

AD-A191 068

MULTIPLE SCATTERING OF WAVES IN DISCRETE RANDOM MEDIA  
(U) PENNSYLVANIA STATE UNIV UNIVERSITY PARK LAB FOR  
ELECTROMAGNET V K VARADAN ET AL 31 DEC 87

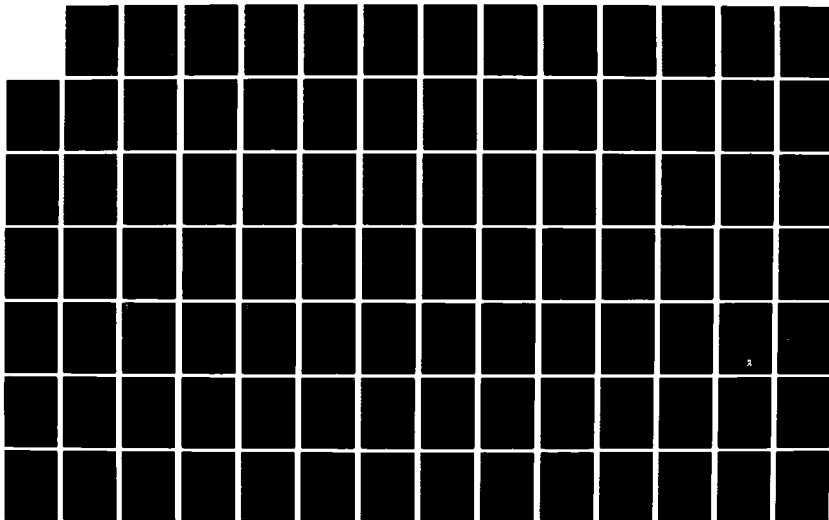
1/2

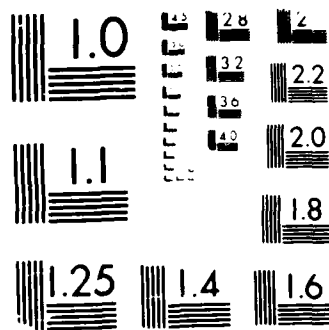
UNCLASSIFIED

ARO-21825 17-GS DRAG29-84-K-0187

F/G 20/11

NL





MICROCOPY RESOLUTION TEST CHART  
ANSI #2 - 1963 - 100% - 100% - 100%

ARO 21825.17-65

(2)

DTIC FILE COPY

**THE PENNSYLVANIA STATE UNIVERSITY**  
*RESEARCH CENTER FOR THE*  
**ENGINEERING OF ELECTRONIC & ACOUSTIC MATERIALS**

**AD-A191 068**

**Multiple Scattering of Waves  
in  
Discrete Random Media**

**Final Report**

**Vijay K. Varadan, Vasundara V. Varadan and Yushieh Ma**

**December 31, 1987**

**DTIC**  
**ELECTE**  
**FEB 04 1988**  
**S H D**

**U.S. Army Research Office**

**Contract No: DAAG29 - 84 - K - 0187**

**Approved for Public Release  
Distribution Unlimited**

**88 1 29 076**

REPORT DOCUMENTATION PAGE		READ INSTRUCTIONS BEFORE COMPLETING FORM
1. REPORT NUMBER ARO 21825.17-65	2. GOVT ACCESSION NO. N/A	3. RECIPIENT'S CATALOG NUMBER N/A
4. TITLE (and Subtitle) Multiple Scattering of Waves in Discrete Random Media		5. TYPE OF REPORT & PERIOD COVERED Final 1 November 1984 - 14 November 1987
		6. PERFORMING ORG. REPORT NUMBER
7. AUTHOR(s) V. K. Varadan and V. V. Varadan, Y. Ma		8. CONTRACT OR GRANT NUMBER(s) DAAG29 - 84 - K - 0187
9. PERFORMING ORGANIZATION NAME AND ADDRESS Laboratory for Electromagnetic and Acoustic Research, 227 Hammond Bldg. Pennsylvania State University		10. PROGRAM ELEMENT, PROJECT, TASK AREA & WORK UNIT NUMBERS
11. CONTROLLING OFFICE NAME AND ADDRESS U. S. Army Research Office Post Office Box 12211 Research Triangle Park, NC 27709		12. REPORT DATE December 31, 1987
14. MONITORING AGENCY NAME & ADDRESS (if different from Controlling Office)		13. NUMBER OF PAGES 144
		15. SECURITY CLASS. (of this report) Unclassified
		15a. DECLASSIFICATION/DOWNGRADING SCHEDULE
16. DISTRIBUTION STATEMENT (of this Report)  Approved for public release; distribution unlimited.		
17. DISTRIBUTION STATEMENT (of the abstract entered in Block 20, if different from Report)  NA		
18. SUPPLEMENTARY NOTES  The view, opinions, and/or findings contained in this report are those of the author(s) and should not be construed as an official Department of the Army position, policy, or decision, unless so designated by other documentation.		
19. KEY WORDS (Continue on reverse side if necessary and identify by block number)  Multiple scattering; discrete random media; effective propagation constant, frequency dependent effective properties, coherent and incoherent intensities, nonspherical scatterers; Monte Carlo simulation; nonspherical statistics, backscattering enhancement; rough surface scattering; wave absorbing materials.		
20. ABSTRACT (Continue on reverse side if necessary and identify by block number)  Multiple scattering of waves in discrete random media was investigated particularly in the scattered intensities (coherent and incoherent). The formalism was applied to examine the effective properties, which are frequency dependent, of either structural composites or wave absorbing composite materials (electronic, elastic and acoustic). The pair correlation function for hard disks was obtained using Monte Carlo simulation and later was used to compute the effective propagation constants for fiber reinforced composites. Nonspherical statistics was employed to study scattering from densely distributed nonspherical scatterers.		

~~UNCLASSIFIED~~

SECURITY CLASSIFICATION OF THIS PAGE(When Data Entered)

in a host medium. The coherent as well as incoherent intensities were computed for spheroidal scatterers and spherical scatterers with different polarizations. The backscattered intensities obtained from our formalism which parallels the diagram method first proposed by Feynman compare favorably with those from optical experiments. Fourteen publications in referred journals and conference proceedings have resulted during this research period from this support.

UNCLASSIFIED

SECURITY CLASSIFICATION OF THIS PAGE(When Data Entered)

# FINAL REPORT

## MULTIPLE SCATTERING OF WAVES IN DISCRETE RANDOM MEDIA

by

V. K. Varadan, V. V. Varadan and Y. Ma

Laboratory for Electromagnetic and Acoustic Research

Department of Engineering Science and Mechanics

and

Center for the Engineering of Electronic and Acoustic Materials

The Pennsylvania State University

University Park, PA 16802

for the period

November 1, 1984 - November 14, 1987

U.S. Army Reserach Office  
Research Triangle Park, NC 27709

Contract No. : DAAG29 - 84 - K - 0187  
December 1987



Accession For	
NTIS GFA&I	<input checked="" type="checkbox"/>
DTIC TAB	<input type="checkbox"/>
Unannounced	<input type="checkbox"/>
Justification	<input type="checkbox"/>
P.	
1. 1. 1. 1. /	
Availability Codes	
Availability Codes	
Dist.	
A-1	

## SUMMARY

During this research period, we concentrated our efforts in two areas. One was to continue our previous investigation of coherent wave propagation in discrete random media. In addition to providing a more rigorous model by considering nonspherical statistics for scatterers of arbitrary shapes, we applied multiple scattering theory to study the frequency dependent effective properties of different kinds of composites (electronic, elastic and acoustic). Such studies enable us to obtain optimal designs of wave absorbing composite materials before conducting any expensive experiment. For preliminary studies, an atmosphere containing aerosols can be modeled as a composite; however, the particles are not stationary and the turbulence in the atmosphere does make the problem even more complicated.

Secondly we began to investigate the incoherently scattered intensity as a result of the multiple scattering of waves in discrete random media. Incoherent intensity becomes extremely important when the magnitude of the second moment of the average wave field cannot be neglected. Consequently, the incoherent intensity not only tells us more about the statistics of the discrete random medium, but also it affects the qualities of the transmitted as well as the reflected signals. Scattered intensities (coherent and incoherent) either from scatterers in a volume or from scatterers on a surface (modeled as rough surface) were theoretically examined. The computed results for backscattered intensity from scatterers compared favorably with those from recently observed backscattering enhancement experiments.

In the following, we outline and summarize, based on the submitted and published papers in either journals or conference proceedings, the work and the obtained results during this period and also propose the tasks which should be pursued in the near future.

- (a) We have demonstrated a scheme for computing the complex propagation characteristics of a medium that is effectively anisotropic. For aligned nonspherical dielectric scatterers in free space, there is a significant difference between the results (for effective permittivity) for parallel and perpendicular polarization of electromagnetic waves. However, the anisotropic effect for spheroidal ice particles in air was not found to be significant when we varied the angle of incidence.
- (b) We employed a more efficient scattering formalism using the scattered field, rather than an earlier exciting field formalism which involves larger matrices. The new formalism is used to compute the phase velocity and attenuation of composite media (circular as well as non-circular scatterers of considerable concentrations) excited by either elastic SH or P and SV waves. To obtain the numerical results, the pair correlation function for "hard" disks using Monte Carlo simulation was used.
- (c) We applied multiple scattering theory to the design of microwave absorbing materials. The scatterers considered were ferrite particles with high dielectric and magnetic loss tangents. Because

the size of the ferrite particles is very small compared to the microwave wavelength, we derived an analytical expression to obtain the complex propagation constant for the composite in the long wavelength limit. The simple formula is able to predict the effective properties of electronic composites in which both scatterers and host materials can be lossy. In the Rayleigh regime, the derived formula covers the volume fraction of scatterers from 0 - 100%. In addition, the characteristics of millimeter and microwave absorbing composites, consisting of piezoelectric or chiral polymer particles, were also examined in wide frequency bands.

(d) Backscattered intensities were studied analytically for spherical scatterers randomly distributed on a plane excited by either a normally incident plane wave or a beam wave. Under these circumstances, waves are essentially multiply scattered by a random rough surface. The formalism used to obtain the backscattered intensities was examined by using the principle of conservation of energy and considering both the coherent and the incoherent intensities. However, current results do not cover nonspherical scatterers and the dense concentration cases which should be pursued further.

(e) Earlier results for electromagnetic wave propagation in discrete random media assumed spherical statistics for describing the spatial distribution of even nonspherical scatterers. We used the Monte Carlo method to generate the appropriate pair correlation functions for nonspherical scatterers (at the present stage, prolate and oblate spheroids with different aspect ratios) which may be either aligned or randomly oriented. The proper pair correlation function is then used to calculate the propagation constants for waves traveling in a medium consisting of randomly and densely distributed nonspherical scatterers. The propagation constant was later used to compute the coherent and incoherent intensities. Considerable differences were found between the previous results using various kinds of approximation for nonspherical statistics, and the current ones using the Monte Carlo simulation.

(f) We developed a computational scheme to obtain numerical results for the second moment (average intensity) of a wave field propagating in a medium consisting of randomly distributed scatterers which are not necessarily simple in shape. The formalism (propagator model) used in our computation parallels the diagram method first proposed by Feynman and clearly shows the various approximations made in the intensity calculations. The back and forth scattering between a pair of scatterers, which has been neglected in the ladder approximation, automatically appears in our formalism taking into account all the multiple scattering between two scatterers through the pair correlation function. The computed scattered intensities in the forward direction compared very well with those measured from microwave experiments. The widths and magnitudes of the backscattered intensity peak compared favorably with those of optical experiments.



LIST OF MANUSCRIPTS SUBMITTED OR PUBLISHED UNDER ARO SPONSORSHIP  
DURING THE PERIOD

V. K. Varadan, V. V. Varadan, Y. Ma, and A. Lakhtakia, "Piezoelectric, ferrite and chiral polymer composites," in Proceedings of Multiple Scattering of Waves in Random Media and Random Rough Surfaces, pp. 503-522, July, 1985.

Y. Ma, V. K. Varadan, and V. V. Varadan, "Scattering of acoustic beam waves by rough surfaces," in Proceedings of Multiple Scattering of Waves in Random Media and Random Rough Surfaces, pp. 695-700, July, 1985.

V. V. Varadan, V. K. Varadan, and Y. Ma, "Multiple scattering theory for acoustic, electromagnetic and elastic waves in discrete random media," in Proceedings of Multiple Scattering of Waves in Random Media and Random Rough Surfaces, pp. 941-952, July, 1985.

V. V. Varadan, Y. Ma, and V. K. Varadan, "Anisotropic dielectric properties of media containing aligned nonspherical scatterers," *IEEE Transactions on Antennas Propagation* AP-33, 886-890, August, 1985.

V. K. Varadan, V. V. Varadan, and Y. Ma, "Multiple scattering of elastic waves by cylinders of arbitrary cross section II. Pair correlated cylinders," *Journal of the Acoustical Society of America* 78(5), 1874-1878, November, 1985.

V. V. Varadan, Y. Ma, and V. K. Varadan, "Propagator model including multiple fields for discrete random media," *Journal of the Optical Society of America* A(2), 2195-2201, December, 1985.

V. K. Varadan, V. V. Varadan, Y. Ma, and W. F. Hall, "Design of ferrites impregnated plastics(PVC) as microwave absorbers," *IEEE Transactions on Microwave Theory and Techniques* MTT-34, 251-258, February, 1986.

Y. Ma, A. H. Magnuson, V. K. Varadan, and V. V. Varadan, "Acoustic response of manganese nodule deposits," *Geophysics* 51, 689-698, March, 1986.

V. K. Varadan, Y. Ma and V. V. Varadan, "Multiple scattering of compressional and shear waves by fiber reinforced composite materials," *Journal of the Acoustical Society of America* 80(1), 333-339, July, 1986.

V. V. Varadan, V. K. Varadan and Y. Ma, "EM wave propagation in discrete random media: nonspherical statistics," presented in the CRDEC Scientific Conference on Obscuration and Aerosol Research, July, 1986.

V. V. Varadan, V. K. Varadan and Y. Ma, "Multiple scattering of waves in random media containing nonspherical scatterers," in the Electromagnetic Wave Propagation Panel Symposium sponsored by AGARD, NATO, May, 1987.

V. V. Varadan, V. K. Varadan and Y. Ma, "Backscattering enhancement of waves in random media," presented in the CRDEC Scientific Conference on Obscuration and Aerosol Research, June, 1987.

Y. Ma, V. V. Varadan and V. K. Varadan, "Average intensity scattered by densely distributed nonspherical particles," presented in the CRDEC Scientific Conference on Obscuration and Aerosol Research, June, 1987.

V. V. Varadan, V. K. Varadan, Y. Ma and W. A. Steele, "Effects of nonspherical statistics on EM wave propagation in discrete random media," *Radio Science* 22, 491-498, July-August, 1987.

Y. Ma, V. V. Varadan and V. K. Varadan, "Scattered intensity of a wave propagating in a discrete random medium," *Applied Optics*, to appear.

## PIEZOELECTRIC, FERRITE AND CHIRAL POLYMER COMPOSITES

V.K. VARADAN, V.V. VARADAN, Y. MA and A. LAKHTAKIA

*Laboratory for Electromagnetic and Acoustic Research,  
Department of Engineering Science and Mechanics,*

*&*

*Research Center for the Engineering of Electronic and Acoustic Materials,  
The Pennsylvania State University,  
University Park, PA 16802.*

### ABSTRACT

*In many applications involving electromagnetic waves, it is desirable to design materials having prescribed frequency-dependent reflection and transmission characteristics; at the same time, they must conform to restrictions on weight, structural properties and geometry, etc. Composite materials that contain a distribution of inclusions of specific concentration, distributional statistics, geometry and material properties, can often achieve the desired absorption characteristics while adhering to other design restrictions. Because of economic and time constraints, the design of such composites must be carried out theoretically. In this paper, the characteristics of millimeter and microwave absorbing composites, consisting of piezoelectric, ferrite or chiral polymer particles, are examined.*

### 1. INTRODUCTION

To investigate the dynamic response of composite materials which are formed as a combination of two discrete phases, i.e., the inclusion (scatterer) and the matrix (host) phases, requires the use of the multiple scattering theory whenever the volume fraction of the inclusion phase becomes even moderately large, which is usually the case for most commercial composites (e.g. carbon fiber or boron fiber composites used in aerospace industry). In this paper, because of the variety of inclusion phases (piezoelectric inclusions are modeled as infinitely long cylinders which are two dimensional scatterers while ferrite and chiral inclusions are treated as three dimensional spherical scatterers) as well as the versatility of the exciting waves (elastic waves and electromagnetic waves which have cylindrical or spherical wavefronts), any effort in trying to formulate a unified algorithm which is suitable for various systems seems to be awkward. However, a general multiple scattering formalism, without going into complicated details, is given also in this proceedings [Varadan *et al.*, 1985c] and can be used for a general reference. Nevertheless, the step-by-step derivations for any specific problem can be found in our previous work [Varadan *et al.*, 1980, 1984, 1985a, 1985b, 1986].

### 2. PIEZOELECTRIC MATERIALS

Ever since the discovery of the piezoelectric effect by Pierre and Jacques Curie [Cady, 1946; Auld, 1973], materials possessing the relevant properties have been widely used in the fabrication of transducers, sensors, filters, resonators, etc. Piezoelectricity is the linear, reversible coupling between the electromagnetic and the elastodynamic energies due to the displacement of charges. If a charge density is created over the surface of a piezoelectric material volume, then internal stress and strain are produced; conversely, the application of mechanical pressure creates a change in the surface charge density, thereby launching an electromagnetic field. Materials which are piezoelectric are either crystals endowed with anisotropy, or they are ceramics with ferroelectric properties which can sustain a

permanent charge polarisation due to dielectric hysteresis. Single crystals are generally suitable for very high frequencies, and, in quartz, elastic wave propagation has been observed at 125 GHz. However, synthetic materials – principally, ferroceramics like uniaxial  $\text{BaTiO}_3$  and lead zirconate titanate (PZT) – have very strong electromagnetic-elastic coupling, and these new materials are increasingly being put to use.

Constitutive relations for piezoelectric materials can be obtained by expressing the thermodynamic internal energy in terms of macroscopic state variables such as strain, electric and magnetic fields. With the assumption that here the piezoelectric materials are non-magnetic, in mixed dyadic/vector notation these relations take the form [Auld, 1973]

$$\mathbf{T} = -\mathbf{e} \cdot \mathbf{E} + \mathbf{c}^E : \mathbf{S}, \quad (2-1a)$$

$$\mathbf{D} = \mathbf{e}^S \cdot \mathbf{E} + \mathbf{e} : \mathbf{S}, \quad (2-1b)$$

$$\mathbf{B} = \mu_0 \mathbf{H}, \quad (2-1c)$$

where  $\mathbf{e}$  is the third rank piezoelectric coupling tensor,  $\mathbf{c}^E$  is the fourth rank stiffness tensor at constant electric field and  $\mathbf{e}^S$  is the second rank permittivity tensor at constant strain and  $\mu_0$  is the permeability of free space. The elastodynamic field variables are  $\mathbf{u}$ , the particle displacement,  $\mathbf{T}$ , the stress tensor, and  $\mathbf{S}$ , the strain tensor, whereas  $\mathbf{E}$ ,  $\mathbf{H}$ , and  $\mathbf{B}$  are the usual electromagnetic field vectors.

In a piezoelectric material, therefore, both the Navier equation and the four Maxwell's equations

$$\nabla \cdot \mathbf{T} = -\rho \omega^2 \mathbf{u}, \quad (2-2)$$

$$\nabla \cdot \mathbf{B} = 0; \nabla \cdot \mathbf{D} = \rho_e; \nabla \times \mathbf{E} = -j\omega \mathbf{B}; \nabla \times \mathbf{H} = j\omega \mathbf{D}, \quad (2-3)$$

must be satisfied by the composite elastic-electromagnetic field subject to the constitutive equations (2-1). In (2-2),  $\rho$  is the mass density, whereas in (2-3),  $\rho_e$  is the volume charge density. Although (2-1) - (2-3) are general, all further discussion in this section is specialized to a cartesian ( $x_1, x_2, x_3$ ) co-ordinate system, with  $x_3$  axis being the preferred direction.

The fourth rank tensor  $\mathbf{c}^E$  is called the stiffness tensor, all elements of which must be positive. Note that not all of its elements are independent of each other, and it turns out that (with the superscript  $E$  omitted, henceforth)

$$c_{ijkl} = c_{klij} = c_{jikl} = c_{ijlk}, \quad i, j, k, l = 1, 2, 3, \quad (2-4)$$

further simplifications coming for transversely isotropic materials [Auld, 1973]. From thermodynamic considerations it can also be shown that the piezoelectric coupling tensor  $\mathbf{e}$  is symmetric. Further, since the stress tensor is symmetric

$$e_{ijk} = e_{ikj} \quad (2-5)$$

Confining the remaining part of this section to transversely ( $x_1$ - $x_2$ ) isotropic media, it is convenient to use an abbreviated index notation due to the particular symmetry of  $c_{ijkl}$ . The upper case letters  $I, J$ , etc., will be used to denote

$I$	$ij$
1	11
2	22
3	33
4	23, 32
5	13, 31
6	12, 21

Thus,  $c_{ij}$  is a  $6 \times 6$  symmetric matrix with only five independent elements for a material with transverse isotropy, and is given by

$$c_{ij} = \begin{bmatrix} c_{11} & c_{12} & c_{13} & 0 & 0 & 0 \\ c_{12} & c_{11} & c_{13} & 0 & 0 & 0 \\ c_{13} & c_{13} & c_{33} & 0 & 0 & 0 \\ 0 & 0 & 0 & c_{44} & 0 & 0 \\ 0 & 0 & 0 & 0 & c_{44} & 0 \\ 0 & 0 & 0 & 0 & 0 & c_{66} \end{bmatrix} \quad (2-6)$$

with  $c_{66} = (c_{11} - c_{12})/2$ . Similarly the piezoelectric coupling tensor  $e$  is written in the abbreviated form as

$$e_{ij} = \begin{bmatrix} 0 & 0 & 0 & 0 & e_{15} & 0 \\ 0 & 0 & 0 & e_{15} & 0 & 0 \\ e_{31} & e_{31} & e_{33} & 0 & 0 & 0 \end{bmatrix} \quad (2-7)$$

which has three independent elements; and the permittivity tensor, after dropping the superscript  $S$ , as

$$\epsilon_{ij} = \begin{bmatrix} \epsilon_{11} & 0 & 0 \\ 0 & \epsilon_{11} & 0 \\ 0 & 0 & \epsilon_{33} \end{bmatrix} \quad (2-8)$$

which has two independent elements.

In order to solve boundary value problems, the appropriate surface conditions on the particle velocity  $v = \{\partial/\partial t\}u$ , the traction force  $T \cdot n$ , and the tangential electric and magnetic fields  $n \times E$  and  $n \times H$  must be satisfied,  $n$  being the unit outward normal to the relevant interface. Reflection and transmission characteristics of planar, piezoelectric half-spaces were probably first examined by Kyame [1949; 1954], and have been dealt at great length by Auld [1973]. Scattering of elastic and electromagnetic waves by transversely isotropic cylinders have been investigated by Moon [1970], whose analysis has been applied by Lakhtakia *et al.* [1986a] to study the properties of cylindrical gratings made of  $\text{BaTiO}_3$  cylinders.

Table 2-1 Comparison of stiffened and unstiffened elastic constants of  $\text{BaTiO}_3$  and PZT-5

$c_{ij}$	PZT - 5		$\text{BaTiO}_3$	
	Unstiffened ( $\times 10^{10} \text{ N/m}^2$ )	Stiffened ( $\times 10^{10} \text{ N/m}^2$ )	Unstiffened ( $\times 10^{10} \text{ N/m}^2$ )	Stiffened ( $\times 10^{10} \text{ N/m}^2$ )
$c_{11}$	12.6	12.9	15.0	15.2
$c_{12}$	7.95	8.27	6.6	6.77
$c_{13}$	8.41	7.25	6.6	5.92
$c_{33}$	11.7	12.0	14.6	14.8
$c_{44}$	2.3	4.22	4.4	5.68

In many practical problems due to the enormous difference in the speed of propagation of acoustic or elastic waves and electromagnetic waves, frequencies pertinent to the former ranging from a few Hertz to 100 MHz are very low with respect to electromagnetic waves. Noting that  $B$  and  $H$  do not explicitly appear in the constitutive equations, it can be assumed that the electromagnetic field reduces to a quasi-static electric field at frequencies less than about 100 MHz. It is, nevertheless, important that the distinction between static and quasi-static is retained. In the quasi-static approximation, one may assume that the  $E$  field is irrotational, noting that it is strictly so in the electrostatic case.

Assuming that the electric field is irrotational, it is possible to write down

$$E = -\nabla \xi, \quad (2-9a)$$

with  $\xi$  being a scalar potential. In which case, the magnetic displacement vector

$$B = 0, \quad (2-9b)$$

by virtue of the fact that  $\nabla \times \nabla \xi = 0$ . This implies an additional relationship between  $\nabla \xi$  and  $S$  via (2-1b), and it can be shown that

$$-e_{11} \{\partial \xi / \partial x_1\} = e_{15} S_5, \quad (2-10a)$$

$$-e_{11} \{\partial \xi / \partial x_2\} = e_{15} S_4, \quad (2-10b)$$

$$-e_{33} \{\partial \xi / \partial x_3\} = e_{31} (S_1 + S_2) + e_{33} S_3. \quad (2-10c)$$

Substitution of (2-10) in (2-1a) yields a stress-strain relationship for the transversely isotropic, piezoelectric medium which does not involve the electromagnetic field explicitly in the quasi-static approximation. Indeed, then it becomes possible to state that

$$T = e \cdot \nabla \xi + \bar{c}^E : S = \bar{c}^E : S, \quad (2-11)$$

where the overbar above  $\bar{c}^E$  signifies piezoelectric stiffening, with its independent elements given by

$$\bar{c}_{11} = c_{11} + (e_{31})^2 / e_{33} \quad \bar{c}_{33} = c_{33} + (e_{31})^2 / e_{33} \quad (2-12a,b)$$

$$\bar{c}_{12} = c_{12} + (e_{31})^2 / e_{33} \quad \bar{c}_{13} = c_{13} + e_{31} e_{33} / e_{33} \quad (2-12c,d)$$

$$\bar{c}_{44} = c_{44} + e_{15}^2 / e_{11} \quad (2-12e)$$

The stiffening can be considerable, especially in the coefficient  $c_{44}$  as Table 2-1 indicates for  $\text{BaTiO}_3$  and PZT-5. In the quasi-static approximation, the appropriate surface conditions on the particle velocity  $v = \{\partial / \partial t\} u$ , the traction force  $T \cdot n$ , the potential  $\xi$  and its normal derivative  $n \cdot \nabla \xi$  must be satisfied.

After the examination of the nature of piezoelectric materials, we are currently investigating the damping characteristics as well as the phase velocity dispersion patterns of piezoelectric composites. In obtaining the numerical results, multiple scattering formalism has been employed in solving the effective wavenumber  $K (= K_1 + iK_2)$  of the piezoelectric composites. The real part  $K_1$  of  $K$  relates to the phase velocity and the imaginary part  $K_2$  is proportional to the attenuation rate which also can be converted to the physical dB scale if the sizes of the inclusions are given.

The piezoelectric composite considered in this paper is transversely isotropic piezoelectric material with properties given in Table 2-2 and the matrix used is soft rubber whose properties are also shown in the same table. Results presented in Figures 1 and 2 are for SH wave incidence. The results from the corresponding problem but for P and SV wave incidence are presented in Figure 3 and 4. However, the properties for such a case are given in Table 2-3.

Table 2-2 Material Properties for Piezoelectric Composites (SH Wave Incidence)

	Case 1	Case 2
$\rho_1$ (kg/m <sup>3</sup> )	6600	7000
$\rho$ (kg/m <sup>3</sup> )	1100	1000
$c_{44}^1$ (N/m <sup>2</sup> )	$8.5 \times 10^9$	$8.5 \times 10^9$
$c_{44}$ (N/m <sup>2</sup> )	$7.0 \times 10^7$	$7.0 \times 10^8$
$e_{15}$ (C/m <sup>2</sup> )	11.6	11.6
$\epsilon_{11}^1$ (F/m)	$300 \epsilon_0$	$56 \epsilon_0$
$\epsilon_{11}$ (F/m)	$6 \epsilon_0$	$20 \epsilon_0$

Table 2-3 Material Properties for Piezoelectric Composites (P and SV Wave Incidence)

	Matrix	Inclusion
$\rho$ (kg/m <sup>3</sup> )	1100	5700
$c_{11}$ (N/m <sup>2</sup> )		$16.6 \times 10^{10}$
$c_{12}$ (N/m <sup>2</sup> )		$7.66 \times 10^{10}$
$e_{31}$ (Coulomb/m <sup>2</sup> )		-4.4
$\epsilon$ (dielectric constant)	$6 \epsilon_0$	
$\epsilon_{33}$		$1450 \epsilon_0$
Lame' Constants (N/m <sup>2</sup> )		
Case 1 $\lambda$	$6.93 \times 10^8$	
$\mu$	$8.91 \times 10^8$	
Case 2 $\lambda$	$2.46 \times 10^9$	
$\mu$	$6.19 \times 10^6$	
Case 3 $\lambda$	$2.28 \times 10^9$	
$\mu$	$9.90 \times 10^7$	
Case 4 $\lambda$	$2.45 \times 10^9$	
$\mu$	$1.10 \times 10^7$	
$\epsilon_0 = 8.854 \times 10^{-12}$ Farad/m $\mu_0 = 4\pi \times 10^{-7}$ Henry/m		

### 3. FERRITES

In spite of the long history of the preparation of ferrite materials, one aspect of the microwave characteristics of ferrites has particularly aroused the interest of researchers in recent days, i.e., the understanding of the mechanism by which electromagnetic energy is dissipated in ferrites. The presence of a high dielectric constant as well as a magnetic loss tangent in a ferrite gives rise to high electromagnetic energy dissipation, which can be fruitfully utilized in the design of efficient microwave absorbing composites.

In our previous work [Varadan *et al.*, 1985b], the attenuation of intensity in composite materials along the wave propagation direction has been shown to be proportional to the imaginary part of the effective wavenumber  $K$ . In other words, by appropriately tailoring the ferrite composites, which in this study is through grounding the sintered ferrite in a ball mill, and then mixing with another material and moulded, we are able to predict the dispersion characteristics of the new material. In

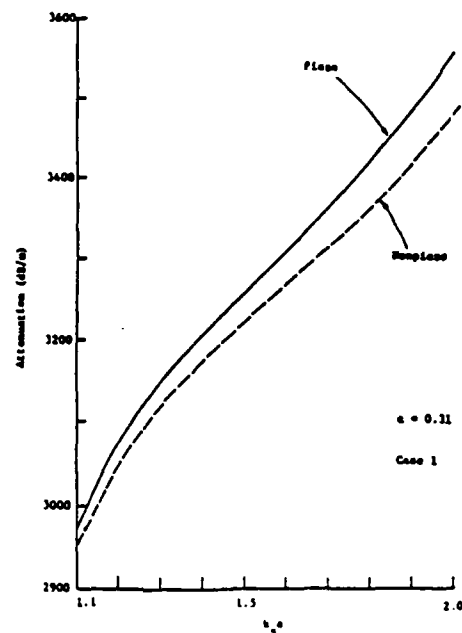


Figure 1 Coherent attenuation vs.  $k_p a$  for piezo- and nonpiezoelectric cylinders for case 1 at  $c = 0.31$ .

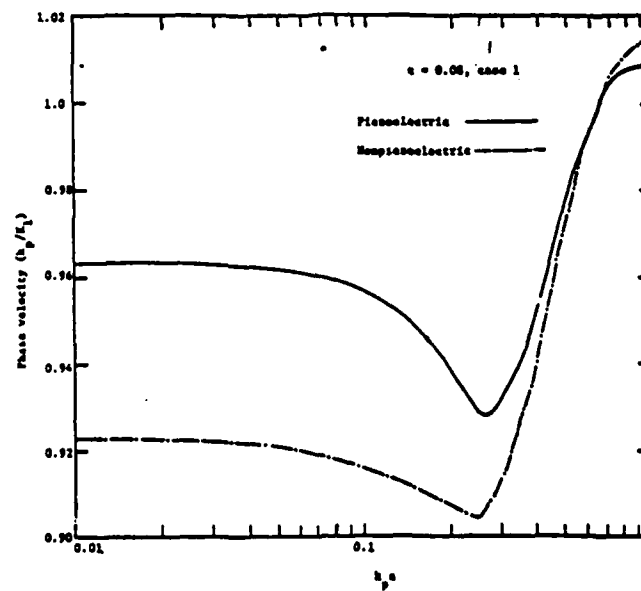


Figure 2 Comparison of phase velocity vs. nondimensional frequency between piezo- and nonpiezoelectric cylinders in an elastic medium of case 1 at  $c = 0.08$ .

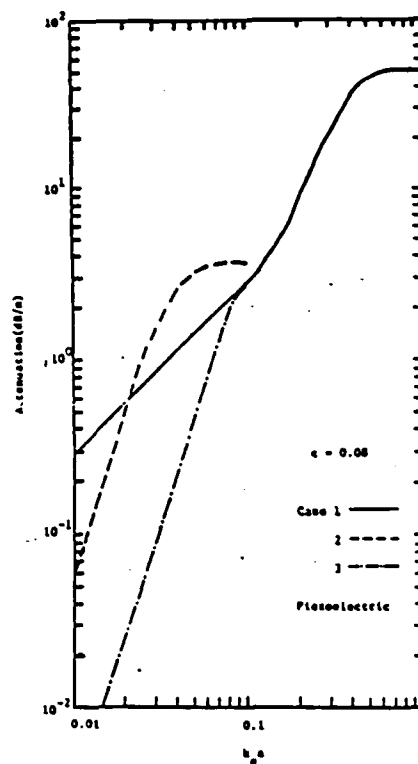
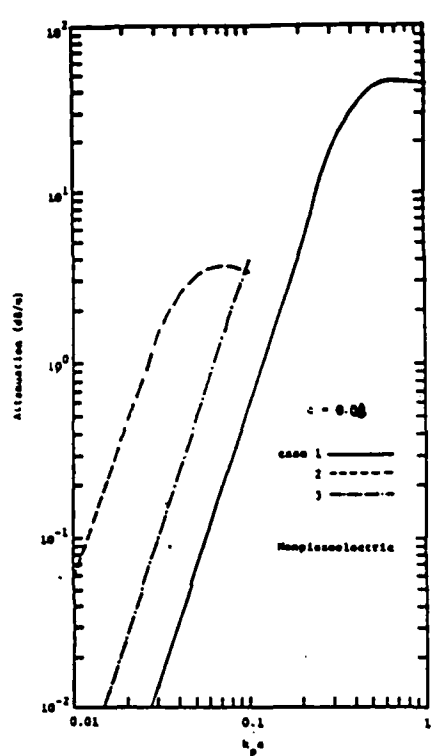


Figure 3 Attenuation vs. nondimensional frequency for nonpiezoelectric cylinders in an elastic medium of cases 1, 2 and 3 at  $c = 0.08$ .

Figure 4 Attenuation vs. nondimensional frequency for piezoelectric cylinders in an elastic medium of cases 1, 2 and 3 at  $c = 0.08$ .



general, the dispersion characteristics depend on the effective wavenumber  $K$ . Although the selection of the matrix material is quite important, the critical parameter in the design of ferrite composites is the inclusion material.

Generally speaking, the effective wavenumber  $K$  is determined through the T-matrix method [Varadan & Varadan, 1980], in which a transfer function for studying the wave scattering as well as absorption characteristics of a single inclusion is considered. However, besides the response of a single inclusion, the low porosity of ferrite composites introduces interactions among inclusions when excited by microwaves and multiple scattering effects have to be included in the analysis. Current efforts are, therefore, directed toward the identification of several categories of ferrite composites whose effective wavenumbers yield high damping coefficients in some specific microwave bands.

Usually, the commercial ferrites with known dispersion curves are the first candidates for the theoretical analysis. Any effort in the preparation of ferrite materials in improving the dispersion patterns whose resonance phenomena highly enhance the attenuation of the composites is strongly encouraged. In most cases, physical properties, in an effective manner, are able to be derived from the effective wavenumber  $K$  of the composite materials. But unfortunately, only the effective quantity of the product of  $\epsilon$  and  $\mu$ , i.e.,  $\langle \epsilon\mu \rangle$ , can be inferred from the effective wavenumber  $K$  of ferrite composites. Although the permittivity of ferrites can be simply obtained using the Lorenz-Lorentz formula [Fröhlich, 1949], there is no direct formula, at least in the current literature, which can be employed to compute the permeability of ferrites. Therefore, the reason for not being able to derive an exact formula for independent  $\epsilon$  and  $\mu$  is probably due to the complex dispersion pattern for the permeability of ferrites.

For magnetized ferrites, the electromagnetic energy can be dissipated due to resonance absorption [Bloembergen, 1950]. One notices that when the signal frequency coincides with the natural precession frequency, maximum energy dissipation occurs. In an infinite medium, the precession frequency is determined by an applied static magnetic field; therefore, it is natural not to expect any precession frequency, and, hence, any significant absorption of microwave energy in an actual sample. However, it is worth noting that an effective field always exists within a sample of finite size due to demagnetizing effects associated with sample or crystalline boundaries and due to crystalline anisotropy.

The absorption mechanism inherited from the effective field, referred to as domain rotation resonance [Polder & Smit, 1953], accounts for an absorption peak which occurs in unmagnetized ferrites at low microwave frequencies (see Fig. 5). It may also account in part for an absorption peak which appears at radio frequencies. However, experiments have shown that the radio frequency magnetic loss in certain ferrite arises from the so called domain wall resonance [Rado *et al.*, 1950]. In Fig. 6, there are two pronounced dispersion regions for the solid ferrite. One occurs at low microwave frequencies while the other at radio frequencies (the low microwave frequency dispersion region is influenced by the domain rotation resonance). In powdered ferrite, one notices that the low frequency peak is completely absent and, since anisotropy would not be affected by powdering, the radio frequency dispersion cannot be due to rotation resonance. Instead, it must therefore be due to domain wall resonance. In low porosity ferrites, domain walls are easily trapped and domain wall motion, consequently, either prevented or restricted. Under these conditions, any resonance observed at low frequencies is quite possibly due to domain rotation resonance in the anisotropy field.

The formalism used to obtain the effective wavenumber of a ferrite composite has been derived [Varadan *et al.*, 1986]. Because the size " $a$ " of the ferrite inclusion is relatively much smaller than the incident wavelength, i.e.,  $ka \ll 1$ , the long wavelength approximation can be made to simplify the whole computation algorithm. For the convenience of the reader, we will briefly cite the final equation which can be used right away in obtaining the effective wavenumber  $K$ .

The normalized effective wavenumber  $\eta$  ( $= K_1/k_2 + jK_2/k_2$ ), according to our previous investigation [Varadan *et al.*, 1986] is given by

$$\eta = 2\{[(\sigma-1-\zeta_1-\zeta_3)+i(v-\zeta_2-\zeta_4+\beta\hat{D}w+\beta\hat{A}w-2wcU\beta/y_1+2wc\beta UV\gamma y_1)]/[(\sigma-4+2\zeta_1+2\zeta_3) + i(v+2\zeta_2+2\zeta_4+4\beta\hat{A}w+4\beta\hat{D}w+4\beta wcU/y_1)]\}^{1/2} \quad (3-1)$$

The normalization factor  $k_2$  is the wavenumber in the matrix material. The parameters in Eq. (3-1) are now defined as follows

$$\begin{aligned} \sigma &= c^2(U - \gamma^2 U - 2\gamma V)/y_2 & v &= c^2(2\gamma U + V - \gamma^2 V)/y_2 \\ \zeta_1 &= c(\hat{B}\gamma + \hat{A})/y_1 & \zeta_2 &= c(\hat{D}\gamma - \hat{C})/y_1 \\ \zeta_3 &= c(\hat{C}\gamma + \hat{D})/y_1 & \zeta_4 &= c(\hat{A}\gamma - \hat{B})/y_1 \\ U &= \hat{B}\hat{C} - \hat{A}\hat{D}, V = \hat{A}\hat{C} + \hat{B}\hat{D} \\ \hat{A} &= 2(B\gamma + A) & \hat{B} &= 2(A\gamma - B) \\ \hat{C} &= 2(C\gamma - D) & \hat{D} &= 2(D\gamma + C) \\ A &= [(\mu_1' - \mu_2')(2\mu_2' + \mu_1') + (\mu_1'' - \mu_2'')(2\mu_2'' + \mu_1'')]/\Delta \\ B &= [(\mu_1'' - \mu_2'')(2\mu_2' + \mu_1') + (\mu_1' - \mu_2')(2\mu_2'' + \mu_1'')]/\Delta \\ C &= [(\epsilon_1' - \epsilon_2')(2\epsilon_2' + \epsilon_1') + (\epsilon_1'' - \epsilon_2'')(2\epsilon_2'' + \epsilon_1'')]/\Delta' \\ D &= [(\epsilon_1'' - \epsilon_2'')(2\epsilon_2' + \epsilon_1') + (\epsilon_1' - \epsilon_2')(2\epsilon_2'' + \epsilon_1'')]/\Delta' \\ \Delta &= (2\mu_2' + \mu_1')^2 + (2\mu_2'' + \mu_1'')^2 & \Delta' &= (2\epsilon_2' + \epsilon_1')^2 + (2\epsilon_2'' + \epsilon_1'')^2 \\ \gamma &= (X_2^3 - 3X_2^2 X_2)/(X_2^3 - 3X_2 X_2^2) & y_2 &= y_1^2 \\ y_1 &= 1 + \gamma^2 & X_2 &= \text{Re}(k_2 a) \\ \beta &= (X_2^3 - 3X_2 X_2^2)/3 & \epsilon_1 &= \epsilon_1' + j\epsilon_1'' \\ \mu_1 &= \mu_1' + j\mu_1'' & k_2 &= \omega(\mu_2 \epsilon_2)^{1/2}/c_0 \\ \epsilon_2 &= \epsilon_2' + j\epsilon_2'' & w &= (1-c)/(1+2c)^2 \\ & & X_2' &= \text{Im}(k_2 a) \\ & & \mu_2 &= \mu_2' + j\mu_2'' \end{aligned}$$

Two kinds of ferrite materials, namely R-1 and R-4, prepared by General Ceramics of Division of Indiana General [Westphal *et al.*, 1972] were used as inclusion materials in our numerical calculation. The dispersion patterns of R-1 and R-4 are presented as Figures 7 and 8 respectively. The matrix material was chosen to be PVC and the dielectric constant of PVC was taken to be  $\epsilon_2 = 2\epsilon_0$  and  $\mu_2 = \mu_0$ . It was assumed that both  $\epsilon_2$  and  $\mu_2$  are nondispersive and lossless at the microwave frequencies. Results for the imaginary part  $K_2$  are presented, using the dB/mm scale, in Figs 9 and 10 for R-1 and R-4 ferrites, respectively. In converting to the dB scale, the ferrite particle was assumed to be 0.4 micron in diameter in each instance. The peak of the attenuation of ferrite composites seems to appear, for both cases, at the frequency having a minimum value of the real permeability constant  $\mu_1$  and is about 3 GHz. This fact has also been observed in our previous results [Varadan *et al.*, 1986] for magnetite  $\text{Fe}_3\text{O}_4$ . Although there is no rigorous proof, it appears that this anti-resonance behavior may be the mechanism causing a high attenuation in ferrite composites. Besides the attenuation pattern of ferrite composites, the phase velocity dispersion patterns are also presented for the R-1 and R-4 ferrites in Figs 11 and 12, respectively.

#### 4. CHIRAL MEDIA

The final class of materials to be discussed here are the chiral materials. The lack of geometric symmetry between an object and its mirror image is referred to as chirality [Bohren, 1974], and the mirror image of such a chiral object cannot be made to coincide with the object itself by any operation involving rotations and/or translations. Chiral objects occur in nature, the readiest available example being the two hands of the reader. The most commonly investigated chiral objects, however, are the L- and the D-type stereo-isomers so familiar to students of organic chemistry. As a garden-variety example, the doubly enantiomorphic sweetener Nutrasweet™, patented by G.D. Searle Company, can occur in four different forms: of these, the taste of L-aspartyl-L-phenylamine methyl ester is sweet, while that of D-aspartyl-D-phenylamine methyl ester is bitter; the isomers with the L-D or the D-L configurations are tasteless [Goodman, 1985]. The basis for the difference in the physical properties of

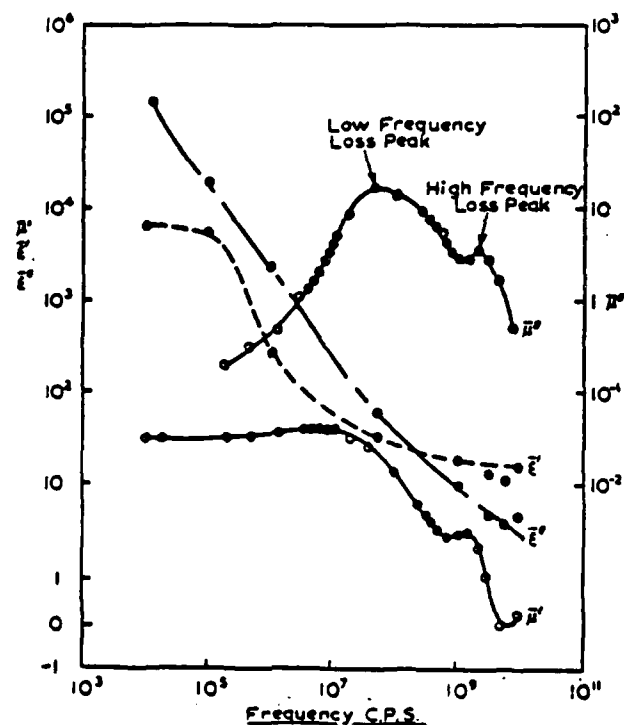


Figure 5 Magnetic and dielectric spectrum of polycrystalline nickel ferrite [Miles *et al.*, 1957].

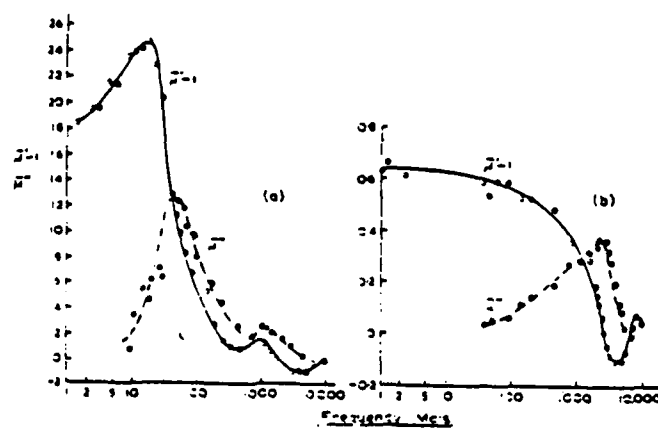


Figure 6 Magnetic spectrum of (a) solid ferramic A ferrite and (b) 70% (by weight) mixture of ferramic A particles and wax [Rado *et al.*, 1950].

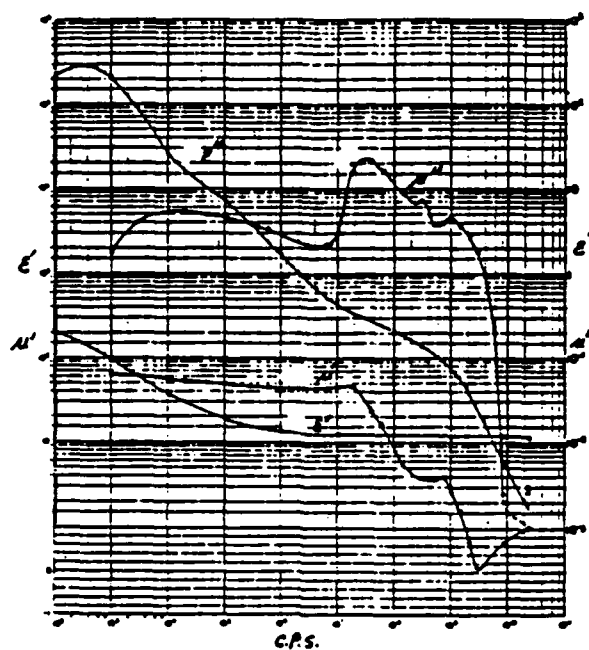


Figure 7 Magnetic and dielectric spectrum of R-1 ferrite [Westphal *et al.*, 1972].

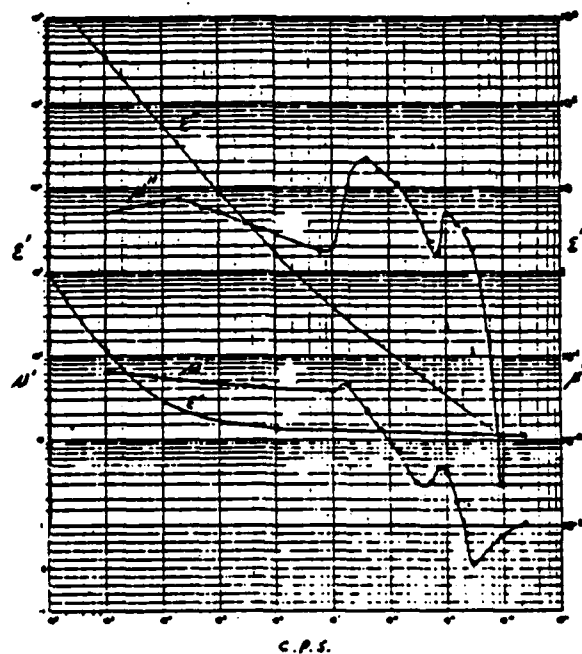


Figure 8 Magnetic and dielectric spectrum of R-4 ferrite [Westphal *et al.*, 1972].

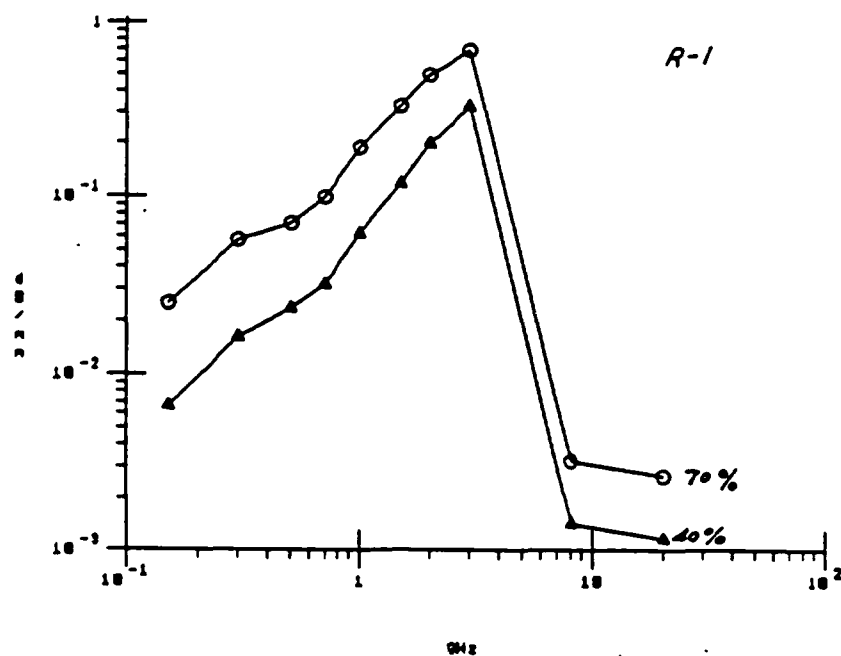


Figure 9 Attenuation vs. frequency for ferrite composites (contain 40% and 70% R-1 ferrites).

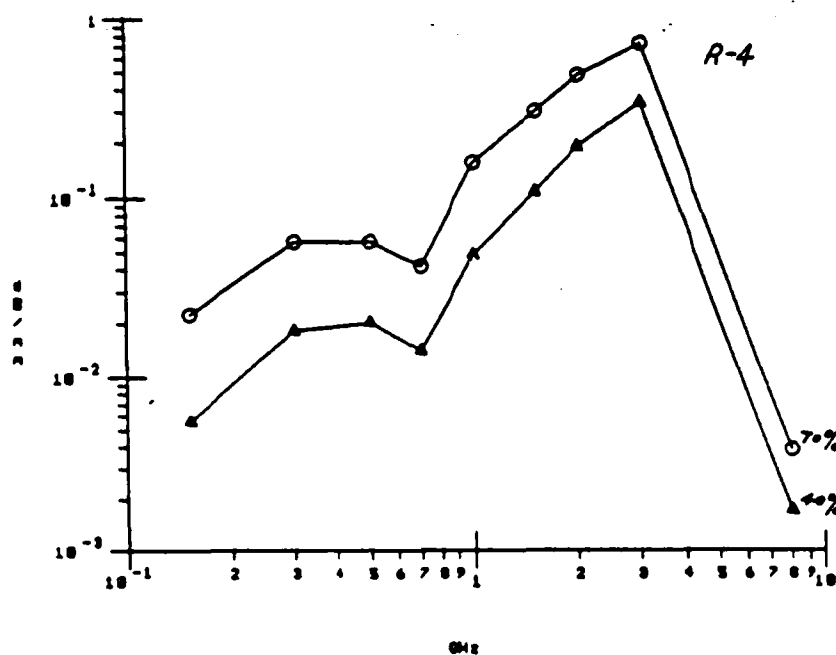


Figure 10 Attenuation vs. frequency for ferrite composites (contain 40% and 70% R-4 ferrites).

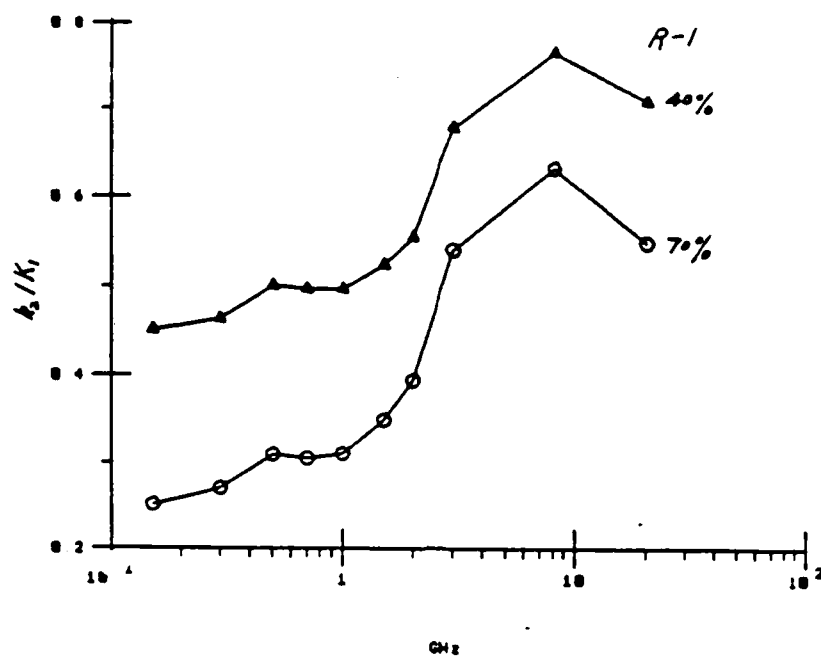


Figure 11 Phase velocity vs. frequency for ferrite composites (contain 40% and 70% R-1 ferrites).

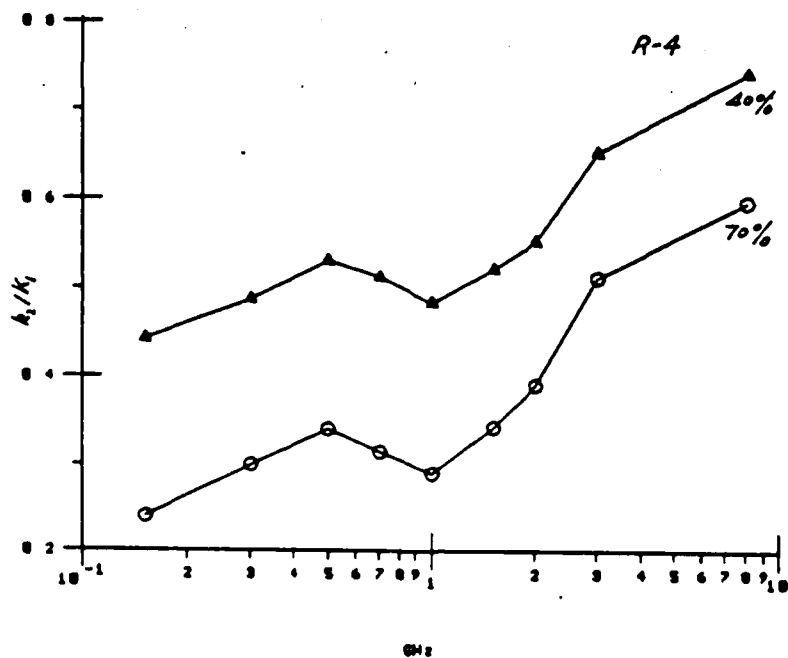


Figure 12 Phase velocity vs. frequency for ferrite composites (contain 40% and 70% R-4 ferrites).

the mirror-conjugates lies in the handedness or the chirality possessed by their molecular configurations. When an electromagnetic disturbance travels through a medium consisting of chiral molecules, it is forced to adapt to the handedness of the molecules. In other words, linearly polarized planewaves cannot be made to propagate through such a medium; whereas left- and right-circularly polarized planewaves, travelling with different phase velocities, are perfectly acceptable solutions of the vector wave equation for this class of media.

Though the phenomenon of chirality is known only at the molecular level, and, therefore, at frequencies in or above the ultraviolet range, it has been suggested [Jaggard *et al.*, 1979; Engheta & Mickelson, 1982] that particles endowed with chirality can exist at even lower frequencies, say, in the GHz range. From recently reported literature, it appears that fluorogold may be exhibiting chirality at a frequency as low as 50 GHz [Birch & Kong, 1986]. This is because chirality, or handedness, is a geometric property: for example, the electromagnetic response of a right-handed helix is different from that of a left-handed one, and the existence of chiral particles made of miniature helices suspended in some host medium has been investigated [Tinoco & Freeman, 1957]. Furthermore, by embedding such chiral particles in a low-loss dielectric medium, that medium, too, will possess handedness. With advances in polymer science, it is conceivable that such artificial media can be manufactured with ease, and their properties tailored by altering the sizes and concentration of the embedded chiral particles.

Because of the fact that the chiral media exhibit circular dichroism [Bohren & Huffman, 1983], the usual constitutive relations  $D = \epsilon E$  and  $B = \mu H$  do not hold due to their incompatibility with the handedness of the medium. Instead, the relations [Eyring *et al.*, 1944; Post, 1962]

$$D = \epsilon E + \alpha \nabla \times E, \quad B = \mu H + \beta \nabla \times H \quad (4-1)$$

hold, the time-reversal symmetry of the fields requiring that  $\alpha = \beta$  [Satten, 1958]. This latter condition due to Satten will be adopted in the ensuing discussion.

Use is now made of the regular Maxwell's equations along with (4-1) along with an  $\exp(-j\omega t)$  time dependence, and following Bohren [1974], the electric and the magnetic fields are transformed to

$$\begin{bmatrix} E \\ H \end{bmatrix} = \begin{bmatrix} 1 & -j(\mu/\epsilon)^{1/2} \\ -j(\epsilon/\mu)^{1/2} & 1 \end{bmatrix} \begin{bmatrix} Q_L \\ Q_R \end{bmatrix} \quad (4-2)$$

where the left- (LCP) and the right- (RCP) circularly polarized fields,  $Q_L$  and  $Q_R$ , respectively, must satisfy the conditions

$$\{\nabla^2 + k_L^2\} Q_L = 0 \quad ; \quad \{\nabla^2 + k_R^2\} Q_R = 0, \quad (4-3a)$$

$$\nabla \times Q_L = k_L Q_L \quad ; \quad \nabla \cdot Q_L = 0, \quad (4-3b)$$

$$\nabla \times Q_R = -k_R Q_R \quad ; \quad \nabla \cdot Q_R = 0. \quad (4-3c)$$

In these equations,

$$k_L = k / \{1 - k\beta\}, \quad (4-4a)$$

$$k_R = k / \{1 + k\beta\}, \quad (4-4b)$$

$$k = \omega \sqrt{\epsilon \mu}. \quad (4-4c)$$

Thus, from (4-2) the electromagnetic field existing in the chiral medium is given by

$$E = Q_L - j(\mu/\epsilon)^{1/2} Q_R \quad ; \quad H = Q_R - j(\epsilon/\mu)^{1/2} Q_L. \quad (4-5)$$

The major consideration now to be faced is to find adequate representations of the functions  $Q_L$  and  $Q_R$  which satisfy the conditions (4-3). In a cartesian (x,y,z) co-ordinate system, if the RCP and the LCP waves are propagating in the x-z plane, then, without loss of generality, these waves can be

set down as [Lakhtakia *et al.*, 1986b]

$$Q_L(r) = (1/k_L) \{ \pm \gamma_L e_x \pm j k_L e_y - \kappa_L e_z \} \exp[j(\kappa_L x \pm \gamma_L z)]; \quad \gamma_L^2 + \kappa_L^2 = k_L^2, \quad (4-6a)$$

$$Q_R(r) = (1/k_R) \{ - \pm \gamma_R e_x \pm j k_R e_y + \kappa_R e_z \} \exp[j(\kappa_R x \pm \gamma_R z)]; \quad \gamma_R^2 + \kappa_R^2 = k_R^2, \quad (4-6b)$$

$e_x$ , etc. being the unit vectors of the co-ordinate system. In a polar  $(\rho, \varphi)$  co-ordinate system, these fields can be conveniently expressed as

$$Q_L(r) = \sum_n f_n [M_n(k_L r) + N_n(k_L r)]; \quad n = 0, \pm 1, \pm 2, \dots \quad (4-7a)$$

$$Q_R(r) = \sum_n g_n [M_n(k_R r) - N_n(k_R r)]; \quad n = 0, \pm 1, \pm 2, \dots \quad (4-7b)$$

where,

$$M_n(kr) = \nabla \times \{ e_z \exp[jn\varphi] Z_n(k\rho) \}; \quad N_n(kr) = (1/k) \nabla \times M_n(kr); \quad (4-7c)$$

$f_n$  and  $g_n$  are the unknown coefficients of expansion; and  $Z_n$  is the cylindrical Bessel function of the first kind if the field has to be regular at the origin, but it is the cylindrical Hankel function of the first kind provided the field satisfies the Sommerfeld radiation conditions at infinity [Morse & Feshbach, 1953]. Finally, in spherical  $(r, \theta, \varphi)$  co-ordinates, vector spherical harmonics [Stratton, 1941] can be used as

$$Q_L(r) = \sum_{v=\sigma mn} f_v [M_v(k_L r) + N_v(k_L r)] \quad (4-8a)$$

$$Q_R(r) = \sum_{v=\sigma mn} g_v [M_v(k_R r) - N_v(k_R r)] \quad (4-8b)$$

with  $v$  being a triple-index -  $\sigma$  is the parity index (even or odd),  $n$  goes from 1 to  $\infty$ , while  $m$  ranges over 0 to  $n$ . The spherical harmonics are given as

$$M_{emn}(kr) = - \{ m z_n(kr)/\sin\theta \} P_n^m(\cos\theta) \sin m\varphi e_\theta - z_n(kr) \{ d/d\theta \} P_n^m(\cos\theta) \cos m\varphi e_\varphi \quad (4-8c)$$

$$M_{omn}(kr) = \{ m z_n(kr)/\sin\theta \} P_n^m(\cos\theta) \cos m\varphi e_\theta - z_n(kr) \{ d/d\theta \} P_n^m(\cos\theta) \sin m\varphi e_\varphi \quad (4-8d)$$

$$N_v(kr) = (1/k) \nabla \times M_v(kr). \quad (4-8e)$$

In the foregoing expressions,  $z_n$  is the spherical Bessel function of the first kind if the field has to be regular at the origin, but it is the spherical Hankel function of the first kind provided the field has to obey the Sommerfeld radiation conditions at infinity;  $P_n^m$  are the associated Legendre polynomial, while  $f_v$  and  $g_v$  are the unknown coefficients of expansion.

The reflection and refraction characteristics of planar achiral-chiral interfaces have been extensively examined [Ramachandran & Ramaseshan, 1961; Lakhtakia *et al.*, 1986b; Silverman, 1986], and it has been observed that by incorporating the chirality parameter  $\beta$  in an otherwise low-loss dielectric medium, the absorption properties of a planar interface can be suitably altered, regardless of the incident polarisation, and over a relatively large range of the angle of incidence [Lakhtakia *et al.*, 1986b]. Boundary value problems involving chiral spheres [Bohren, 1974], spherical shells [Bohren, 1975], and cylinders [Bohren, 1978] have also been recently solved. Lakhtakia *et al.* [1985] have applied the T-matrix method [Waterman, 1969] to solve for the scattering and absorption characteristics of low-loss, dielectric, chiral spheroids.

Though the exact value of the chiral parameter  $\beta$  is not known for "chiral" media in the microwave frequency range and must await experimentation [Lakhtakia *et al.*, 1985; Silverman, 1986], we have observed from numerical calculations that the specific value of  $\beta$  can change the scattering



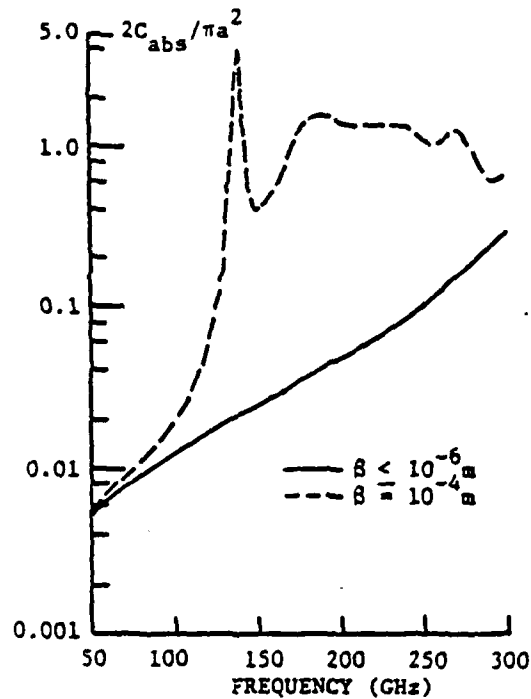


Figure 13 Normalized absorption cross-section,  $2C_{abs}/\pi a^2$ , for a 0.2 mm radius chiral, lossy dielectric sphere exposed to a linearly polarized planewave as a function of frequency. The relative permittivity of the sphere  $\epsilon/\epsilon_0 = 5.0 + j0.1$ , while its relative permeability  $\mu/\mu_0 = 1.0$ .

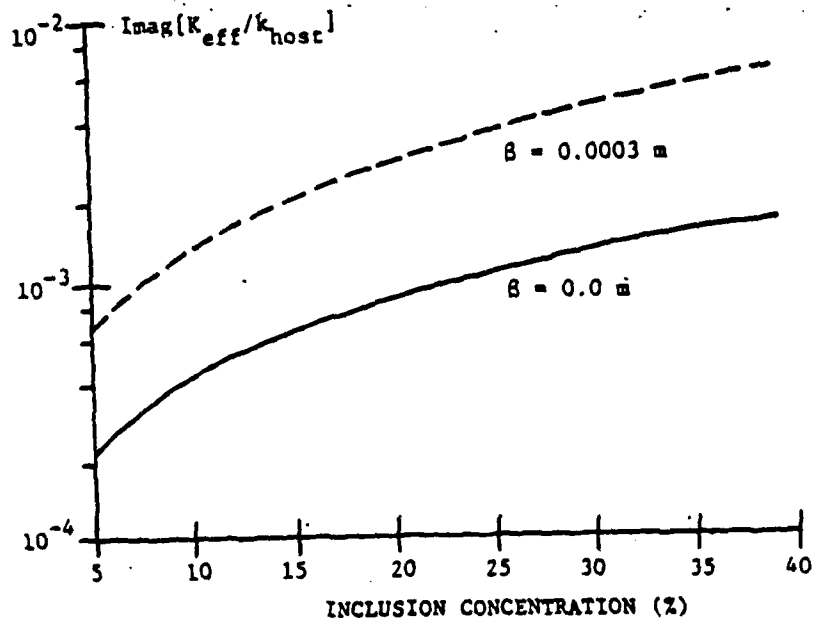


Figure 14 Computed value of the coherent attenuation  $\text{Im}\{K_{eff}/k_{host}\}$  for a composite in which the host is epoxy ( $\epsilon/\epsilon_0 = 4.0$ ), and the chiral inclusions ( $\epsilon/\epsilon_0 = 2.9 + j0.029$ ;  $\beta = 0.0003$  m) are spheres of radius  $a$ . The normalized frequency is  $k_{host}a = 0.026$  for inclusion concentrations varying from 5 - 40%.

characteristics of a dielectric particle drastically. For instance, shown in Fig. 13 is the absorption cross-section  $C_{abs}$  of a chiral sphere  $\{\epsilon/\epsilon_0 = 5.0 + j0.1\}$  of radius  $a = 0.2$  mm, suspended in free space, and irradiated by a linearly polarized planewave for  $\beta \leq 10^{-6}$  m and  $\beta = 10^{-4}$  m over the 50 - 300 GHz frequency range. To be noted is the fact that unless  $|(k_L - k_R)/k| > 0.1$  inside the chiral scatterer,  $\beta$  will not enhance either the absorption or the scattering cross-section significantly; if, however,  $\beta$  is large enough, then the scatterer can appreciably retard the progress of a linearly polarized planewave even though it may not be very lossy itself. Furthermore, if  $\epsilon$  of the scatterer is purely real, no enhancement in the absorption cross-section may be obtained simply by the incorporation of a non-zero  $\beta$ .

A chiral composite would consist of chiral inclusions dispersed in a non-chiral host medium, the small chiral inclusions themselves made up of microminiature helices suspended in some other, or the same, host medium. As a wave traverses such a composite medium, it will be multiply scattered by the inclusions. Besides actual absorption inside the chiral inclusions, scattering into other directions will also retard the progress of the wave in the forward direction. These considerations have been taken into account in the formulation of a self-consistent multiple scattering theory employed by our group. Shown in Fig. 14 is the computed value of the attenuation  $\text{Im}\{K_{eff}/k_{host}\}$  for a composite in which the host is epoxy  $\{\epsilon/\epsilon_0 = 4.0\}$ , and the chiral inclusions  $\{\epsilon/\epsilon_0 = 2.9 + j0.029; \beta = 0.0003$  m) are spheres of radius  $a$ . These computations were performed at a normalized frequency of  $k_{host}a = 0.026$  for inclusion concentrations varying from 5 - 40%. As can be observed from the graph, the presence of a non-zero  $\beta$  has greatly enhanced the coherent attenuation inside the composite. From the sample computations made, it is clear that while our assays of their utility are still in the preliminary stages, the role of chiral media in electromagnetic applications holds vast promise and merits further exploration. In particular, the typical values of  $\beta$  for chiral materials in the microwave frequency range need to be determined by experimentation.

## REFERENCES

1. Auld, B.A. [1973] *Acoustic Fields and Waves in Solids*, Wiley, New York.
2. Birch, J.P. and F.P. Kong [1986] *Infrared Phys.* 26, 131.
3. Bohren, C.F. [1974] *Chem. Phys. Lett.* 29, 458.
4. Bohren, C.F. [1975] *J. Chem. Phys.* 62, 1566.
5. Bohren, C.F. [1978] *J. Coll. Interface Sci.* 66, 105.
6. Bohren, C.F. and D.R. Huffman [1983] *Absorption and Scattering of Light by Small Particles*, Wiley, New York.
7. Bloembergen, N. [1950] *Phys. Rev.* 78, 572.
8. Cady, W.G. [1946] *Piezoelectricity*, McGraw-Hill, New York.
9. Engheta, N. and A.R. Mickelson [1982] *IEEE Trans. Antennas. Propagat.* 30, 1213.
10. Eyring, H., J. Walter and G.E. Kimball [1944] *Quantum Chemistry*, Wiley, New York.
11. Fröhlich, H. [1949] *Theory of Dielectrics, Dielectric Constants and Dielectric Loss*, Oxford University Press.
12. Goodman, M. [1985] *Biopolymers* 24, 137.

13. Jaggard, D.L., A.R. Mickelson and C.H. Papas [1979] *Appl. Phys.* 18, 211.
14. Kyame, J.J. [1949] *J. Acoust. Soc. Am.* 21, 159.
15. Kyame, J.J. [1954] *J. Acoust. Soc. Am.* 26, 990.
16. Lakhtakia, A., V.K. Varadan and V.V. Varadan [1985] *Appl. Opt.* 24, 4146.
17. Lakhtakia, A., V.K. Varadan and V.V. Varadan [1986a] *J. Wave-Mat. Interact.* 1, 97.
18. Lakhtakia, A., V.V. Varadan and V.K. Varadan [1986b] *IEEE Trans. Electromag. Compat.* 28, 90.
19. Miles, P.A., W.B. Westphal and A. Von Hippel [1957] *Rev. Modern Phys.* 29, 302.
20. Moon, F.C. [1970] *J. Acoust. Soc. Am.* 48, 254.
21. Morse, P.M. and H. Feshbach [1953] *Methods of Theoretical Physics, Vol. II*, McGraw-Hill, New York.
22. Polder, D. and J. Smit [1953] *Rev. Modern Phys.* 25, 89.
23. Post, E.J. [1962] *Formal Structure of Electromagnetics*, North-Holland, Amsterdam.
24. Rado, G.T., R. Wright and W. Emmerson [1950] *Phys. Rev.* 80, 273.
25. Ramachandran, G.N. and S. Ramaseshan [1961] *Encyclopedia of Physics, Vol. XXVII*, Springer, Berlin.
26. Satten, R.A. [1958] *J. Chem. Phys.* 28, 742.
27. Silverman, M.P. [1986] *J. Opt. Soc. Am. A* 3, 830.
28. Stratton, J.A. [1941] *Electromagnetic Theory*, McGraw-Hill, New York.
29. Tinoco, Jr., I. and M.P. Freeman [1957] *J. Phys. Chem.* 61, 1196.
30. Varadan, V.K. and V.V. Varadan, ed. [1980] *Acoustic, Electromagnetic and Elastic Wave Scattering - Focus on the T-matrix Approach*, Pergamon Press, New York.
31. Varadan, V.K., Y. Ma, and V.V. Varadan [1984] *Radio Sci.* 19, 1445.
32. Varadan, V.K., V.V. Varadan and Y. Ma [1985a] *Technical Report PSU/LEAR-85-3*, Pennsylvania State University.
33. Varadan, V.K., Y. Ma and V.V. Varadan [1985b] *J. Acoust. Soc. Am.* 77, 375.
34. Varadan, V.V. and V.K. Varadan [1985c], see paper in this Proceedings.
35. Varadan, V.K., V.V. Varadan, Y. Ma and W.F. Hall [1986] *IEEE Trans. Microwave Theory Tech. MIT-34*, 251.

36. Waterman, P.C. [1969] *Alta Frequenza* 38, 348.
37. Westphal, W.B. and A. Sils [1972] *Technical Report AFML-TR-72-39*, Massachusetts Institute of Technology.

## SCATTERING OF ACOUSTIC BEAM WAVES BY ROUGH SURFACES

Y. MA, V.K. VARADAN, and V.V. VARADAN  
Laboratory for Electromagnetic and Acoustic Research,  
Department of Engineering Science and Mechanics,  
&  
Research Center for the Engineering of Electronic and Acoustic Materials,  
The Pennsylvania State University,  
University Park, PA 16802.

### ABSTRACT

We model the rough surface as scatterers of different sizes randomly distributed on an acoustically transparent plane. This problem has its application in studying the reflectivity of marine mineral deposits. In fact, the roughness of the plane can be characterized by various size distributions of scatterers. The T-matrix, which is essentially a scattering transfer function, enables us to acquire the acoustic signature of any arbitrary shaped single scatterer and is used to obtain the frequency spectrum of the reflectivity of an ensemble of those scatterers. In this paper, the backscattered response of a random distribution of scatterers on a plane subjected to a normally incident, narrow beamform acoustic wave is investigated and the beam effect on the average backscattered field is found to be small and can be neglected for further analysis of multiple scattering problems of rough surfaces.

### 1. INTRODUCTION

Most investigators use plane wave excitation to analyze the scattering problem from a plane of scatterers [Twersky, 1957; Biot, 1968; Hong, 1980; Ma et al., 1986]. The results yield a scattered wave which is analogous to the reflection of a plane wave on a rough surface characterized by an equivalent reflection coefficient [Twersky, 1957]. In marine geophysics it is customary to use the ray theory [Clay et al., 1977] together with the plane wave reflection coefficient to study the reflections at sea floor, i.e. rough subbottom. Therefore, the present study uses the normally incident plane wave as this closely represents the equipment (see Fig. 1) used in the remote sensing. The narrow beam spherical wave (as an acoustic source) analysis is done here to indicate the accuracy of its usage and justify the plane wave analysis for the scattering problem. The normal incidence of a narrow beam is also used so that one can obtain a physical interpretation of the analysis without going into too much complexity in mathematics. Typical echo sounders use beam widths of at least 60 degree for the acoustic beam so as to accommodate the roll and pitch of the survey ship. However, in the deep sea sounding environment high intensity is required to overcome transmission losses occurring in the water column. In order to do this the narrow beam width is beneficial because it concentrates the acoustic energy into a smaller area on the bottom. Therefore in the market much smaller beams are becoming common, with 6 degree being representative [Myers et al., 1969].

### 2. GAUSSIAN BEAMFORM ACOUSTIC WAVE

The acoustic source which is located a distance  $H$  above the bottom plane (see Fig. 2), radiates a spherically spreading pressure wave with a Gaussian beamform

$$\psi_j(\mathbf{R}) = \psi_a R_0 \exp[-(ik + \mu)|\mathbf{R} - \mathbf{z}|] \exp(-\alpha \delta^2 / |\mathbf{R} - \mathbf{z}|). \quad (1)$$

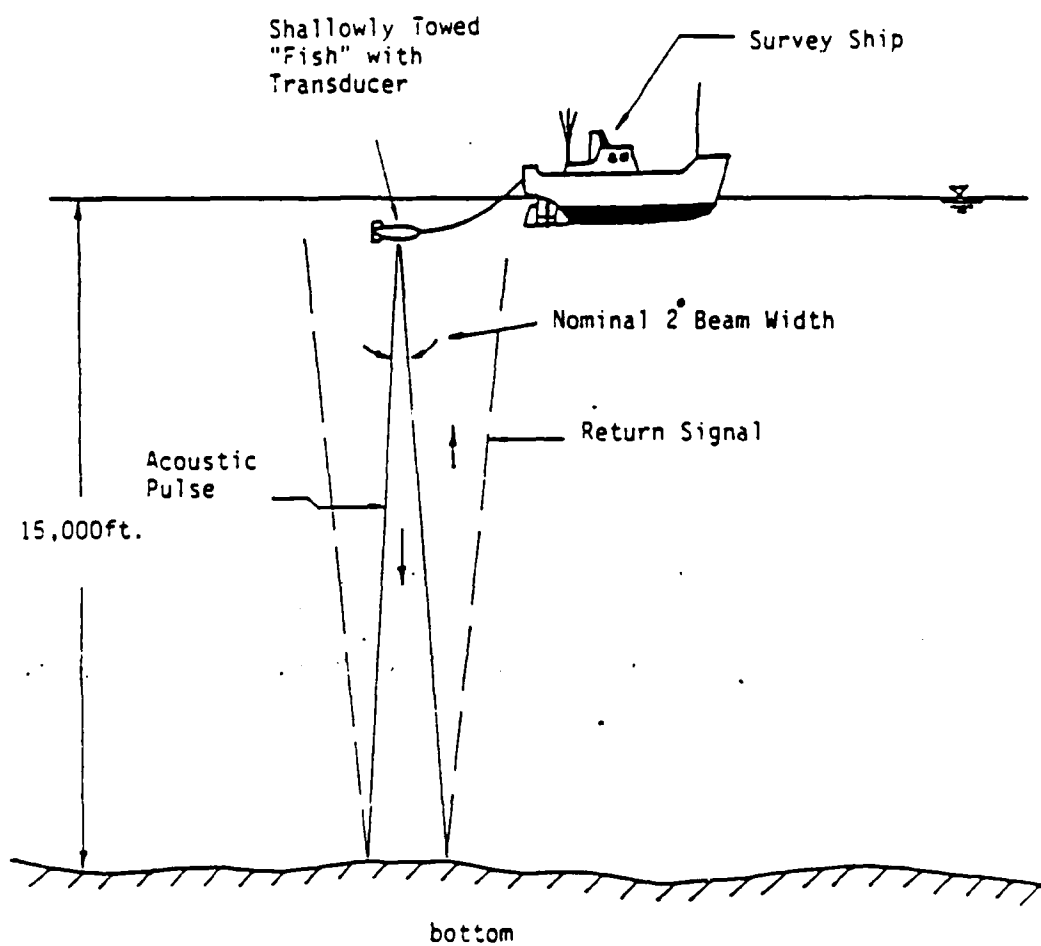


Figure 1 Proposed Prospecting System (Acoustic Sounding).

in which  $\psi$  is the acoustical potential,  $z = (0,0,H)$ ,  $\mu$  the absorption coefficient in the fluid medium (ocean),  $R_0$  the reference distance (usually one meter),  $\delta$  the beam width (in radian),  $1/|R - z|$  the spreading factor and  $\alpha$  the Gaussian beamform coefficient defined as

$$\alpha = \ln 4 / \delta_{HP}^2 \quad (2)$$

where  $\delta_{HP}$ , the half power beam width, is shown in Fig. 3.

On the bottom plane, i.e.  $z = 0$ , at a distance  $r_j$  from the beam axis the incident wave field becomes

$$\psi_i(r_j) = \psi_a R_0 \exp[-(ik + \mu)D] \exp(-\alpha \delta_j^2 / D), \quad (3)$$

where  $D$  is the distance between the transducer and  $r_j$ . The incident field at the image point, i.e.  $z = -H$  or  $D = 2H$ , is

$$\psi_i(z = -H) = \psi_a R_0 \exp[-(ik + \mu)2H] / 2H. \quad (4)$$

### 3. SCATTERED WAVE FIELD

A single scatterer located at  $r_j$  on the bottom plane ( $z = 0$ ) will radiate a spherically spreading wave due to the excitation by the incident wave. Here we consider a planar distribution of scatterers suspended in a fluid medium and this approximation based on the fact that the water-saturated subbottom in which the scatterers are actually distributed has an acoustic impedance that closely matches the acoustic impedance in water. The strength of the radiated wave depends on both the external wave field and the scatterer's characteristics which can be described by the T-matrix [Varadan and Varadan, 1980]. The backscattered field ( $\theta_j = 0$ ) at  $z = H$  of the single scatterer at  $r_j$  can thus be defined as

$$u_j(b.s.) = T \exp[-(ik + \mu)D] \psi_i(r_j) / D = T \psi_a R_0 \exp[-(ik + \mu)2D] \exp(-\alpha \delta_j^2 / D^2). \quad (5)$$

In which the subscript b.s. denotes the backscattering and  $T$  is the average T-matrix defined as

$$T(R-r_j) = \int T(a_j, R-r_j) q(a_j) da_j$$

and  $q(a)$  is the size distribution function. One sees from Eq. (5) that the spreading factor is now  $1/D^2$  for the scattered field  $u_j(b.s.)$ .

If there is a sparse distribution of scatterers on the surface, the total backscattered field is simply the sum of the fields scattered from each scatterer. In other words, the external field of each scatterer is due to the incident wave alone and is the first order approximation of the multiple scattering processes. The average total backscattered field can be found as

$$\langle U_{b.s.} \rangle = \rho T R_0 \psi_a \int_0 \exp[-(ik + \mu)2D] \exp(-\alpha \delta_j^2 / D^2) 2\pi r_j dr_j, \quad (6)$$

where the axial symmetry and the polar integration for a large area

$$\int_A dr_j = \int_0^{2\pi} \int_0 r_j dr_j d\theta = 2\pi \int_0 r_j dr_j$$

have been employed and  $\rho$  is the number of scatterers per unit area. From the symmetry (Fig. 2) one sees

$$\tan \delta_j = r_j / H$$

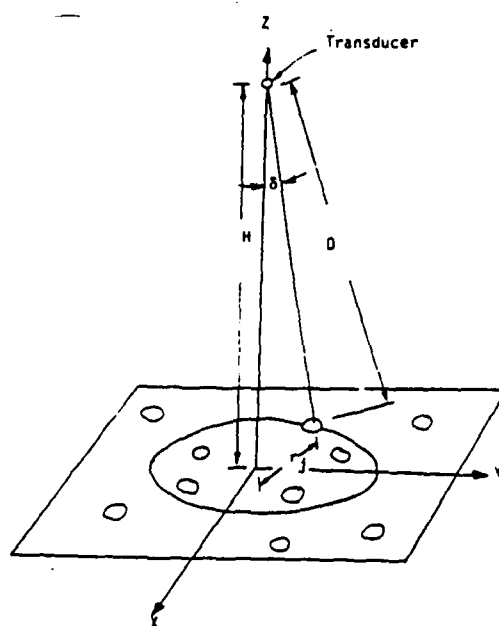
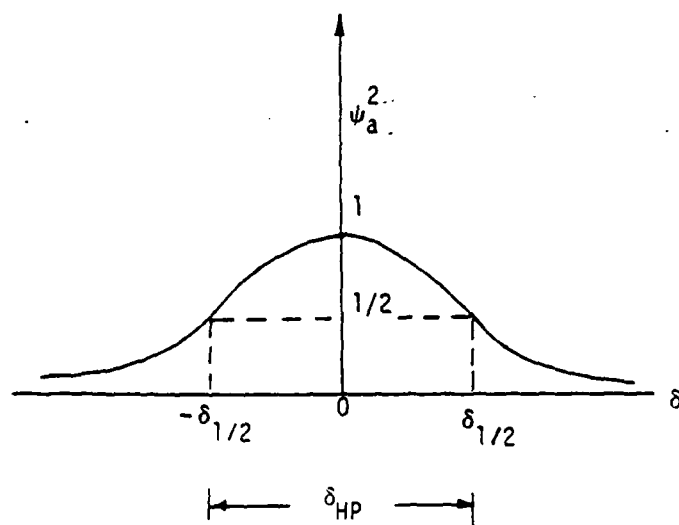


Figure 2 Geometry of the Narrow Beam Analysis.



$\delta_{HP}$  = Half Power Beam Width =  $2\delta_{1/2}$

Figure 3 Gaussian Beam Form.



$$D^2 = H^2 + r_j^2.$$

Using the above relationships and changing the integration variable by (instead of  $r_j$  integration,  $\delta_j$  integration is used)

$$r_j dr_j = H^2 [r_j / H] d(r_j / H) = H^2 \tan \delta_j \sec^2 \delta_j d\delta_j$$

in Eq. (6), the average of the total backscattered field becomes

$$\langle U_{b.s.} \rangle = 2\pi \rho T \psi_a R_0 \int_0^{2\pi} \exp[-2(ik + \mu)H \sec \delta_j \exp(-\alpha \delta_j^2) \tan \delta_j] d\delta_j. \quad (7)$$

The integral in the above equation can be done using the principle of stationary phase [Lamb, 1932]. The magnitude of  $kH$  is always much larger than that of  $\alpha \delta_j^2$  (see Table 1 for comparison). For  $kH \gg 1$ , which is a phase control factor, the integral can be converted to the following form

$$\int_0^{2\pi} \exp[-ikHg(\delta_j)] \tan \delta_j d\delta_j, \quad (8)$$

in which  $g(\delta_j) = (2 + 2\mu/ik) \sec \delta_j + \alpha \delta_j^2 / ikH$ .

The phase angle  $\gamma$  is obtained by solving the  $\delta_j$  which makes

$$g'(\delta_j) = (2 + 2\mu/ik) \sec \delta_j \tan \delta_j + \alpha \delta_j^2 / ikH = 0$$

and is found to be zero, i.e.  $\gamma = 0$ , in this case (in the interval of 0 and  $2\pi$ ). The second derivative of  $g(\delta_j)$  evaluated at the phase angle  $\gamma = 0$  is

$$g''(0) = 2 + 2\mu/ik + 2\alpha/ikH$$

Using the stationary phase principle, Eq.(8) can be written in the following manner

$$g(\gamma) \int_0 \exp[-ikHg''(\gamma) \zeta^2 / 2] \zeta d\zeta \quad (9)$$

in which  $\zeta$  is the parameter in the Taylor expansion around the phase angle  $\gamma$ , i.e.

$$g(\delta_j) = g(\gamma + \zeta) = g(\gamma) + g'(\gamma)\zeta + g''(\gamma)\zeta^2/2! + \dots$$

$$\tan \delta_j = \tan(\gamma + \zeta) = \tan \gamma + \sec^2 \gamma \zeta + \dots$$

Substituting  $\gamma = 0$  and the expression for  $g(\gamma)$  and  $g''(\gamma)$  into Eq. (9) one obtains

$$\exp[-ik(1 + \mu/ik)2H] \int_0 \exp[-ikH(1 + \mu/ik + \alpha/ikH)\zeta^2] \zeta d\zeta. \quad (10)$$

Finally after substituting Eq. (10) into (9) and carrying out the integral in (10) the average of the total backscattered field becomes

$$\langle U_{b.s.} \rangle = (2\pi \rho T / ik)(1 + \alpha/ikH + \mu/ik)^{-1} (R_0 \exp[-(ik + \mu)2H] \psi_a / 2H). \quad (11)$$

One sees from the above equation that the last term is actually the incident field at the image point, i.e.  $z = -H$ , comparing with Eq. (3). The beam effect which involves in the second term  $\alpha/ikH$  can be evaluated. As can be seen from Table 2 at large depth, unless a very narrow beam width under the low frequency is used, the beam effect on the average backscattered field is very small and can be neglected for further analysis of multiple scattering problems. The first term is thus recognized as an equivalent plane wave reflection coefficient which relates the average backscattered field to the incident

wave field by just a simple proportionality. This is physically the phenomenon of the plane wave excitation and thus the validity of the plane wave analysis for rough surface scattering problems has been verified through the narrow beam investigation.

Table 1 Comparison between the Magnitudes of  $kH$  and  $\alpha\delta^2$

Frequency	$kH$	$\delta_{HP}$	$\alpha\delta^2$
1 kHz	20943	2 degree	2807
10 kHz	209430	4 degree	701
100 kHz	2094300	6 degree	312

$H = 5000$  m, acoustic wave velocity = 1500 m/sec,  $\delta = 90$  degree

Table 2 Beam Width Correction Factor ( $\alpha/kH$ )

Frequency	Half Power Beam Width $\delta_{HP}$		
	1 degree	5 degree	10 degree
1 kHz	0.22	0.0087	0.0022
10 kHz	0.022	0.00087	0.00022
100 kHz	0.0022	0.000087	0.000022

$H = 5000$  m, acoustic wave velocity = 1500 m/sec,  $\delta = 90$  degree

## REFERENCES

1. Biot, M.A. [1968] *J. Acoust. Soc. Am.* 44, 1616.
2. Clay, C.S. and H. Medwin [1977] *Acoustical Oceanography*, John Wiley and Sons, New York.
3. Hong, K.M [1980] *J. Optical Soc. Am.* 70, 821.
4. Lamb, H. [1932] *Hydrodynamics*, Dover Pub. Co., New York.
5. Mathur, N.L. and K.C. Yeh [1964] *J. Math. Phys.* 5, 1619.
6. Myers, J.J., C.H. Holm and R.F. McAllister [1969] *Handbook of Ocean and Underwater Engineering*, McGraw-Hill Book Co, New York.
7. Ma, Y., A.H. Magnuson, V.K. Varadan and V.V. Varadan [1986] *Geophysics* 51, No 3, 689.
8. Twersky, V. [1957] *J. Acoust. Soc. Am.* 29, 209.
9. Varadan, V.K. and V.V. Varadan, ed. [1980] *Acoustic, Electromagnetic and Elastic Wave Scattering - Focus on the T-matrix Approach*, Pergamon Press, New York.

## MULTIPLE SCATTERING THEORY FOR ACOUSTIC, ELECTROMAGNETIC AND ELASTIC WAVES IN DISCRETE RANDOM MEDIA

V. V. VARADAN, V. K. VARADAN AND Y. MA  
Department of Engineering Science and Mechanics and  
Center for the Engineering of Electronic and Acoustic Materials  
The Pennsylvania State University Park  
University Park, PA 16802

### ABSTRACT

A multiple scattering theory is presented using a T-matrix to characterize the response of a single inclusion to an arbitrary incident field. The multiple scattering series can be represented in diagrammatic form. A partial resummation of the series is equivalent to the Quasi-Crystalline Approximation (QCA). This results in a new Green's function or propagator for the effective medium whose singularities or poles are given by the zeroes of the dispersion equation satisfied by the coherent field. The QCA requires a knowledge of the two particle pair correlation function and this is included explicitly so that volume fractions of scatterers greater than 5% can be considered. Since all fields are generally expanded in vector spherical functions, keeping functions of the appropriate polarization one can directly use this formalism for acoustic, electromagnetic and elastic waves by using the T-matrix that is appropriate for the particular boundary value problem for the single scatterer. Excellent agreement with experimental results has been obtained for all three fields. Recent work using non-spherical statistics resulting from Monte Carlo simulation for a distribution of spheroids has also been implemented in evaluating the effective wavenumber for media containing dense distributions of spheroids which was not possible before.

### 1. INTRODUCTION

The average or effective properties of a random medium containing inclusions of one material or voids distributed in some fashion in a second material called the host or matrix material can be conveniently studied by analyzing the propagation of plane waves in such materials and solving the resulting dispersion equations. Since waves propagating in such a two phase system will undergo multiple interactions with the scatterer phase, it becomes natural to consider multiple scattering theory and ensemble averaging techniques if the distribution of the inclusion phase is random. In this paper, a multiple scattering theory is presented that utilizes a T-matrix to describe the response of each scatterer to an incident field. The T-matrix is simply a representation of the Green's function for a single scatterer in a basis of spherical or cylindrical functions. In this definition, it simply relates the expansion coefficients of the field that is incident on or excites a scatterer to the expansion coefficients of the field scattered when both fields are expanded in the same spherical wave basis [1]. In theory, the T-matrix is infinite, but in practice the T-matrix is truncated at some size that depends on the ratio of size of scatterer to the wavelength and the complexity of the geometry. Formally the T-matrix includes a multipole description of the field scattered by the inclusion and this requires a propagator for multipole fields to describe the propagation from one scatterer to the next. Finally, the technique presented here is for a random distribution of scatterers which requires an ensemble average over the position of the scatterers and requires a knowledge of the positional correlation functions.

The formalism presented is generally applicable to acoustic, electromagnetic, and elastic waves.

The notation  $\phi_n = \phi_{\tau lm \sigma}$  is used to represent the vector spherical functions. The polarization index  $\tau = 1, 2, 3$  denotes the irrotational component and the two solenoidal components respectively. The other indices describe the multipole nature of the fields, with  $l = 0, 1, 2, \dots$ ;  $m = 0, 1, 2, \dots, l$ ; and  $\sigma$  denotes the even or odd azimuthal parity in spherical coordinates. The acoustic field being completely irrotational will be described by  $\tau = 1$  only, the electromagnetic field by  $\tau = 2, 3$  and the elastodynamic field by  $\tau = 1, 2, 3$ . The procedure for computing the T-matrix for each field has been described in several publications, in particular we refer the interested reader to Varadan and Varadan [2]. In the multiple scattering formalism that is presented below, if proper identification of the polarization index is made and the appropriate T-matrix substituted, all three types of wave propagation problems can be studied.

Good agreement has been obtained with available experimental results for all three types of waves for a wide range of wavelengths, scatterer concentration and properties [3,4,5]. The theory presented here most closely resembles the work of Twersky [6,7] and Tsang and Kong [8]. The infinite hierarchy of equations that results in a multiple scattering formalism when the exciting field is averaged has usually been truncated by using the Quasi-Crystalline Approximation first proposed by Lax [9]. In this approximation, which is shown to be completely equivalent to a partial resummation of the multiple scattering series, only a knowledge of the two body correlation function is required. In previous studies [10,11], we relied on spherical statistics for hard spheres, generated by Monte Carlo simulation or by the Percus-Yevick approximation even for non-spherical scatterers. Essentially, this increased the exclusion volume surrounding the non-spherical scatterer, and artificially restricted us to smaller concentrations in order to prevent the statistical spheres from overlapping. In the present study, these restrictions are removed by using a new Monte Carlo simulation developed by Steele [12] for non-spherical scatterers, that is based on expanding the two body correlation functions in Legendre polynomials. This permits us to consider the angular correlations that exist for non-spherical oriented scatterers. The final equation for the formalism is the dispersion equation which describes the propagation characteristics of the coherent or average field in the effective medium. The numerical solution of this equation yields the effective complex, frequency dependent propagation number which is also a function of the size, geometry and distribution of the inclusion phase. The effective wavenumber is a function of the direction of propagation in the effective medium if the medium is effectively anisotropic. If, for example the scatterers are spheres or if the non-spherical scatterers are randomly oriented, the effective medium will be isotropic, but if the medium contains aligned non-spherical scatterers the effective medium will be anisotropic. The effective wavenumber can be related to the effective material properties of the medium which are also complex and frequency dependent. For anisotropic materials, by solving the dispersion equation for different directions of propagation with respect to the aligned non-spherical scatterers, we can construct all components of the material property tensors of the effective medium such as the elastic stiffness tensor or the dielectric tensor, see [13].

Numerical results for aligned and randomly oriented oblate and prolate spheroids using the new correlation functions have been obtained and compared with previous calculations for spheroids that used spherical statistics. We foresee important applications of these new results to electromagnetic wave propagation through aerosols, which are non-spherical and often consist of aggregates and also in other cases where non-spherical scatterers are involved.

## 2. EFFECTIVE WAVENUMBER FOR THE AVERAGE FIELD IN A DISCRETE RANDOM MEDIUM

Let the random medium contain  $N$  scatterers in a volume  $V$  such that  $N \rightarrow \infty$ ,  $V \rightarrow \infty$ , but  $n_0 = N/V$  the number density of scatterers is finite. Let  $u$ ,  $u^0$ ,  $u_i^e$ ,  $u_i^s$  be respectively the total field, the incident or primary plane, harmonic wave of frequency  $\omega$ , the field incident or exciting the  $i$ -th scatterer and the field which is in turn scattered by the  $i$ -th scatterer. These fields are defined at a point  $r$  which is not occupied by any one of the scatterers. In general, these fields or potentials which can be used to describe them satisfy the scalar or vector wave equation. Let  $\text{Re } \phi_n$  and  $\text{Ou } \phi_n$  denote the

basis of orthogonal functions which are eigenfunctions of the Helmholtz equation, see Morse and Feshbach [14]. As explained in the introduction the subscript 'n' is an abbreviated superindex and vector notation is implied. The qualifiers Re and Ou denote functions which are regular at the origin (Bessel functions) and outgoing at infinity (Hankel functions) which are respectively appropriate for expanding the field which is incident on a scatterer and that which it scatters. Thus, we can write the following set of self-consistent equations:

$$u = u^0 + \sum_{i=1}^N u_i^s = u_i^e + u_i^s = u^0 + \sum_{j=1}^N u_j^s + u_i^s, \quad (1)$$

$$u^0(r) = p \exp(ik_0 \cdot r) = \sum_n a_n^i \text{Re } \phi_n(r - r_i), \quad (2)$$

$$u_i^e = \sum_n \alpha_n^i \text{Re } \phi_n(r - r_i); \quad a < |r - r_i| < 2a, \quad (3)$$

$$u_i^s = \sum_n f_n^i \text{Ou } \phi_n(r - r_i), \quad |r - r_i| > a; \quad (4)$$

where  $a_n^i$  and  $f_n^i$  are unknown expansion coefficients. We observe in Eqs.(3) and (4) that "a" is the radius of the sphere or cylinder (for 2-D problems) circumscribing the scatterer and that all expansions are with respect to a coordinate origin located in a particular scatterer.

The T-matrix by definition simply relates the expansion coefficients of  $u_i^e$  and  $u_i^s$  provided  $u_i^e + u_i^s$  is the total field which is consistent with the definitions in Eq. (1). Thus [1],

$$f_n^i = \sum_{n'} T_{nn'}^i a_{n'}^i, \quad (5)$$

and the following addition theorem for the basis functions is invoked,

$$\text{Ou } \phi_n(r - r_j) = \sum_{n'} \sigma_{nn'}(r_i - r_j) \text{Re } \phi_{n'}(r - r_i). \quad (6)$$

Substituting Eqs. (2) - (6) in Eq. (1), and using the orthogonality of the basis functions we obtain

$$\alpha^i = a^i + \sum_{j \neq i} \sigma(r_i - r_j) T^j \alpha^j. \quad (7)$$

This is a set of coupled algebraic equations for the exciting field coefficients which can be iterated and leads to a multiple scattering series.

For randomly distributed scatterers, an ensemble average can be performed on Eq. (7) leading to

$$\langle \alpha^i \rangle_i = a^i + \langle \sigma(r_i - r_j) T^j \alpha^j \rangle_{ij} \quad (8)$$

where  $\langle \rangle_{ijk\dots}$  denotes a conditional average and Eq. (8) is an infinite hierarchy involving higher and higher conditional expectations of the exciting field coefficients. In actual engineering applications, a knowledge of higher order correlation functions is difficult to obtain, usually the hierarchy is truncated so that at most only the two body positional correlation function is required.

To achieve this simplification the Quasi-Crystalline Approximation (QCA), first introduced by Lax [9] is invoked, which is stated as

$$\langle \alpha^j \rangle_{ij} \equiv \langle \alpha^j \rangle_j. \quad (9)$$

Then, Eq. (8) simplifies to

$$\langle \alpha^i \rangle_i = a^i + \langle \sigma(r_i - r_j) T^j \langle \alpha^j \rangle_j \rangle_i ; \quad (10)$$

an integral equation for  $\langle \alpha^i \rangle_i$  which in principle can be solved. We observe that the ensemble average in Eq. (10) only requires  $P(r_j|r_i)$ , the joint probability distribution function. In particular, the homogeneous solution of Eq. (10) leads to a dispersion equation for the effective medium in the quasi-crystalline approximation. Defining the spatial Fourier transform of  $\langle \alpha^i \rangle_i$  as

$$\langle \alpha^i \rangle_i = \int e^{iK \cdot r_i} C^i(K) dK \quad (11)$$

and substituting in Eq. (10), we obtain for the homogeneous solution

$$C^i(K) = \sum_{j \neq i} \int \sigma(r_i - r_j) T^j P(r_j|r_i) e^{iK \cdot (r_i - r_j)} dr_j C^j(K) . \quad (12)$$

If the scatterers are identical

$$C^i(K) = C^j(K) = C(K) \quad (13)$$

and thus for a non-trivial solution to  $\langle \alpha^i \rangle_i$ , we require

$$\left| 1 - \sum_{j \neq i} \int \sigma(r_i - r_j) T^j P(r_j|r_i) e^{iK \cdot (r_i - r_j)} dr_j \right| = 0 . \quad (14)$$

In Eqs. (12) and (14),  $P(r_j|r_i)$  is the joint probability distribution function. For isotropic statistics,

$$P(r_j|r_i) = \begin{cases} 0; & |r_i - r_j| < 2a \\ g(|r_i - r_j|) / V; & |r_i - r_j| > 2a \end{cases} \quad (15)$$

where we have assumed that the scatterers are impenetrable with a minimum separation between the centers being the diameter  $2a$  of the circumscribing sphere in 3-D and circle in 2-D. Equation (14) can hence be simplified to

$$\left| 1 - n_0 \int \sigma(r_1 - r_2) T g(|r_1 - r_2|) e^{iK \cdot (r_1 - r_2)} dr_1 \right| = 0 \quad (16)$$

where  $(1/V) \sum_{j \neq i} = (N-1)/V \approx n_0$ . The integral in Eq. (16) is simply the spatial Fourier transform of  $\sigma T g$ . The zeroes of the determinant as expressed by Eq. (16), yield the allowed values of  $K$  as a function of the microstructure as determined by the  $T$ -matrix, the number density  $n_0$  and the statistics of the distribution as determined by the pair correlation function. In general  $K$ , the effective wavenumber is complex and frequency dependent.

In order to perform the integration in Eq. (16), we need a model for the pair correlation function. For non-spherical scatterers, the pair correlation function depends not only on the length of the vector connecting the centers of the scatterers, but also on the direction of this vector and the orientation of each scatterer. If the scatterers are spherical, then there is no dependence on direction and orientation and the statistics are said to be spherical or isotropic. In both cases, the scatterers are not allowed to overlap, i.e. an infinite repulsive potential is assumed between scatterers. In the statistical mechanics literature, several schemes are available for calculating the pair correlation function of 'hard' particles. For spherical hard particles, analytical results can be obtained for sparse concentrations in the form of

a density expansion or virial series, and for higher concentrations the Percus-Yevick, the self-consistent approximation, and Monte Carlo simulations have all been used for distributions of spheres, see [10,11]. If spherical statistics are used, then the so called 'hole correction integral' on the excluded surface can be done analytically, resulting in a matrix that is diagonal. This simplifies some portions of the calculation considerably. Results, explicitly for non-spherical scatterers are not readily available, and in previous calculations, we artificially surrounded the non-spherical scatterer by a transparent sphere that enclosed it, or considered a sphere of equivalent volume. In the first approximation, the non-overlap of the statistical spheres severely limited the concentrations that we could consider, and the second approximation, although better than the first did not lead to satisfactory results at volume fractions exceeding 10%.

It is interesting to examine what type of multiple scattering terms contribute to the quasi-crystalline approximation. If Eq. (8) is iterated, we obtain

$$\begin{aligned} \langle \alpha^i \rangle_i &= a^i + \langle \sum_{j \neq i} \sigma^{ij} T^j a^j \rangle_i \\ &+ \langle \sum_{j \neq i} \sigma^{ij} T^j \langle \sum_{k \neq j} \sigma^{jk} T^k a^k \rangle_{ij} \rangle_i + \dots \end{aligned} \quad (17)$$

here the abbreviation  $\sigma^{ij} = \sigma(r_i - r_j)$  has been used, and matrix multiplication is implied throughout. We recall that  $\sigma$  and  $T$  are suitably truncated matrices and  $\alpha$  and  $a$  are suitably truncated vectors. Suppose the QCA is invoked for each term in Eq. (17), i.e.

$$\langle \sigma^{jk} T^k a^k \rangle_{ij} = \langle \sigma^{jk} T^k a^k \rangle_j \quad (18)$$

Then we note that only two body correlations are required and the multiple scattering series in Eq. (17) can be easily summed by spatial Fourier transform techniques using the convolution theorem. Symbolically, the multiple scattering series in Eq. (17) may be represented as

$$\langle \alpha^i \rangle_i = a^i_j + \text{---} \overset{\text{---}}{\underset{\text{---}}{\text{---}}} \text{---} + \text{---} \overset{\text{---}}{\underset{\text{---}}{\text{---}}} \overset{\text{---}}{\underset{\text{---}}{\text{---}}} \text{---} + \dots \quad (17')$$

where  $\text{---} \bullet \text{---}$  denotes  $\sigma_{jk}$ ,  $\overset{\text{---}}{\underset{\text{---}}{\text{---}}} \bullet$  denotes  $p(r_j | r_k)$ ,  $\bullet_j$  denotes  $T^j$  and  $\bullet_k \text{---}$  denotes  $a^k$ . Eq. (17) or its alternate form (17') can be summed and written as

$$\langle \alpha^i \rangle_i = \int [1 - n_0 \int \sigma(x) T g(x) e^{-iK \cdot x} dx]^{-1} (\exp iK \cdot r_i) a^i dK \quad (19)$$

In Eq. (19), the matrix inverse is the spatial Fourier transform of the Green's function or propagator for the effective medium in the QCA as given in Eq. (18). The dispersion equation for the medium is given by the zeroes of the spatial Fourier transform of the Green's function. Thus, the dispersion equation resulting from Eq. (19) is identical to the one obtained from Eq. (15).

The dispersion equation as given in Eq. (16) is very well suited for computation. Using appropriate forms of the basis functions  $\phi_n$  which are solutions of the field equations, the T-matrix of the single scatterer can be computed; for example, see Varadan and Varadan [2]. The translation matrix  $\sigma$ , although complicated in form for cylindrical and spherical functions, can nevertheless be computed in a straight forward manner. The spatial Fourier transform of  $\sigma T g$  is fairly easy to compute because the integrand is well behaved for large values of the interparticle distance. In the results presented for different types of wavefields, tabulated Monte Carlo values for impenetrable spheres [15] were substituted for  $g$  at various concentrations. The roots of the resulting determinant were found using Muller's method by giving initial guesses using the analytic expressions for  $K$  which can be obtained from Eq. (15) in the long wavelength limit. The real and imaginary parts of the effective wavenumber can be related respectively to the phase velocity and attenuation in the effective medium. The attenuation is due to geometric dispersion or scattering which may be further enhanced if there are losses associated with the material properties of the scatterer and/or the host.

In recent years, considerable progress has been made in Monte Carlo simulation to describe the statistics for non-spherical hard ( impenetrable ) particles by Steele [12]. He has expanded the joint probability functions in a series of spherical harmonics and radial functions with unknown coefficients. The coefficients are evaluated directly in the Monte Carlo simulation. For aligned prolate and oblate spheroids, these results have just become available. The excluded volume for these geometries is also spheroidal. The hole correction integral can only be done numerically, and the resulting matrix is no longer diagonal. This has been implemented in calculations of the effective wavenumber in media containing random distributions of aligned spheroidal particles [19]. It can be seen that correct statistics conforming to the shape of the particle is needed to get correct results at volume fractions exceeding 5%.

### 3. NUMERICAL RESULTS

In this paper we have given a general formalism to describe multiple scattering of waves in a discrete random medium, which leads to a dispersion equation that is numerically tractable for acoustic, electromagnetic and elastic waves. Here we simply refer the reader to several papers that already contain numerical results for the phase velocity ( real part of the effective wavenumber ) and attenuation ( imaginary part of the effective wavenumber ). The attenuation of the coherent field in the random medium may be due to real losses associated with the lossy properties if any of the scatterers but is also due to geometric dispersion or multiple scattering. Thus a composite material is effectively lossy even if the constituent phases are non-lossy. The numerical results that have been published are for spherical and spheroidal particles that are randomly distributed at volume fractions in the range of 0 - 45% whose sizes are comparable to the wavelength of the propagating wave. The spheroidal scatterers can be aligned [16], or randomly oriented [17]. At the volume fractions considered, multiple scattering and the effects of statistical correlations cannot be ignored and were crucial in the excellent agreement we obtained with experimental results, for acoustic waves see [18], for electromagnetic waves, see [3], and for elastic waves see [5].

#### (a) Acoustic properties of a two phase fluid

The scatterers in this case can be penetrable elastic solid or fluid particles, acoustically hard or acoustically soft spheres. The adiabatic compressibility of the effective medium can be obtained from the definition

$$\frac{K^2(\omega)}{k^2} = \frac{\langle \chi \rangle \langle \rho \rangle}{\chi_0 \rho_0} \quad (20)$$

where  $k$  is the wavenumber in the host medium,  $\langle \rho \rangle = (1 - c) \rho_0 + c \rho_s$ , the average mass density,  $\rho_0$  and  $\rho_s$  being the density of the host and scatterer materials,  $\chi_0$  is the adiabatic compressibility of the host material,  $\langle \chi \rangle$  is the effective compressibility of the composite fluid and  $c$  the volume fraction of scatterers. For the case of a random distribution of bubbles in water, excellent agreement has been obtained with the experimental results of Silberman [18] (see Figure 1). The calculations reproduce the long wavelength bubble resonances that result in an anomalous dispersion of the phase velocity and a peak in the attenuation as a function of frequency.

#### (b) Effective properties of structural composites

In a fiber reinforced composite, for P - (longitudinal), SV - (transversely polarized shear wave) and SH - (shear waves polarized parallel to the fibers) wave propagation, if the fibers are circular and parallelly-oriented, the effective medium is transversely isotropic and will be characterized by five elastic constants. By calculating  $K_p$ ,  $K_{sv}$  and  $K_{sh}$ , three of the five elastic constants can be found as a function of frequency, fiber geometry and concentration. If wave propagation along the fibers is considered, then the remaining constants can also be found. In the long wavelength limit analytical



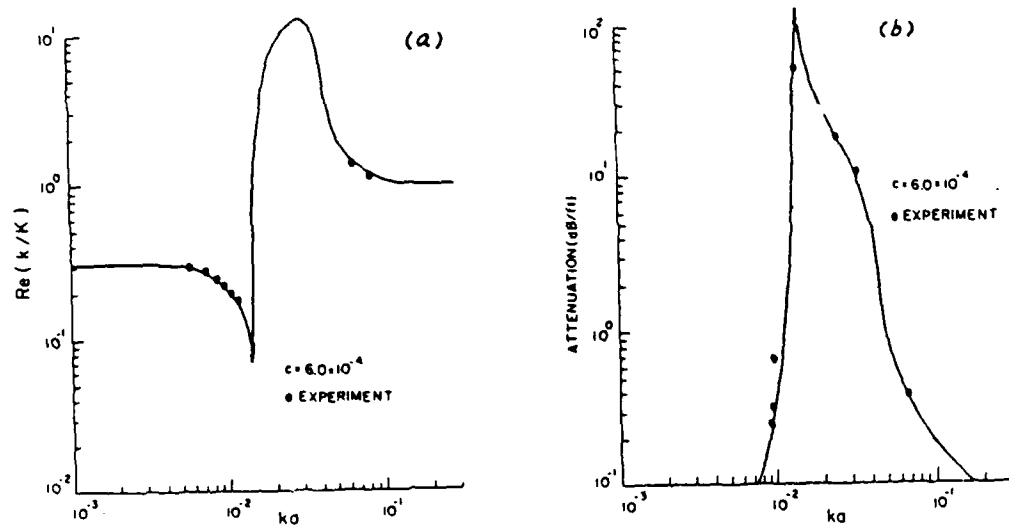


Figure 1 (a) Normalized phase velocity versus nondimensional frequency  $ka$  for bubbles in water (Ref. [19]).  
(b) Coherent attenuation versus nondimensional frequency  $ka$  for bubbles in water (Ref. [19]).

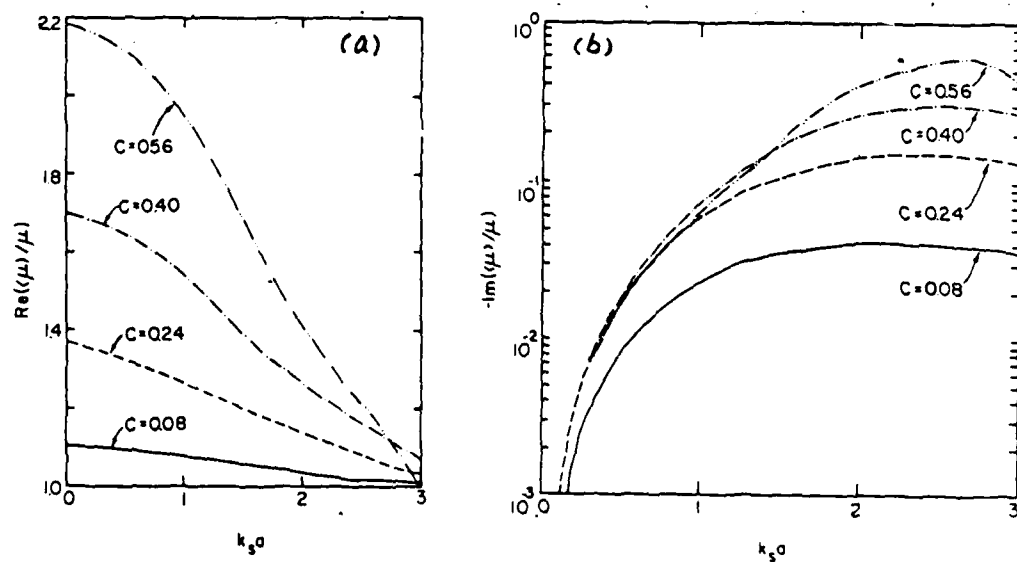


Figure 2 (a) Real part of shear modulus versus nondimensional frequency (Ref. [13]).  
(b) Imaginary part of shear modulus versus nondimensional frequency (Ref. [13]).

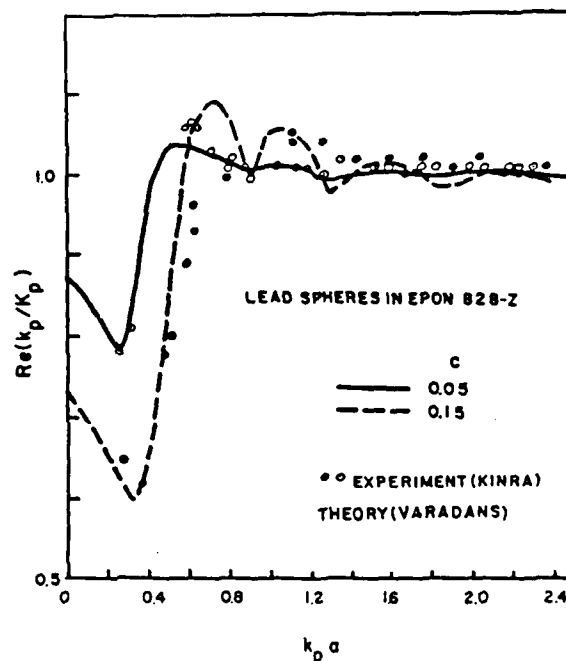


Figure 3 Comparison between theory and experiment - phase velocity versus frequency for lead spheres in Epon 828-Z (Ref. [5]).

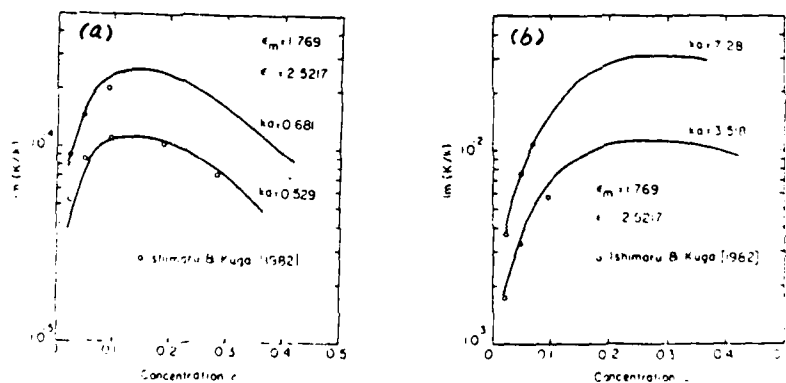


Figure 4 (a) Coherent attenuation versus concentration for latex spheres in water for  $ka < 1$  (Ref. [3]).  
(b) Coherent attenuation versus concentration for latex spheres in water for  $ka > 1$  (Ref. [3]).

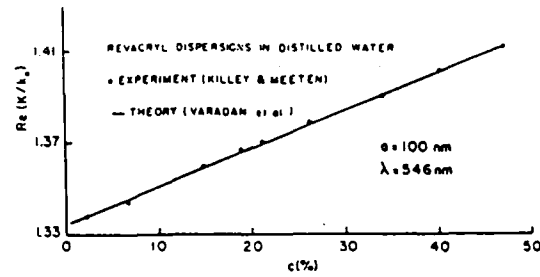


Figure 5 (a) Phase velocity versus concentration  $c$  for Revacryl dispersions in distilled water at wavelength = 546 nm (Ref. [4]).

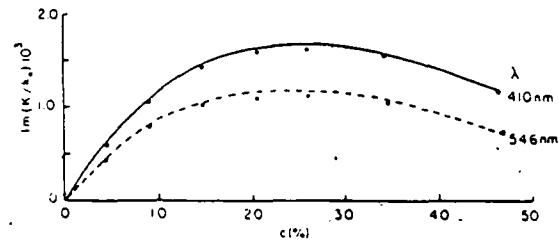


Figure 5 (b) Coherent attenuation versus concentration  $c$  for Revacryl dispersions in distilled water at wavelength = 410 and 546 nm (Ref. [4]).

shown in Figure 2 are calculated effective shear moduli for boron fiber reinforced aluminum composites.

(c) Effective elastic properties of particulate composites

For spherical particles randomly distributed in a host material, the composite material is effectively isotropic and hence characterized by two effective elastic constants which can be obtained by solving the dispersion equations for  $K_p$  and  $K_s$ , see [5,20]. Here again for particulate composites, we have obtained excellent agreement with the experimental results of Kinra who measured the phase velocity as a function of frequency for a distribution of lead spheres in epoxy [5] (see Figure 3).

(d) Effective dielectric properties of dielectric composites

For a random distribution of dielectric or metal spheres distributed in a dielectric host material, the medium is effectively isotropic and characterized by just one dielectric function which can be obtained from the effective wavenumber  $K$  via  $\langle \epsilon \rangle = \epsilon_0 \langle K^2 \rangle / k^2$ , where  $\epsilon_0$  is the dielectric function of the host material, see [16]. For a dense distribution of polystyrene spheres in air again we obtained excellent agreement with the experimental results of Ishimaru [3] (see Figure 4). For optical experiments, our theoretical results compared extremely well with those obtained by Killey and Meeten [4] (see Figure 5).

## ACKNOWLEDGEMENT

The work reported here was supported in part by the U.S. Army Research Office through contract # DAAG29-84-K-0187 and DAAG29-85-K-0234 awarded to the Pennsylvania State University. The authors are grateful to Dr. Walter A. Flood for several helpful discussions and suggestions during the course of this work. They also wish to express their appreciation to Professor W. A. Steele who provided tabulated values of the pair statistics using Monte Carlo simulation.

## REFERENCES

- (1) V.N. Bringi, T.A. Seliga, V. K. Varadan and V. V. Varadan, "Bulk Propagation Characteristics of Discrete Random Media," in Multiple Scattering and Waves in Random Media, P.L. Chow, W.E. Kohler and G.C. Papanicolaou, editors; North-Holland Publishing Co. (1981).
- (2) V.K. Varadan and V.V. Varadan, editors, Acoustic, Electromagnetic and Elastic Wave Scattering - Focus on the T-Matrix Method, Pergamon Press (1980).
- (3) V. K. Varadan, V. N. Bringi, V. V. Varadan, and A. Ishimaru, "Multiple Scattering Theory for Waves in Discrete Random Media and Comparison with experiments," Radio Science **18**, pp. 321-327 (1983).
- (4) V. V. Varadan, Y. Ma and V. K. Varadan, "Propagator Model including Multipole Fields for Discrete Random Media," J. Opt. Soc. Am. **A2**, pp. 2195 - 2201 (1985).
- (5) V.K. Varadan, Y. Ma and V.V. Varadan, "A Multiple Scattering Theory for Elastic Wave Propagation in Discrete Random Media," J. Acoust. Soc. Am. **77**, pp. 375 - 385 (1985).
- (6) V. Twersky, "Coherent Electromagnetic Waves in Pair-Correlated Random Distributions of Aligned Scatterers," J. Math. Phys. **19**, pp. 215- 230 (1978).
- (7) V. Twersky, "Acoustic Bulk Parameters in Distributions of Pair-Correlated Scatterers," J. Acoust. Soc. Am. **64**, pp. 1710 - 1719 (1978).

- (8) L. Tsang and J.A. Kong, "Multiple Scattering of Electromagnetic Waves by Random Distributions of Discrete Scatterers with Coherent Potential and Quantum Mechanical Formalism," *J. Appl. Phys.* **51**, pp. 3465 - 3485 (1980).
- (9) M. Lax, "Multiple Scattering of Waves II. The Effective Field in Dense Systems," *Phys. Rev* **85**, pp. 621 - 629 (1952).
- (10) V. N. Brongi, V. V. Varadan and V. K. Varadan, "Effects of the Pair Correlation Function on Coherent Wave Attenuation in Discrete Random Media," *IEEE Trans.* **AP-30**, pp. 805 - 808 (1982).
- (11) V. N. Brongi, V. K. Varadan and V. V. Varadan, "Average Dielectric Properties of Discrete Random Media Using Multiple Scattering Theory," *IEEE Trans.* **AP-31**, pp. 371 - 375 (1983).
- (12) Y. D. Chen and W. A. Steele, *J. Chem. Phys.* **50**, p. 1428 (1969).
- (13) V.K. Varadan, Y. Ma and V.V. Varadan, "Multiple Scattering of Compressional and Shear Waves by Fiber Reinforced Composite Materials," *J. Acoust. Soc. Am.* **80**, pp. 333 - 339 (1986).
- (14) P. M. Morse and H. Feshbach, *Methods of Theoretical Physics*, Vol. II, p. 1865, McGraw-Hill (1953).
- (15) J. A. Barker and D. Henderson, "Monte Carlo Values for the Radial Distribution Function of a System of Fluid Hard Spheres," *Mol. Phys.* **21**, pp.187-191 (1971).
- (16) V.V. Varadan, Y. Ma and V.K. Varadan, "Anisotropic Dielectric Properties of Media Containing Aligned Non-Spherical Scatterers," *IEEE Trans.* **AP-33**, pp. 886 - 890 (1985).
- (17) V.K. Varadan, Y. Ma and V.V. Varadan, "Coherent Electromagnetic Wave Propagation through Randomly Distributed and Oriented Pair-Correlated Dielectric Scatterers," *Radio Science* **19**, pp. 1445 - 1449 (1984).
- (18) V.K. Varadan, V.V. Varadan and Y. Ma, "A Propagator Model for Multiple Scattering of Waves by Bubbles in Water," *J. Acoust. Soc. Am.* **78**, pp. 1879 - 1881 (1985).
- (19) V.V. Varadan, V.K. Varadan, Y. Ma and W.A. Steele, "Effects of Non-Spherical Statistics on EM Wave Propagation in Discrete Random Media," *Radio Science*, submitted (1987).
- (20) V.K. Varadan, V.V. Varadan and Y. Ma, "Frequency Dependent Elastic Properties of Rubber like Materials Containing a Random Distribution of Voids," *J. Acoust. Soc. Am.* **76**, pp. 296 - 300 (1984).

## Anisotropic Dielectric Properties of Media Containing Aligned Nonspherical Scatterers

VASUNDARA V. VARADAN, MEMBER, IEEE, Y. MA, AND  
VUAY K. VARADAN, MEMBER, IEEE

**Abstract**—Electromagnetic wave propagation in a medium containing a random distribution of aligned, pair-correlated nonspherical scatterers is studied using the  $T$ -matrix to characterize the single scatterer response, the quasicrystalline approximation (QCA) and the correlation function. The resulting dispersion equation for the average medium is numerically solved as a function of frequency and the direction of propagation. Numerical results are presented for the attenuation of electromagnetic waves versus frequency, concentration, and direction of propagation.

### INTRODUCTION

It is well-known that in a medium with microstructure in the form of discrete-random inhomogeneities, electromagnetic waves undergo attenuation as well as dispersion. If the inhomogeneities are either spherically symmetric or randomly oriented, the medium is macroscopically or on the average isotropic. The attenuation and phase velocity are independent of the direction of propagation. However, the medium can be effectively anisotropic if the scatterers are nonspherical and aligned. In this case the propagation characteristics of the medium are a function of the angle with respect to the axis of alignment (taken as the  $z$ -axis).

Such problems have been studied in detail by Twersky [1], [2] for both acoustic and electromagnetic waves. He has presented analytical results for elliptical cylinders and ellipsoids in the long wavelength approximation including the effects of the pair correlation function. The formulation that we present is quite similar but is, however, more suited [3] for numerical computations at higher frequencies requiring smaller matrices to yield convergent results. The dispersion equation that we solve numerically is compared to that obtained by Twersky. Both treatments rely on the quasicrystalline approximation (QCA) to break the hierarchy of equations for the ensemble average of the field exciting a particular scatterer. As a result only a knowledge of the two particle correlation function is required. In a recent report [4] we have shown what type of multiple scattering processes are included in the QCA and which ones are neglected. The response of a single scatterer to the field exciting it is characterized by a  $T$ -matrix. The  $T$ -matrix is numerically generated on a basis of vector spherical functions using Waterman's extended boundary condition method [5], [6]. Earlier work using this general scheme was restricted to randomly oriented nonspherical scatterers or for wave propagation restricted to the alignment axis [8]–[11]. Numerical results are presented for aligned spheroidal scatterers as a function of frequency, volume fraction of scatterers and the direction of propagation.

Very recently Tsang [12] has also reported some results for non-spherical, randomly oriented particles.

### Wave Propagation in Media with Aligned Nonspherical Scatterers

Consider an isotropic medium characterized by a refractive index  $\sqrt{\epsilon}$  in which aligned rotationally symmetric scatterers are randomly distributed. The rotational axis of symmetry is taken to be the  $z$ -axis. Plane harmonic waves of frequency  $\omega$ , propagate in the direction  $\hat{k}_o(\alpha, \beta)$ . If  $\vec{U}^o$ ,  $\vec{U}_i^e$ , and  $\vec{U}_i^s$  specify the incident field, the field exciting the  $i$ th scatterer and the field scattered by the  $i$ th scatterer respectively, then self-consistency requires that

$$\vec{U}_i^s = \vec{U}^o + \sum_{j \neq i} \vec{U}_j^s. \quad (1)$$

The exciting and scattered fields are expanded on a basis of vector spherical functions, as follows [6]:

$$\vec{U}_i^e(\vec{r}) = \sum_{\tau=1}^2 \sum_{lm\sigma} \alpha_{\tau lm\sigma}^i \text{Re } \vec{\psi}_{\tau lm\sigma}(\vec{r} - \vec{r}_i), \quad |\vec{r} - \vec{r}_i| \leq 2a \quad (2)$$

$$\vec{U}_i^s(\vec{r}) = \sum_{\tau=1}^2 \sum_{lm\sigma} f_{\tau lm\sigma}^i \text{Ou} \vec{\psi}_{\tau lm\sigma}(\vec{r} - \vec{r}_i), \quad |\vec{r} - \vec{r}_i| \geq 2a \quad (3)$$

where  $r_i$  denotes the center of the  $i$ th scatterer and  $a$  is the radius of the circumscribing sphere.

Using the extended boundary condition method [5] we can derive a  $T$ -matrix to relate the unknown coefficients  $\alpha$  and  $f$  as follows:

$$f_{\tau lm\sigma}^i = \sum_{\tau' l' m' \sigma'} T_{\tau lm\sigma, \tau' l' m' \sigma'}^i \alpha_{\tau' l' m' \sigma'}^i \quad (4)$$

where  $T^i$ , the  $T$ -matrix of the  $i$ th scatterer, depends only on the frequency  $\omega$  and the geometry and nature of the scatterer.

Substituting (2), (3), and (4) in (1) and using the translation addition theorem for the vector spherical functions, we obtain

$$\alpha_n^i = 4\pi i^l \vec{A}_n(\hat{k}_o) e^{ik\hat{k}_o \cdot \vec{r}_i} + \sum_{j \neq i} \sum_{n'} \sum_{n''} \alpha_{n'n}(\vec{r}_i - \vec{r}_j) T_{n'n''}^j \alpha_{n''}^j \quad (5)$$

where the abbreviated index  $n$  represents the set  $\{\tau, l, m, \sigma\}$ ,  $\vec{A}_n$  are vector spherical harmonics,  $\vec{A}_1 = r \nabla Y_{lm\sigma}$ ,  $\vec{A}_2 = r \times \vec{A}_1$ , and  $\alpha_{n'n}$  is the translation matrix [9].

A configurational average is performed in (5) over the random positions of the scatterers and the QCA is invoked in the usual manner [9]. For identical scatterers, we obtain

$$\langle \alpha_n^i \rangle_i = 4\pi i^l \vec{A}_n(\hat{k}_o) e^{ik\hat{k}_o \cdot \vec{r}_i} + \sum_{j \neq i} \sum_{n'} \sum_{n''} T_{n'n''} \int \langle \alpha_{n''}^j \rangle_j \alpha_{n'n}(\vec{r}_i - \vec{r}_j) p(\vec{r}_j | \vec{r}_i) d\vec{r}_j \quad (6)$$

Manuscript received October 29, 1984; revised March 11, 1985. This work was supported by the U.S. Army Research Office under Contract DAAG29-83-K-0097.

The authors are with the Department of Engineering Science and Mechanics, Pennsylvania State University, University Park, PA 16802.

where  $p(\vec{r}_i|\vec{r}_i)$  is the conditional probability distribution function and  $\langle \alpha_n^i \rangle_j$  is the conditional expectation of  $\alpha_n$  with a scatterer fixed at  $\vec{r}_i$ .

The average exciting field is assumed to propagate with the wavenumber  $K$  of the effective medium.  $K = K_1 + iK_2$  is a complex frequency dependent function unlike the wavenumber  $k = \omega/c$  of the host medium. Thus

$$\langle \alpha_n^i \rangle_i = X_n e^{iK\hat{k}_o \cdot \vec{r}_i} \quad (7)$$

when substituted into (6) permits us to evaluate a portion of the integral for impenetrable particles, i.e.,  $p(\vec{r}_i|\vec{r}_i) = 0$  if  $|\vec{r}_i - \vec{r}_j| \leq 2a$  and  $p(\vec{r}_i|\vec{r}_i) = (1/V)g(|\vec{r}_i - \vec{r}_j|)$  for  $|\vec{r}_i - \vec{r}_j| > 2a$  where  $V$  is the large volume of the system such that the number density  $n_o (= N/V)$  is finite. For details we refer to our earlier work in [9], the difference in this case being  $\hat{k}_o \neq \hat{z}$ .

If the scatterers are rotationally symmetric, then the  $T$ -matrices are diagonal in the azimuthal index, i.e.,  $m' = m''$ . In this case we can assume, without loss of generality, that  $\hat{k}_o$  is in the  $x-z$  plane since there is a complete symmetry in the  $x-y$  plane. Further there is a very simple relationship between the dispersion equations that result for wave propagation with polarization parallel to the  $x-z$  plane and perpendicular to the  $x-z$  plane. For this case (7) when substituted into (6) results in the following equations for the coefficients  $X_{1lm}$  and  $X_{2lm}$ :

$$\begin{aligned} X_{1lm} = n_o \sum_{l'm'} \sum_{l''=\lambda-l}^{l'+1} i^\lambda \{ [T_{1l'o,1l''o}^{m'} X_{1l''o}^{m'}] \\ + T_{1l'o,2l''e}^{m'} X_{2l''e}^{m'} \} \cdot \{ B^{11,+} \\ \cdot Y_{\lambda,m'-m,e}(\hat{k}_o)(-1)^m - B^{11,-} Y_{\lambda,m'+m,e}(\hat{k}_o) \} \\ + \{ T_{2l'e,1l''o}^{m'} X_{1l''o}^{m'} + T_{2l'e,2l''e}^{m'} X_{2l''e}^{m'} \} \\ \cdot \{ B^{21,+} Y_{\lambda,m'-m,e}(\hat{k}_o)(-1)^m \\ - B^{21,-} Y_{\lambda,m'+m,e}(\hat{k}_o) \} \left\{ \frac{16\pi a^2}{k^2 - K^2} (JH)_\lambda + 4\pi I_\lambda \right\} \end{aligned} \quad (8a)$$

and

$$\begin{aligned} X_{2lm} = n_o \sum_{l'm'} \sum_{l''=\lambda-l}^{l'+1} i^\lambda \{ [T_{1l'o,1l''o}^{m'} X_{1l''o}^{m'}] \\ + T_{1l'o,2l''e}^{m'} X_{2l''e}^{m'} \} \{ B^{12,+} Y_{\lambda,m'-m,e}(\hat{k}_o)(-1)^m \\ - B^{12,-} Y_{\lambda,m'+m,e}(\hat{k}_o) \} \\ + \{ T_{2l'e,1l''o}^{m'} X_{1l''o}^{m'} + T_{2l'e,2l''e}^{m'} X_{2l''e}^{m'} \} \\ \cdot \{ B^{22,+} Y_{\lambda,m'-m,e}(\hat{k}_o)(-1)^m \\ + B^{22,-} Y_{\lambda,m'+m,e}(\hat{k}_o) \} \left\{ \frac{16\pi a^2}{k^2 - K^2} (JH)_\lambda + 4\pi I_\lambda \right\} \end{aligned} \quad (8b)$$

where

$$\begin{aligned} (JH)_\lambda &= k/\lambda (2Ka) Y'_\lambda(2ka) \\ &- K'_\lambda (2Ka) h_\lambda(2ka) \end{aligned}$$

and

$$I_\lambda = \int_{2a}^\infty [g(x) - 1] j_\lambda(Kx) h_\lambda(Kx) x^2 dx. \quad (10)$$

The four quantities  $B^{11,+}$ ,  $B^{22,+}$ ,  $B^{12,+}$ ,  $B^{21,+}$  are vestiges of the translation matrix after the angular and radial parts have been absorbed in the integration. Expressions for them may be found in terms of the Wigner coefficients and are given below:

$$\begin{aligned} B^{11,+} = B^{22,+} &= (-1)^{m'+m} (\pi \epsilon_m \epsilon_{m'}/4 \epsilon_{m'} \epsilon_m)^{1/2} \\ &\cdot (-1)^{(l-l'+\lambda)/2} \left[ \frac{(2l+1)(2l'+1)(2\lambda+1)}{l(l+1)l'(l'+1)} \right]^{1/2} \\ &\cdot \begin{pmatrix} l & l & \lambda \\ 0 & 0 & 0 \end{pmatrix} \begin{pmatrix} l' & l & \lambda \\ m' & m & m+m' \end{pmatrix} \\ &\cdot [l'(l'+1) + l(l+1) - \lambda(\lambda+1)] \end{aligned} \quad (11)$$

and

$$\begin{aligned} B^{12,+} = B^{21,+} &= (-1)^{m'+m} (\pi \epsilon_m \epsilon_{m'}/4 \epsilon_{m'} \epsilon_m)^{1/2} i^{l-l'+\lambda+1} \\ &\cdot \left[ \frac{(2l+1)(2l'+1)(2\lambda+1)}{l(l+1)l'(l'+1)} \right]^{1/2} \begin{pmatrix} l' & l & \lambda-1 \\ 0 & 0 & 0 \end{pmatrix} \\ &\cdot \begin{pmatrix} l' & l & \lambda \\ m' & m & m+m' \end{pmatrix} \\ &\cdot [\lambda^2 - (l-l')^2]^{1/2} [(l'+l+1)^2 - \lambda^2]^{1/2}. \end{aligned} \quad (12)$$

Equations (8a) and (8b) may be written in vector matrix notation in the form

$$X_i = M_{ij} X_j. \quad (13)$$

The dispersion equation for the effective medium then becomes

$$|\delta_{ij} - M_{ij}(\omega, K, \hat{k}_o)| = 0 \quad (14)$$

where  $M_{ij}$  itself is an infinite matrix for each  $i, j$ . The determinantal equation must be solved numerically using suitable forms of the pair correlation function  $g(x)$ , for given  $\omega$ ,  $\hat{k}_o$ ,  $n_o$ , and  $T$ . It is seen that the solution will depend explicitly on the direction of wave propagation  $\hat{k}_o$ , rendering the medium effectively anisotropic.

#### RELATIONSHIP TO TWERSKY'S DISPERSION EQUATION

In a series of papers, Twersky [1], [2] has derived the dispersion equation invoking the quasicrystalline approximation and including the effects of pair correlation for both acoustic and electromagnetic wave propagation in pair correlated random distributions of aligned scatterers. For spherically symmetric statistics, i.e., requiring a spherical excluded volume even for nonspherical scatterers, we can show that the dispersion derived by Twersky [2] is identical to (8a) and (8b) when the scattered field is written as an expansion in vector spherical harmonics.

In [2, eq. (81)], the dispersion equation for electromagnetic wave propagation in aligned, random distributions is given as

$$\begin{aligned} C_{nm} = - \sum_{\substack{l's \\ \mu\nu}} \left\{ \alpha_{n\nu}^{m\mu} \left[ C_1 \begin{pmatrix} -\mu & l' \\ \nu & s \end{pmatrix} C_{sr} - C_2 \begin{pmatrix} -\mu & l' \\ \nu & s \end{pmatrix} B_{sr} \right] \right. \\ \left. + \beta_{n\nu}^{m\mu} \left[ C_2 \begin{pmatrix} -\mu & l' \\ \nu & s \end{pmatrix} C_{sr} + C_1 \begin{pmatrix} -\mu & l' \\ \nu & s \end{pmatrix} B_{sr} \right] \right\} \end{aligned} \quad (15a)$$

and

$$B_{nm} = - \sum_{\substack{t \neq s \\ \mu \nu}} \left\{ \gamma_{n\nu}^{m\mu} \left[ C_1 \begin{pmatrix} -\mu & t \\ \nu & s \end{pmatrix} C_{st} - C_2 \begin{pmatrix} -\mu & t \\ \nu & s \end{pmatrix} B_{st} \right] \right. \\ \left. + \delta_{n\nu}^{m\mu} \left[ C_2 \begin{pmatrix} -\mu & t \\ \nu & s \end{pmatrix} C_{st} + C_1 \begin{pmatrix} -\mu & t \\ \nu & s \end{pmatrix} B_{st} \right] \right\} \quad (15b)$$

where in our notation

$$C_{nm} \rightarrow X_{1nm}, \quad B_{nm} \rightarrow X_{2nm}, \\ n \in [0, \infty], \quad m \in [0, \infty]$$

are the scattered field coefficients.

$$\begin{bmatrix} \alpha_{n\nu}^{m\mu} & \beta_{n\nu}^{m\mu} \\ \gamma_{n\nu}^{m\mu} & \delta_{n\nu}^{m\mu} \end{bmatrix} \rightarrow \begin{bmatrix} T^{11} & T^{12} \\ T^{21} & T^{22} \end{bmatrix}$$

is the  $T$ -matrix of an individual scatterer and the two symbols  $C_1$  and  $C_2$  are related to the Fourier transform of the product of the pair correlation function and the translation matrix as in (6).

In the notation of the present paper and the abbreviated index notation we may write Twersky's equation, (15a) (15b), in the form

$$\begin{pmatrix} X_1 \\ X_2 \end{pmatrix} = \begin{bmatrix} T^{11} & T^{12} \\ T^{21} & T^{22} \end{bmatrix} \begin{bmatrix} C_1 & -C_2 \\ C_2 & C_1 \end{bmatrix} \begin{pmatrix} X_1 \\ X_2 \end{pmatrix} \quad (16)$$

We note that (8a) and (8b) may be multiplied from the left by the  $T$ -matrix, so that the dispersion equation is in terms of the average scattered field coefficients rather than the exciting field. Then using  $\langle f_n^i \rangle_{ij} \approx \langle f_n^i \rangle_i = X_n^{iK} \hat{k}_o \cdot \hat{r}_i$  we can rewrite the dispersion equation in the form

$$X_n^i = a_n + n_o \sum_{n'n''} T_{nn'} \int a_{n'n''}(\hat{r}_{ij}) e^{iK \hat{k}_o \cdot \hat{r}_{ij}} X_{n''}^i g(|\hat{r}_{ij}|) d\hat{r}_{ij} \quad (17)$$

We further note that using the integral representation of the vector spherical functions the translation matrix can be written in the form

$$a_{nn'}(k\hat{x}) = 2 \int_{C_2} d\hat{\gamma} \hat{A}_n(\hat{\gamma}) \cdot \hat{A}_{n'}(\hat{\gamma}) [i(1 - \delta_{rr'}) \\ \cdot (-1)^{r'} + \delta_{rr'}] e^{ik\hat{\gamma} \cdot \hat{x}} \quad (18)$$

where  $C_2$  are the contours. Using properties of the scalar products of vector spherical harmonics of the same argument as given for example by Twersky [2], we can show that

$$\int a_{nn'}(k\hat{x}) e^{iK \hat{k}_o \cdot \hat{x}} g(|\hat{x}|) d\hat{x} = \begin{bmatrix} C_1 & -C_2 \\ C_2 & C_1 \end{bmatrix} \quad (19)$$

as defined in [2, eq. (80)] so that the dispersion equation derived here is identical to that of Twersky.

## RESULTS AND DISCUSSION

The dispersion equation (14) was programmed on an IBM 370. The main parts of the program consist of subroutines that 1) generate the  $T$ -matrix for a given  $\omega$  and shape of scatterer, 2) set up the matrix  $\delta_{ij} - M_{ij}$ , 3) special function programs, 4) determinant solver, 5) complex root finder based on Müller's

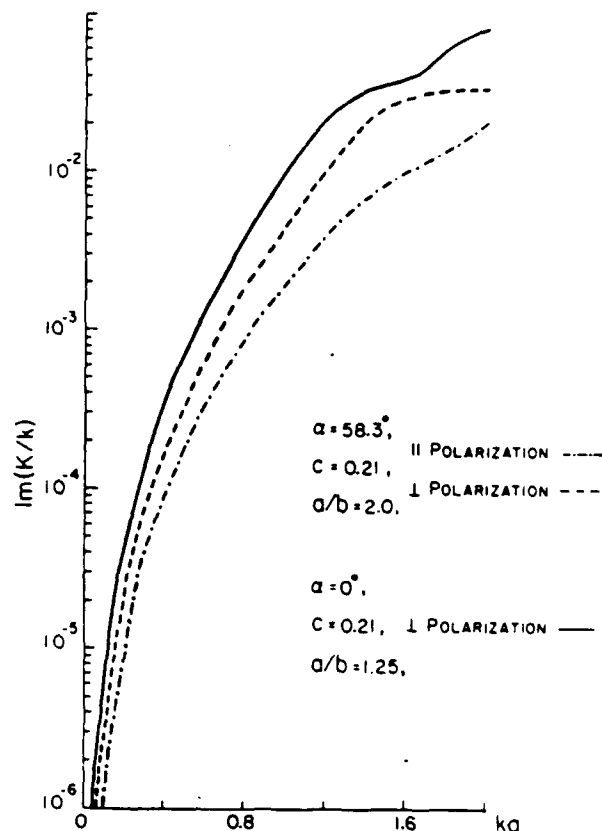


Fig. 1. Plot of attenuation versus normalized wavenumber for a distribution of aligned spheroids for wave propagation at  $\alpha = 58.3^\circ$  and  $\alpha = 0^\circ$ .

method and a main program that specifies the parameters  $\omega$ ,  $n_o$ ,  $a$ ,  $\hat{k}_o$  and the shape and nature of the scatterer. The root finder returns the value of  $K = K_1 + iK_2$  that renders  $|\delta_{ij} - M_{ij}| = 0$ . This is then the complex, frequency dependent effective wavenumber of the medium. Although simple relations exist between the dispersion equations for parallel and perpendicular polarization, the resulting wavenumbers  $K^{\parallel}$  and  $K^{\perp}$  are in general different.

The truncation sizes of both  $T$  and  $M$  are varied till convergence is obtained. The computation is more time consuming than for the case when  $\hat{k}_o = \hat{z}$  because an additional summation on the azimuthal index is involved, i.e., the azimuthal modes are no longer uncoupled. This involves the storage of fairly large matrices. Typical computation time for a lossless oblate spheroidal dielectric scatterer of aspect ratio 2:1 with the dielectric constant  $\epsilon_r = 3.168$  for a given  $\omega$ ,  $n_o$  and  $\hat{k}_o$  is about 60 s after the program has been tested for the correct matrix size.

We now present results in the form of plots of the imaginary part of the relative effective dielectric constant  $\langle \epsilon \rangle$  as a function of  $ka = \omega a/c$ ,  $k_o(\alpha, \beta = 0)$  and  $c = n_o 4\pi a^3/3$  where  $a$  is the semi-major axis of the oblate spheroid of aspect ratio 2:1 and 1.25:1. We recall that  $\langle \epsilon \rangle = K^2/k^2$ , at  $ka \sim 1.7$  when a crossover occurs. In Fig. 1, the attenuation given by  $\text{Im}(K/k)$  is plotted as a function of  $ka$  for both parallel and perpendicular polarization for  $\alpha = 58.3^\circ$  and  $c = 0.21$ . Also included in the figure is the attenuation for  $\alpha = 0$  and aspect ratio 1.25:1. In Fig. 2 the attenuation is plotted as a function of  $\alpha$  varying from  $0^\circ$  to  $90^\circ$ . The attenuation is a slowly varying function of  $\alpha$  and is maximum at  $\alpha = 0^\circ$ .

In Fig. 3, the complex plane plot of the relative effective



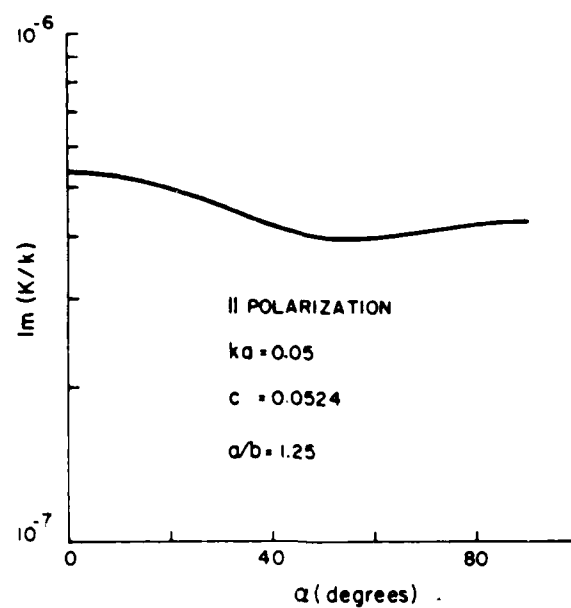


Fig. 2. Plot of attenuation versus direction of wave propagation for aligned spheroids, parallel polarization.

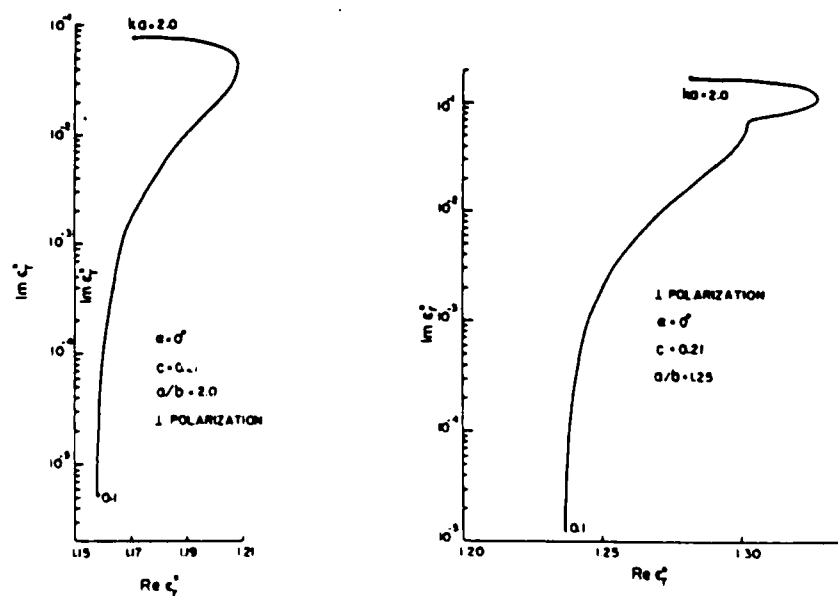


Fig. 3. Complex plane plot of the dielectric constant at different frequencies for aligned spheroids.

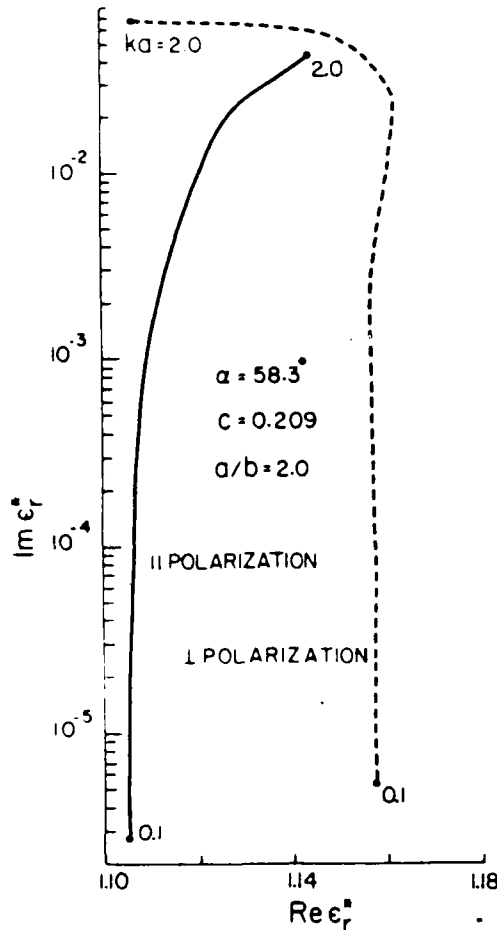


Fig. 4 Complex plane plot of the dielectric constant at different frequencies for aligned spheroids.

dielectric constant ( $\epsilon$ ) is plotted for perpendicular polarization for both  $a/b = 2.0$  and  $1.25$ . In Fig. 4, the complex plane plots of ( $\epsilon$ ) are shown for  $\alpha = 58.3^\circ$  for parallel and perpendicular polarization. Fig. 5 shows the comparison of our results with those by other methods. The curve denoted as "Twersky" resulted from computations based on Twersky's formalism as given in [2]. The curve marked "self-consistent," uses the self-consistent approximation to the pair correlation function (see [10]) and Monte Carlo computations for the pair correlation as given by Barker and Henderson [13] were used for purposes of comparison. All curves are in good agreement for the range of parameters considered.

In conclusion, we have demonstrated a scheme for computing the complex propagation characteristics of a medium that is effectively anisotropic. Although, the effects are not dramatic, there is a significant (measurable) difference between the results for parallel and perpendicular polarization. The effect of polarization is more significant than that of propagation direction. Finally we have also discussed how our dispersion equation for a medium with pair correlated aligned scatterers compares with Twersky's equation for the same system.

#### ACKNOWLEDGMENT

Many helpful discussions with Dr. W. A. Flood and Dr. G. S. Brown are gratefully acknowledged.

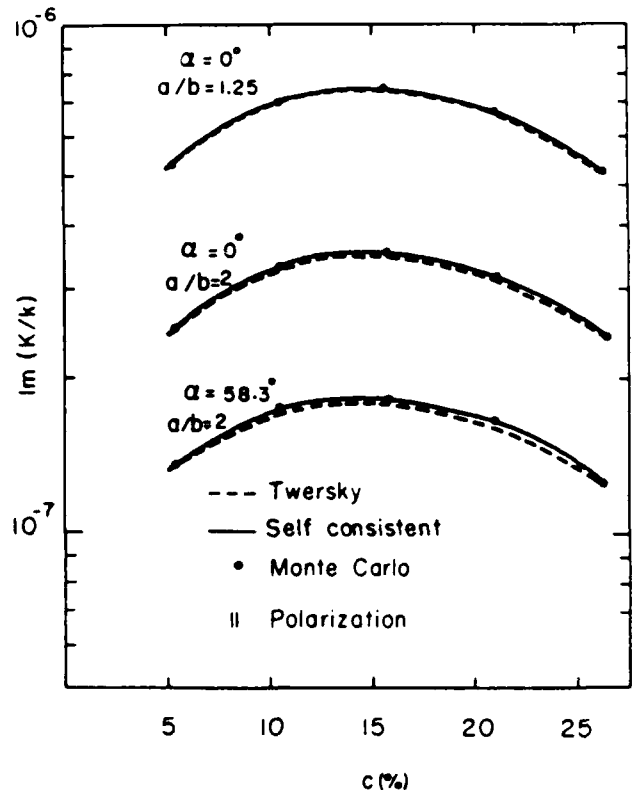


Fig. 5 Comparison of our results with those by other methods at  $ka = 0.05$ .

#### REFERENCES

- [1] V. Twersky, "Coherent scalar field in pair-correlated random distribution of aligned scatterers," *J. Math. Phys.*, vol. 18, pp. 2468-2486, 1977.
- [2] —, "Coherent electromagnetic waves in pair-correlated random distribution of aligned scatterers," *J. Math. Phys.*, vol. 19, pp. 215-230, 1978.
- [3] Y. Ma, V. V. Varadan, and V. K. Varadan, "Multiple scattering theory for wave propagation in discrete random media," *Int. J. Eng. Sci.*, vol. 22, pp. 1130-1148, 1984.
- [4] V. V. Varadan and V. K. Varadan, "The quasi-crystalline approximation and multiple scattering of waves in random media," submitted.
- [5] P. C. Waterman, "Symmetry, unitarity and geometry in electromagnetic scattering," *Phys. Rev. D*, vol. 3, pp. 825-839, 1971.
- [6] V. K. Varadan and V. V. Varadan, Eds., *Acoustic, Electromagnetic and Elastic Wave Scattering—Focus on the T-Matrix Approach*. New York: Pergamon, 1980.
- [7] V. N. Brongi, V. V. Varadan, and V. K. Varadan, "Coherent wave attenuation by a random distribution of particles," *Radio Sci.*, vol. 17, pp. 946-952, 1982.
- [8] —, "Average dielectric properties of discrete random media using multiple scattering theory," *IEEE Trans. Antennas Propagat.*, vol. AP-31, pp. 371-375, 1983.
- [9] V. N. Brongi, T. A. Seliga, V. K. Varadan and V. V. Varadan, "Bulk propagation characteristics of discrete random media," in *Multiple Scattering and Waves in Random Media*, P. L. Chow, W. E. Kohler, and G. Papanicolaou, Eds. Amsterdam: North Holland, 1981.
- [10] V. K. Varadan, V. N. Brongi, V. V. Varadan, and A. Ishimau, "Multiple Scattering theory for waves in discrete random media and comparison with experiments," *Radio Sci.*, vol. 18, pp. 321-327, 1983.
- [11] V. V. Varadan, V. N. Brongi, and V. K. Varadan, "Frequency dependent dielectric constants of discrete random media," in *Macroscopic Properties of Disordered Media*, R. Burridge, S. Childrens, and G. Papanicolaou, Eds. New York: Springer-Verlag, 1982.
- [12] J. A. Barker and D. Henderson, "Monte Carlo values for the radial distribution function of a system of fluid hard sphere," *Molecular Phys.*, vol. 21, pp. 187-191, 1971.

# Multiple scattering of elastic waves by cylinders of arbitrary cross section. II. Pair-correlated cylinders

V. K. Varadan, V. V. Varadan, and Y. Ma

Laboratory for Electromagnetic and Acoustic Research, Department of Engineering Science and Mechanics, The Pennsylvania State University, University Park, Pennsylvania 16802

(Received 23 September 1984; accepted for publication 28 June 1985)

Multiple scattering of elastic waves by randomly distributed cylinders of arbitrary cross section has been considered. Because the pair-correlation function, as well as the quasicrystalline approximation, has been incorporated in the presented formalism, the effective phase velocity, as well as the coherent attenuation in dense systems, has been investigated. A more efficient scattering formalism (SF) has been employed rather than the exciting field formalism (EF) used earlier by the authors. Closed form expressions for the phase velocity and the attenuation are given in the Rayleigh limit, and numerical results are presented for a wide range of frequencies and concentrations.

PACS numbers: 43.20.Fn

## INTRODUCTION

In a previous paper,<sup>1</sup> we presented an exciting field multiple scattering formalism for cylinders using the concept of a scattering operator—the  $T$  matrix.<sup>2</sup> This formulation used the  $T$  matrix to characterize the scattering by a single isolated scatterer followed by configurational averaging techniques. Lax's quasicrystalline approximation (QCA)<sup>3</sup> was used to truncate the resulting hierarchy of equations. This yielded a set of "hole correction" integrals which were evaluated analytically, and the extinction theorem was invoked to yield the dispersion relation characterizing the bulk or effective properties of the medium which was solved numerically. Computations of the effective coherent wave attenuation as a function of the nondimensional wavenumber  $ka$  ("a" being a characteristic dimension of the obstacle) were presented in Ref. 1 for various concentrations ( $c$ ). The formalism based on a sparse distribution of correlated scatterers leads to unphysical nulls in the plots of coherent attenuation at high values of the concentration (which disappear at higher values of  $ka$ ). Moreover, in the Rayleigh limit, the formalism gives only the phase velocity and does not provide the analytical expression for coherent attenuation.

The incorporation of the complete correlation function between the positions of the scatterers provides the effective properties, coherent attenuation, etc., for dense systems. If the QCA is invoked, it has been shown by Twersky<sup>4-7</sup> that only a knowledge of the two-body (pair) correlation function is required. Twersky has considered a general formalism for scalar waves in Refs. 4-6 and for electromagnetic waves in Ref. 7.

In this paper, we consider the multiple scattering of elastic  $SH$  waves by randomly distributed cylinders incorporating the QCA and the pair-correlation function as given by Twersky.<sup>6</sup> We studied the problem using a scattered field formalism (SF) rather than the exciting field formalism (EF), since SF provides a more convenient basis for scattering of elastic longitudinal ( $P$  -) and shear ( $SV$  -) waves<sup>8</sup> by elastic scatterers and by piezoelectric scatterers<sup>9</sup> which couple both elastic and electromagnetic fields. The SF employed

here is precisely the formalism introduced by Twersky in the 50's. When performing the numerical calculations, we find that the SF is more suited for computations at higher frequencies requiring smaller matrices than the EF reported by us earlier.<sup>1</sup> Closed form expressions for the phase velocity and attenuation are presented in the long wavelength limit, and it is shown that our results for circular and elliptical cylinders agree with those given by Twersky<sup>5</sup> for all concentrations. Numerical results are presented for both phase velocity and coherent attenuation for higher frequencies.

## I. DISPERSION EQUATION USING SF FORMALISM

In this section only the essential details and the final result for the dispersion equation based on the SF (scattered field) formalism are presented. The equations presented here are identical to those given by Twersky<sup>4-7,10</sup> if the notation used here is properly interpreted.

We consider  $N$  ( $N \rightarrow \infty$ ) arbitrary shaped (rotationally symmetric), long, and parallel cylindrical scatterers embedded in an infinitely extended elastic solid (matrix). Let  $\rho_1, \mu_1$  be the density and rigidity of the matrix and  $\rho_2, \mu_2$  those of the scatterers. A plane  $SH$  wave of unit amplitude, frequency  $\omega$ , and wavenumber  $k$  is incident perpendicular to the axis of the cylinders in the direction  $\hat{k}_0$ .

From Ref. 1, one can obtain an equation relating the scattered field coefficients in the form

$$b_n^i = \sum_n T_{nn'}^i \left( a_n^0 + \sum_{j=1}^N \sum_{n'} (-1)^{n'+n} \psi_{n'-n}(\mathbf{r}_{ij}) b_{n'}^j \right), \quad (1)$$

where the  $T$  matrix  $T_{nn'}^i$  relates the exciting and scattered field coefficients for a particular ( $i$ th) scatterer,  $a_n^0 = i^{n'} e^{ik\hat{k}_0 \cdot \mathbf{r}_i}$  are the known incident field coefficients,  $\mathbf{r}_{ij} = \mathbf{r}_i - \mathbf{r}_j$  is the vector connecting the  $i$ th and  $j$ th scatterers, and  $\psi_n$  are outgoing cylindrical wavefunctions. Equation (1) is precisely the same as introduced by Twersky in the 50's.<sup>10</sup>

Since the number of scatterers is large, it is more meaningful to perform a configurational average over the random

positions of all scatterers except the  $i$ th, which is assumed to be fixed. The details can be found in Ref. 5. We thus have for identical scatterers

$$\langle b_n^i \rangle_i = \sum_n T_{nn} \left( a_n^0 + (N-1) \sum_{n'} \int_S (-1)^{n'+n} \right. \\ \left. \times \psi_{n'-n}(\mathbf{r}_j) \langle b_n^i \rangle_{ij} p(\mathbf{r}_j | \mathbf{r}_i) d\mathbf{r}_j \right), \quad (2)$$

where  $\langle \rangle_i$  and  $\langle \rangle_{ij}$  denote the configurational average with the  $i$ th scatterer held fixed and both the  $i$ th and  $j$ th scatterers held fixed, respectively, and  $p(\mathbf{r}_j | \mathbf{r}_i)$  is the conditional probability distribution function. For impenetrable cylinders,  $p(\mathbf{r}_j | \mathbf{r}_i) = 0$  if  $|\mathbf{r}_j - \mathbf{r}_i| < 2a$ , where " $a$ " is the largest dimension of the cylinders and  $p(\mathbf{r}_j | \mathbf{r}_i) = g(|\mathbf{r}_j - \mathbf{r}_i|/S)$ , where  $S$  is the large area over which the cylinders are distributed. Here, we have assumed isotropic or circular statistics even for noncircular cylinders and the function  $g(x)$  is the radial distribution function. Equation (2) yields an infinite coupled hierarchy for the conditionally averaged scattered field coefficients. It can be truncated by using the quasicrystalline approximation (QCA) suggested by Lax<sup>3</sup> and Twersky. In this approximation,  $\langle b_n^i \rangle_{ij} \approx \langle b_n^i \rangle_i$ , which has been proved valid for a wide range of concentrations. Further, we assume the existence of a coherent field propagating in the direction  $\hat{k}_0$  of the incident field with an effective, complex, frequency dependent wavenumber  $K = K_1 + iK_2$  of the form

$$\langle b_n^i \rangle = X_n e^{iK_0 \cdot \mathbf{r}_i}, \quad (3)$$

where  $X_n$  is an unknown constant.

Equation (3) is substituted in Eq. (2) and the extinction theorem can be invoked to cancel the incident wave term on the right-hand side of Eq. (2) (refer to Twersky<sup>5</sup> for details). The resulting equation is

$$X_n = n_0 \sum_{n'} \sum_m T_{nn'} I_{lm,m} X_m, \quad (4)$$

where

$$I_{lm,m} = 2\pi i^{m-l} \{ (k^2 - K^2)^{-1} [2kaJ_{m-l}(2Ka) \\ \times H'_{m-l}(2ka) - 2KaH_{m-l}(2ka)J'_{m-l}(2Ka)] \\ + 4a^2 \int_0^\infty H_{m-l}(2kax)J_{m-l}(2Kax) \\ \times [g(x) - 1]x dx \}. \quad (5)$$

In Eq. (4), we have assumed that  $N$  and  $S$  are infinitely large with the number density  $n_0 = (N-1)/S$ . Equations (4) and (5) are identical to those obtained by Twersky<sup>5</sup> if the  $T$  matrix is interpreted as the single scattering coefficients.

Equation (4) is a system of linear simultaneous equations for the coefficients  $X_n$ . For a nontrivial solution of the coherent field, we must require the determinant of the coefficient matrix to vanish. This is the required dispersion equation, which can be solved for the effective propagation constant  $K$  as a function of  $k$  and  $c$ . This will be discussed in Sec. II. The values of  $g(x)$  obtained by Monte Carlo calculations are used in our numerical computations.<sup>11,12</sup>

## II. RAYLEIGH LIMIT SOLUTION

The dispersion relation derived in Eq. (4) can be solved in detail to predict the phase velocity and coherent attenuation for a two-phase composite medium. Although the system of equations requires a numerical approach to yield solutions for higher values of frequency, analytical results can be obtained for low-frequency approximations. Including the effects of correlation between scatterers, it is seen that an attenuation factor is obtained in the Rayleigh limit. Analytical results are seen to mainly depend on the form of correlation assumed. The  $g(x)$  obtained from the virial series and the geometrical considerations by Twersky<sup>5,6</sup> agree very well with Monte Carlo calculations. Using Twersky's results for  $g(x)$ , we hence obtain the dispersion equations for both elastic circular and elliptical cylinders, respectively, embedded in an elastic matrix:

circular cylinder

$$\frac{K^2}{k^2} = \left[ \left( 1 + c(d-1) \right) \left( 1 + c \frac{1-m}{1+m} \right) \left( 1 - c \frac{1-m}{1+m} \right)^{-1} \right. \\ \left. + \frac{i\pi}{4} k^2 a^2 c (1-c)^3 \left[ \left( 1 + c \right) \left( 1 - c \frac{1-m}{1+m} \right)^2 \right]^{-1} \right. \\ \left. \times \left\{ 2 \left( \frac{1-m}{1+m} \right)^2 [1 + c(d-1)] \right. \right. \\ \left. \left. + (d-1)^2 \left[ 1 - c^2 \left( \frac{1-m}{1+m} \right)^2 \right] \right\} \right] \quad (6)$$

and

elliptical cylinder

$$\frac{K^2}{k^2} = \left[ \left( 1 + c_1(d-1) \right) \left( 1 + c_1 \frac{(1-m)(a+b)}{2(mb+a)} \right) \right. \\ \left. \times \left( 1 - c_1 \frac{(1-m)(a+b)}{2(mb+a)} \right)^{-1} \right. \\ \left. + \frac{i\pi}{4} k^2 a^2 \left[ c(1-c)^3 \right] \right. \\ \left. \times \left[ \left( 1 + c \right) \left( 1 - c_1 \frac{(1-m)(a+b)}{2(mb+a)} \right)^2 \right]^{-1} \right. \\ \left. \times \left\{ 2 \left( \frac{(1-m)(a+b)}{2(mb+a)} \right)^2 [1 + c_1(d-1)] \right. \right. \\ \left. \left. + (d-1)^2 \left[ 1 - c_1^2 \left( \frac{(1-m)(a+b)}{2(mb+a)} \right)^2 \right] \right\} \right],$$

$$c = n_0 \pi a^2, \quad c_1 = cb/a < c. \quad (7)$$

These results agree exactly with those of Twersky<sup>5</sup> if we put  $d = C'$  and  $m^{-1} = B'$  in his Eq. (70).<sup>5</sup> In this paper, we present numerical results at higher frequencies for various aspect ratios of elliptical cylinders. This is discussed in Sec. III.

## III. NUMERICAL RESULTS AND CONCLUSIONS

The analytical expressions for the phase velocity and coherent attenuation as obtained above could be derived only for very low values of  $ka$ , as higher approximations would lead to unwieldy expressions. A quantitative estimate of the multiple scattering process at resonant and higher frequencies can be obtained by numerically solving the disper-

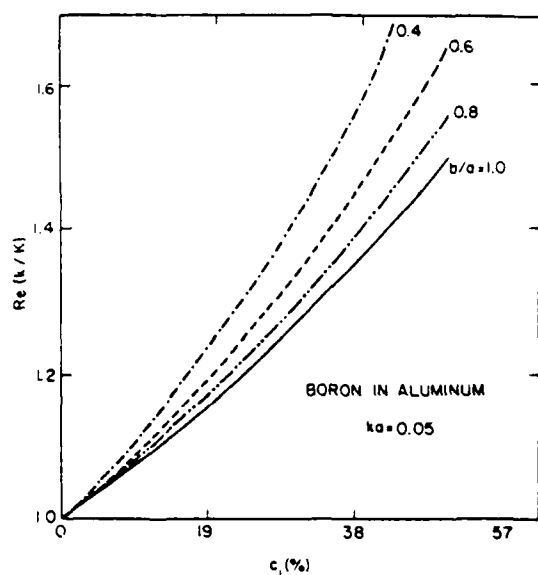


FIG. 1. Normalized phase velocity versus concentration  $c_1$  for different aspect ratios.

sion equation, Eq. (4). The computational scheme has been described previously<sup>1</sup> and will not be repeated here.

To study the frequency dependent phase velocity and attenuation of composite materials, we consider an aluminum matrix reinforced by boron fibers whose density ratio  $d = 0.93$  and shear modulus ratio  $m = 6.46$ . In order to show the effect of density and shear modulus on the wave propagation characteristics through composites, the composite of  $\text{BaTiO}_3$  fibers in polyurethane which gives  $d = 5.18$  and  $m = 0.69 \times 10^4$  is also used.

In the Rayleigh region ( $ka \ll 1$ ), the phase velocity of the composite is computed for different fiber concentrations for various aspect ratios  $b/a$  and the numerical results are presented in Fig. 1, where the phase velocity is normalized with respect to the shear velocity in the host medium (unless specially mentioned, calculations are made for boron-aluminum composite). One sees that the phase velocity increases

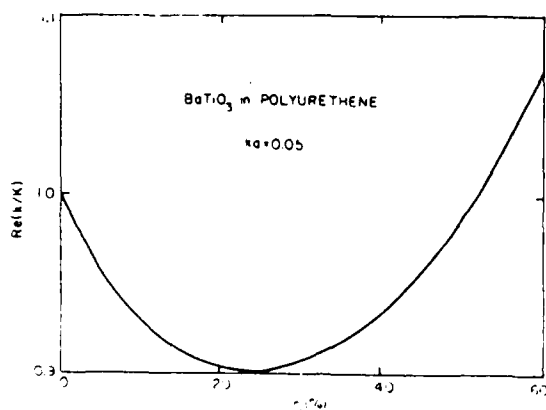


FIG. 2. Normalized phase velocity versus concentration  $c$  for circular  $\text{BaTiO}_3$  fibers in polyurethane.

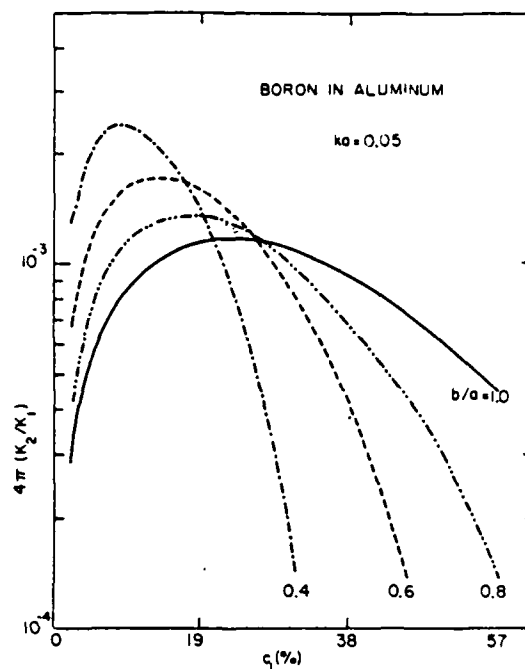


FIG. 3. Attenuation coefficient versus concentration  $c_1$  for different aspect ratios.

with increasing concentration for the same aspect ratio. However, for the same concentration, the phase velocity increases with the decreasing aspect ratio since the number of scatterers becomes larger when the smaller aspect ratio fibers are used.

For circular  $\text{BaTiO}_3$  fibers in polyurethane, the characteristics of the phase velocity against concentration are greatly affected by the larger shear modulus ratio which can

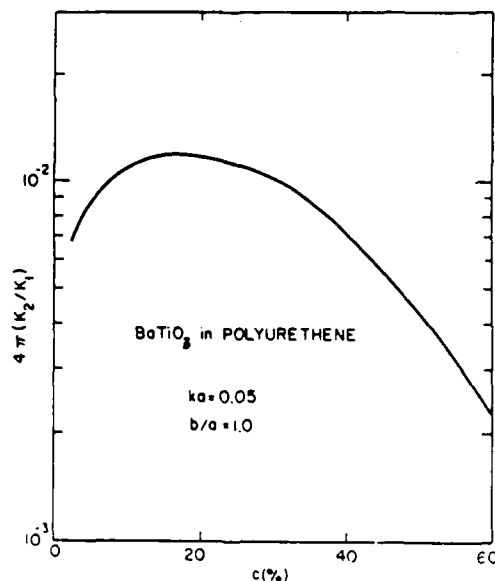


FIG. 4. Attenuation coefficient versus concentration for  $\text{BaTiO}_3$  in polyurethane.

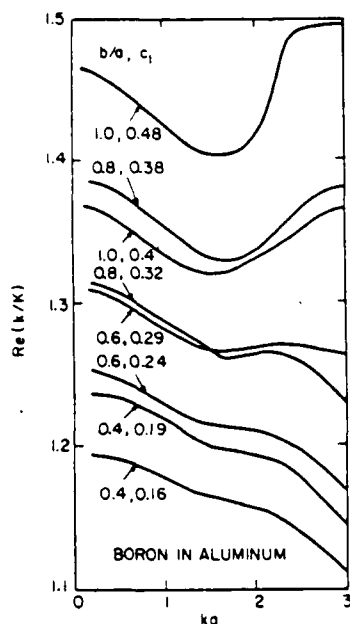


FIG. 5. Normalized phase velocity versus nondimensional frequency  $ka$  for different aspect ratio and concentration.

be seen from Fig. 2. The phase velocity ratio first becomes less than 1 and then increases to become greater than 1 after  $c = 0.5$ . Figure 3 presents the attenuation for different fiber concentrations and various aspect ratios. One is able to observe that in the long wavelength limit the peak of the attenuation occurs at a smaller concentration for smaller aspect ratio fibers. The larger the number of scatterers, the faster the attenuation rises and falls for the same concentration. In other words, the transition phenomenon in the two-phase medium may occur at a smaller concentration if the smaller aspect ratio fibers are used in the low-frequency range. A similar attenuation trend is also found for  $\text{BaTiO}_3$  fibers as presented in Fig. 4.

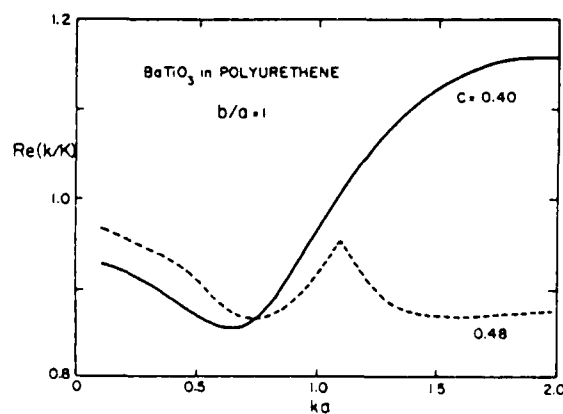


FIG. 6. Normalized phase velocity versus nondimensional frequency  $ka$  for circular  $\text{BaTiO}_3$  fibers in polyurethane.

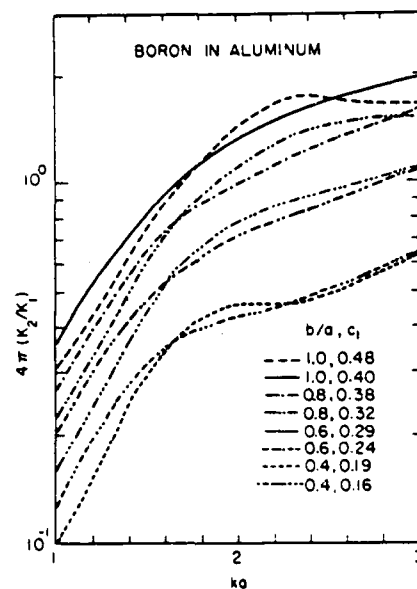


FIG. 7. Attenuation coefficient versus nondimensional frequency  $ka$  for different aspect ratio and concentration.

Figure 5 presents numerical results of the frequency dependent phase velocity for different concentrations as well as aspect ratios. When the aspect ratio  $b/a$  is close to unity, the phase velocity gradually decreases and then increases with the increasing frequency. Nevertheless, this behavior becomes quite different when a smaller aspect ratio is employed. As can be seen in Fig. 5, instead of increasing, the

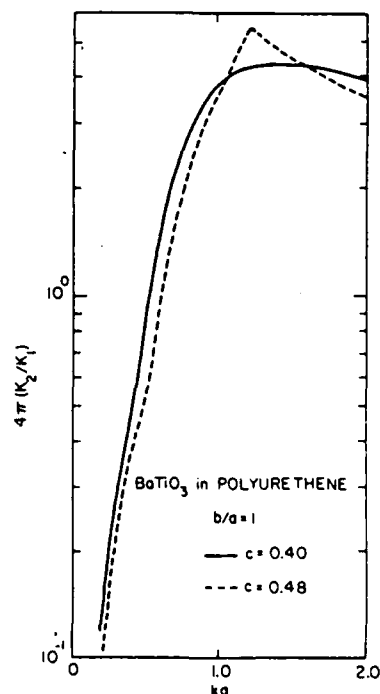


FIG. 8. Attenuation coefficient versus nondimensional frequency  $ka$  for circular  $\text{BaTiO}_3$  fibers in polyurethane.

phase velocity gradually decreases after  $ka$  is about 2.0. But when the same aspect ratio fibers are used, the higher the concentration, the larger is the phase velocity, as expected.

If a different composite is used, i.e., BaTiO<sub>3</sub> fibers in polyurethane, the characteristic of the phase velocity against concentration is totally changed, which is depicted in Fig. 6. It is noted that the density and shear modulus play an important role in the results. The results show a resonant phenomenon which is typical for composites reinforced by materials with a much larger density and elastic modulus at high concentrations.

In Fig. 7, we have plotted the attenuation coefficient  $\alpha (= 4\pi K_2/K_1)$  vs  $ka$  for two values of concentration  $c$ . In all cases, the attenuation first increases rapidly with increasing frequency up to about  $ka = 1.6$ , which is generally valid following an extension of the Rayleigh scattering law [ $\alpha \sim (ka)^2$ ]. After this frequency, the attenuation increases at a milder rate and behaves differently for different aspect ratio fibers due to the higher mode vibrations. One general observation is that the smaller the concentration, the higher attenuation for  $ka$  less than about 1.6. After this value there is a transition range of  $ka$ , where the fibers of larger concentrations produce higher attenuation and the larger the aspect ratio, the narrower and transition frequency band. We do emphasize that the concentration used in the calculation is quite large and the attenuation is, therefore, reduced with the increasing concentration which can be found in Fig. 3.

The trend of the attenuation curve is also applied to the

composite of BaTiO<sub>3</sub> in polyurethane, which is shown in Fig. 8. However, the magnitude of the attenuation is about ten times larger than that of the aluminum composite due to the much larger shear modulus used.

## ACKNOWLEDGMENTS

The authors would like to thank the reviewers for their suggestions and comments. The use of the departmental VAX 11/730 minicomputer is gratefully acknowledged.

<sup>1</sup>V. K. Varadan, V. V. Varadan, and Y. H. Pao, J. Acoust. Soc. Am. 63, 1310 (1978).

<sup>2</sup>*Acoustic, Electromagnetic and Elastic Wave Scattering—Focus on the T-matrix Approach*, edited by V. K. Varadan and V. V. Varadan (Pergamon, New York, 1980).

<sup>3</sup>M. Lax, Phys. Rev. 85, 621 (1952).

<sup>4</sup>V. Twersky, J. Math. Phys. 18, 2468 (1977).

<sup>5</sup>V. Twersky, J. Acoust. Soc. Am. 64, 1710 (1978).

<sup>6</sup>V. Twersky, J. Acoust. Soc. Am. 73, 68 (1983).

<sup>7</sup>V. Twersky, J. Math. Phys. 19, 215 (1978).

<sup>8</sup>V. K. Varadan, V. V. Varadan, and Y. Ma, "Multiple Scattering of Elastic Waves by Cylinders of Arbitrary Cross Section. III. P- and SV-Waves," Report No: PSU/LEAR-84-2, Laboratory for Electromagnetic and Acoustic Research, June 1984.

<sup>9</sup>V. K. Varadan, V. V. Varadan, and Y. Ma, "Multiple Scattering of Elastic Waves by Piezoelectric Cylinders," Report No: PSU/LEAR-84-3, Laboratory for Electromagnetic and Acoustic Research, July 1984.

<sup>10</sup>V. Twersky, *Electromagnetic Waves*, edited by R. G. Langer (University of Wisconsin, Madison, WI, 1962), pp. 361–389.

<sup>11</sup>N. Metropolis, A. W. Rosenbluth, M. N. Rosenbluth, A. H. Teller, and E. Teller, J. Chem. Phys. 21, 1087 (1953).

<sup>12</sup>W. W. Wood, J. Chem. Phys. 48, 415 (1968).

# Propagator model including multipole fields for discrete random media

V. V. Varadan, Y. Ma, and V. K. Varadan

Laboratory for Electromagnetic and Acoustic Research, Department of Engineering Science and Mechanics, The Pennsylvania State University, University Park, Pennsylvania 16802

Received May 29, 1985; accepted August 14, 1985

A propagator model using Feynman diagrams is presented for studying the first and the second moments of the electromagnetic field in a discrete random medium. The major difference between our work and previous treatments of this type is that all diagrams are in a basis of vector spherical functions. Each propagator or infinite-medium Green's function is the translation matrix for spherical functions, and each scatterer is characterized by a T matrix that, in turn, is a representation of the Green's function of the scatterer in a basis of spherical functions. All orders of multipoles are formally retained, in contrast to previous work involving the dipole approximation. Partial resummations of the scattering diagrams are shown to be related to the quasi-crystalline approximation and the first-order smoothing approximation. The lowest-order term of the ladder approximation for the incoherent intensity is evaluated. Sample numerical results are presented and compared with available experimental results.

## INTRODUCTION

We consider the propagation of plane coherent electromagnetic waves in an infinite medium containing identical, lossless, randomly distributed particles. Our aim here is to characterize the random medium by an effective complex wave number  $K$  (which would be a function of particle concentration, the electrical size, and the statistical description of the random positions of the scatterers) and to study both coherent and incoherent intensities as a function of frequency for various values of the concentration  $c$  (the fractional volume occupied by the scatterers). Although the formulation is generally valid for nonspherical, aligned, or randomly oriented scatterers, initial calculations are confined to spherical scatterers, which generally give us a better picture of the order of magnitude of the different contributions to the intensity without the additional complications of nonspherical geometry and orientation.

Extensive work by Twersky<sup>1-5</sup> has laid the foundation for multiple-scattering theory in discrete random media. A related approach using the T matrix of a single scatterer<sup>6</sup> together with configurational averaging procedures have been used by the authors to develop a computational method for the electromagnetic-wave-propagation problem in inhomogeneous media.<sup>7-9</sup> Lax's<sup>10</sup> quasi-crystalline approximation (QCA) is used in conjunction with suitable models for the pair correlation function to obtain an effective wave number  $K (= K_1 + iK_2)$  that is complex and frequency dependent. In a classic paper, Frisch<sup>11</sup> has demonstrated formally the relationship between the present problem and its analog in quantum mechanics. He used Feynman diagrams to show that the mean Green's function for the random medium is analogous to the Dyson equation, whereas the second moment of the Green's function is analogous to the Bethe-Salpeter equation. More interestingly, he showed that retaining only two-body correlations and summing all terms involving sequential scattering and correlation is equivalent to the first-order smoothing approximation first

introduced by Bourret<sup>12</sup> and used by Keller<sup>13</sup> and his co-workers.

In this paper, we represent the multiple-scattering series in a basis of vector spherical functions using the T matrix to characterize each scatterer. Formally, the T matrix includes a detailed description of the scatterer to all orders in a multipole expansion, this in contrast to previous treatments that invoked the dipole approximation. The so-called propagator or Green's function that propagates the signal from one scatterer to the next is again represented in a basis of vector spherical functions. This again is a consequence of not invoking the dipole approximation to describe the scatterer. Thus instead of simply using a full-space Green's function of the form  $\exp(ikr)/kr$ , as would be appropriate for point scatterers, the propagation matrix used here describes the propagation of a complex, multipole field to the next scatterer.

The partial resummations that can be performed by retaining only two-body correlations including only sequential scattering lead to so-called dressed propagators. These propagators describe a medium with a different propagation constant. One of the new observations we make is that the QCA first used by Lax<sup>10</sup> and the first-order smoothing approximation of Bourret<sup>12</sup> and Keller<sup>13</sup> appear to be the resummation of the same class of diagrams. This does not seem to have been commented on before.

In addition, the intensity of the electromagnetic field is also represented with the help of Feynman diagrams. The so-called coherent intensity is the summation of all diagrams that involve two independent field lines, whereas the incoherent intensity is the summation of all diagrams that involve two distinct field lines intercepting different scatterers but that are, however, coupled by positional correlations between scatterers. The lowest approximation to the incoherent intensity leads to the ladder diagrams. We also refer to the work by Tsang and Kong,<sup>14</sup> who have computed the backscattered intensity in single-scattering approximation.



Sample numerical results are presented for the first and the second moments of the field and compared with the experiments of Killey and Meeten.<sup>15</sup>

### MULTIPLE-SCATTERING FORMULATION

Consider wave propagation in an infinite medium of volume  $V \rightarrow \infty$  containing a random distribution of  $N$  scatterers,  $N \rightarrow \infty$ , such that  $n_0 = N/V$ , the number density of scatterers, is finite. Plane harmonic waves of frequency  $\omega$  propagate in the medium and undergo multiple scattering. Let  $E$ ,  $E^0$ ,  $E_i^e$ , and  $E_i^s$  denote, respectively, the total field, the incident field, the field exciting the  $i$ th scatterer, and the field scattered by the  $i$ th scatterer. Then self-consistency requires the following relationships among the fields<sup>7-9</sup>:

$$E = E^0 + \sum_{i=1}^N E_i^s \quad (1)$$

and

$$E_i^e = E^0 + \sum_{j \neq i} E_j^s. \quad (2)$$

Let  $O_u \psi_n$  generally denote outgoing functions (Hankel functions) and functions regular at the origin (Bessel functions). We dispense with vector notation, and the abbreviated index may denote  $n \rightarrow r, l, m, \sigma; r = 2, 3; l \in [0, \infty]; m \in [0, l]$ ; see Refs. 7-9.

At a field point  $r$  in the host medium, the incident, scattered, and exciting fields are expanded as follows:

$$E^0(r) = \sum_n a_n \text{Re} \psi_n(r), \quad (3)$$

$$E^e(r) = \sum_n \alpha_n^i \text{Re} \psi_n(r - r_i), \quad |r - r_i| < 2a, \quad (4)$$

$$E^s(r) = \sum_n f_n^i O_u \psi_n(r - r_i), \quad (r - r_i), \quad |r - r_i| > 2a, \quad (5)$$

where  $r_i$  denotes the center of the  $i$ th scatterer and  $a$  is the radius of the sphere circumscribing any scatterer. The coefficients  $a_n$  are known, whereas the coefficients  $f_n^i$  and  $\alpha_n^i$  are unknown but are, however, related through the T matrix<sup>6</sup>:

$$f_n^i = \sum_{n'} T_{nn'} \alpha_{n'}^i. \quad (6)$$

Substituting Eqs. (3)-(6) into Eq. (2) and using the translation-addition theorems for spherical wave functions and the orthogonality properties of spherical harmonics,<sup>8</sup> we obtain

$$\alpha_n^i = \alpha_n^i + \sum_{j \neq i} \sum_{n'} \sum_{n''} \sigma_{nn'}(r_j - r_i) T_{n'n''} \alpha_{n''}^j, \quad (7)$$

where

$$O_u \psi_n(r - r_j) = \sum_{n'} \sigma_{nn'}(r_i - r_j) \text{Re} \psi_{n'}(r - r_i) \quad (8)$$

and  $\sigma_{nn'}$  is the translation matrix for spherical wave functions.

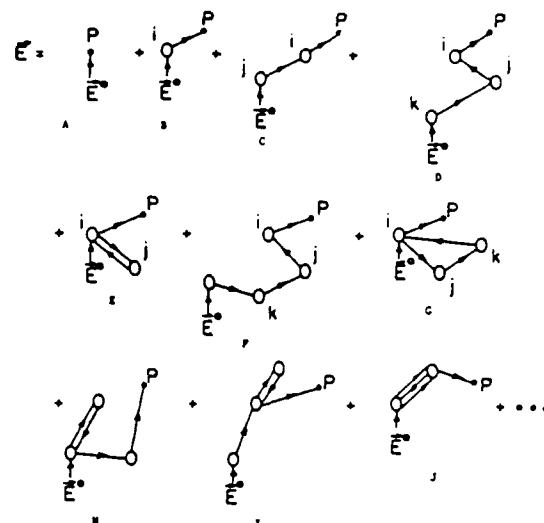


Fig. 1. A diagrammatic representation of multiple-scattering processes.

If we substitute Eqs. (7) and (5) in Eq. (1) and iterate, we obtain

$$E(r) = E^0(r) + \sum_i O_u \psi_n(r - r_i) T_{nn'} a_{n'}^i + \sum_{i,j} O_u \psi_n(r - r_i) T_{nn'} \sigma_{n'n''}(r_{ij}) T_{n''n'''} a_{n'''}^j + \sum_{i,j,k} O_u \psi_n(r - r_i) T_{nn'} \dots + \dots, \quad (9)$$

where  $r_{ij} = (r_j - r_i)$ .

The first term in Eq. (9) is the incident field reaching the observation point  $r$  denoted by  $P$  in Fig. 1A. The second term of Eq. (9) is a sum of  $N$  contributions, each of which can be represented by a diagram of the type shown in Fig. 1B. The thin line represents the incident field  $E^0$ , and the thick solid line represents the propagator  $O_u \psi_n(r - r_i) T_{nn'}$  that propagates the field from scatterer  $i$  to observation point  $r$ . The sum of all  $N$  diagrams of this type is termed single scattering. The third term of Eq. (9) is a sum of  $N(N-1)$  contributions, each involving a pair of particles, and is represented by the diagram of Fig. 1C. There are also  $N(N-1)$  terms of the form given in Fig. 1D that involve only a pair of particles. There are  $N(N-1)(N-2)$  terms of the type shown in Fig. 1E. As seen from Fig. 1, the three-body process can include any number of scattering in any order among the three objects.

### FIRST MOMENT OF THE FIELD AND THE QUASI-CRYSTALLINE APPROXIMATION

Equation (9) can be averaged over the positions of the particles to yield the coherent, average, or first moment of the field:



the QCA neglects back and forth scattering and includes only sequential scattering. By assuming that the average field propagates with an effective propagation constant  $K$ , i.e.,

$$\langle \alpha_n^{(j)} \rangle \simeq X_n \exp(iK\mathbf{k}_0 \cdot \mathbf{r}_j), \quad (21)$$

and using expressions (20) and (21) in Eq. (19), we formally obtain

$$X_n = n_0 \int \sigma_{nn'}(\mathbf{r}_{ij}) T_{nn'} p(\mathbf{r}_j | \mathbf{r}_i) \exp[i\mathbf{K} \cdot (\mathbf{r}_j - \mathbf{r}_i)] d\mathbf{r}_j X_n. \quad (22)$$

This is a homogeneous set of equations for  $X_n$ . For a non-trivial solution, the determinant of the coefficient matrix should vanish, leading to

$$|1 - n_0 \overline{\sigma g}(\mathbf{K}) T| = 0, \quad (23)$$

which is identical to Eq. (18).

Thus invoking the QCA is identical to a partial resummation of the multiple-scattering series represented by the diagrams in Eq. (11b). Although this has been generally known, no formal proof has been given before, especially when the full multipole description for each scattering is used. The more interesting observation is that Frisch<sup>11</sup> has shown that Eqs. (11) are also equivalent to the first-order smoothing approximation. Thus it would seem that the first-order smoothing and the QCA are equivalent. There appears to have been no discussion of this in previous literature on the subject.

## SECOND MOMENT OF THE FIELD INTENSITY

The intensity or the second moment of the field with polarization  $\hat{u}$  at  $\mathbf{r}$  is simply defined as

$$I_u(\mathbf{r}, \omega) = \hat{u} \cdot \langle \mathbf{E}(\mathbf{r}, \omega) \mathbf{E}(\mathbf{r}, \omega) \rangle \cdot \hat{u}. \quad (24)$$

If Eq. (9) is substituted for  $E$  in Eq. (24), we get the multiple-scattering series for the intensity. Diagrammatically each field line in Eq. (24) can be represented as in Fig. 1. When both fields are multiplied and then averaged together we get correlations between scatterers on both field lines. Using the same notation as before, the following diagrams result:

$$I_u(\mathbf{r}, \omega) = (\hat{u} \cdot \mathbf{E}^0)^2 + \left\{ \begin{array}{l} \text{Diagram 1} + \text{Diagram 2} + \dots \\ \text{Diagram 3} + \text{Diagram 4} + \dots \\ \text{Diagram 5} + \dots \\ \text{Diagram 6} + \dots \end{array} \right\} \quad (25)$$

where we have allowed only sequential two-body correlations and grouped the terms into four categories. The first term is, of course, the incident intensity. The second group contains two field lines that are uncorrelated from one to another but contain correlations within themselves. The third group contains two field lines that, however, interact with the same particles. The last group contains the ladder diagrams but also allows sequential correlations within each field line. All the other possible terms that contain diagrams of the type



have been neglected.

The first two groups of terms contribute to the coherent intensity, and the last two groups contribute to the incoherent intensity or spectral density of the field fluctuations. The diagrams can be resummed by introducing the so-called dressed propagators, if we refer to the translation operator  $\sigma_{nn'}(\mathbf{r}_{ij})$  in the host medium as a bare propagator. The dressed propagator is the propagator in a medium that allows only QCA-type sequential-scattering terms with sequential correlations and is identical to Eq. (16). Such propagators are represented by bold lines in contrast to the bare propagators. Thus

$$I_u(\mathbf{r}, \omega) = \left\{ \text{Diagram 1} \right\}_{(a)} + \left\{ \text{Diagram 2} \right\}_{(b)} + \left\{ \text{Diagram 3} + \text{Diagram 4} + \dots \right\}_{(c)}. \quad (26)$$

The terms in (b) can be summed by using Fourier transforms and convolution techniques, but the ladder diagrams in (c) do not lend themselves very easily to resummation by Fourier-transform techniques. The relative contribution of the terms in (b) and (c) is studied numerically in the next section.

## NUMERICAL RESULTS

Three types of results are presented in this section. The first type is the calculation of effective propagation constant by solving the roots of the determinantal equation [Eq. (18)]. The numerical procedure for doing this has been described in detail in Refs. 7 and 8 and will not be repeated here. The computation requires the T matrix of the scatterer; here we have used the multipole field for spherical scatterers. The concentration  $c$  of scatterers (fractional volume occupied by the scatterers) and the frequency are the other parameters required. In addition, the pair correlation function is required. We have used values generated by Monte Carlo simulation for hard or impenetrable spheres as a function of distance between the spheres and the concentration of spheres. The details may be found in Ref. 16.

In Figs. 2 and 3, the real and the imaginary part of the effective propagation constant in a distribution of Revacryl spheres is plotted as a function of concentration for two different frequencies denoted by the wavelengths  $\lambda = 410$  nm and  $\lambda = 546$  nm. These wavelengths were chosen because our calculations could be compared with the experiments of Killey and Meeten.<sup>15</sup> The agreement is very good, as can be seen from the graphs. The refractive index for Revacryl spheres used in the computation was taken to be  $n = 1.48$ , and the host medium is distilled water with  $n = 1.334$ .

In Fig. 4, the lowest approximation to the coherent intensity that is given by the first term in Eq. (26) was used to compute the coherent intensity. In lowest approximation,

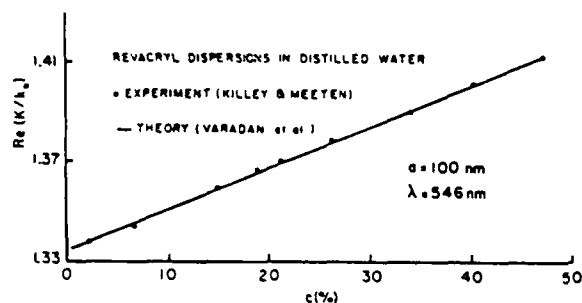


Fig. 2. Phase velocity versus concentration  $c$  for Revacryl dispersions in distilled water at  $\lambda = 546$  nm.

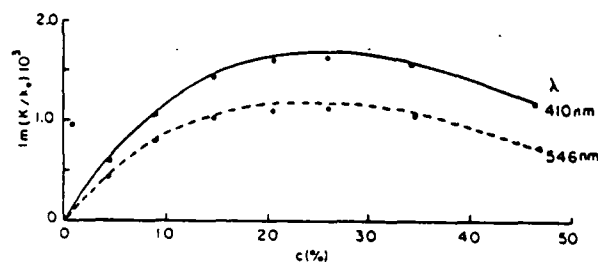


Fig. 3. Coherent attenuation versus concentration  $c$  for Revacryl dispersions in distilled water at  $\lambda = 410$  and  $546$  nm.

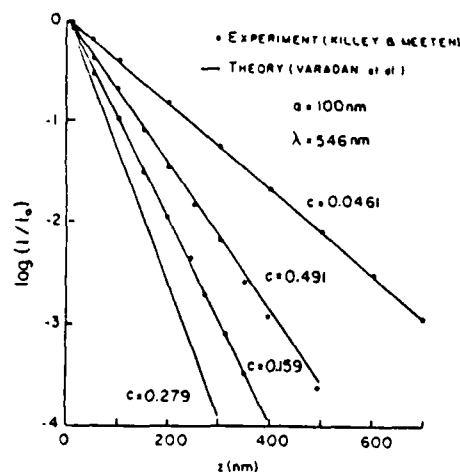


Fig. 4. Coherent intensity as a function of propagation depth  $z$  for various values of  $c$  at  $\lambda = 546$  nm.

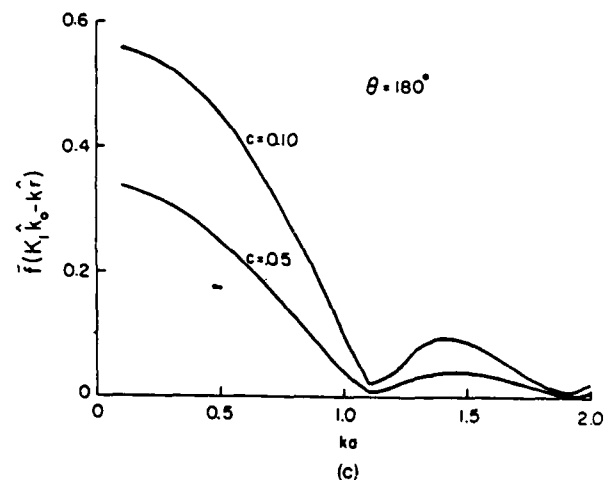
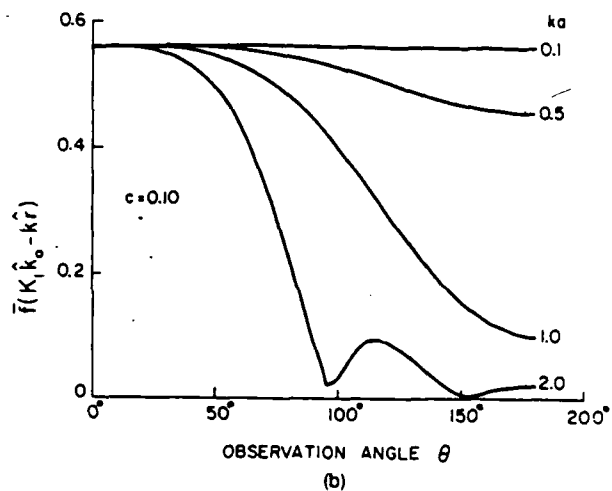
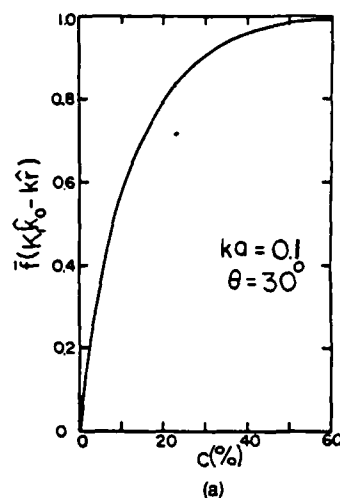


Fig. 5. (a) The spatial Fourier transform  $\tilde{f}(K_1 k_0 - k_r)$  of  $g(|x|) - 1$  as a function of concentration  $c$  for  $ka = 0.1$  and  $\theta = 30^\circ$ . (b) The spatial Fourier transform  $\tilde{f}(K_1 k_0 - k_r)$  of  $g(|x|) - 1$  as a function of observation angle  $\theta$  for  $c = 0.10$  and  $ka = 0.1, 0.5, 1.0$ , and  $2.0$ . (c) The spatial Fourier transform  $\tilde{f}(K_1 k_0 - k_r)$  of  $g(|x|) - 1$  as a function of  $ka$  in the backscattering direction for  $c = 0.05$  and  $0.10$ .

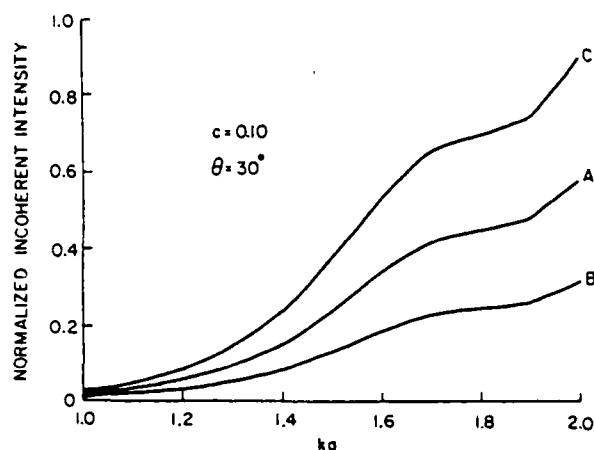


Fig. 6. Normalized incoherent intensity that is due to single scattering from correlated scatterers as a function of  $ka$  for  $c = 0.10$  and  $\theta = 30^\circ$ .

the intensity decays exponentially with penetration into the random medium, the rate of decay being twice the imaginary part of the effective propagation constant ( $K = K_1 + iK_2$ ) in the medium. The rate is a function of the frequency, the size of scatterers, the concentration of scatterers, and the material properties. Again the results normalized with respect to the incident intensity in Fig. 3 for Revacryl spheres comes quite favorably with the results of Killey and Meeten.

In Figs. 5 and 6, the leading term for the incoherent intensity involving only single scattering from one scatterer (A) or two correlated scatterers (B) is plotted for various parameters. The total single-scattering result is denoted by C in Fig. 6. The exact expression used in the computations is given below:

$$\begin{aligned}
 I_\theta(\mathbf{r}, \omega) &= \hat{\theta} \cdot (\mathbf{E}(\mathbf{r}, \omega) \mathbf{E}^*(\mathbf{r}, \omega)) \cdot \hat{\theta} \\
 &= \frac{n_0}{(kr)^2} \left| \sum_n \hat{\theta} \cdot \mathbf{A}_n(\hat{\mathbf{r}}) T_n a_n(\hat{\mathbf{k}}_0) \right|^2 V_s \\
 &\quad \times \left\{ 1 + n_0 \int (g(\mathbf{x}) - 1) \exp[-i(K_1 \hat{\mathbf{k}}_0 - k\hat{\mathbf{r}}) \cdot \mathbf{x}] d\mathbf{x} \right\} \\
 &= \frac{N}{(kr)^2} \left| \sum_n \hat{\theta} \cdot \mathbf{A}_n(\hat{\mathbf{r}}) T_n a_n(\hat{\mathbf{k}}_0) \right|^2 \underbrace{[1]}_A + \underbrace{\tilde{f}(K\hat{\mathbf{k}}_0 - k\hat{\mathbf{r}})}_B.
 \end{aligned} \quad (27)$$

$\hat{\mathbf{k}}_0$  is the direction of propagation of the incident wave,  $a_n(\hat{\mathbf{k}}_0)$  are the incident-wave field coefficients,  $\tilde{f}(K_1 \hat{\mathbf{k}}_0 - k\hat{\mathbf{r}})$  is the spatial Fourier transform of  $[g(\mathbf{x}) - 1]$ , and  $\mathbf{A}_n = \mathbf{A}_{\tau i m \tau}$  are vector spherical harmonics with  $\tau = 1, 2, 3$ .

In order to study the difference in the order of magnitude of corresponding terms (equal number of T matrices), one can simply plot expressions A and B in Eq. (27) as a function of concentration. Although these terms will be a function of frequency for higher-order terms of the multiple-scattering series, we can get a feel for the relative contribution of these terms. They are plotted in Fig. 5(a) and one can see that, even at a concentration of 10%, the value of the correlation integral [term B of Eq. (27)] is approximately 36% of A. This implies that there is no point in summing higher-order

terms in (b) of Eq. (26) without also retaining higher-order ladder diagrams.

In Fig. 5(b),  $\tilde{f}(K_1 \hat{\mathbf{k}}_0 - k\hat{\mathbf{r}})$  in Eq. (27) is plotted as a function of observation angle for different values of  $ka$ . It can be seen that for  $\theta = 180^\circ$ , the contribution from  $\tilde{f}$  to the incoherent intensity is greatly dependent on the value of  $ka$  under consideration. In Fig. 5(c),  $\tilde{f}$  is plotted for two values of  $c = 0.05$  and  $0.1$  and  $\theta = 180^\circ$  (backscattering) as a function of  $ka$ .

The conclusion from Figs. 5(a)–5(c) is that the incoherent intensity has contributions from both (b) and (c) in Eq. (26), and more studies are indicated to neglect one in favor of the other.

In Fig. 6, the normalized incoherent intensity is plotted as a function of  $ka$  at  $c = 0.1$  for an observation angle of  $30^\circ$ . The curve labeled C is the total contribution that is due to single scattering; the curve A is due to completely correlated or single scattering from the same particle I, and B is due to I. It is clear that B is not negligible compared to A.

## ACKNOWLEDGMENT

This research was supported by the U.S. Army Research Office under contract no. DAAG 29-84-K-0187 to The Pennsylvania State University.

## REFERENCES

1. V. Twersky, "Coherent scalar field in pair-correlated random distributions of aligned scatterers," *J. Math. Phys.* 18, 2468–2486 (1977).
2. V. Twersky, "Coherent electromagnetic waves in pair-correlated random distributions of aligned scatterers," *J. Math. Phys.* 19, 215–230 (1978).
3. V. Twersky, "Multiple scattering of waves by periodic and by random distributions," in *Electromagnetic Scattering*, P. L. E. Uslenghi, ed. (Academic, New York, 1978), pp. 221–251.
4. V. Twersky, "Acoustic bulk parameters in distribution of pair-correlated scatterers," *J. Acoust. Soc. Am.* 64, 1710–1719 (1978).
5. V. Twersky, "Propagation and attenuation in composite media," in *Macroscopic Properties of Disordered Media*, Vol. 154 of *Lecture Notes in Physics*, R. Burridge and S. Childress, eds. (Springer-Verlag, New York, 1982), pp. 258–271.
6. V. K. Varadan and V. V. Varadan, eds., *Acoustic, Electromagnetic and Elastic Wave Scattering—Focus on the T-Matrix Approach* (Pergamon, New York, 1980).
7. V. V. Varadan, V. N. Brongi, and V. K. Varadan, "Frequency dependent dielectric constants of discrete random media," in *Macroscopic Properties of Disordered Media*, Vol. 154 of *Lecture Notes in Physics*, R. Burridge and S. Childress, eds. (Springer-Verlag, New York, 1982), pp. 272–284.
8. V. N. Brongi, V. K. Varadan and V. V. Varadan, "Coherent wave attenuation by a random distribution of particles," *Radio Sci.* 17, 946–952 (1982).
9. V. K. Varadan, V. N. Brongi, V. V. Varadan, and A. Ishimaru, "Multiple scattering theory for waves in discrete random media and comparison with experiments," *Radio Sci.* 18, 321–327 (1983).
10. M. Lax, "Wave propagation and conductivity in random media," in *Proceedings of the SIAM-AMS Conference on Stochastic Differential Equations* (American Mathematical Society, Providence, R.I., 1970), Vol. VI, pp. 35–95.
11. V. Frisch, "Wave propagation in random media," in *Probabilistic Methods in Applied Mathematics*, A. T. Bharucha-Reid, ed. (Academic, New York, 1968).
12. R. C. Bourret, "Stochastically perturbed fields, with applications to wave propagation in random media," *Nouvo Cimento* 26, 1–31 (1962).
13. J. B. Keller, "Wave Propagation in Random media," in *Pro-*

- ceedings of the Symposium on Applied Mathematics* (American Mathematical Society, Providence, R.I., 1962), Vol. 13, pp. 227-246.
14. L. Tsang and J. A. Kong, "Scattering of electromagnetic waves from a half space of density distributed dielectric scatterers," *Radio Sci.* 18, 1260-1272 (1983).
  15. A. Killey and G. H. Meeten, "Optical extinction and refraction of concentrated latex dispersions," *J. Chem. Soc., Faraday Trans. 2*, 587-599 (1981).
  16. J. A. Barker and D. Henderson, "Monte Carlo values for the radial distribution function of a system of fluid hard spheres," *Mol. Phys.* 21, 187-191 (1971).

# Design of Ferrite-Impregnated Plastics (PVC) as Microwave Absorbers

VIJAY K. VARADAN, MEMBER, IEEE, VASUNDARA V. VARADAN, MEMBER, IEEE,  
YUSHIEH MA, AND W. F. HALL

**Abstract**—This paper is concerned with the modeling of absorption of microwaves in a composite containing a random distribution of  $\text{Fe}_3\text{O}_4$  particles embedded in PVC. The theoretical model based on a self-consistent multiple scattering formalism, including the effect of statistical correlations in the positions of the particles. A T-matrix is used to characterize the response of individual ferrite particles to any incident excitation. An analytical expression is obtained for the complex propagation constant in the composite in the long wavelength limit.

In addition to presenting results for a variety of materials including Ni ferrite compounds, it is shown that a particular set of assumed values of the complex magnetic permeability and dielectric function leads to very good agreement with the experimental data of Ueno *et al.* [2].

## I. INTRODUCTION

THE HIGH DIELECTRIC and magnetic loss tangents of the magnetite  $\text{Fe}_3\text{O}_4$  makes it an ideal candidate for applications to microwave absorbing materials. Generally, the  $\text{Fe}_3\text{O}_4$  particles in the form of spheres or cylinders are held together by a binder such as PVC. Since weight and the structural integrity of the composite is also of concern in many applications, it is desirable to choose the optimum volume fraction of  $\text{Fe}_3\text{O}_4$  particles and adjust the shape, size, and distribution of particles to obtain the required mass density and microwave absorbing properties. A reliable theoretical model that can predict effective properties for various values of these parameters is an economical way to arrive at the optimum configuration. Such a model is proposed in this paper.

Since the use of ferrites in microwave absorbing composites is relatively new, measured values of the electrical and magnetic properties of ferrites are difficult to find in the literature. For many types of ferrites, it is hard to measure the complex permeability and the complex permittivity due to the high electrical conductivity of  $\text{Fe}_3\text{O}_4$ . For some materials, such as the Ni ferrite compounds, one can find measured values of complex permeability but not of permittivity. This may be due to the fact that completely different techniques are called for the two measurements. One may refer to Lax and Button [1].

Recently, Ueno *et al.* [2] have reported experimental results for iron oxide ( $\text{Fe}_3\text{O}_4$ ) impregnated plastics (PVC)

in the 0.1–10-GHz range of frequencies. Plots of  $\mu'$ ,  $\mu''$ ,  $\epsilon'$ , and  $\epsilon''$  of the composite are plotted as a function of frequency. The reflection and transmission coefficients of the composite slab for various angles of incidence are also plotted as a function of layer thickness as well as angle of incidence. The only other reference that provides some useful information on the material properties is the book by Smit and Wijn [3]. We believe that there may be other sources, especially in the internal research reports of various industrial and government research laboratories, that may be of a proprietary nature and, hence, not easily available.

The plan of this paper is as follows. In Section II, the multiple scattering formalism is presented. In Section III, long wavelength approximation are invoked to obtain a closed-form solution of the dispersion equation for a ferrite composite. The equation can be explicitly solved for spherical particles, for arbitrary concentration within the limitations imposed by the quasi-crystalline approximation. Analytical expressions for the effective complex wave-number are presented. In Section IV, the calculations and results for  $\text{Fe}_3\text{O}_4$  composites are explained and the comparison with the experimental results of Ueno *et al.* is discussed. A short summary and conclusions end the paper.

## II. MULTIPLE SCATTERING FORMALISM

Consider the propagation of plane-harmonic electromagnetic waves along the  $z$  axis of an  $xyz$  coordinate system in a medium referred to as the host or matrix characterized by real values of the dielectric function  $\epsilon_2$  and magnetic permeability  $\mu_2$ . Embedded in the matrix is a random distribution of randomly oriented scatterers characterized by a complex permittivity  $\epsilon_1 = \epsilon'_1 + i\epsilon''_1$  and complex permeability  $\mu_1 = \mu'_1 + i\mu''_1$ . In this paper, the time dependence  $e^{-i\omega t}$  is assumed throughout. The number of scatterers  $N$  and the embedding volume  $V$  are both large, but when  $N/V = n_0$ , the number density is finite.

The total field at any point in the host medium is the sum of the incident field and the fields scattered by all the scatterers. The field that excites a given scatterer (say, the  $i$ th scatterer),  $\vec{E}_i^{\text{inc}}$ , however, is the incident field  $\vec{E}^{\text{inc}}$ , plus the fields scattered from all the other scatterers  $\vec{E}_j^{\text{sc}}$

$$\vec{E}_i^{\text{sc}}(\vec{r}) = \vec{E}^{\text{inc}}(\vec{r}) + \sum_{j \neq i}^N \vec{E}_j^{\text{sc}}(\vec{r} - \vec{r}_j) \quad (1)$$

Manuscript received March 18, 1985; revised September 25, 1985.  
V. K. Varadan, V. V. Varadan, and Y. Ma are with the Laboratory for Electromagnetic and Acoustic Research, Department of Engineering Science, Pennsylvania State University, University Park, PA 16802.  
W. F. Hall is with Rockwell International Science Center, Thousand Oaks, CA 91360.  
IEEE Log Number 8406471

where  $\vec{r}$  and  $\vec{r}_j$  are the observation point and the position of the  $j$ th scatterer, respectively. Expanding all the fields in terms of vector spherical functions and employing the translation theorem and the orthogonality of the basis functions, we obtain (see Varadan *et al.* [4] and Brangi *et al.* [5])

$$b_n^{m(i)} = \frac{2n+1}{n(n+1)} i^n \frac{e^{i\vec{k} \cdot \vec{r}_i}}{2i} [\delta_{m,1} + n(n+1)\delta_{m,-1}] \\ + \sum_{j=1}^N \sum_{n_1=0}^{\infty} \sum_{m_1=-n_1}^{n_1} [B_{n_1}^{m_1(i)} B_{m_1 n_1}^{m n}(\vec{r}_i - \vec{r}_j) \\ + C_{n_1}^{m_1(i)} C_{m_1 n_1}^{m n}(\vec{r}_i - \vec{r}_j)] \quad (2)$$

$$c_n^{m(i)} = \frac{2n+1}{n(n+1)} i^n \frac{e^{i\vec{k} \cdot \vec{r}_i}}{2i} [\delta_{m,1} + n(n+1)\delta_{m,-1}] \\ + \sum_{j=1}^N \sum_{n_1=0}^{\infty} \sum_{m_1=-n_1}^{n_1} [B_{n_1}^{m_1(i)} C_{m_1 n_1}^{m n}(\vec{r}_i - \vec{r}_j) \\ + C_{n_1}^{m_1(i)} B_{m_1 n_1}^{m n}(\vec{r}_i - \vec{r}_j)] \quad (3)$$

where  $\Sigma'$  denotes  $j \neq i$ ,  $\delta_{mn}$  is the Kronecker delta, and  $k$  is the wavenumber in the host medium.  $B_n^m$  and  $C_n^m$  are the scattered field coefficients,  $b_n^m$  and  $c_n^m$  are the exciting field coefficients, and  $B_{n_1}^{m_1(i)}$  and  $C_{n_1}^{m_1(i)}$  are the functions resulting from the translation theorem of the vector spherical functions.

Now we introduce the T-matrix of a single scatterer which relates the scattered field expansion coefficients to the exciting field expansion coefficients as follows (see, for example, [6]):

$$\begin{pmatrix} B \\ C \end{pmatrix} = \begin{bmatrix} T^{11} & T^{12} \\ T^{21} & T^{22} \end{bmatrix} \begin{pmatrix} b \\ c \end{pmatrix} = (T) \begin{pmatrix} b \\ c \end{pmatrix}. \quad (4)$$

For aligned identical scatterers, if the T-matrix is computed with respect to the  $xyz$  axes, then the T-matrix of all  $N$  scatterers is the same. However, if the orientation of each scatterer with respect to the  $xyz$  axes is defined by the Euler angles  $\alpha, \beta, \gamma$ , then the T-matrix of the  $i$ th scatterer is a function of the Euler angles and is defined by

$$T = D \hat{T} D^{-1} \quad (5)$$

where  $\hat{T}$  is the T-matrix of a scatterer evaluated with respect to the set of coordinate axes natural to the scatterer ( $XYZ$  axes), and is independent of position and orientation and is, hence, the same for identical scatterers.  $D$  is the rotation matrix given by Edmonds [7]

$$D_{nm}^n(\alpha, \beta, \gamma) = e^{im\alpha} d_{nm}^n(\beta) e^{in\gamma} \quad (6)$$

where

$$d_{nm}^n(\beta) = \left[ \frac{(n+m)!(n-m)!}{(n+m')!(n-m')!} \right]^{1/2} \left( \cos \frac{\beta}{2} \right)^{n+m'} \\ \cdot \left( \sin \frac{\beta}{2} \right)^{m-m'} P_{n-m}^{(n-m', m'-m)}(\cos \beta). \quad (7)$$

In (7),  $P$  is the Jacobi polynomial, which can be expressed in terms of the associated Legendre polynomials (see Edmonds [7]).

The T-matrix averaged over all possible orientations of the scatterer may then be written as

$$\langle T_{nm, n'm'} \rangle = \frac{1}{8\pi^2} \int_0^{2\pi} d\alpha \int_0^{2\pi} d\gamma \int_0^\pi d\beta \sin \beta \\ \cdot \sum_{m_1, m_2} [D_{m m_1}^n(\alpha, \beta, \gamma) \hat{T}_{n m_1, n' m_2} \\ \cdot (D^{-1})_{m_2 m'}^{n'}(\alpha, \beta, \gamma)] \\ = \frac{1}{2n+1} \sum_{m_1, m_2} \hat{T}_{n m_1, n' m_2} \delta_{m m_1} \delta_{m_2 m'} = \hat{T}_{n m, n' m'}. \quad (8)$$

If (2) and (3) are multiplied by  $\langle T \rangle$  from (8), we obtain a set of coupled equations for the scattered field expansion coefficients which are averaged over all possible orientations.

It remains now to perform an average over all possible positions. To this end, one can introduce a probability density function of finding the first scatterer at  $\vec{r}_1$ , the second scatterer at  $\vec{r}_2$ , and so forth by  $p(\vec{r}_1, \vec{r}_2, \dots, \vec{r}_N)$ , which in turn may be expressed in terms of conditional probability  $p(\vec{r}_j|\vec{r}_i)$ , of finding a scatterer at  $\vec{r}_j$  if a scatterer is known to be at  $\vec{r}_i$ . The two-point joint probability function  $p(\vec{r}_i|\vec{r}_j)$  is in turn defined in terms of the radial distribution function  $g(|\vec{r}_j - \vec{r}_i|)$  as follows:

$$p(\vec{r}_j|\vec{r}_i) = \begin{cases} \frac{1}{V} g(|\vec{r}_j - \vec{r}_i|), & |\vec{r}_j - \vec{r}_i| \geq 2a \\ 0, & |\vec{r}_j - \vec{r}_i| < 2a \end{cases} \quad (9)$$

where  $V$  is the large but finite volume occupied by the scatterers and  $2a$  is the largest dimension of the scatterer. Here, the scatterers are not permitted to penetrate one another. Several models of  $g(r)$  are available and are briefly outlined in Brangi *et al.* [8]. The radial distribution functions obtained using the self-consistent approximation, which is a linear combination of the Percus-Yevick and hypernetted chain approximations, seem to be good for a wide range of concentrations, and are also used in our computations here. Improved forms of  $g(r)$  as outlined by Twersky [9] for nonspherical statistics can also be employed if it can be extended to higher orders of concentration. Performing the configurational averaging and invoking the quasi-crystalline approximation as outlined in Twersky [10] and Varadan *et al.* [11], [12]. We obtain the average scattered field coefficients as follows:

$$\begin{bmatrix} \langle B_{nm}^i \rangle \\ \langle C_{nm}^i \rangle \end{bmatrix} = \begin{bmatrix} \langle T^{11} \rangle & \langle T^{12} \rangle \\ \langle T^{21} \rangle & \langle T^{22} \rangle \end{bmatrix} \begin{bmatrix} \langle \psi_{n, m_1}^i \rangle \\ \langle \chi_{n, m_1}^i \rangle \end{bmatrix} \quad (10)$$



where

$$\begin{aligned} \langle \psi'_{n_1 m_1} \rangle &= \frac{2n_1+1}{n_1(n_1+1)} i^{n_1} \frac{e^{i\vec{k} \cdot \vec{r}_i}}{2i} \left[ \delta_{m_1,1} + n_1(n_1+1) \delta_{m_1,-1} \right] \\ &+ \frac{1}{V} \sum_{j=1}^N \sum_{n_2=0}^{\infty} \sum_{m_2=-n_2}^{n_2} \int_{V'} \left[ \langle B'_{n_2 m_2} \rangle B_{n_1 m_1}^{n_2 m_2}(\vec{r}_i - \vec{r}_j) \right. \\ &\left. + \langle C'_{n_2 m_2} \rangle C_{n_1 m_1}^{n_2 m_2}(\vec{r}_i - \vec{r}_j) \right] g(|\vec{r}_j - \vec{r}_i|) d\vec{r}_j \quad (11) \end{aligned}$$

and

$$\begin{aligned} \langle \chi'_{n_1 m_1} \rangle &= \frac{2n_1+1}{n_1(n_1+1)} i^{n_1} \frac{e^{i\vec{k} \cdot \vec{r}_i}}{2i} \left[ \delta_{m_1,1} + n_1(n_1+1) \delta_{m_1,-1} \right] \\ &+ \frac{1}{V} \sum_{j=1}^N \sum_{n_2=0}^{\infty} \sum_{m_2=-n_2}^{n_2} \int_{V'} \left[ \langle B'_{n_2 m_2} \rangle C_{n_1 m_1}^{n_2 m_2}(\vec{r}_i - \vec{r}_j) \right. \\ &\left. + \langle C'_{n_2 m_2} \rangle B_{n_1 m_1}^{n_2 m_2}(\vec{r}_i - \vec{r}_j) \right] g(|\vec{r}_j - \vec{r}_i|) d\vec{r}_j. \quad (12) \end{aligned}$$

In (11) and (12),  $V'$  denotes the volume of the medium excluding a sphere of radius  $2a$ . For identical scatterers  $\sum_{j=1}^N = N-1$  and  $4\pi(N-1)a^3/3V = c$ , the volume concentration of "scatterers" provided  $N$  is large enough.

To find the average propagation constant  $K$  for the composite medium, we assume a plane-wave propagation with effective wavenumber  $\vec{K}$  in the same direction as the incident wave direction with unknown amplitudes  $Y$  and  $Z$

$$\begin{aligned} \langle B_{nm}^i \rangle &= Y_{nm} e^{i\vec{K} \cdot \vec{r}_i} \\ \langle C_{nm}^i \rangle &= Z_{nm} e^{i\vec{K} \cdot \vec{r}_i}. \quad (13) \end{aligned}$$

Equation (13) is substituted in (10) and the extinction theorem can be invoked to cancel the incident wave term on the right-hand side of (11) and (12). The resulting equations are

$$\begin{aligned} Y_{nm} &= \sum_{q=|n_1-n_2|}^{|n_1+n_2|} \sum_{n_1=0}^{\infty} \sum_{n_2=0}^{\infty} \sum_{m_1=-n_1}^{n_1} \sum_{m_2=-n_2}^{n_2} (-1)^{m_2/n_2-n_1} \delta_{m_1, m_2} (JH)_q \\ &\cdot \left\{ Y_{n_2 m_2} \left[ \langle T^{11} \rangle_{nm, n_1 m_1} a(n_2, n_1, q) a(m_2, n_2 | -m_1, n_1 | q) \right. \right. \\ &- \langle T^{12} \rangle_{nm, n_1 m_1} b(n_2, n_1, q) a(m_2, n_2 | -m_1, n_1 | q, q-1) \Big] \\ &+ Z_{n_2 m_2} \left[ \langle T^{12} \rangle_{nm, n_1 m_1} a(n_2, n_1, q) a(m_2, n_2 | -m_1, n_1 | q) \right. \\ &\left. \left. - \langle T^{11} \rangle_{nm, n_1 m_1} b(n_2, n_1, q) a(m_2, n_2 | -m_1, n_1 | q, q-1) \right] \right\} \quad (14a) \end{aligned}$$

and

$$Z_{nm} = \dots \quad (14b)$$

where (14b) can be obtained from (14a) by replacing  $\langle T^{11} \rangle$  and  $\langle T^{12} \rangle$  by  $\langle T^{21} \rangle$  and  $\langle T^{22} \rangle$ , respectively. The term  $(JH)_q$  is given by

$$\begin{aligned} (JH)_q &= \frac{6c}{(ka)^2 - (Ka)^2} \left[ 2kaj_q(2Ka)h'_q(2ka) \right. \\ &- 2Kah_q(2ka)j'_q(2Ka) \Big] \\ &+ 24c \int_1^\infty x^2 [g(x) - 1] \\ &\cdot h_q(2kax)j_q(2Kax)dx. \quad (15) \end{aligned}$$

In (14) and (15),  $j_q$  and  $h_q$  are the spherical Bessel functions, and the primes denote differentiation with respect to the argument. The expressions for "a" and "b" occurring in (14) are related to the Wigner 3-j symbols and are given by Cruzan [13]. Setting the determinant of the coefficient matrix generated from (14) to zero, we can solve for the average propagation constant  $K = K_1 + iK_2$ . The real part  $K_1$  is related to the phase velocity, while the imaginary part  $K_2$  is related to the coherent attenuation. For ferrites, it is not possible to obtain the values of  $\mu$  and  $\epsilon$  separately from a knowledge of the wavenumber alone. For nonmagnetic materials with  $\mu = \mu_0$ , this is possible.

### III. ANALYTICAL SOLUTION FOR THE EFFECTIVE WAVENUMBER IN A FERRITE COMPOSITE FOR MICROWAVE FREQUENCIES

Equations (14) and (15) of the previous section can be solved numerically as illustrated in several papers by Varadan *et al.* [11], [12]. For the problem at hand, it was more convenient to solve the truncated set of dispersion equations analytically. At frequencies in the gigahertz range, the wavelength in PVC is of the order of several millimeters. Radar absorbing composites have to be designed such that enough attenuation and reflection reduction is achieved in a coating which is a millimeter or two in thickness. The ferrite particles are much smaller than a millimeter in diameter. Thus, one can safely solve the dispersion equation in the long wavelength approximation.

Retaining only the dipole terms in (14), we obtain

$$\begin{vmatrix} (T^{11})_{11}(JH_0 + \frac{1}{2}JH_2) - 1 & \frac{1}{2}(T^{22})_{11}JH_1 \\ \frac{1}{2}(T^{11})_{11}JH_1 & (T^{22})_{11}(JH_0 + \frac{1}{2}JH_2) - 1 \end{vmatrix} = 0. \quad (16)$$

The hole correction and the correlation integral of (15) can be written analytically as

$$\begin{aligned} JH_n &= \frac{6c}{(ka)^2 - (Ka)^2} \left[ 2kaj_n(2Ka)h'_n(2ka) \right. \\ &- 2Kah_n(2ka)j'_n(2Ka) \Big] \\ &+ 24c \int_1^\infty x^2 [g(x) - 1] \\ &\cdot h_n(2kax)j_n(2Kax)dx. \quad (17) \end{aligned}$$

For spherical particles, the dipole term of the T-matrix

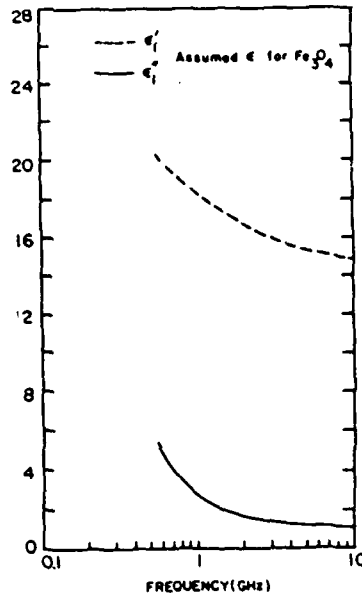


Fig. 1. Permittivity versus frequency.

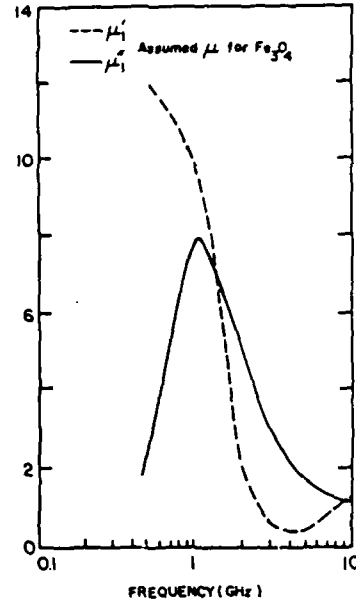


Fig. 2. Permeability versus frequency.

takes the form

$$(T^{11})_{11} = \frac{-\{\mu_1 j_{11}[2j_{12} - (k_2 a)j_{22}] - \mu_2 j_{12}[2j_{11} - (k_1 a)j_{21}]\}}{\{\mu_1 j_{11}[2h_{12} - (k_2 a)h_{22}] - \mu_2 h_{12}[2j_{11} - (k_1 a)j_{21}]\}}$$

$$(T^{22})_{11} = \frac{-\{\mu_1 j_{12}[2j_{11} - (k_1 a)j_{21}] - \mu_2 \frac{\epsilon_1 \mu_1}{\epsilon_2 \mu_2} j_{11}[2j_{12} - (k_2 a)j_{22}]\}}{\{\mu_1 h_{12}[2j_{11} - (k_1 a)j_{21}] - \mu_2 \frac{\epsilon_1 \mu_1}{\epsilon_2 \mu_2} j_{11}[2h_{12} - (k_2 a)h_{22}]\}} \quad (18)$$

According to the symmetry of the T-matrix for a spherical scatterer

$$(T^{12})_{11} = 0 \quad \text{and} \quad (T^{21})_{11} = 0.$$

Here, the following notation has been used:

$$j_{nm} = j_n(k_m a) \quad \text{spherical Bessel function}$$

$$h_{nm} = h_n(k_m a) \quad \text{spherical Hankel function,}$$

$$n, m = 1, 2$$

and the subscripts 1 and 2 for  $k$  (or subscripts 1 and 2 for  $\mu$  and  $\epsilon$ ) represent the properties of the scatterer and the matrix, respectively.

In the microwave frequency range, the solution to the effective properties of a ferrite composite, which is a mixture of ferrite particles embedded in a plastic matrix, is given as

where  $\eta = (K_1/k_0) + i(K_2/k_0)$ . The real part of  $\eta$  enables us to calculate the effective index of refraction, while the attenuation in the composite is inferred by the imaginary part of  $\eta$ .

The parameters in (19) are now defined as follows:

$$\sigma = c^2(U - \gamma^2 U - 2\gamma V)/y_2 \quad \nu = c^2(2\gamma U + V - \gamma^2 V)/y_2$$

$$\zeta_1 = C(\hat{B}\gamma + \hat{A})/y_1 \quad \zeta_2 = C(\hat{D}\gamma - \hat{C})/y_1$$

$$\zeta_3 = C(\gamma\hat{C} + \hat{D})/y \quad \zeta_4 = C(\hat{A}\gamma - \hat{B})/y_1$$

$$U = \hat{B} \cdot \hat{C} - \hat{A} \cdot \hat{D}$$

$$V = \hat{A} \cdot \hat{C} + \hat{B} \cdot \hat{D}$$

$$\hat{A} = 2(B\gamma + A), \quad \hat{B} = 2(A\gamma - B),$$

$$\hat{C} = 2(C\gamma - D), \quad \hat{D} = 2(D\gamma + C)$$

$$A = [(\mu'_1 - \mu'_2)(2\mu'_2 + \mu'_1) + (\mu''_1 - \mu''_2)(2\mu''_2 + \mu''_1)]/\Delta$$

$$B = [(\mu'_1 - \mu'_2)(2\mu'_2 + \mu'_1) - (\mu''_1 - \mu''_2)(2\mu''_2 + \mu''_1)]/\Delta$$

$$C = [(\epsilon'_1 - \epsilon'_2)(2\epsilon'_2 + \epsilon'_1) + (\epsilon''_1 - \epsilon''_2)(2\epsilon''_2 + \epsilon''_1)]/\Delta'$$

$$D = [(\epsilon'_1 - \epsilon'_2)(2\epsilon'_2 + \epsilon'_1) - (\epsilon''_1 - \epsilon''_2)(2\epsilon''_2 + \epsilon''_1)]/\Delta'$$

$$\eta^2 = \frac{4(\sigma - 1 - \zeta_1 - \zeta_3) + 4i(\nu - \zeta_2 - \zeta_4 + \beta\hat{D}w + \beta\hat{A}w - 2wcU\beta/y_1 + 2wc\beta UV/y_1)}{(\sigma - 2 + 2\zeta_1 + 2\zeta_3) + i[\nu + 2\zeta_2 + 2\zeta_4 + 4\beta\hat{A}w + 4\beta\hat{D}w + (4\beta wcU/y_1)]} \quad (19)$$

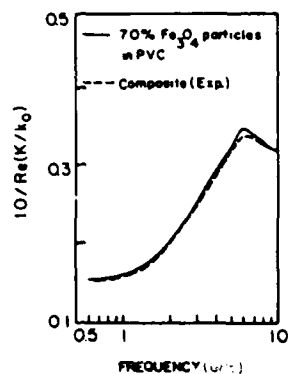


Fig. 3. Normalized value of the real part of the effective wavenumber versus frequency.

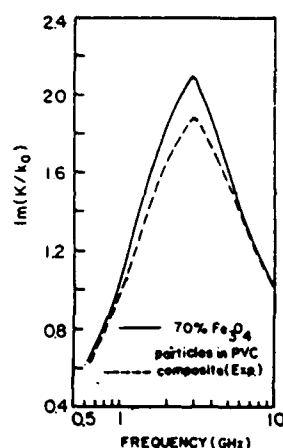


Fig. 4. Normalized value of the imaginary part of the effective wavenumber versus frequency.

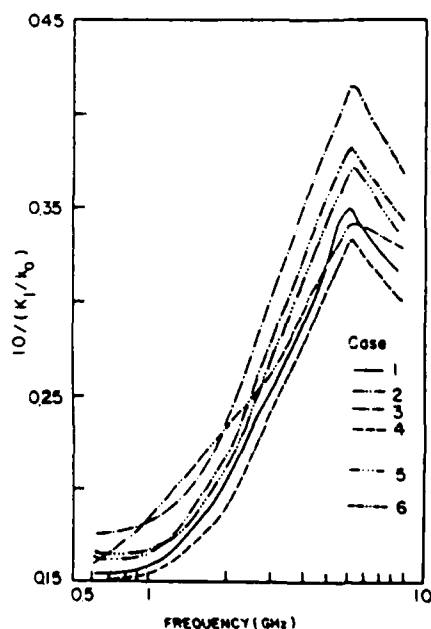


Fig. 5. Normalized value of the real part of the effective wavenumber versus frequency for different cases.

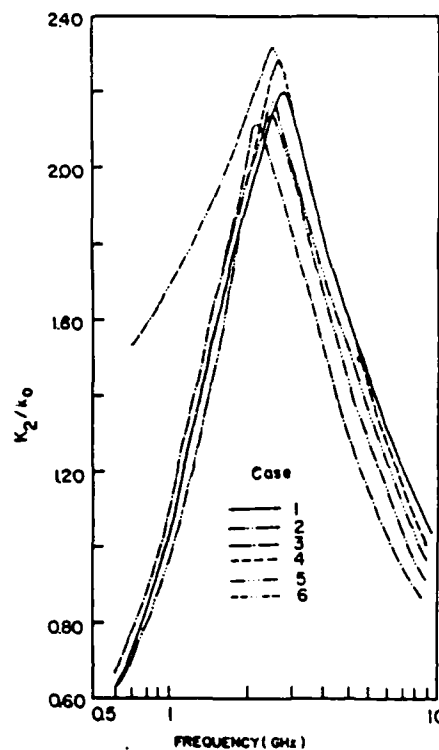


Fig. 6. Normalized value of the imaginary part of the effective wavenumber versus frequency for different cases.

TABLE I

Case 1. Assumed properties for  $\text{Fe}_3\text{O}_4$  which match well with the experimental data ( $\epsilon_1'$ ,  $\epsilon_1''$ ,  $\mu_1'$ , and  $\mu_1''$  for  $\text{Fe}_3\text{O}_4$  can be found in Figure 1).

Case 2. Properties of case 1, but reduce  $\mu_1$  by 20%.

Case 3. Properties of case 1, but reduce  $\mu_1$  by 33 1/3%.

Case 4. Properties of Case 1, but increase  $\epsilon_1$  by 20%.

Case 5. Properties of case 1, but reduce  $\epsilon_1$  by 20%.

Case 6.  $\epsilon_1$  in case 1, but  $\mu_1$  as for  $\text{NiFe}_2\text{O}_4$  ( $d=4.18$ ).

The properties for PVC

$\epsilon_2' = 2$ ,  $\epsilon_2'' = 0$   
 $\mu_2' = 1$ ,  $\mu_2'' = 0$   
 (values are relative to free space)

$$\Delta = (2\mu_2' + \mu_1')^2 + (2\mu_2'' + \mu_1'')^2$$

$$\Delta' = (2\epsilon_2' + \epsilon_1')^2 + (2\epsilon_2'' + \epsilon_1'')^2$$

$$\gamma = (X_2^3 - 3X_2^2 X_2') / (X_2^3 - 3X_2 X_2'^2)$$

$$y_1 = (1 + \gamma^2)$$

$$W = (1 - c)^4 / (1 + 2c)^2$$

$$y_2 = y_1^2$$

$$\beta = (X_2^3 - 3X_2 X_2'^2) / 3$$

$$X_2 = \text{Re}(k_2 a)$$

$$X_2' = \text{Im}(k_2 a)$$

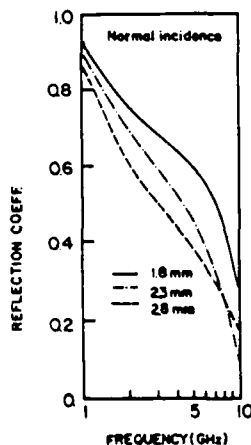
$$\mu_2 = \mu_2' + i\mu_2''$$

$$\epsilon_2 = \epsilon_2' + i\epsilon_2''$$

$$k_2 = \omega / (\mu_2 \epsilon_2)^{1/2}$$

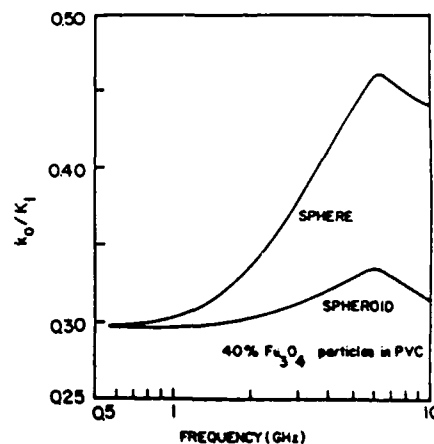
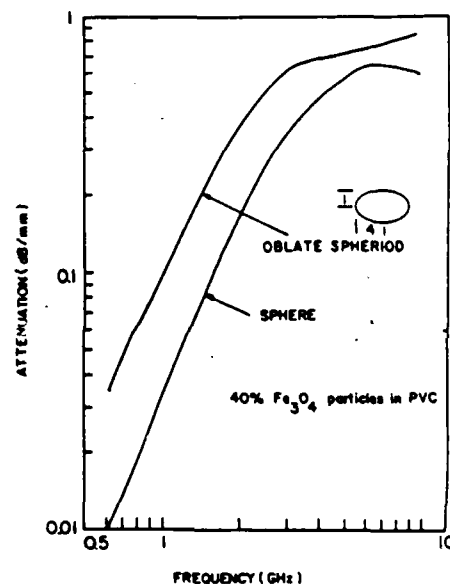
TABLE II

Frequency (GHz)	Case	$K_1/k_0 (k_0/K_1)$	$K_2/k_0$
0.6	1	6.43(0.156)	0.62
	2	6.12(0.163)	0.62
	3	5.87(0.170)	0.66
	4	6.68(0.150)	0.61
	5	6.09(0.164)	0.62
	Exp.	6.48(0.154)	0.60
1.0	1	6.37(0.157)	1.02
	2	6.07(0.165)	1.08
	3	5.85(0.171)	1.08
	4	6.64(0.151)	1.04
	5	6.03(0.166)	0.98
	Exp.	6.26(0.160)	0.95
2.0	1	5.00(0.200)	1.93
	2	4.58(0.218)	1.99
	3	4.35(0.230)	2.02
	4	5.23(0.191)	2.09
	5	4.73(0.211)	1.91
	Exp.	4.24(0.236)	2.14
3.0	1	3.90(0.256)	2.15
	2	3.47(0.288)	1.99
	3	3.19(0.313)	1.87
	4	4.02(0.249)	2.21
	5	3.63(0.275)	2.01
	Exp.	3.82(0.262)	2.17
5.0	1	2.86(0.350)	1.42
	2	2.61(0.383)	1.29
	3	2.40(0.417)	1.15
	4	2.99(0.334)	1.48
	5	2.69(0.372)	1.34
	Exp.	2.91(0.344)	1.48
10.0	1	1.17(0.315)	0.99
	2	2.91(0.344)	0.91
	3	2.71(0.369)	0.85
	4	3.32(0.301)	1.04
	5	2.98(0.336)	0.94
	Exp.	3.03(0.330)	1.08
70% $\text{Fe}_3\text{O}_4$ particles in PVC, $K = K_1 + iK_2$			

Fig. 7. Reflection coefficient versus frequency for  $\text{Fe}_3\text{O}_4$  composite slab for different slab thicknesses.

## IV. RESULTS AND CONCLUSIONS

The complex effective wavenumber  $K = K_1 + iK_2$  as given in (16) was computed as a function of frequency for  $\text{Fe}_3\text{O}_4$  particles dispersed in a PVC matrix. The dielectric constant of PVC was taken to be  $\epsilon_2 = 2\epsilon_0$  and  $\mu_2 = \mu_0$ . It was assumed that both  $\epsilon_2$  and  $\mu_2$  are nondispersive and

Fig. 8. Normalized value of the real part of the effective wavenumber versus frequency for spherical and spheroidal  $\text{Fe}_3\text{O}_4$  particles in PVC.Fig. 9. Attenuation versus frequency for spherical and spheroidal  $\text{Fe}_3\text{O}_4$  particles in PVC.

nonlossy at the frequencies of interest. As mentioned in the Introduction, measured electric and magnetic properties of  $\text{Fe}_3\text{O}_4$  particles in isolation are not available in the literature. The high conductivity of  $\text{Fe}_3\text{O}_4$  is cited as reason for the difficulty in measurements [14]. Measured values of the composite properties for 70 percent volume fraction of  $\text{Fe}_3\text{O}_4$  particles in PVC have been reported by Ueno *et al.* [2].

They have presented measured data for the real and imaginary parts of the dielectric function  $\langle \epsilon \rangle = \langle \epsilon' \rangle + i\langle \epsilon'' \rangle$  and  $\langle \mu \rangle = \langle \mu' \rangle + i\langle \mu'' \rangle$  as a function of frequency.

In our calculations, we had to assume the properties of  $\epsilon_1 = \epsilon'_1 + i\epsilon''_1$  and  $\mu_1 = \mu'_1 + i\mu''_1$  that were reasonable [3] and lead to approximate agreement with the measured values of Ueno *et al.* [2] for the composite properties.

For most ferrites (iron oxides), in the frequency range between 0.25 – 2–3 GHz, the imaginary part of the mag-

netic permeability displays a characteristic peak due to the natural ferrimagnetic spin resonance of the iron oxide. It is this high value of  $\mu_1''$  and the high conductivity of the ferrite that results in a large  $\epsilon_1''$  (imaginary part of the dielectric function) that leads to the high absorption of EM waves. At frequencies lower than 0.5 GHz,  $\epsilon_1''$  increases with decreasing frequency while  $\mu_1''$  decreases with decreasing frequency. Thus, there are two loss mechanisms present that span the very low to high frequencies leading to the desired absorption. In Figs. 1 and 2, the assumed values of  $\mu_1$  and  $\epsilon_1$  for  $\text{Fe}_3\text{O}_4$  are presented as a function of frequency. In Figs. 3 and 4, the computed normalized values of the real and imaginary parts of the effective wavenumber in the composite are plotted and compared with the experimental values.

In Figs. 5 and 6, the real and imaginary parts of the effective wavenumber are presented and compared for six different cases. Case 1 is the same as the computed results of Figs. 3 and 4 with properties as assumed in Figs. 1 and 2. In cases 2–6,  $\epsilon_1$  and  $\mu_1$  were varied as explained in Table I. In Table II, the effective wavenumber normalized by the free-space value is tabulated for the six different cases at selected frequencies along with the measured values. It was concluded that if the measured values as reported by Ueno *et al.* [2] are correct, then the values of  $\epsilon_1$  and  $\mu_1$  as shown in Figs. 1 and 2 are expected to be quite close to the actual values for  $\text{Fe}_3\text{O}_4$  in isolation since they provide the best fit with experimental data.

It can be seen that case 3, which corresponds to a decrease in the value of  $\mu_1 = \mu_1' + i\mu_1''$  by 20 percent, leads to much lower values of absorption, indicating the important role of  $\mu_1''$  on the imaginary part of the effective wavenumber in the composite.

In Figs. 7 and 8, the reflection coefficient of a slab of the  $\text{Fe}_3\text{O}_4$ -PVC composite in free space is plotted as a function of frequency for three different slab thicknesses. The reflection coefficient generally decreases as a function of frequency but is nevertheless high at the lower frequencies due to the high-volume fraction of  $\text{Fe}_3\text{O}_4$ . It is suggested that the composite should be constructed in a graded fashion so as to reduce the initial reflection by matching its impedance to the free-space value.

Finally the effects of a nonspherical shape was studied to a limited extent. In Fig. 9, the real and imaginary parts of the wavenumber for disk-shaped particles (oblate spheroids of aspect ratio 4:1) that are parallelly oriented with waves incident along the axis of symmetry are compared with those of spherical particles. For this particular orientation, the attenuation produced by the spherical particles is considerably less than for the disk-shaped particles. Calculations are in progress for needle-shaped particles, parallelly oriented or randomly oriented.

If one is interested in specific materials for which no measured spectra of the magnetic and electrical properties are available, it may be possible to arrive at reasonable values  $\epsilon_1'$ ,  $\epsilon_1''$ ,  $\mu_1'$ , and  $\mu_1''$  by fitting them to simple equations that involve the characteristic resonance frequency or relaxation time of the material and the asymptotic values

of  $\epsilon$  and  $\mu$ . These values will have to be obtained from measurements, but these are easier to measure than the full spectrum.

#### ACKNOWLEDGMENT

Helpful discussions with Profs. L. E. Cross and R. E. Newnham of Pennsylvania State University are gratefully acknowledged. The authors would like to thank the reviewers for carefully reading the manuscript and for their suggestions and comments.

#### REFERENCES

- [1] B. Lax and K. J. Button, *Microwave Ferrites and Ferrimagnetics* New York: McGraw-Hill, 1962.
- [2] R. Ueno, N. Ogasawara, and T. Inui, "Ferrites—or iron oxide—impregnated plastics serving as radio wave scattering suppressors," in *Proc. Int. Conf. Ferrites* (Japan), 1980, pp. 890–893.
- [3] J. Smit and H. P. J. Wijn, *Ferrites* Holland: Philips' Technical Library, 1959.
- [4] V. K. Varadan, V. N. Brngi, and V. V. Varadan, "Coherent electromagnetic wave propagation through randomly distributed dielectric scatterers," *Phys. Rev. D*, vol. 19, pp. 2480–2489, Apr. 1979.
- [5] V. N. Brngi, T. A. Seliga, V. K. Varadan, and V. V. Varadan, "Bulk propagation characteristics of discrete random media," in *Multiple Scattering of Waves in Random Media*, P. L. Chow, W. E. Kohler, and G. Papanicolaou, Eds. Amsterdam: North-Holland, 1981, pp. 43–75.
- [6] V. K. Varadan and V. V. Varadan, Eds., *Acoustic, Electromagnetic and Elastic Wave Scattering—Focus on the T-Matrix Approach*. New York: Pergamon Press, 1980.
- [7] A. R. Edmonds, *Angular Momentum in Quantum Mechanics*. Princeton, N.J.: Princeton University Press, 1957.
- [8] V. N. Brngi, V. V. Varadan, and V. K. Varadan, "The effects of pair correlation function on coherent wave attenuation in discrete random media," *IEEE Trans. Antennas Propagat.*, vol. AP-30, pp. 805–808, July 1982.
- [9] V. Twersky, "Reflection and scattering of sound by correlated rough surfaces," *J. Acoust. Soc. Am.*, vol. 73, pp. 85–94, Jan. 1983.
- [10] V. Twersky, "Coherent electromagnetic waves in pair-correlated random distribution of aligned scatterers," *J. Math. Phys.*, vol. 19, pp. 215–230, Jan. 1978.
- [11] V. K. Varadan, V. N. Brngi, V. V. Varadan, and A. Ishimaru, "Multiple scattering theory for waves in discrete random media and comparison with experiments," *Radio Sci.*, vol. 18, pp. 321–327, 1983.
- [12] V. K. Varadan, Y. Ma, and V. V. Varadan, "Coherent electromagnetic wave propagation through randomly distributed and oriented pair-correlated dielectric scatterers," *Radio Sci.*, vol. 19, pp. 1445–1449, 1984.
- [13] O. R. Cruzan, "Translation additional theorems for spherical vector wave equations," *Q. Appl. Math.*, vol. 20, p. 33, 1962.
- [14] R. Newnham, private communication.



Vijay K. Varadan (M'82) received the M.S. degree in engineering mechanics from Pennsylvania State University in 1969. In 1974, he obtained the Ph.D. degree in theoretical and applied mechanics from Northwestern University.

During 1974–1977, he was a faculty member in the Department of Applied Mechanics at Cornell University. From 1977 to 1983, he was on the faculty of the Engineering Mechanics Department at Ohio State University. In 1983, he joined the faculty of the Engineering Science and

Mechanics Department at Pennsylvania State University as a Professor, where he is also a faculty member of the Graduate Program in Acoustics and the Material Research Laboratory and the Director of the Laboratory for Electromagnetic and Acoustic Research. His current research interests are in the general area of wave phenomena as it applies to acoustics, electromagnetic, and elastodynamic fields, propagation in random media, design of composite materials for specific electromagnetic and acoustic properties, numerical techniques for the solution of scattering, and its inverse problems.

Dr. Varadan is a Fellow of the Acoustical Society of America and a member of ASME.



**Vasundara V. Varadan** (M'82) received the M.S. and Ph.D. degrees in physics from the University of Illinois at Chicago in 1970 and 1974, respectively. She was in the Theoretical and Applied Mechanics Department at Cornell University as a post-doctoral Associate during 1974-1977.

From 1977 to 1983, she was on the faculty of the Engineering Mechanics department at Ohio State University. In 1983, she joined the Engineering Science and Mechanics Department at Pennsylvania State University as an Associate

Professor, where she is also a faculty member of the Graduate Program in Acoustics and the Materials Research Laboratory. Her research interests are in the general area of wave phenomena as it applies to acoustic, electromagnetic, and elastodynamic fields, propagation in random media, design of composite materials for specific electromagnetic and acoustic properties, numerical techniques for the solution of scattering problems, and inverse problems.

Dr. Varadan is a Fellow of the Acoustical Society of America, a member of the American Academy of Mechanics, and the Society of Engineering Science.



**Yushieh Ma** received the M.S. degree in coastal and oceanographic engineering from the University of Florida in 1979. In 1982, he obtained the Ph.D. degree in aerospace and ocean engineering from the Virginia Polytechnic Institute and State University. From 1982-1983, he worked as a post-doctoral researcher at Ohio State University.

In late 1983, he joined the faculty in the Department of Engineering Science and Mechanics at Pennsylvania State University, where he is

now an Assistant Professor. His research interests include remote sensing in geophysics, underwater acoustics and multiple scattering of waves in random media.

Dr. Ma is a member of the Acoustical Society of America, American Society of Civil Engineers, and the American Institute of Aeronautics and Astronautics.



**W. F. Hall** received the Ph.D. degree in physics from the University of California in 1964.

From 1961 to 1964, his work experience entailed preliminary design for guidance, navigation, and control systems at Northrop Northronics, Palos Verdes, CA. From 1965 to the present, he has worked as a Research Physicist, Member of Technical Staff, and currently as Group Leader at the Rockwell Science Center. In 1970 (spring semester), he was co-Instructor, Mathematical Methods in Research at Harvey Mudd College,

Claremont, CA, funded under a Sloan Foundation Grant to explore new methods in teaching. He has made significant scientific contributions in the following areas. 1) Charged-particle scattering in crystals: His work with R. E. DeWames and G. W. Lehman was the first to point out and evaluate the importance of quantum effects in channeling, a phenomenon in which charged particles penetrate a crystal lattice to great depths. In later work, the conditions which govern the transition of this phenomenon from quantum to classical behavior were established. 2) Properties of magnetic systems: He has contributed to the understanding of a wide range of phenomena in magnetic systems, including magnetic bubble-domain dynamics, surface magnetization near the transition temperature, and thermal properties of the magnetization in the vicinity of a magnetic impurity. 3) Viscoelastic effects in polymer solutions: With R. E. DeWames and M. C. Shen, he has investigated and extended the currently accepted theories of the frequency-dependent viscosity in polymer solutions, applying these theories to the calculation of the relaxation-time spectrum of block co-polymers. 4) Characteristics of compound semiconductor interfaces: He has derived a relationship between the current-voltage characteristic of a semiconductor heterojunction and the variation in material properties in the vicinity of metallurgical interface. In conjunction with W. E. Tennant, J. Cape, and J. S. Harris, he has developed an optical technique for probing the position dependence of the bandgap near the interface. In addition to his research in the above areas, he has collaborated in the investigation of a number of diverse topics, including distributed-feedback lasers, magnetic suspension viscosity, dielectric properties of salt solutions, and various applications of electromagnetic theory.

Dr. Hall is a member of the American Physical Society, Pi Mu Epsilon, and Sigma Pi Sigma, and has 40 publications.

## Acoustic response of manganese nodule deposits

Y. Ma\*, A. H. Magnuson†, V. K. Varadan\*, and V. V. Varadan\*

### ABSTRACT

Backscattered acoustic intensities are studied analytically for manganese nodule deposits excited by a normally incident plane wave. The primary objective is to use this remote-sensing technique to infer the nodule concentration as well as its size distribution from the frequency spectrum of the acoustic response.

For sparse distributions of scatterers, multiple scattering theory has been used to obtain the coherent reflection and transmission coefficients from the sea floor covered with manganese nodules. The derived equations can also be used for densely distributed configurations when considering higher-order statistics between scatterers. The validity of the formalism is examined by using the principle of conservation of energy and considering both the coherent and the incoherent intensities.

Numerical results of acoustic intensities are highly frequency-dependent, especially when the nondimensional frequency  $ka$  is greater than 1. The strength of the acoustic intensity is proportional to nodule concentration. Different size distributions of nodules can be distinguished through use of the intensity measurements. However only a minor difference is observed in the low-frequency range between uniform and Rayleigh size distributions.

### INTRODUCTION

Manganese nodules, which also contain other minerals such as nickel and copper, are of economic importance due to their natural abundance on the deep ocean floor. Because 70 to 80 percent of the metals they contain are currently imported into the United States, Graff (1984) and Spiess et al. (1983) predicted that the mining and exploration of manganese nodule deposits will become increasingly important and feasible. The physics of nodule deposits was discussed in Glasby (1977) and Greenslate (1977). Magnuson et al. (1981, 1982) described how an acoustic remote-sensing technique could be used to infer

the area weight density (tons of nodule per unit area) and the average nodule size, which, in turn will indicate the appropriate type of mining equipment to be used.

Remote acoustic sensing techniques provide an economical way to infer the presence and abundance of manganese nodule deposits on the deep ocean floor. The coherent acoustic reflection from the ocean bottom is analyzed over a nondimensional frequency range  $ka = 2\pi fa/c$  from 0.2–5.0, where  $f$  is the frequency in hertz,  $a$  is the mean nodule radius, and  $c$  is the acoustic wave speed in water. Previous studies were confined to an analysis of the coherent reflectivity only and provided only limited information about the nodule distribution. Measurement of the incoherent intensity provides additional information. An improved theoretical model is presented for determining both the coherent and incoherent intensities.

Acoustic intensity measurements are common in underwater acoustics. To compare the field measurements with the theoretical calculations, the incoherent intensity must also be considered because it becomes significant as the sounding frequency increases. An intensity calculation based on the energy principle for nonabsorbing scatterers, which was investigated in Twersky (1957), is discussed here, and conservation of energy is used to check the numerical accuracy. The study, although, restricted to sparse nodule distributions so that higher-order scattering can be neglected, nevertheless includes some interaction among the nodules. The use of multiple scattering theory to accommodate denser concentrations of nodules is currently being investigated. In addition, any given size distribution of these nodules can also be considered, as described in Ma et al. (1983). Calculations are presented here for uniform and Rayleigh size distributions.

### REFLECTED AND TRANSMITTED FIELDS

We consider a planar distribution of nodules modeled as elastic spheres suspended in water. The interstitial space between the nodules and the region below the nodule field is assumed to be occupied by water. This is an approximation, but the soft, water-saturated mud in which the nodules are actually distributed has an acoustic impedance that closely matches the acoustic impedance in water relative to the

Presented at the 107th Acoustical Society of America Meeting, May 10, 1984, Norfolk. Manuscript received by the Editor May 10, 1984; revised manuscript received June 25, 1985.

\*Laboratory for Electromagnetic and Acoustic Research, Department of Engineering Science and Mechanics, The Pennsylvania State University, University Park, PA 16802.

†Ocean Engineering Program, Texas A & M University, College Station, TX 77843.

© 1986 Society of Exploration Geophysicists. All rights reserved.

## LIST OF SYMBOLS

$A$  = Area  
 $a$  = Size of nodule (radius)  
 $c$  = Concentration ( $N\pi a^2/A$ )  
 $\hat{e}_r$  = Unit radial vector in spherical coordinates  
 $\hat{e}_z$  = Unit vector in the positive  $z$  direction in rectangular coordinates  
 $f(\theta)$  = Scattering function  
 $g$  = Density ratio  
 $H$  = Depth measured from receiver  
 $h_n^{(1)}$  = Spherical Hankel function of the first kind  
 $\text{Im}(\cdot)$  = Imaginary part of  $(\cdot)$   
 $i$  = Imaginary unit ( $i^2 = -1$ )  
 $j_n(\cdot)$  = Spherical Bessel function  
 $k$  = Wavenumber  
 $N$  = Total number of scatterers  
 $n_0$  = Number density ( $N/A$ )  
 $O(\cdot)$  = Order of  $(\cdot)$   
 $P_n(\cos \theta)$  = Legendre polynomials  
 $p$  = Pressure  
 $R$  = Reflection coefficient  
 $\text{Re}(\cdot)$  = Real part of  $(\cdot)$   
 $r$  = Distance between nodules and the reference origin  
 $T$  = Transmission coefficient  
 $U$  = Total scattered field  
 $u$  = Individual scattered field  
 $v$  = Velocity vector

$x, y, z$  = Rectangular coordinates  
 $y_n(\cdot)$  = Spherical Neumann function  
 $\theta$  = Scattering angle  
 $\omega$  = Angular frequency  
 $\Omega$  = Solid angle  
 $\rho$  = Mass density of fluid medium  
 $\sigma$  = Scattering cross-section  
 $\nabla$  = Gradient operator  
 $\psi$  = Wave function (acoustic potential)  
 $\langle \cdot \rangle$  = Configurational average  
 $\langle \cdot \rangle_i$  = Configurational average holding  $i$ th scatterer fixed  
 $\langle \cdot \rangle_{jk}$  = Configurational average holding  $j$ th and  $k$ th scatterers fixed

## SUBSCRIPTS

$L$  = Longitudinal wave  
 $m, n$  = Indices (integer)  
 $T$  = Transverse wave

## SUPERSCRIPTS

$\text{inc}$  = Refers to incident wave  
 $*$  = Complex conjugate  
 $+$  =  $z > 0$  plane  
 $-$  =  $z < 0$  plane

manganese nodules that are highly reflecting (high-impedance mismatch to water). The theoretical model of the problem is based on the earlier work of Twersky (1957) and Foldy (1945). In contrast to Twersky, who considered rigid spheres, we consider elastic spheres and retain all necessary terms in order to model the field scattered by a single nodule exactly.

Plane harmonic waves of frequency  $\omega$  are incident normal to the nodule field. The  $z$ -axis points upward from the nodule field at  $z = 0$ . The average field above the nodule distribution is the sum of the downgoing incident wave of amplitude  $\Psi_0$  and upgoing reflected wave whose amplitude differs from the incident field by the reflection coefficient  $R$ . In the region  $z < 0$ , there is a transmitted field of amplitude  $T\Psi_0$ . The reflected and transmitted fields are due to scattering from the nodules that includes multiple scattering effects. The average field on the plane  $z = 0$  must be independent of position. Twersky (1957) approximated this field as the sum of the incident fields and the mean value of the reflected and transmitted fields evaluated at  $z = 0$ . Foldy (1945), in his description of the multiple scattering of waves by a random distribution of spheres, assumed that the incident field that excites each sphere is simply the average field in the medium. This has come to be known as Foldy's approximation and leads to a simple equation for the effective propagation constant in the composite medium. We emphasize that this is not a single scattering approximation. In our model we used Twersky's approximation for the average field at  $z = 0$  and took this to be the field exciting the nodules in the spirit of Foldy's formalism. The fields scattered by the nodules can be expanded using outgoing spherical functions with coefficients that depend upon the reflection and transmission coefficients which have

yet to be determined. The details of determining the scattered field are given in Appendix A.

The total field above and below the nodule field can be written as

$$\Psi(\mathbf{R}) = \Psi^{\text{inc}}(\mathbf{R}) + \sum_{j=1}^N u_j^s(\mathbf{R} - \mathbf{r}_j) = \Psi^{\text{inc}}(\mathbf{R}) + U^s(\mathbf{R}), \quad (1)$$

where  $\mathbf{R}$  is the field point which in our model is also the location of the receiver and transmitter. In equation (1),  $u_j^s$  is the field scattered by the  $j$ th nodule located at  $\mathbf{r}_j$  on the  $z = 0$  plane, and  $N$  is the total number of nodules distributed over a large area  $A$  such that  $N \rightarrow \infty$ ,  $A \rightarrow \infty$ , but  $n_0 = N/A$  (the number density of the nodules) is finite.

We are interested only in the ensemble averaged fields, because the position of individual nodules does not affect the response to a great extent. The configurational average (Appendix B) of equation (1) over all possible positions of the nodules weighted by the joint probability distribution function  $p(\mathbf{r}_1, \mathbf{r}_2, \dots, \mathbf{r}_N)$  and the size distribution function  $q(a_j)$  is denoted by

$$\langle \Psi_{\text{tot}} \rangle = \int da_1 \int da_2 \dots \int da_N \int d\mathbf{r}_1 \int d\mathbf{r}_2 \dots \int d\mathbf{r}_N \times \Psi(\mathbf{R}) p(\mathbf{r}_1, \mathbf{r}_2, \dots, \mathbf{r}_N) q(a_1, a_2, \dots, a_N)$$

The incident field is independent of the nodule locations and we concentrate on the average total scattered field. According to Foldy (1945), the field exciting each nodule may be



approximately described by the average total field given in equation (1). From Appendix A, we write

$$u_j^*(\mathbf{R} - \mathbf{r}_j) = F(a_j, \mathbf{R} - \mathbf{r}_j) \langle \Psi \rangle(\mathbf{r}_j), \quad (3)$$

where

$$F(a_j, \mathbf{R} - \mathbf{r}_j) = \sum_n \frac{(2n+1)}{(1+iC_n)} i^n h_n^{(1)}(k|\mathbf{R} - \mathbf{r}_j|) p_n(\cos \theta_j). \quad (4)$$

The terms in equation (4) are explained in Appendix A. In equation (3)  $\langle \Psi \rangle(\mathbf{r}_j)$  is simply the average field evaluated at  $\mathbf{r}_j$ .

The ensemble average of equation (3) may be written. Note that it depends only on the location of the  $j$ th scatterer and that

$$\int d\mathbf{r}_2 \cdots \int d\mathbf{r}_N p(\mathbf{r}_1, \mathbf{r}_2, \dots, \mathbf{r}_N) = p(\mathbf{r}_j) = \frac{1}{A}, \quad (5)$$

where  $p(\mathbf{r}_j)$ , the probability of locating a nodule at  $\mathbf{r}_j$ , is simply  $1/A$  for a random distribution. Averaging equation (3) yields

$$\left\langle \sum_{j=1}^N u_j^* \right\rangle = n_0 \int \overline{F(\mathbf{R} - \mathbf{r}_j)} \langle \Psi \rangle(\mathbf{r}_j) d\mathbf{r}_j, \quad (6)$$

where

$$\overline{F(\mathbf{R} - \mathbf{r}_j)} = \int F(a_j, \mathbf{R} - \mathbf{r}_j) q(a_j) da_j, \quad (7)$$

and  $q(a)$  is the size distribution function obtained from analyzing pictures of nodule deposits on the sea floor. This is used to describe statistically how different nodule sizes are distributed on the sea floor.

The average field should depend only on the angle of incidence  $\pi$  and the height of the receiver-transmitter. Introducing reflection and transmission coefficients,

$$\langle \Psi(\mathbf{R}) \rangle = \Psi^{inc}(\mathbf{R}) + R[\Psi^{inc}]^*, \quad z > 0, \quad (8)$$

and

$$\langle \Psi(-\mathbf{R}) \rangle = \Psi^{inc}(1+T), \quad z < 0, \quad (9)$$

where the complex conjugate denotes an upward propagating wave (Figure 1). Thus if

$$\Psi^{inc} = \Psi_0 e^{-ikz}, \quad (10)$$

then

$$\langle \Psi \rangle = \Psi_0 (e^{-ikz} + R e^{ikz}), \quad z > 0, \quad (11)$$

and

$$\langle \Psi \rangle = \Psi_0 (1+T) e^{-ikz}, \quad z < 0. \quad (12)$$

We note that the average field at  $z=0$  is independent of the coordinates. The average field is constant and can be written (following Twersky, 1957) as

$$\Psi_z = \Psi_0 + \Psi_0 (R+T)/2, \quad z=0. \quad (13)$$

Equation (13) is used in equation (6) as the field incident on a nodule at  $\mathbf{r}_j$ . For the total average scattered field, we obtain

$$\overline{F(\mathbf{R} - \mathbf{r}_j)} = \langle U \rangle = n_0 \Psi_0 \int \overline{F(\mathbf{R} - \mathbf{r}_j)} [1 + (R+T)/2] d\mathbf{r}_j, \quad (14)$$

For remote sensing the receiver-transmitter is in the far field of nodules, such that  $k|\mathbf{R} - \mathbf{r}_j| \gg 1$ . Then we use the asymptotic form of the Hankel function in equation (4) as given in equation (A-10) and obtain

$$\langle U \rangle = n_0 \Psi_0 \int_0^\infty r dr \int_0^{2\pi} d\phi \frac{e^{ik|\mathbf{R} - \mathbf{r}|}}{|\mathbf{R} - \mathbf{r}|} \times \overline{f(\theta)} [1 + (R+T)/2], \quad (15)$$

where

$$\overline{f(\theta)} = \frac{1}{k} \sum_{n=0}^\infty \int \frac{(2n+1)}{1+iC_n} (-1)^n P_n(\cos \theta) q(a) da,$$

and we use cylindrical polar coordinates so that

$$d\mathbf{r} = r dr d\phi. \quad (16)$$

From Figure 2 we note that

$$|\mathbf{R} - \mathbf{r}| = H/\cos \theta. \quad (17)$$

We further note that the integral in equation (15) is independent of the angle  $\phi$  and hence

$$\langle U \rangle = 2\pi n_0 \Psi_0 \int_0^{\pi/2} \overline{f(\theta)} [1 + (R+T)/2] e^{ikH/\cos \theta} \times (-H \tan \theta / \cos \theta) d\theta. \quad (18)$$

To solve equation (18) for  $kH \gg 1$ , the principle of stationary phase (Lamb, 1932) is used. The solution can thus be written in terms of the stationary phase angle  $\gamma$  as

$$\langle U \rangle = (2\pi n_0 i \Psi_0 / k) [1 + (R+T)/2] \overline{f(\gamma)} e^{ikH/\cos \gamma}. \quad (19)$$

The stationary phase angle  $\gamma$  is obtained by solving

$$d(ikH/\cos \theta)/d\theta = 0, \quad (20)$$

and found to be  $\gamma = n\pi$  ( $n = 0, 1, 2, \dots$ ) for this case.

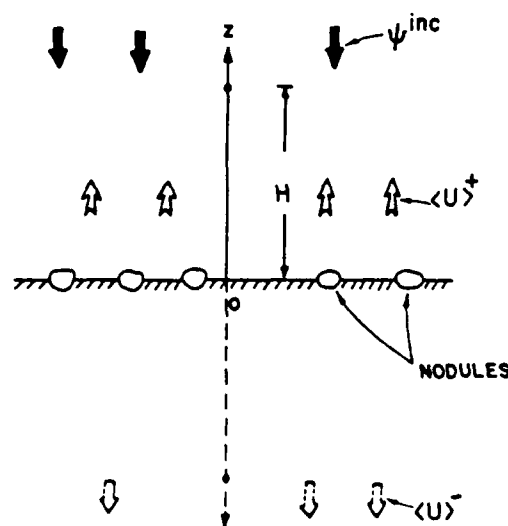


FIG. 1. The average scattered field excited by a normally incident plane wave.

From equation (18) it can be seen that  $\langle U \rangle$  can be solved by integrating  $\theta$  from 0 to  $\pi/2$ . The only appropriate phase angle in this region is zero. Therefore, for  $z > 0$ , the total scattered field  $\langle U \rangle^+$  is found to be

$$\begin{aligned} \langle U \rangle^+ &= (2\pi n_0 i \Psi_0 / k) [(1 + T/2) \overline{f(0)} + (R/2) \overline{f(\pi)}] e^{ikz} \\ &= R \Psi_0 e^{ikz}. \end{aligned} \quad (21)$$

In equation (21), instead of  $\overline{f(0)}$  multiplied by the reflection coefficient  $R$ , the scattering function at  $\theta = \pi$  (which is a compensation angle of zero degrees) is used. The reason is that the transmitted and reflected waves are different in propagation directions by an angle of 180 degrees. This is also clear from Twersky (1957). Similarly,

$$\begin{aligned} \langle U \rangle^- &= (2\pi n_0 i \Psi_0 / k) [(1 + T/2) \overline{f(\pi)} + (R/2) \overline{f(0)}] e^{-ikz} \\ &= T \Psi_0 e^{-ikz} \end{aligned} \quad (22)$$

The reflection and transmission coefficients, the two unknowns, can now be solved simultaneously from equations (21) and (22) using Cramer's rule. The result is

$$R = \beta_0 / [1 - \beta_+ + (\beta_+^2 + \beta_0^2)/4], \quad (23)$$

and

$$T = [\beta_+ - (\beta_+^2 + \beta_0^2)/2] / [1 - \beta_+ + (\beta_+^2 + \beta_0^2)/4], \quad (24)$$

where

$$\beta_0 = 2\pi n_0 \overline{f(0)} / k,$$

and

$$\beta_+ = 2\pi n_0 \overline{f(\pi)} / k.$$

Substituting the expressions for  $R$  and  $T$  into equations (21) and (22), respectively, we obtain

$$\langle U \rangle^+ = [\beta_0 + \beta_0 \beta_+ + O(\beta_0^3)] \Psi_0 e^{ikz}, \quad z > 0 \quad (25)$$

and

$$\langle U \rangle^- = [\beta_+ + (\beta_+^2 + \beta_0^2)/2 + O(\beta_+^3)] \Psi_0 e^{-ikz}, \quad z < 0. \quad (26)$$

The first terms on the right-hand sides of equations (25) and (26) are due to a single scattering whose excitation is the incident plane wave  $\psi^{inc}$  only. This can be obtained by substituting  $\psi^{inc}$  at  $z = 0$  for  $\langle \psi(r_j) \rangle$  in equation (6). The second term is obtained using the self-consistent approach. This is essentially Picard's process based on initially approximating  $\psi$  by the incident field  $\psi^{inc}$  plus the single scattered wave, which in turn gives a series of orders-of-scattering for  $\psi$  in terms of single scattering functions. Foldy (1945) introduced this method to explain the orders of scattering because the higher-order scattering is approximated by iteration using the lower-order scattering terms. The idea is that the average scattered field  $\langle U \rangle^+$  (or  $\langle U \rangle^-$ ) can be obtained from a Neumann series

$$\langle U(R) \rangle = u_1^+ + \sum_{m=2}^{\infty} u_m^+, \quad (27)$$

where

$$\begin{aligned} u_m^+ &= n_0 \int \{ [u_{m-1}^+(r_j) + u_{m-1}^-(r_j)] / 2 \} [F(R - r_j)] dr_j, \\ u_1^+ &= \beta_0 \Psi_0 e^{+ikz}, \quad z > 0, \end{aligned}$$

and

$$u_1^- = \beta_+ \Psi_0 e^{-ikz}, \quad z < 0.$$

It can be seen from equation (27) that  $m = 1, 2$ , and 3 correspond to single, double, and triple scattering, respectively.

Generally speaking, for a sparse distribution of nodules, i.e.,  $n_0 v \ll 1$  ( $n_0 v = C = n_0 \pi a^2$ ) in equations (25) and (26) the successive terms are smaller compared to the previous terms. Therefore, the higher-order scattering containing a high-order value of  $n_0 v$  can be neglected in the approximation of the average scattered field  $\langle U \rangle$ .

#### CONFIGURATIONAL AVERAGE OF THE SQUARE OF THE TOTAL FIELD $\langle \Psi^2 \rangle$

Because nodules are randomly distributed on the sea floor, their positions are not prepared in advance, we have no interest in studying wave scattering by one particular distribution. Instead, an average picture better describes the nodule field. We define "coherent scattering" or "coherent propagation" only as an average over the ensemble of configurations which are, in the present case, different top views from areas covered with nodules. When an experiment has been performed on a particular configuration, we can estimate the properties of the average over an ensemble with a high probability of accuracy. In experiments several samples are used to guard this probability. Interested readers can refer to any text on statistical mechanics for further elucidation. Because the nodules are randomly distributed, the scattered field  $U$  is not constant: scatterers make an otherwise homogeneous medium inhomogeneous. The magnitude and phase of  $U$  will fluctuate in a random manner. Thus the total field at  $R$ , i.e.,  $\psi(R)$ , is also a random function and can usually be divided into average field  $\langle \psi \rangle$  and the fluctuating field  $\psi'$ .

The square of the magnitude of the coherent field  $|\langle \psi \rangle|^2$  is the coherent component. The average of the square of the magnitude of the incoherent field is the incoherent component. The reason for introducing the incoherent field here is that the

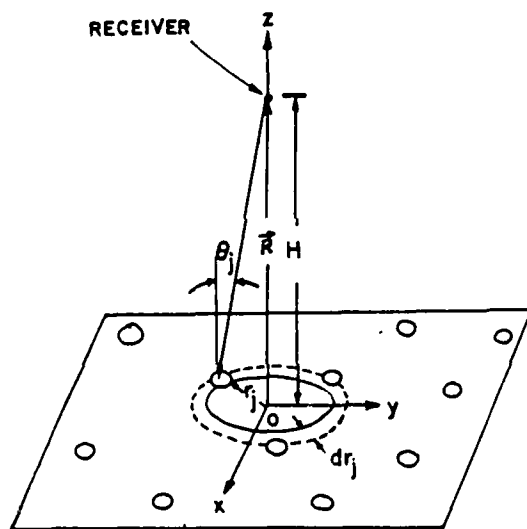


FIG. 2. Geometry of scattering from nodules on a plane.

"incoherent intensity," which is quadratic in the field amplitude, must be computed separately. This is because the averaging process will not commute with the nonlinear operator of squaring the absolute magnitude of a field quantity. These values correspond to those which would be obtained experimentally by employing amplitude-sensitive and energy-sensitive measuring devices. Here the incoherent field is simply the difference between  $\langle |\psi|^2 \rangle$  and  $\langle |\psi\rangle|^2$ . Its usefulness is explained in obtaining the second statistical moment of a fluctuating field in statistical mechanics. This extra information also enables us to describe the amount accurately, as well as the size distribution, of an average nodule field which has at least two unknown physical quantities. This is impossible to achieve without solving higher-moment equations. The sum of the coherent and incoherent components is the average of the square of the magnitude of the acoustic field, i.e.,

$$\langle |\psi|^2 \rangle = \langle |\psi\rangle|^2 + \langle |\psi'|^2 \rangle, \quad (28)$$

where  $\psi'$  is related to  $U$  as  $\psi' = U - \langle U \rangle$ , or

$$\langle |\psi'|^2 \rangle = \langle |U|^2 \rangle - \langle |U\rangle|^2. \quad (29)$$

The coherent component  $\langle |\psi\rangle|^2$  can be obtained directly from the known coherent field  $\langle \psi \rangle$  [equation (4)]. It is of interest here to find the incoherent component  $\langle |\psi'|^2 \rangle$  only. Substituting the expression for  $U$

$$\left( U = \sum_{j=1}^N u_j \right)$$

into equation (29) yields

$$\begin{aligned} \langle |\psi'|^2 \rangle &= \langle \sum_j u_j^* \sum_k u_k \rangle - \sum_j \langle u_j \rangle^* \sum_k \langle u_k \rangle \sum_j \langle u_j \rangle \\ &= \sum_{j,k} \langle u_j^* u_k \rangle + \sum_j \langle |u_j|^2 \rangle - \sum_j \langle u_j \rangle^* \langle u_j \rangle. \end{aligned} \quad (30)$$

The above equation can also be written in the form

$$\begin{aligned} \langle |\psi'|^2 \rangle &= n_0^2 \iint [(N-1) \langle u_j^* u_k \rangle_{jk} / N \\ &\quad - \langle u_j \rangle^* \langle u_k \rangle] dr_j dr_k \\ &\quad + n_0 \int \langle |u_j|^2 \rangle_j dr_j \end{aligned} \quad (31)$$

by using the definition of the configurational average. To calculate the incoherent component  $\langle |\psi'|^2 \rangle$  in equation (31), two approximations were also introduced. First,  $(N-1)/N$  is replaced by unity. This is valid for large  $N$ . Second, we use

$$\langle u_j^* u_k \rangle_{jk} \sim \langle u_j \rangle^* \langle u_k \rangle, \quad (32)$$

as suggested by Twersky (1957). For sparsely distributed scatterers, equation (32) may be interpreted physically as neglecting contributions to the excitation of a scatterer that arise from fluctuations of the average radiation that has been scattered by the other scatterers.

It should be noted from equations (30) and (31) that

$$\sum_{j,k} \langle u_j^* u_k \rangle$$

can be approximated using  $\langle |U|^2 \rangle$ . This implies that

$$\sum_{j,k} \langle u_j (\nabla / -ik) u_k \rangle,$$

or the average of the  $j$ th scattered field multiplied by the gradient of the  $k$ th scattered field can be estimated as

$$\sum_{j,k} \left\langle u_j^* \frac{\nabla}{-ik} u_k \right\rangle^+ \sim \langle |U|^2 \rangle^+ \hat{e}_z, \quad z > 0, \quad (33)$$

and

$$\sum_{j,k} \left\langle u_j^* \frac{\nabla}{-ik} u_k \right\rangle^- \sim \langle |U|^2 \rangle^- \hat{e}_z, \quad z < 0, \quad (34)$$

where  $\hat{e}_z$  is the unit vector in the positive  $z$  direction. Although the gradient of  $u_j$  gives the radial direction, the average direction should be in the  $z$  direction. This is to be expected from the symmetry of the problem (the energy flux is canceled out along the  $x$  and  $y$  directions). Both equations (33) and (34) are thus important approximations in considering the energy conservation.

#### CONFIGURATIONAL AVERAGE OF ENERGY FLUX $\langle S \rangle$

The energy flux (intensity) is defined as (Morse and Ingard, 1968),

$$S = (p^* v + p v^*)/2, \quad (35)$$

an important quantity in wave propagation theory for considering energy conservation. Because we define

$$v = \nabla \psi \quad (36)$$

from potential theory, we obtain

$$p = i\omega\rho\psi \quad (37)$$

from the linearized momentum equation. Therefore, the energy flux can be expressed in terms of  $\psi$  as

$$S = i\omega\rho(\psi^* \nabla \psi - \psi \nabla \psi^*)/2. \quad (38)$$

The configurational average of the energy flux becomes

$$\langle S \rangle = i\omega\rho[\langle \psi^* \nabla \psi \rangle - \langle \psi \nabla \psi^* \rangle]/2, \quad (39)$$

and it now contains both the coherent and the incoherent components.

Because  $\psi = \psi^{\text{inc}} + U$ , substituting it into equation (27) gives (taking the real part for magnitude)

$$\begin{aligned} \langle S \rangle &= \omega\rho k \operatorname{Re} \left[ \frac{\psi^{\text{inc}*} \nabla \psi^{\text{inc}}}{-ik} + \frac{\psi^{\text{inc}*}}{-ik} \nabla \langle U \rangle \right. \\ &\quad \left. + \frac{\langle U \rangle^* \nabla \psi^{\text{inc}}}{-ik} + \frac{\langle U^* \nabla U \rangle}{-ik} \right]. \end{aligned} \quad (40)$$

Because the operations of taking the gradient and the integration involved performing the configurational average commute,

$$\langle \nabla U \rangle = \nabla \langle U \rangle, \quad (41)$$

and this relationship has been used in obtaining equation (40).

For scattered waves  $\langle S \rangle$  is expected to be going outward away from the plane on which the nodules lie. Because the scattering characteristics are different in the positive and negative  $z$  directions, it is necessary to separate  $\langle S \rangle$  into two parts. Let

$$\langle S \rangle = \langle S \rangle^+, \quad z > 0, \quad (42)$$

and

$$\langle S \rangle = \langle S \rangle^-, \quad z < 0, \quad (43)$$

where the expressions for  $\langle S \rangle^+$  and  $\langle S \rangle^-$  are

$$\begin{aligned} \langle S \rangle^+ = \omega p k \operatorname{Re} & \left[ \frac{\psi^{\text{inc}*} \psi^{\text{inc}}}{-ik} + \frac{\psi^{\text{inc}*}}{-ik} \nabla \langle U \rangle^+ \right. \\ & \left. + \frac{\langle U \rangle^+ \nabla \psi^{\text{inc}}}{-ik} + \frac{\langle U^* \nabla U \rangle^+}{-ik} \right], \end{aligned} \quad (44)$$

and

$$\begin{aligned} \langle S \rangle^- = \omega p k \operatorname{Re} & \left[ \frac{\psi^{\text{inc}*} \psi^{\text{inc}}}{-ik} + \frac{\psi^{\text{inc}*}}{-ik} \nabla \langle U \rangle^- \right. \\ & \left. + \frac{\langle U \rangle^- \nabla \psi^{\text{inc}}}{-ik} + \frac{\langle U^* \nabla U \rangle^-}{-ik} \right]. \end{aligned} \quad (45)$$

By substituting the expressions for  $\psi^{\text{inc}}$ ,  $\langle U \rangle^+$ , and  $\langle U \rangle^-$  into equations (44) and (45), we obtain

$$\langle S \rangle^+ = \omega p k \left[ -\psi_0^2 \hat{e}_z + \operatorname{Re} \left( \frac{\langle U^* \nabla U \rangle^+}{-ik} \right) \right], \quad (46)$$

and

$$\begin{aligned} \langle S \rangle^- = \omega p k & \times \left[ -\psi_0^2 \hat{e}_z - (C^- + C^{-*}) \psi_0^2 \hat{e}_z + \operatorname{Re} \left( \frac{\langle U^* \nabla U \rangle^-}{-ik} \right) \right]. \end{aligned} \quad (47)$$

The second term on the right-hand side of equation (46) [or the third term on the right-hand side of equation (47)] can be further separated into two parts. Thus

$$\frac{\langle U^* \nabla U \rangle^\pm}{-ik} = \sum_{j,k} \sum_i \left\langle u_j \frac{\nabla}{-ik} u_k \right\rangle^\pm + \sum_{j'} \left\langle u_j \frac{\nabla}{-ik} u_{j'} \right\rangle^\pm. \quad (48)$$

Using equations (48), (33), and (34), the average energy flux  $\langle S \rangle^\pm$  becomes

$$\langle S \rangle^+ = \omega p k [\psi_0^2 (-\hat{e}_z) + (|\langle U \rangle^+|^2 \hat{e}_z + \mathbf{I}^+)], \quad (49)$$

and

$$\begin{aligned} \langle S \rangle^- = \omega p k [\psi_0^2 (-\hat{e}_z) + \psi_0^2 (T + T^*) (-\hat{e}_z) \\ + (|\langle U \rangle^-|^2 (-\hat{e}_z) + \mathbf{I}^-)], \end{aligned} \quad (50)$$

where

$$\begin{aligned} \mathbf{I}^+ &= \operatorname{Re} \left( \sum_j \left\langle u_j \frac{\nabla}{-ik} u_j \right\rangle^+ \right) \\ &= \operatorname{Re} \left( \frac{n_0}{-ik} \langle u_j^* \nabla u_j \rangle_j^+ d\mathbf{r}_j \right), \end{aligned} \quad (51)$$

and

$$\begin{aligned} \mathbf{I}^- &= \operatorname{Re} \left( \sum_i \left\langle u_j^* \frac{\nabla}{-ik} u_j \right\rangle^- \right) \\ &= \operatorname{Re} \left( \frac{n_0}{-ik} \langle u_j^* \nabla u_j \rangle_j^- d\mathbf{r}_j \right). \end{aligned} \quad (52)$$

The energy principle simply states that the mean energy

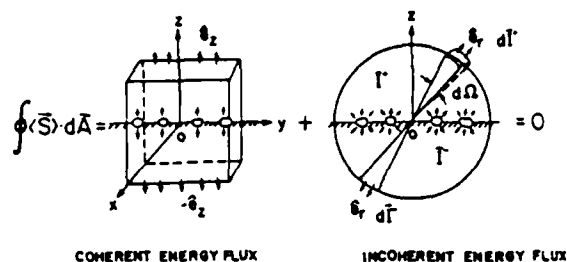


FIG. 3. Control volume for energy flux consideration.

outflow, for nondissipative scatterers, from any enclosed volume vanishes (Twersky, 1957), i.e.,

$$\int \langle S \rangle \cdot d\mathbf{A} = 0. \quad (53)$$

To verify this, a simple control volume is assumed (Figure 3). For the upper half-plane ( $z > 0$ ), we have

$$\begin{aligned} \langle S \rangle^+ \cdot d\mathbf{A} &= \omega p k [\psi_0^2 (-\hat{e}_z) + (|\langle U \rangle^+|^2 \hat{e}_z) \cdot \hat{e}_z \\ &+ \omega p k \int \mathbf{I}^+ \cdot d\mathbf{A}. \end{aligned} \quad (54)$$

For the lower half-plane ( $z < 0$ ), we have

$$\begin{aligned} \int \langle S \rangle^- \cdot d\mathbf{A} &= \omega p k [\psi_0^2 [(-\hat{e}_z) + (T + T^*) (-\hat{e}_z)] \\ &+ (|\langle U \rangle^-|^2 \hat{e}_z) \cdot (-\hat{e}_z) + \omega p k \int \mathbf{I}^- \cdot d\mathbf{A}. \end{aligned} \quad (55)$$

Note from Figure 3 that the total average energy flux has two separate parts. One is the coherent energy flux which has components either in the positive or negative  $z$  direction, but not in the  $x$  and  $y$  directions. The other is the power scattered into all directions (specified by  $\hat{e}_z$ ), called the incoherent energy flux,  $\mathbf{I}^+$  and  $\mathbf{I}^-$ . After adding equation (55) to equation (54),

$$\begin{aligned} \int \langle S \rangle \cdot d\mathbf{A} &= \omega p k [\psi_0^2 (T + T^*) + |\langle U \rangle^+|^2 + |\langle U \rangle^-|^2] \\ &+ \omega p k \int \mathbf{I} \cdot d\mathbf{A}. \end{aligned} \quad (56)$$

The term  $u_j^* (\nabla / -ik) u_j$  appearing in  $\mathbf{I}^+$  and  $\mathbf{I}^-$  in the  $p$  term is related to the scattering cross-section  $\sigma$  (Appendix A), and we can show that

$$\begin{aligned} \int \mathbf{I}^+ \cdot d\mathbf{A} &= n_0 \bar{\sigma}^+ \psi_0^2, \\ \int \mathbf{I}^- \cdot d\mathbf{A} &= n_0 \bar{\sigma}^- \psi_0^2, \end{aligned} \quad (57)$$

and

$$\mathbf{I} \cdot d\mathbf{A} = n_0 (\bar{\sigma}^+ + \bar{\sigma}^-) \psi_0^2 = n_0 \bar{\sigma} \psi_0^2,$$

where

$$\bar{\sigma} = \int \sigma q(a) da.$$

After dividing equation (56) by  $\psi_0^2 \omega \rho k$  and neglecting the terms  $|\langle U \rangle|^2$  and  $|\langle U \rangle|^{-2}$  (of order  $|R|^2$  and  $|T|^2$ , which are small compared with  $|R|$  and  $|T|$ , respectively), we obtain

$$\int \langle S \rangle \cdot dA = (T + T^*) + n_0 \bar{\sigma}. \quad (58)$$

The first term on the right-hand side of equation (58) becomes [by using equation (12)]

$$(T + T^*) = -4\pi n_0 \operatorname{Im} [\bar{f}(\pi)]/k. \quad (59)$$

Substituting equation (59) back into equation (58), it can be seen [by using the forward scattering theorem (Morse and Ingard, 1968)] that

$$\int \langle S \rangle \cdot dA = n_0 [\bar{\sigma} - 4\pi \operatorname{Im} (\bar{f}(\pi))/k] = 0. \quad (60)$$

Equation (60) states that the energy flux coherently transmitted is canceled by the energy flux incoherently scattered. This verifies the energy principle for nonabsorbing scatterers as mentioned in Twersky (1957). The proof of the conservation of energy, in other words, is done exactly as in the case of a single scatterer by computing the net flux due to the exciting and the scattered fields through a close surface containing one scatterer. This is also explained in Waterman and Truell's paper (1960).

## RESULTS AND DISCUSSION

Tolstoy (1983) modeled nodule deposits as hard (rigid) scatterers on a hard ocean floor and considered only low-frequency cases. Nevertheless, the results are heuristic and the modeling is not realistic. We modeled manganese nodules as elastic spheres whose measured properties are shown in Table 1. However, calculations using rigid spheres as nodules are also done for the purpose of comparison.

For a low area coverage of nodules, e.g., 0.2 percent, the nodule field is estimated to have about 150 tons/km<sup>2</sup> nodule deposit on the sea floor if a 3 cm nodule in radius is assumed. Although the area coverage is low, the rather high area weight density proves to be interesting enough to the mining industry. Note that in our calculations the bottom plane reflectivity was taken as zero to model more accurately the nearly acoustically transparent sedimentary bottom in the Central Pacific Basin (Mizuno et al., 1976). In Figures 4 and 5 we present the computed values of the acoustic intensities which have been divided by  $\rho \omega k \psi_0^2$  as a function of the nondimensional frequency  $ka$  for sparse distributions of nodules.

We see from Figures 4 and 5 that the contribution of the coherent intensity toward the total backscattered intensity is quite small; therefore, it can be neglected for high values of  $ka$ . As expected, the coherent intensity is a hundred times larger

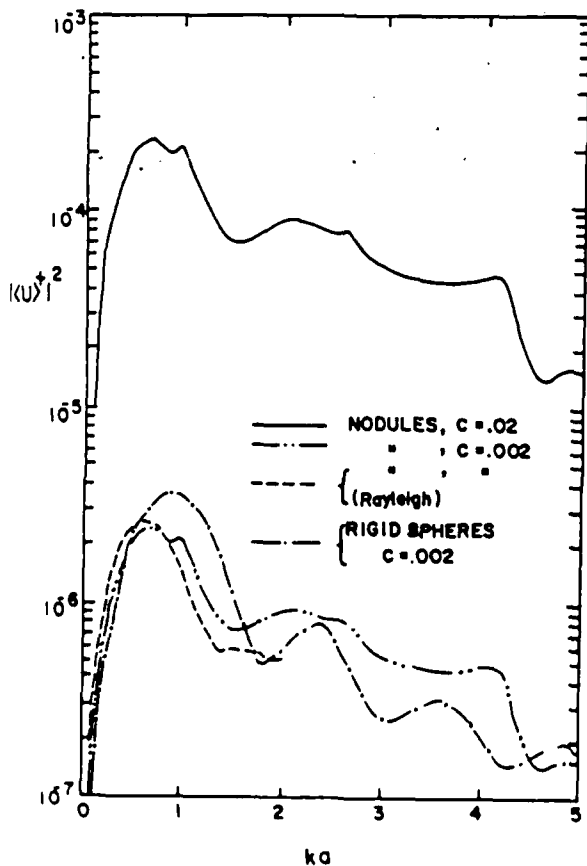


FIG. 4 Nondimensional coherent acoustic intensity versus nondimensional frequency.

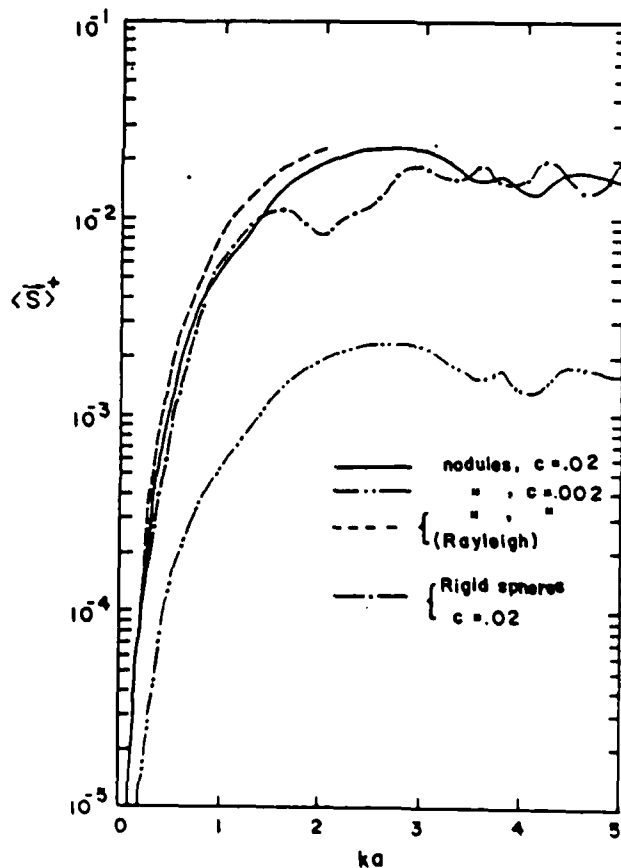


FIG. 5 Nondimensional total acoustic intensity versus nondimensional frequency.

Table 1. Acoustical properties of manganese nodules.

Concretion type	Wave speeds			Density (kg/m <sup>3</sup> )
	$C_L$ (m/s)	$C_T$ (m/s)	$C_T/C_L$	
Pacific nodules	1 950–2 500 [2 350]	1 615–2 450 [2 000]	0.83–0.98	1 910–1 960
Atlantic nodules	2 125–3 215 [2 605]	1 625–2 580 [1 980]	0.69–0.80	1 890–2 070

[ ] = average value

when the concentration changes from 0.002 to 0.02 while the total intensity is only ten times larger. The size distribution does not seem to affect the intensity very much. This may be because it is a Rayleigh distribution and the cutoff size is limited from the real nodule size distributions. However, this should be investigated further for an even denser distribution.

The refinement of the elastic sphere model can actually provide a more accurate intensity calculation because nodules are, in general, potato-shaped scatterers. Precisely speaking, they cannot be modeled as identically shaped scatterers. However, the randomness in shape can also be included in the configurational average consideration. Varadan and Varadan (1980) suggested using the T matrix to solve for different shape scatterers. Future modification of the present model is feasible, depending upon the required numerical accuracy.

We take into account the interactions among nodules, but the higher-order scattering terms are ignored due to the sparse distribution and low concentration of nodules. For high concentrations of nodules, the complete introduction of the higher-order scattering terms, plus the appropriate distribution function, are required to analyze the problem using multiple scattering theory. This is currently being investigated.

## REFERENCES

Foldy, L. L., 1945, The multiple scattering of waves: Phys. Rev., 67, 107–119.

- Glasby, G. P., 1977, Marine manganese deposits: Elsevier Oceanography Series, 15.  
 Graff, G., 1984, Mineral mining heads out to sea: High Technology, January, 26–28.  
 Greenslate, J., 1977, Manganese concentration weight density—a marine geochemistry constant: Moore, J. R., Ed., in Marine Mining, Crane, Russak & Co. Inc., 1, 125.  
 Lamb, H., 1932, Hydrodynamics: Dover Publications Inc.  
 Ma, Y., Varadan, V. K., Varadan, V. V., and Bedford, K. W., 1983, Multifrequency remote acoustic sensing of suspended materials in water: J. Acoust. Soc. Am., 74, 581–585.  
 Magnuson, A. H., Sundkvist, K., Ma, Y., and Smith, K., 1981, Acoustic sounding for manganese nodules: 13th Offshore Tech. Conf., no. 4133, Houston, May.  
 Magnuson, A. H., Sundkvist, K., Ma, Y., Riggins, D., and Sen, R., 1982, Remote acoustic sensing of manganese nodule deposits: 14th Offshore Tech. Conf., no. 4260, Houston, May.  
 Mizuno, A., and Moritani, T., 1976, Manganese nodule deposits of the Central Pacific basin: World Mining and Metals Tech., 267–281.  
 Morse, P. M., and Ingard, K. U., 1968, Theoretical acoustics: McGraw-Hill Book Co. Inc.  
 Spiess, F. N., 1980, Ocean remote acoustic sensing of the sea floor, NOAA Workshop on Ocean Acoustic Remote Sensing, II, NOAA Office of Sea Grant, Rockville, 11–1; 11–38.  
 Spiess, F. N. and Weydert, M. P., 1983, Variability of acoustic reflectivity over a manganese nodule field: 106th Acoust. Soc. of Am. Mtg., no. HHH2, San Diego.  
 Tolstoy, I., 1983, Acoustic estimation of deep sea floor nodule densities: Geophysics, 48, 1450–1452.  
 Twersky, V., 1957, On scattering and reflection of sound by rough surfaces: J. Acoust. Soc. Am., 29, 208–225.  
 Varadan, V. K., and Varadan, V. V., 1980, Acoustic, electromagnetic and elastic wave scattering—Focus on the T-matrix approach: Pergamon Press.  
 Waterman, P. C., and Truell, R., 1961, Multiple scattering of waves: J. Math. Phys., 2, 512–537.

## APPENDIX A

For an elastic sphere in a fluid medium

$$C_n = \frac{y_{n1}D - g(x_1/x_3)y'_{n1}E}{-j_{n1}D + g(x_1/x_3)y'_{n1}E}$$

$$x_1 = ka, \quad x_2 = k_L a, \quad x_3 = k_T a$$

$$j_{n1} = j_n(x_1), \quad j_{n2} = j_n(x_2), \quad j_{n3} = j_n(x_3)$$

$$h = k_L/k_T$$

$$j'_{n1} = d[j_n(kr)]/d[kr], \quad r = a$$

$$j'_{n2} = d[j_n(k_L r)]/d[k_L r], \quad r = a$$

$$j'_{n3} = d[j_n(k_T r)]/d[k_T r], \quad r = a$$

$$j''_{n1} = d^2[j_n(k_L r)]/[d(k_L r)]^2, \quad r = a$$

$$j''_{n2} = d^2[j_n(k_T r)]/[d(k_T r)]^2, \quad r = a$$

(A-1)

$$j''_{n3} = d^2[j_n(k_T r)]/[d(k_T r)]^2, \quad r = a$$

$$y_{n1} = y_n(x_1)$$

$$y'_{n1} = d[y_n(kr)]/d(kr), \quad r = a$$

$g$  = density ratio of scatterer to fluid medium,

$$D = 2n(n+1)[1 - (j_{n2}/x_2 j'_{n2})] - (x_3^2 j'_{n3}) - n^2 - n + 2$$

and

$$E = 4n(n+1)(1 - j_{n2}/x_2 j'_{n2})(1 - x_3 j'_{n3}/j_{n3})$$

$$- 2x_2[x_3^2 j'_{n3}/j_{n3} + n^2 + n + 2]$$

$$\times [(1/2h^2 - 1)j_{n2}/j'_{n2} - j'_{n2}/j'_{n2}]$$

For a rigid sphere in a fluid medium

$$C_n = -y'_{n1}/j_{n1},$$

(A-2)

$$\sigma = \int_0^{4\pi} I_s R^2 d\Omega / I_i, \quad (A-3)$$

$I_s$  = Scattered wave intensity,

$I_i$  = Incident wave intensity,

$$\sigma = 2\pi \int_0^\pi |p_s|^2 R^2 \sin \theta d\theta / |p_i|^2, \quad (A-4)$$

for spherical coordinates,

$p_s$  = scattered wave pressure,

$p_i$  = incident wave pressure,

$$\sigma^- = 2\pi \int_{\pi/2}^\pi |p_s|^2 R^2 \sin \theta d\theta / |p_i|^2, \quad (A-5)$$

$$\sigma^+ = 2\pi \int_0^{\pi/2} |p_s|^2 R^2 \sin \theta d\theta / |p_i|^2, \quad (A-6)$$

and

$$\sigma = \sigma^+ + \sigma^- = (4\pi/k^2) \sum_{n=0}^{\infty} (2n+1)/(1+C_n^2). \quad (A-7)$$

Rayleigh size distribution function

$$q(a) = (2a^3/0.74\bar{a}^4) \exp(-a^4/1.48\bar{a}^4). \quad (A-8)$$

Uniform size distribution function

$$q(a) = \begin{cases} 0, & a \neq \bar{a} \\ 1, & a = \bar{a} \end{cases} \quad (A-9)$$

Asymptotic expression for the spherical Hankel function of the first kind

$$h_n^{(1)}(kr) \sim \frac{1}{kr} e^{ikr - (n+1/2)\pi/2}, \quad kr \gg 1. \quad (A-10)$$

## APPENDIX B

### CONFIGURATIONAL AVERAGE

Consider  $N$  scatterers which are statistically distributed on a plane. An ensemble of configurations can be characterized by a probability distribution function of  $r_j$ ,

$$p = p(r_1, r_2, \dots, r_N). \quad (B-1)$$

Equation (B-1) specifies the probability that the first scatterer lies in the element of area  $dr_1$  about the position  $r_1$  and the second scatterer lies in the element of area  $dr_2$  about the position  $r_2$ , etc. The probability of finding such a configuration can thus be represented as

$$p dr_1 dr_2, \dots, dr_N. \quad (B-2)$$

Now we introduce a random scalar function  $F$  which is a function of  $r_j$ ,  $F = F(r_1, r_2, \dots, r_N)$ . The configurational average of  $F$  over the ensemble of configurations can be given in terms of  $p$  as

$$\langle F \rangle = \int \dots \int F p dr_1 dr_2, \dots, dr_N. \quad (B-3)$$

The conditional probability distribution function

$$p(r_1, r_2, \dots, r_N/r_j) = p(r_1, r_2, \dots, r_{j-1}, r_{j+1}, \dots, r_N/r_j),$$

which is useful in the averaging process, represents the probability of finding the  $N-1$  scatterers located at the appropriate intervals of  $r + dr$  with the  $j$ th scatterer at the fixed position  $r_j$ . In the same manner, the conditional probability distribution function

$$p(r_1, r_2, \dots, r_N/r_j, r_k)$$

$$= p(r_1, r_2, \dots, r_{j-1}, r_{j+1}, \dots, r_{k-1}, r_{k+1}, \dots, r_N/r_j, r_k),$$

represents two nodules at the fixed positions  $r_j$  and  $r_k$ .

According to the law for the conditional probability, it can be seen that

$$p(r_1, r_2, \dots, r_N) = p(r_j) p(r_1, r_2, \dots, r_N/r_j),$$

and

(B-4)

$$p(r_1, r_2, \dots, r_N) = p(r_j, r_k) p(r_1, r_2, \dots, r_N/r_j, r_k),$$

where  $p(r_j)$  is the probability of the scatterer occurring between  $r_j$  and  $dr_j$  and  $p(r_j, r_k)$  is the probability of the  $j$ th and the  $k$ th scatterers occurring simultaneously as specified.

The conditional configurational average of a random function  $F$  over the ensemble of configurations of  $N-1$  nodules holding the  $j$ th nodule fixed can thus be defined in terms of the conditional probability distribution function  $p(r_1, r_2, \dots, r_N/r_j)$  as

$$\langle F \rangle_j = \int_{N-1} \dots \int F p(r_1, r_2, \dots, r_N/r_j) \prod_{n=1, n \neq j}^N dr_n. \quad (B-5)$$

where

$$\prod_{n=1}^N dr_n = dr_1, dr_2, \dots, dr_{N-1},$$

and the integration, equation (B-5), is not performed over  $dr_j$ . Similarly,

$$\langle F \rangle_{jk} = \int_{N-2} \dots \int F p(r_1, r_2, \dots, r_N/r_j, r_k) \prod_{n=1, n \neq j, k}^N dr_n. \quad (B-6)$$

Using equations (B-4), (B-5), and (B-6),  $\langle F \rangle$  and  $\langle F \rangle_j$  can be expressed in terms of  $\langle F \rangle_j$  and  $\langle F \rangle_{jk}$  in the following manner:

$$\langle F \rangle = \int \langle F \rangle_j p(r_j) dr_j,$$

and

(B-7)

$$\langle F \rangle_j = \int \langle F \rangle_{jk} \frac{p(r_j, r_k)}{p(r_j)} dr_k.$$

## APPENDIX C

## BACKGROUND OF THE REMOTE-SENSING TECHNIQUE

Existing prospecting techniques for manganese nodule deposits require lowering instruments, sensors, etc. by cable several miles to the ocean floor. For example, side-scan sonar imaging at ultrasonic frequencies is in wide use and provides a detailed picture of the bottom, including profiles of individual nodules (Spiess, 1980).

However, side-scan sonar imaging must be done relatively close to the bottom and requires a long tow cable. Survey speeds are consequently slow and the process is, therefore, expensive. Moreover, ultrasonic frequencies are severely attenuated with distance so that remote sensing is ruled out when sounding in a typical water depth of 5 000 m with high-frequency transducers.

To increase the speed of surveillance and to reduce the prospecting cost, the cable from which the instrumentation is suspended should be eliminated. To do this, mount the instrument in or near the survey ship to form a remote-sensing system. After sending the acoustic pulses remotely from the exploration vessel, the reflected return sound pulses are ana-

lyzed to infer the presence and amount of nodules.

The remote-sensing technique is based on the expected acoustic signature of the bottom in the presence of nodules. The characteristic acoustic response (as a function of frequency) of nodule deposits is that of a "high-pass filter" (Magnuson et al., 1981). The break frequency increases with increasing nodule size. If the mean size is fixed, the strength of the return signal will increase with increasing nodule concentration. The expected high-pass filter characteristic of the nodule response is the basis of the research. Ocean bottoms without nodules have a relatively flat spectrum and the response is less independent of frequency. If a return from the bottom exhibits a high-pass filter characteristic, we conclude that nodules (or other rounded objects) are down there. It is the qualitative difference between bottoms with and without nodules that makes it possible (in principle) to sense nodules remotely. As for the quantitative results, detailed analysis is required and we present one here.

## APPENDIX D

## BRIEF REVIEW OF TWERKSY'S (1957) WORK

Twersky (1957) in his pioneering paper "On scattering and reflections of sound by rough surfaces" considered rough surfaces as a random distribution of arbitrary identical scatterers (e.g., circular semicylinders and hemispheres) on free or rigid base planes.

Starting with the boundary-value problem for a single configuration of scatterers (it was considered at that time to be difficult to calculate the far-field scattering amplitude of a single scatterer due to the lack of good computing facilities) the goal was to find the analytical, rather than numerical, results of the corresponding ensemble average energy flux from rough surfaces excited by a plane acoustic wave.

The physical restrictions in Twersky's paper were primarily from the assumed sparse distribution of scatterers, i.e., the

average separation of scatterers is large compared to their sizes. However, this assumption made his heuristic approximation (that the average field with two scatterers held fixed could be replaced by the average with one fixed) feasible and allowed the development of an initial practical formalism without loss of generality. For the case of a dense distribution of scatterers, multiple scattering involving a higher-order statistics has to be considered. This is now under investigation by the authors for the scattering problem of nodule deposits.

Finally, the reflection coefficients, as well as differential scattering cross-sections per unit area of rough surfaces (mutually consistent in fulfilling the principle of conservation of energy) were obtained by Twersky considering multiple-scattering effects.



# Multiple scattering of compressional and shear waves by fiber-reinforced composite materials

V. K. Varadan, Y. Ma, and V. V. Varadan

Laboratory for Electromagnetic and Acoustic Research, Department of Engineering Science and Mechanics, The Pennsylvania State University, University Park, Pennsylvania 16802

(Received 15 October 1985; accepted for publication 19 December 1985)

A multiple scattering formalism using a  $T$  matrix to characterize the response of a single fiber to an incident wave is presented to describe  $P$ - and  $SV$ -wave propagation in a fiber-reinforced composite. A convenient numerical procedure is then developed to compute the effective elastic moduli, attenuation, and phase velocity as a function of frequency and fiber concentration.

PACS numbers: 43.20.Fn

## INTRODUCTION

In the design of fiber-reinforced composite materials for structural applications, it is important to know the dynamic properties of the composite as a function of frequency, fiber properties, concentration, and distribution. It is the dynamic structural properties that determine the response of a structure to transient loads. The dynamic properties of the composite can be predicted by studying the propagation of elastic ( $P$  and  $SV$  or  $SH$ ) waves in such materials either experimentally or theoretically. Waves propagating in such a medium will undergo multiple scattering, geometric dispersion, and attenuation. The resulting effective propagation constant is hence complex and frequency dependent, the real part being directly related to the elastic properties of the composite. Previously, we have given a multiple scattering formalism for the propagation of  $SH$  waves in a medium containing a random distribution of correlated fibers.<sup>1</sup> The formalism is based on the quasicrystalline approximation (QCA) which requires only a knowledge of two body correlations and the  $T$  matrix of a fiber of arbitrary cross section.

In this paper, we consider the more realistic problem of compressional- ( $P$ -) and shear- ( $SV$ -) wave propagation perpendicular to circular fibers. The only relevant theoretical studies of this type are those of Bose and Mal<sup>2</sup> and Datta<sup>3</sup> in the low-frequency limit (Rayleigh range). The appropriate correlation between fibers is not incorporated in their investigations. Even though they could obtain reliable values for phase velocity in the Rayleigh limit, the relevant coherent attenuation was not presented in Ref. 3, while some approximate value was presented in Ref. 2. However, the computations of frequency-dependent elastic properties such as dilatational modulus, shear modulus, Young's modulus, etc., require both phase velocity and coherent attenuation as a function of frequency for a range of concentration. This paper provides analytical and numerical multiple scattering approaches for such a study. We have derived analytical expressions for the effective propagation constant in the Rayleigh limit from our multiple scattering formalism. Our results of phase velocity agree with those of Ref. 2 and the Hashin-Rosen<sup>4</sup> bounds. Further, we have obtained numerical results for higher frequencies and higher fiber concentrations. The results are presented in the form of plots of the attenuation and phase velocity of  $P$  and  $SV$  waves and the

effective elastic moduli as a function of frequency and concentration.

## I. SCATTERING FIELD FORMALISM

Consider a random distribution of  $N$  number of long, parallel elastic cylinders embedded in an infinitely extended elastic solid (matrix) which are referred to as a coordinate system, as shown in Fig. 1. Here,  $O_i$  and  $O_j$  denote the centers of the  $i$ th and  $j$ th cylinders and can be represented by polar coordinates  $r_i$  and  $\theta_i$  and  $r_j$  and  $\theta_j$ , respectively. The  $z$  axis is taken parallel to the axis of the cylinder, and  $P$  is any point in the matrix which is denoted by polar coordinate system centered at  $O_j$ .

Let  $\lambda, \mu, \rho$  be the elastic constants and density of the matrix medium and  $\lambda_1, \mu_1, \rho_1$  be those of the cylinders.

Assume that either a time harmonic plane compressional ( $P$ ) or shear ( $SV$ ) wave of unit amplitude and frequency  $\omega$  propagates normal to the cylinders. Choose a Cartesian coordinate system (see Fig. 1) such that the direction of propagation of the incident wave is along the  $x$  axis while

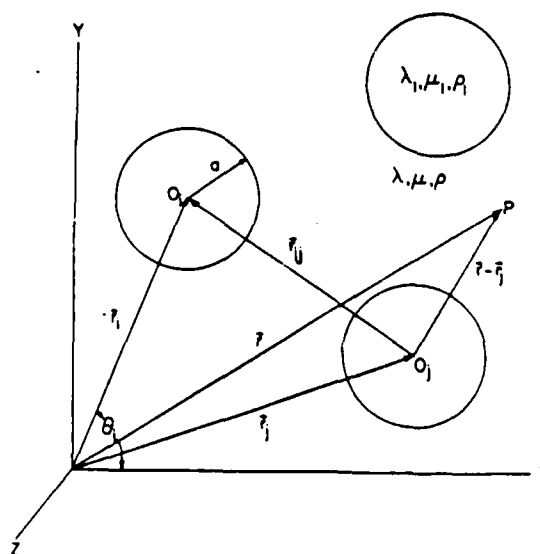


FIG. 1. Random distribution of circular cylinders and the geometry.

the displacement vector of the incident shear wave is along the  $y$  axis. Suppressing the time dependence  $e^{-i\omega t}$ , the displacement vector corresponding to the incident wave is denoted by

$$u^0 = \begin{cases} e^{ik_p x} \hat{x}, & (P) \text{ wave,} \\ e^{ik_{SV} x} \hat{y}, & (SV) \text{ wave,} \end{cases} \quad (1)$$

where  $k_p$  and  $k_{SV}$  are the wavenumbers of the  $P$  and  $SV$  waves in the matrix,

$$\begin{aligned} k_p &= \omega/c_p; \quad k_{SV} = \omega/c_{SV}; \quad c_p = \sqrt{(\lambda + 2\mu)/\rho}; \\ c_{SV} &= \sqrt{\mu/\rho}. \end{aligned} \quad (2)$$

The waves undergo multiple scattering when they impinge on the cylinders, giving rise to a displacement field inside the cylinder also. The displacement vector corresponding to the scattered field is denoted by  $u^s$  while that corresponding to the refracted field is denoted by  $u_i$ . The displacement fields  $u^s$  and  $u_i$  satisfy equations of motion given by

$$[(k_p^{-2} - k_{SV}^{-2})\nabla\nabla\cdot + k_{SV}^{-2}\nabla^2]u^s + u^s = 0, \quad (3)$$

$$[(k_i^{-2} - k_{SV}^{-2})\nabla\nabla\cdot + k_{SV}^{-2}\nabla^2]u_i + u_i = 0. \quad (4)$$

In Eq. (4),

$$\begin{aligned} k_i &= \omega/c_i; \quad k_{SV} = \omega/c_{SV}; \\ c_i &= \sqrt{(\lambda_i + 2\mu_i)/\rho_i}; \quad c_{SV} = \sqrt{\mu_i/\rho_i} \end{aligned} \quad (5)$$

are the  $P$  and  $SV$  wavenumbers and wave velocities, respectively, inside the cylinder.

The displacement vector can be constructed using two scalar potentials  $\phi$  and  $\psi$  which are solutions of the scalar wave equation for compressional ( $\phi$ ) and shear ( $\psi$ ) waves and is given by

$$u = \nabla\phi + k_{SV}\nabla\times(\hat{z}\psi). \quad (6)$$

The expansion of the solution of the scalar wave equation in terms of cylindrical functions, namely, products of Bessel or Hankel functions and trigonometric functions, is well known. The outgoing scattered waves centered at the origin of the cylinder are given in terms of Hankel functions, while the exciting field must be regular at the origin and hence given by Bessel functions.

The total displacement field at any point (say  $P$ ) in the matrix is the sum of the incident field and the fields scattered by all the cylinders. The field that excites the  $j$ th cylinder  $u_j^s$  is, however, the result of the incident field  $u^0$  and the fields scattered from all the remaining scatterers. Thus, at any point  $r$  in the vicinity of the  $j$ th cylinder,

$$u_j^s(r) = u^0(r) + \sum_{i \neq j}^N u_i^s(r - r_i). \quad (7)$$

We now expand the scattered and exciting fields in terms of vector cylindrical basis functions  $\phi_n$  and  $\psi_n$ :

$$u_i^s(r) = \sum_{n=-\infty}^{\infty} [\alpha_n^i \phi_n(r - r_i) + \beta_n^i \psi_n(r - r_i)], \quad (8)$$

$$\begin{aligned} u_j^s(r) = \sum_{n=-\infty}^{\infty} [A_n^j \text{Re } \phi_n(r - r_j) \\ + B_n^j \text{Re } \psi_n(r - r_j)], \end{aligned} \quad (9)$$

where

$$\phi_n = \nabla\phi_n = (1/k_n)\nabla[H_n(k_n|r - r_i|)e^{in\theta_i}], \quad (10)$$

$$\psi_n = k_n\nabla\times(\hat{z}\psi_n) = (1/k_n)\nabla\times[2H_n(k_n|r - r_i|)e^{in\theta_i}]. \quad (11)$$

The  $\text{Re } \phi_n$  and  $\text{Re } \psi_n$  are given by (10) and (11) with Hankel function replaced by Bessel function  $J_n$ , and  $\alpha_n, \beta_n, A_n$ , and  $B_n$  are undetermined coefficients. In Eq. (11),  $\theta_i$  refers to the angle that  $r - r_i$  makes with the  $x$  axis (see Fig. 1).

Since  $(u_i^s + u_j^s)$  is the total field in the matrix medium, the expansion coefficients of the field scattered by the  $i$ th cylinder may be formally related to the coefficients of the field that excites the  $i$ th cylinder through the  $T$  matrix:

$$\begin{pmatrix} \alpha_n^i \\ \beta_n^i \end{pmatrix} = \sum_{m=-\infty}^{\infty} \begin{pmatrix} T_{nm}^{11} & T_{nm}^{12} \\ T_{nm}^{21} & T_{nm}^{22} \end{pmatrix} \begin{pmatrix} A_m^i \\ B_m^i \end{pmatrix}. \quad (12)$$

Substituting (8) and (9) in (7), we obtain

$$\begin{aligned} \sum_n [A_n^j \text{Re } \phi_n(r - r_j) + B_n^j \text{Re } \psi_n(r - r_j)] \\ = u^0(r) + \sum_{i \neq j}^N \sum_m [\alpha_m^i \phi_m(r - r_i) + \beta_m^i \psi_m(r - r_i)]. \end{aligned} \quad (13)$$

It should be noted that the series on the right-hand side of (13) is expressed with respect to the center of the  $i$ th cylinder. In order to express these quantities with respect to the center of the  $j$ th cylinder, the following addition theorem for cylindrical vector wave functions is invoked:

$$\phi_i(r - r_i) = \sum_m (-1)^{l+m} \text{Re } \phi_m(r - r_j) \phi_{l-m}(r_{ij}), \quad (14)$$

$$\psi_i(r - r_i) = \sum_m (-1)^{l+m} \text{Re } \psi_m(r - r_j) \psi_{l-m}(r_{ij}),$$

where  $r_{ij} = r_i - r_j$ .

Substituting (14) in (13) and simultaneously expanding the incident wave in a Fourier-Bessel series expansion and then employing the orthogonality relations for the vector basis functions, we obtain

$$\begin{pmatrix} A_n^j \\ B_n^j \end{pmatrix} = \begin{pmatrix} L_n^j \\ M_n^j \end{pmatrix}. \quad (15)$$

In Eq. (15),

$$L_n^j = i^n e^{in\theta_j} \delta_{1P} + \sum_{i \neq j}^N \sum_m (-1)^{m+n} \alpha_m^i \phi_{m-n}(r_{ij}), \quad (16)$$

$$M_n^j = i^n e^{in\theta_j} \delta_{2P} + \sum_{i \neq j}^N \sum_m (-1)^{m+n} \beta_m^i \psi_{m-n}(r_{ij}),$$

where  $\delta_{ij}$  is the Kronecker delta. For  $P$ -wave incidence,  $P = 1$ , and for  $S$ -wave incidence,  $P = 2$ . In Eq. (15),  $L$  and  $M$  contain unknown coefficients  $\alpha$  and  $\beta$  of the scattered field. The coefficients  $\alpha$  and  $\beta$  are, however, related to  $A$  and  $B$  of the exciting field through the  $T$  matrix as defined in Eq. (12). Substituting Eq. (15) in Eq. (12), we obtain a system of linear equations for the scattered field coefficients:

$$\begin{pmatrix} \alpha_n^j \\ \beta_n^j \end{pmatrix} = \sum_m \begin{pmatrix} T_{nm}^{11} & T_{nm}^{12} \\ T_{nm}^{21} & T_{nm}^{22} \end{pmatrix} \begin{pmatrix} L_m^j \\ M_m^j \end{pmatrix}. \quad (17)$$

In the sequel, we continue the analysis for  $P$ -wave incidence and study the phase velocity, coherent attenuation, dynamic moduli, etc., both for low and higher frequencies. Without much detailed presentation, we also present similar results for  $S$ -wave incidence.

For only  $P$ -wave incidence, Eq. (17) can be rewritten for identical cylinders as

$$\alpha'_n = \sum_{n'} T_{nn'}^{11} \left( a_n^0 + \sum_{j \neq n}^N \sum_{n''} (-1)^{n' + n''} \alpha'_{n''} \phi_{n'' - n'}(r_y) \right) + \sum_{n'} T_{nn'}^{12} \left( \sum_{j \neq n}^N \sum_{n''} (-1)^{n' + n''} \beta'_{n''} \psi_{n'' - n'}(r_y) \right), \quad (18)$$

and

$$\beta'_n = \sum_{n'} T_{nn'}^{21} \left( a_n^0 + \sum_{j \neq n}^N \sum_{n''} (-1)^{n' + n''} \alpha'_{n''} \phi_{n'' - n'}(r_y) \right) + \sum_{n'} T_{nn'}^{22} \left( \sum_{j \neq n}^N \sum_{n''} (-1)^{n' + n''} \beta'_{n''} \psi_{n'' - n'}(r_y) \right), \quad (19)$$

where

$$a_n^0 = r^{n'} e^{ik_n r'},$$

It can be seen from Eqs. (18) and (19) that the scat-

tered field coefficients  $\alpha_n$  and  $\beta_n$  are coupled. To uncouple these equations, we multiply Eq. (18) by  $(T^{12})^{-1}$  and Eq. (19) by  $(T^{22})^{-1}$  and subtract to obtain

$$\beta'_n = (T^{22})(T^{12})^{-1} \alpha'_n - [(T^{22})(T^{12})^{-1} T^{11} - T^{21}] \times \left( a^0 + \sum_{j \neq n}^N \sigma^1(r_y) \alpha'_j \right), \quad (20)$$

where  $\sigma^1(r_y)$  stands for the propagator term given by  $(-1)^{n' + n''} \phi_{n'' - n'}$  for  $P$  waves. In writing (20), we have dropped all the summation and subscripts to avoid cumbersome looking expressions. With Eq. (20), Eq. (18) now explicitly gives the scattered field formalism for elastic wave propagation through the composite medium.

In Eqs. (18) and (19), the scattered field coefficients explicitly depend on the positions of the cylinders. For a system with a large number of cylinders, it is more meaningful to study the effective propagation characteristics in the medium rather than the details of the multiple scattering processes that take place. Thus a configurational average is performed in Eqs. (18) and (19) over the positions of all cylinders except the  $j$ th, which is assumed to be held fixed. The details can be found in Ref. 1. We thus have, for identical scatterers, the average scattered field coefficients of the scattered  $P$  wave given by

$$\langle \alpha' \rangle_j = T^{11} \left( a^0 + (N-1) \int_{S'} \langle \alpha' \rangle_y \sigma^1(r_y) p(r_j | r_i) dr_i \right) + T^{12} T^{22} (T^{12})^{-1} \int_{S'} \langle \alpha' \rangle_y \sigma^2(r_y) p(r_j | r_i) dr_i - T^{12} [T^{22} (T^{12})^{-1} T^{11} - T^{21}] \left( \int_{S'} a^0 p(r_j | r_i) \sigma^2(r_y) dr_i + \int_{S'} \int_{S'} \langle \alpha' \rangle_y \phi_{jk} p(r_j | r_i, r_k) \sigma^2(r_y) \sigma^1(r_k) dr_i dr_k \right), \quad (21)$$

where  $\langle \rangle$ , and  $\langle \rangle_y$  denote the configurational averages with the  $i$ th scatterer and both the  $i$ th and  $j$ th scatterers held fixed, respectively, and  $p(r_j | r_i)$  and  $p(r_k, r_j | r_i)$  are the joint probability distribution functions. The notation  $\sigma^2(r_y)$  stands for  $(-1)^{n' + n''} \psi_{n'' - n'}$ , the propagator for  $S$  waves. In Eq. (21),  $S'$  denotes the cross-sectional area of the medium excluding the circular area of radius " $2a$ " which is the hard core radius or the minimum distance between two scatterers, each of radius " $a$ ."

The above equation is a hierarchy which, when iterated, will involve higher-order conditional probability distribution functions. However, the hierarchy can be truncated by invoking the quasicrystalline approximation (QCA) suggested by Lax.<sup>5</sup> According to the QCA,

$$\langle \alpha' \rangle_y \sim \langle \alpha' \rangle_j, \quad j \neq i, \quad (22)$$

$$\langle \alpha' \rangle_{jk} \sim \langle \alpha' \rangle_k, \quad i \neq j \neq k.$$

The probability distribution function in Eq. (21) can be conveniently written as  $p(r_k, r_j | r_i) = p(r_k | r_i) p(r_j | r_i)$  and

$$p\left(\frac{r_j}{r_i}\right) = \begin{cases} g(x)/S, & x > 1, \\ 0, & x < 1, \end{cases} \quad (23)$$

where we have assumed that the scatterers are impenetrable and that for a translationally invariant system,  $p(r_j | r_i)$  depends only on  $|r_y| = 2ax$ . In the statistical mechanics literature,  $g(x)$  is known as the radial distribution function.

For uncorrelated, impenetrable cylinders  $g(x) = 1$  or  $1/(1-c)$  for  $x > 1$ , where  $c$  is the concentration of cylinders and  $g(x) = 0$  for  $x < 1$ . This approximation is valid only for very low values of  $c$  (very sparse distribution of cylinders). Several models of the radial distribution function such as the Percus-Yevick approximation, the convolution-hypernetted chain approximation, the Born-Green-Yvon approximation, and the self-consistent approximation are widely adopted in numerical computations.

In our calculations, the Monte Carlo calculations of  $g(x)$ ,<sup>6</sup> which give a virtually exact solution to the equations of state, are used for  $c$  up to 0.55.

To study the coherent or average  $P$ -wave field in the effective medium, we assume that the average field is a plane  $P$  wave propagating in the  $x$  direction just as the original plane wave incident in the matrix but with a complex propagation constant  $K_p = K_p^r + iK_p^i$ , which is frequency dependent. The real part  $K_p^r$  is related to the phase velocity and the imaginary part  $K_p^i$  is proportional to the coherent attenuation of the  $P$  wave. Thus

$$\langle \alpha' \rangle_j = X_n e^{iK_p^r x}. \quad (24)$$

Equations (22)-(24) are substituted in Eq. (21) and the extinction theorem can be invoked to cancel the incident wave term on the right-hand side of Eq. (21). The resulting equation is

$$X_n = T_{nn}^{11} I_{n-n}^1 X_{n-} + T_{nn}^{12} I_{n-n}^2 [T_{n-n}^{22} (T_{n-n}^{12})^{-1} X_{n-} - T_{n-n}^{22} (T_{n-n}^{12})^{-1} T_{n-n}^{11} I_{n-n}^1 X_{n-} + T_{n-n}^{21} I_{n-n}^1 X_{n-}] , \quad (25)$$

where

$$I_{n-n}^1 = I^{1-n} 2\pi n_0 \left( \frac{1}{k_p^2 - K_p^2} [2k_p a J_{n-n}(2K_p a) H'_{n-n}(2k_p a) - 2K_p a H_{n-n}(2k_p a) J'_{n-n}(2K_p a)] \right. \\ \left. + 4a^2 \int_1^\infty H_{n-n}(2k_p ax) J_{n-n}(2K_p ax) [g(x) - 1] x dx \right) , \quad (26)$$

and  $I_{n-n}^2$  is obtained by replacing  $k_p$  in Eq. (26) by  $k_s$ . In Eq. (26),  $n_0 (= N/S)$  is the number density of the cylinders in the matrix.

To obtain a similar expression for the average  $S$  wave in the effective medium, we assume that the average field is a plane  $S$  wave propagating along the  $x$  direction just as the original plane  $S$  wave incident in the matrix but with a complex propagation constant  $K_s = K_s' + iK_s''$  which is frequency dependent. By assuming  $\langle \beta_{n-}^j \rangle_j = Y_n e^{iK_s x}$ , we can obtain a dispersion equation for  $Y_n$ .

Equation (25) is a system of homogeneous linear simultaneous equations for the coefficients  $X_n$  for  $P$  waves. For a nontrivial solution, the determinant of the coefficient matrix can be set equal to zero which yields the desired dispersion equation.

The dispersion equation obtained for  $P$ - or  $SV$ -wave incidence can be solved for the effective propagation constant  $K_p$  or  $K_s$ , respectively, as a function of  $k_p$ ,  $k_s$ , and number density of the cylinders  $n_0$ . The determination of  $K_p$  or  $K_s$  is necessarily numerical except in the long wavelength or Rayleigh limit. This will be discussed in Sec. II.

## II. RAYLEIGH LIMIT SOLUTION

In the Rayleigh or low-frequency limit, the size of the scatterer is considered to be very small compared to the incident wavelength. It is then sufficient to take only the lowest order coefficients in the expansion of the fields and the  $T$ -matrix elements<sup>7</sup> and the set of simultaneous equations for the unknown  $X_0$ ,  $X_1$ ,  $X_{-1}$ ,  $X_2$ , and  $X_{-2}$  for effective  $P$ -wave properties and  $Y_0$ ,  $Y_1$ ,  $Y_{-1}$ ,  $Y_2$ , and  $Y_{-2}$  for effective shear-wave properties. The dispersion equations in terms of effective  $P$  and  $S$  wavenumbers  $K_p$  and  $K_s$  are obtained as follows:

for  $P$ -wave incidence,

$$\left( \frac{K_p}{k_p} \right)^2 = \frac{Z_p}{F_p} + ic \frac{(1-c)^3}{1+c} \frac{\pi}{4} (k_p a)^2 \frac{(F_p H_p - Q_p Z_p)}{F_p^2} , \quad (27)$$

where

TABLE I. Material properties used in calculations

	Density $\rho$ (kg/m <sup>3</sup> )	Lame constants	
		$\lambda$ (N/m <sup>2</sup> )	$\mu$ (N/m <sup>2</sup> )
Boron	2530	$16.67 \times 10^{10}$	$25 \times 10^{10}$
Aluminum	2720	$6.86 \times 10^{10}$	$3.87 \times 10^{10}$

$$Z_p = (1 + ct_0)(1 + 2ct_1)[1 + ct_2(1 + \epsilon)] ,$$

$$F_p = 1 - ct_2(1 - \epsilon) - 2c^2 t_0 t_2 ,$$

$$H_p = [1 + ct_2(1 + \epsilon)](t_0 + t_1 + 3ct_0 t_1) \\ + t_2(1 + ct_0)(1 + 2ct_1)(1 + \epsilon^{3/2}) \\ + \epsilon^{1/2} t_1 [1 + ct_2(1 + \epsilon)](1 + ct_0) ,$$

$$Q_p = [1 + ct_2(1 + \epsilon)](t_0 + t_1) \\ - 2ct_2[t_0 + t_1(1 + ct_0)] + t_2(1 + \epsilon^{3/2}) \\ + \epsilon^{1/2} t_1 [1 + ct_2(1 + \epsilon) - 2ct_2(1 + ct_0)] ,$$

$$\epsilon = (c_p/c_s)^2 ,$$

$$t_0 = -(\lambda_1 + \mu_1 - \lambda - \mu)/(\lambda_1 + \mu_1 + \mu) ,$$

$$t_1 = (\rho_1 - \rho)/2\rho ,$$

$$t_2 = -\mu(\mu_1 - \mu)/[\mu_1(\lambda + 3\mu) + \mu(\lambda + \mu)] ;$$

for  $S$ -wave incidence,

$$\left( \frac{K_s}{k_s} \right)^2 = \frac{Z_s}{F_s} + ic \frac{(1-c)^3}{1+c} \frac{\pi}{4} (k_s a)^2 \frac{(F_s H_s - Q_s Z_s)}{F_s^2} , \quad (28)$$

where

$$Z_s = (1 + 2ct_1)[1 + ct_2(1 + \epsilon)] , \quad F_s = 1 + ct_2(1 - \epsilon) ,$$

$$H_s = t_1(1 + \epsilon^{-1/2})[1 + ct_2(1 + \epsilon)]$$

$$+ t_2\epsilon(1 + \epsilon^{-3/2})(1 + 2ct_1) ,$$

$$Q_s = t_1(1 + \epsilon^{-1/2})[1 + ct_2(1 - \epsilon)] + t_2\epsilon(1 + \epsilon^{-3/2}) .$$

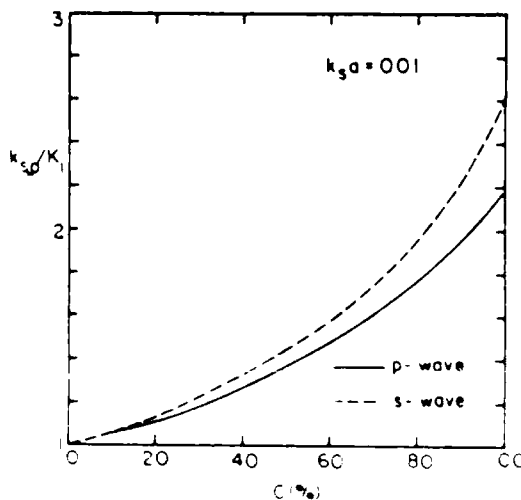


FIG. 2. Phase velocity versus concentration for boron in aluminum in the Rayleigh region

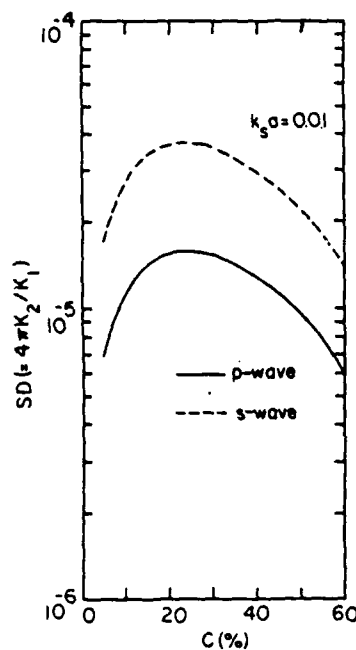


FIG. 3. Attenuation versus concentration in the Rayleigh region.

Following the work of Christensen,<sup>8,9</sup> one could define a two-dimensional bulk modulus as  $\langle E_{2D} \rangle = \langle \lambda + \mu \rangle$ , an expression which can be derived from Eq. (27), as given by

$$\langle E_{2D} \rangle = (\lambda + \mu) + (\lambda + 2\mu) \times \frac{c(\lambda_1 - \mu_1 - \lambda - \mu)}{(1-c)(\lambda_1 + \mu_1) + c\lambda + (1+c)\mu},$$

which agrees exactly with Eq. (28) of Ref. 9.

From Eq. (28), one could obtain an expression for the effective shear modulus  $\langle \mu \rangle / \mu$  also as given by

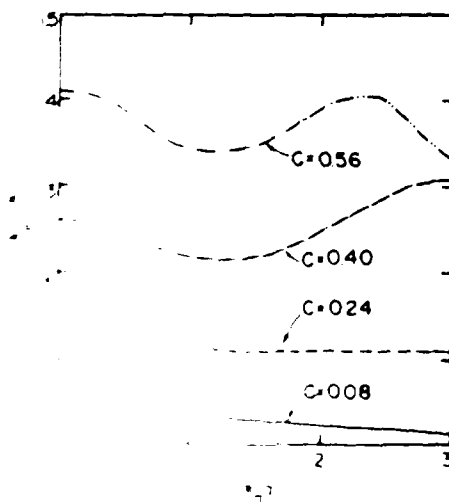


FIG. 4. Attenuation versus nondimensional frequency for P waves.

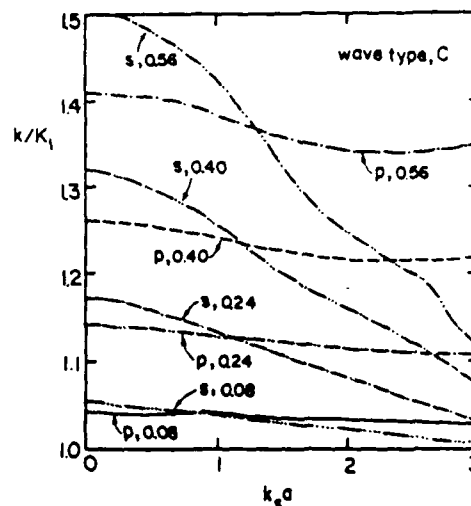


FIG. 5. Comparison of phase velocity versus nondimensional frequency between P and S waves.

$$\frac{\langle \mu \rangle}{\mu} = 1 + c \left[ \left( \frac{\mu}{\mu_1 - \mu} \right) + (1-c) \frac{(b + 7\mu/3)}{(2b + 8\mu/3)} \right]^{-1},$$

where  $b = \lambda + 2\mu/3$  is the bulk modulus. The equation is in exact agreement with Eq. (4.26) of Ref. 9.

### III. NUMERICAL RESULTS AND CONCLUSIONS

Computations of specific damping or coherent P- (SV-) wave attenuation  $K_2^2/k_p$ , (or  $K_2^2/k_s$ ) and phase velocity

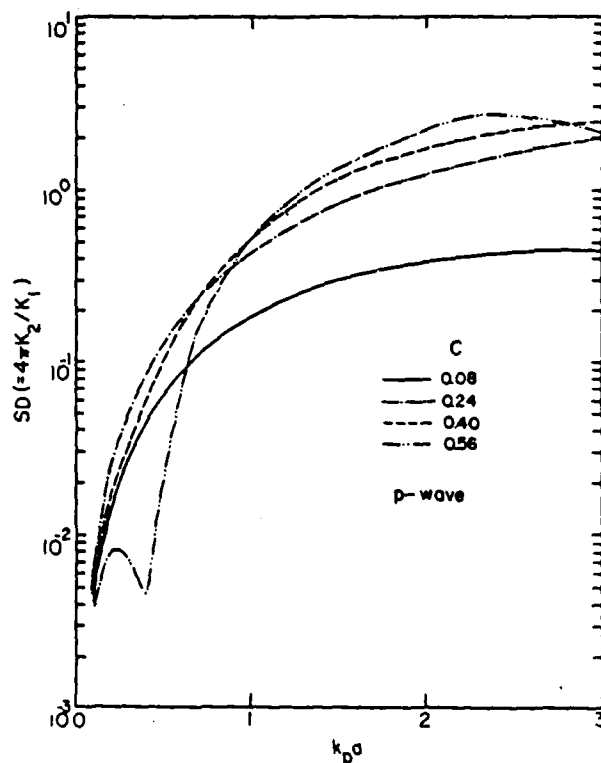


FIG. 6. Attenuation versus nondimensional frequency for P waves.

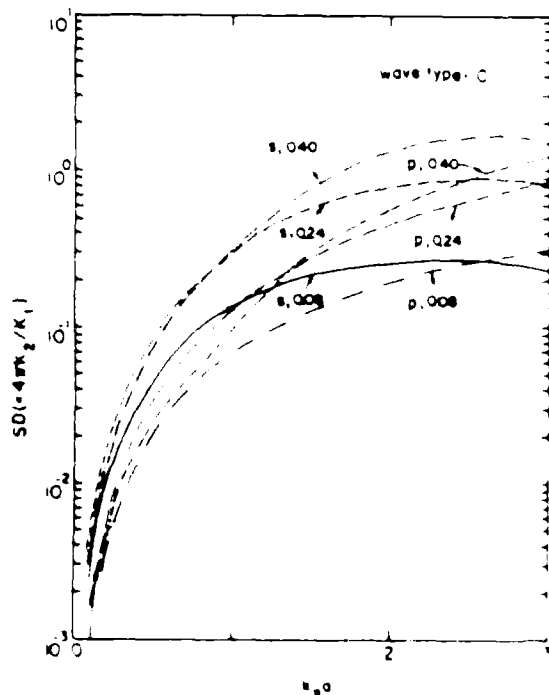


FIG. 7. Comparison of attenuation versus nondimensional frequency between *P* and *S* waves.

$k_p/K_p$  (or  $k_s/K_s$ ) as a function of nondimensionalized frequency  $k_p a$  (or  $k_s a$ ) at concentration  $C (= n_p \pi a^2)$  are performed by determining the singular values of the coefficient matrix of  $X_p$  (or  $Y_p$ ) obtained from Eq. (25). The computation involves an iterative procedure for determining the dominant root in the complex plane in terms of  $k_p a$  (or  $k_s a$ ) using Müller's method. Good initial guesses are provided by Eqs. (27) and (28) at low values of  $k_p a$  ( $k_s a$ ) and these could be used systematically to obtain quick convergence of roots at high values of  $k_p a$  (or  $k_s a$ ).

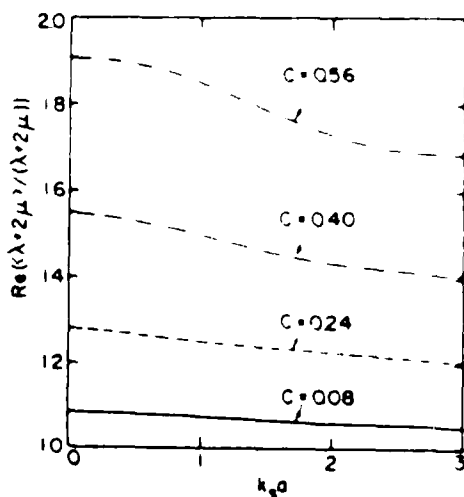


FIG. 8. Real part of elastic modulus versus nondimensional frequency.

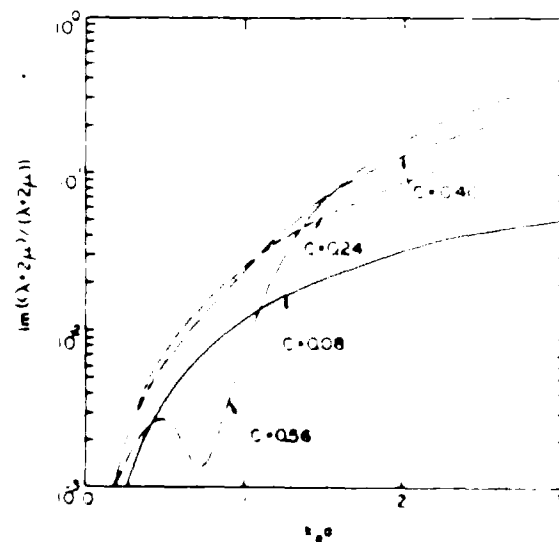


FIG. 9. Imaginary part of elastic modulus versus nondimensional frequency.

Numerical results for phase velocity, attenuation, and frequency-dependent elastic properties such as effective dilatation modulus, shear modulus, etc., are presented in Figs. 2–12 for boron–aluminum composite. The material properties of the scatterer (boron) and those of aluminum matrix are given in Table I.

In Fig. 2, the phase velocity for both *P* and *S* waves is plotted as a function of concentration for  $k_p a = 0.01$ , while Fig. 3 depicts the corresponding specific damping  $S_p^0 = 4\pi(K_p^0/K_p^0)$  for the compressional wave and  $S_s^0 = 4\pi(K_s^0/K_s^0)$  for the shear wave. As can be seen from the plots, the shear wave dominates the scattering response in the long wavelength region.

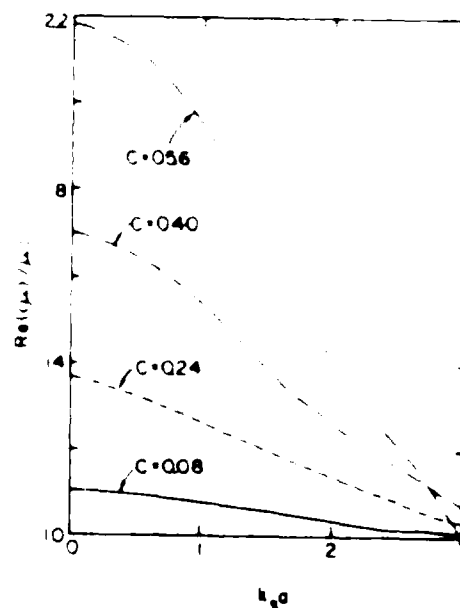


FIG. 10. Real part of shear modulus versus nondimensional frequency.

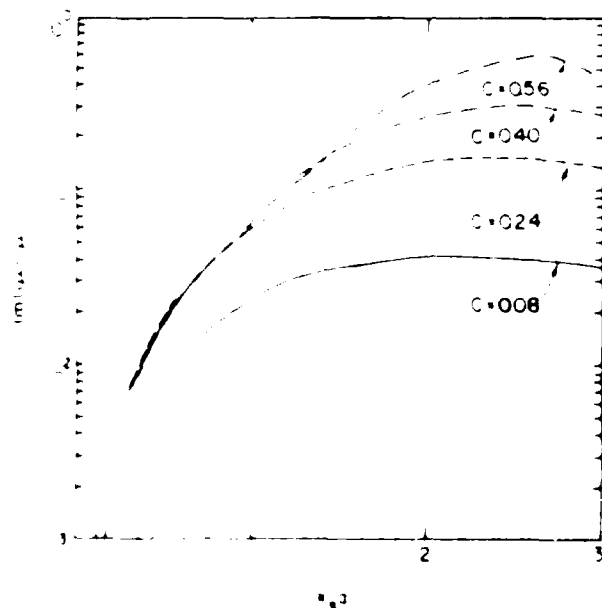


FIG. 1 Imaginary part of shear modulus versus nondimensional frequency.

Figures 4 and 5 present the frequency spectrum of the phase velocity for *P* and *S* waves, respectively, for four different concentrations. For the case of *S*-wave incidence, the phase velocity is always higher at lower frequencies for all *c*. However, for *P*-wave incidence, there is transition region where the phase velocity increases at higher frequencies at higher concentrations. This behavior may be due to an eminent resonance for a high-concentration composite. A similar behavior has also been observed by Kins<sup>10</sup> and Varadan *et al.*<sup>11</sup> earlier in the study of 3-D particulate composites.

The corresponding results for specific damping are

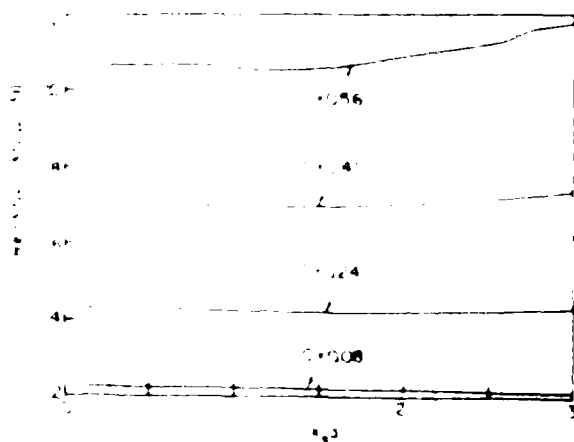


FIG. 2 Real part of 2-D bulk modulus versus nondimensional frequency.

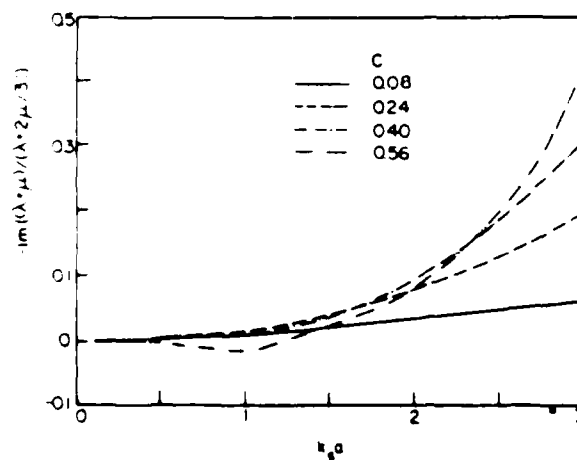


FIG. 3 Imaginary part of 2-D bulk modulus versus nondimensional frequency.

shown in Figs. 6 and 7. The anomaly of the attenuation for  $c = 0.55$  is simply the result of strong multiple scattering effects for such a highly packed system. This seems possible only for *P*-wave incidence as seen in Fig. 6.

From the effective wavenumbers  $K_y a$  or  $K_y a$ , one could easily compute frequency-dependent elastic properties as shown in Figs. 8–13. These properties are very useful in the design of fiber-reinforced composites.

#### ACKNOWLEDGMENTS

This work was supported, in part, by Rockwell International. The authors would like to thank the reviewers for their helpful comments and suggestions.

- <sup>1</sup>V. K. Varadan, V. V. Varadan, and Y. Ma, *J. Acoust. Soc. Am.* **78**, 1874 (1985).
- <sup>2</sup>S. K. Bose and A. K. Maji, *J. Mech. Phys. Solids* **22**, 217 (1974).
- <sup>3</sup>S. K. Datta, "Scattering by a random distribution of inclusions and effective elastic properties," in *Continuum Model of Discrete Systems*, edited by J. W. Prosser (University of Waterloo, Waterloo, IL, 1978).
- <sup>4</sup>Z. Hama and B. W. Rosen, *J. Appl. Mech.* **31**, 223 (1964).
- <sup>5</sup>M. Lax, *Phys. Rev.* **85**, 621 (1952).
- <sup>6</sup>W. W. Wood, *J. Chem. Phys.* **40**, 415 (1964).
- <sup>7</sup>V. K. Varadan and V. V. Varadan (Eds.), *Acoustic, Electromagnetic and Elastic Wave Scattering—Focus on the T-Matrix Approach* (Pergamon, New York, 1980).
- <sup>8</sup>R. M. Christensen and K. H. Lo, "Solutions for effective shear properties in three phase sphere and cylinder models," *J. Mech. Phys. Solids* **27**, 315 (1979).
- <sup>9</sup>R. M. Christensen, *Mechanics of Composite Materials* (Wiley, New York, 1979).
- <sup>10</sup>V. K. Kins and A. Anand, *Int. J. Solids Struct.* **18**, 367 (1982).
- <sup>11</sup>V. K. Varadan, Y. Ma, and V. V. Varadan, *J. Acoust. Soc. Am.* **77**, 375 (1985).

# EFFECTS OF NONSPHERICAL STATISTICS ON EM WAVE PROPAGATION IN DISCRETE RANDOM MEDIA

V.V. Varadan, V.K. Varadan, Y. Ma, and W.A. Steele\*

*Laboratory for Electromagnetic and Acoustic Research*

*Department of Engineering Science and Mechanics*

*and*

*Center for the Engineering of Electronic and Acoustic Materials*

*\*Department of Chemistry*

*The Pennsylvania State University, University Park, PA 16802*

## ABSTRACT

*Earlier results for electromagnetic wave propagation in discrete random media assumed spherical statistics in describing the spatial distribution even for nonspherical scatterers. The appropriate pair correlation function for nonspherical scatterers can be, in general, obtained by the Monte Carlo method which is essential in analyzing the nonspherical statistics. This paper presents new results using the nonspherical statistics in the investigation of multiple EM wave scattering by aligned dielectric prolate as well as oblate spheroids randomly distributed in space. The comparison between the previous results and those using spherical statistics show that approximating the spatial distribution of nonspherical scatterers using the spherical statistics will yield either high or low effective properties of the random media.*

## 1. INTRODUCTION

In the extant wave scattering literature, scatterers are generally being modeled as spherical ones and the complexity of the analytical problem can therefore be reduced. However, in nature, most scatterers are not spherical in shape. Thus, the sphere model will not be appropriate in some real applications. Even worse, when consider wave propagation and scattering in a collection of nonspherical scatterers with a considerable concentration, in addition to the shape of scatterers, the spatial distribution of scatterers cannot simply be described using spherical statistics. The fact is that the possibility in finding another scatterer in the neighborhood of a given scatterer becomes uneven in the radial direction which is not the case for a randomly distributed spherical scatterers due to the unsymmetry of the problem.

To make the problem tractable, nonspherical scatterers with rotational symmetry properties randomly distributed in free space are first considered. Fortunately, scattering responses from most nonspherical scatterers of this kind are able to be respresented by the T-matrix [Varadan and Varadan, 1980]. But unless the concentration of those nonspherical scatterers (in this case, lossless dielectric prolate(oblate) spheroids for EM wave study) remains at a lower level, the spatial distribution of those nonspherical scatterers cannot be, even known from our intuition, correctly described by the spherical statistics. To just see the shape effect and distiguish this from those previous approximations made using the spherical statistics even for nonspherical scatterers, we consider only the aligned case which means the symmetry axes of the spheroids are all parallel to the direction of the incident wave.

The nonspherical statistics involved in the analysis is to introduce the pair correlation function for aligned



spheroids. With the help of high speed digital computers, the Monte Carlo method can be employed to obtain the pair correlation function for aligned spheroids and some numerical values of the function are presented in this paper. Finally, computations of the effective attenuation rate as well as the phase velocity using the nonspherical statistics in studying the electromagnetic wave propagation through randomly distributed aligned spheroids are performed. When compared with numerical results for nonspherical scatterers using the spherical statistics approximations, the attenuation is found to be either over or under-estimated.

### Multiple Scattering Formulation

We consider  $N(N \rightarrow \infty)$  rotationally symmetric oriented scatterers randomly distributed in a volume  $V(V \rightarrow \infty)$  so that the number of particles per unit volume  $n_0 = N/V$  is finite, see Figure 1. Only the most important details that lead to the dispersion equation involving the pair correlation are presented and for all intermediate steps, we refer the reader to [V.K. Varadan et al., 1979].

Monochromatic plane electromagnetic wave giving rise to an electric field  $E^0$  are assumed to propagate parallel to the rotational axis of symmetry of the scatterers (the z-axis), see Figure 1. The field scattered by the  $i$ th scatterer is denoted by  $E_i^s$  so that the total field  $E$  at a point  $r$  outside the scatterers is given by

$$E(r) = E^0(r) + \sum E_i^s(r). \quad (1)$$

The field exciting the  $i$ th scatterer  $E_i^e$  is given by

$$E_i^e(r) = E^0(r) + \sum E_j^s(r). \quad (2)$$

From (1) and (2), we note that

$$E(r) = E_i^e(r) + E_i^s(r) \quad (3)$$

so that the exciting and scattered fields must be defined in a self-consistent manner. These fields are expanded in a set of vector spherical functions as follows:

$$E_i^e(r) = \sum \sum \sum [b_{\sigma m l} {}^i \text{Re} M_{\sigma m l}(r - r_i) + c_{\sigma m l} {}^i \text{Re} N_{\sigma m l}(r - r_i)]; \quad a < |r - r_i| < 2a \quad (4)$$

and

$$E_i^s(r) = \sum \sum \sum [B_{\sigma m l} {}^i M_{\sigma m l}(r - r_i) + C_{\sigma m l} {}^i N_{\sigma m l}(r - r_i)]; \quad |r - r_i| > 2a \quad (5)$$

where  $\{b, c\}$  and  $\{B, C\}$  are expansion coefficients of the exciting and scattered fields, respectively. The vector spherical functions  $\{M, N\}$  are defined by [Stratton, 1941].

These expansions are substituted into (2) with the following definition of the T-matrix of a single scatterer

$$\begin{aligned} B_{\sigma m l}^j &= (T_{\sigma' m' l}^{\sigma m l})^{11} & (T_{\sigma' m' l}^{\sigma m l})^{12} & b_{\sigma' m' l}^j \\ C_{\sigma m l}^j &= (T_{\sigma' m' l}^{\sigma m l})^{21} & (T_{\sigma' m' l}^{\sigma m l})^{22} & c_{\sigma' m' l}^j \end{aligned} \quad (6)$$

(where the T-matrix is independent of the position of the scatterer) which results in an equation for the exciting field coefficients  $\{b, c\}$  alone. This equation averaged over the position of all scatterers where the QCA [Lax, 1952] is involved, and we arrive at an equation for the configurational average  $\langle b \rangle$  and  $\langle c \rangle$  of the exciting field coefficients with one scatterer held fixed.

We assume that this average field (the coherent field) propagates in a medium with an effective complex wavenumber  $\mathbf{K} = (K_1 + iK_2)\mathbf{k}$  in the direction of the original incident field in the discrete medium. Thus, we obtain

$$\langle b_{\sigma m l}^j \rangle_1 = i Y_{\sigma m l} e^{i\mathbf{K} \cdot \mathbf{r}_1} \quad (7)$$

and

$$\langle c_{\sigma m l}^j \rangle_1 = i Z_{\sigma m l} e^{i\mathbf{K} \cdot \mathbf{r}_1} \quad (8)$$

where  $\{Y, Z\}$  are expansion coefficients of the average exciting field. The dispersion equations then take the following form:

$$\begin{aligned} i^n Y_{01n} &= \sum \sum \sum i^p (-i)^\lambda (JH)_\lambda \{ Y_{01p} [(T_{01p}^{01n})^{11} \psi_{00}(n, n, \lambda) + (T_{01p}^{eln})^{21} \chi_{e0}(n, n, \lambda)] \\ &+ Z_{elp} [(T_{elp}^{01n})^{12} \psi_{00}(n, n, \lambda) + (T_{elp}^{eln})^{22} \chi_{e0}(n, n, \lambda)] \} \end{aligned} \quad (9)$$

$$\begin{aligned} i^n Z_{01n} &= \sum \sum \sum i^p (-i)^\lambda (JH)_\lambda \{ Y_{01p} [(T_{01p}^{01n})^{11} \chi_{0e}(n, n, \lambda) + (T_{01p}^{eln})^{21} \psi_{ee}(n, n, \lambda)] \\ &+ Z_{elp} [(T_{elp}^{01n})^{12} \chi_{0e}(n, n, \lambda) + (T_{elp}^{eln})^{22} \psi_{ee}(n, n, \lambda)] \} \end{aligned} \quad (10)$$

where the functions  $\{\psi, \chi\}$  are defined in [Brngi et al., 1981] and  $(JH)_\lambda$  is an integral given by

$$(JH)_\lambda(K, k, n_0) = 2\pi n_0 (2\lambda + 1) \int_0^\pi \sin \theta d\theta \int_0^\infty G(r, \theta) j_\lambda(Kr) h_\lambda(kr) P_\lambda(\cos \theta) P_q(\cos \theta) r^2 dr \quad (11)$$

In the above equation,  $G(r, \theta)$  is the pair correlation function for aligned spheroidal scatter,  $P(\cos \theta)$  is the Legendre polynomials and  $j$  and  $h$  are the spherical Bessel and Hankel functions, respectively. For spherical scatterers, Eq (11) can be reduced to the following form

$$\begin{aligned} (JH)_\lambda &= 6c(2ka)_\lambda(2Ka)h_\lambda(2ka) - 2Kah_\lambda(2ka)j_\lambda(2Ka) / \{(ka)^2 - (Ka)^2\} \\ &+ 24c \int_1^\infty [g(x) - 1] h_\lambda(2kax) j_\lambda(2Kax) x^2 dx \end{aligned} \quad (12)$$

Eq (12) is actually a special case of (11) by neglecting the azimuthal angle dependence for the pair correlation function. Therefore,  $g(x)$  in Eq.(12) is simply the pair correlation function for spherical scatterers.  $c$  is the concentration ( $c = 4\pi a^3 n_0 / 3$ ) and  $a$  is the radius of the scatterer. The prime denotes the derivative

## THE PAIR CORRELATION FOR ALIGNED SPHEROIDS

The pair correlation function for aligned spheroidal particles can be expanded in the Legendre polynomials as

$$G(r) = \sum_n g_n(r) P_n(\cos\theta) \quad (13)$$

where the coefficients depend only on the distance between particles and azimuthal angle (see Figure 1). The coefficients  $g_n(r)$  can be evaluated during the Monte Carlo simulation [Metropolis, et al., 1953] by using the orthogonality of Legendre polynomials. For a system of hard particles, the required probability in Monte Carlo simulation is simply checking the overlap criterion. Overlap is decided whether the center to center distance for a pair of spheroids is less than  $d$  which is defined by

$$d = (2b/\eta)(1 - \cos^2\theta + \cos^2\theta/\eta^2)^{-1/2} \quad (14)$$

where  $\eta$  is the aspect ratio of the spheroid such that  $\eta > 1$  for prolate and  $< 1$  for oblate spheroids and  $b$  is half the length of the axis of symmetry for the spheroid (see Figure 1). The plot of  $g_n(r)/(2n+1)$  vs. normalized radial distance, i.e.  $r/b$ , for aspect ratio 2.0 and 15.7% concentration is shown in Figure 2. For comparison, the center-center correlation function  $g_0(r)$  calculated using Percus-Yevick approximation is also presented.

## RESULTS AND DISCUSSION

The real and imaginary part, i.e.  $K_1$  and  $K_2$  respectively, of the effective wavenumber  $K$ , are related to the phase velocity and attenuation of the effective medium. They can be obtained by solving the dispersion equations (9) and (10) simultaneously.

In order to show the difference in electromagnetic wave propagation characteristics, e.g.  $K_1$  and  $K_2$ , results based on the approximation for randomly distributed spheroids using the spherical statistics (Circumscribing Sphere Approximation and Equivalent Volume Approximation [Varadan et al., 1986]) are compared with those using nonspherical statistics. Moreover, without considering interaction among scatterers, results based on single scattering theory are also included to justify multiple scattering effects for scatterers with considerable concentrations.

In Table I, numerical results for phase velocity as well as for attenuation are presented for prolate spheroids with an aspect ratio 1.5 and 15 percent concentration under different considerations. One sees that the results obtained from single scattering theory give much higher attenuation than all other cases and this also has been observed for all the subsequent computations. Generally speaking, the circumscribing sphere assumption predicts lower attenuation while the equivalent volume assumption predicts a higher attenuation. However, the phase velocity is much less sensitive to the statistics considered. As a matter of fact, the phase velocity for a nonresonant discrete random medium will not be critically affected by the pair correlation function. For oblate spheroids, this observation also holds and can be shown in Table II which is for oblate spheroids with an aspect ratio 0.667 and 15 percent concentration.

In conclusion, we would like to emphasize the importance in introducing the nonspherical statistics in

analyzing the scattering from densely distributed nonspherical scatterers. The approximations made for the spatial distribution of nonspherical scatterers can produce results which either over or under-estimate the effective properties which, in this case, is the attenuation of the effective medium.

## REFERENCES

- N. Metropolis, A.W. Rosenbluth, N. Rosenbluth, A.H. Teller and E. Teller, "Equation of state calculation by fast computing machines," J. Chem. Phys. 21, No. 6, pp. 1087-1092, 1953.
- V.K. Varadan and V.V. Varadan, eds., Acoustic, electromagnetic and Elastic Wave Scattering-Focus on the T-matrix Approach (Pergamon Press, New York, 1980)
- M. Lax, "Multiple scattering of waves, II. Effective field in dense systems," Phys. Rev. 85, pp. 621-629, 1952.
- V.K. Varadan, V.N. Brongi, and V.V. Varadan, "Coherent electro- magnetic wave propagation through randomly distributed dielectric scatterers," Phys. Rev. D, Vol. 19, pp. 2480-2489, 1979.
- J.A. Stratton, Electromagnetic Theory (McGraw-Hill, New York, 1941).
- V.N. Brongi, T.A. Seliga, V.K. Varadan and V.V. Varadan, "Bulk propagation characteristics of discrete random media," in Multiple Scattering of Waves in Random Media, P.L. Chow, W.E. Kohler and G. Papanicolaou, Eds. (North Holland, Amsterdam, 1981).
- V.V. Varadan, V.K. Varadan, Y. Ma, and W.A. Steele, "Effects of nonspherical statistics on wave propagation in discrete random media" submitted for publication, Radio Science.

Table I Effective K for prolate spheroids with an aspect ratio 1.5 and 15.7 percent concentration

kb	Monte Carlo Simulation		Equival Volume Assumption		Circumscribing sphere Assumption		Single Scattering Theory
	$K_1/k$	$K_2/k$	$K_1/k$	$K_2/k$	$K_1/k$	$K_2/k$	$K_2/k$
0.1	1.0947	0.4822(-5)	1.0947	0.3340(-5)			0.1090(-4)
0.2	1.0950	0.3481(-4)	1.0950	0.2677(-4)	1.0950	0.1054(-5)	0.8721(-4)
0.3	1.0955	0.1048(-3)	1.0955	0.9060(-4)	1.0953	0.1050(-4)	0.2945(-3)
0.4	1.0960	0.2170(-3)	1.0961	0.2156(-3)	1.0957	0.4235(-4)	0.6989(-3)
0.5	1.0967	0.3894(-3)	1.0970	0.4232(-3)	1.0963	0.8415(-4)	0.1366(-2)
0.6	1.0977	0.6346(-3)	1.0980	0.7357(-3)	1.0971	0.1623(-3)	0.2363(-2)
0.7	1.0988	0.9984(-3)	1.0992	0.1176(-2)	1.0980	0.2884(-3)	0.3749(-2)
0.8	1.1000	0.1519(-2)	1.1006	0.1768(-2)	1.0991	0.4539(-3)	0.5585(-2)
0.9	1.1013	0.2175(-2)	1.1022	0.2534(-2)	1.1004	0.6841(-3)	0.7916(-2)
1.0	1.1027	0.2894(-2)	1.1040	0.3495(-2)	1.1021	0.1038(-2)	0.1078(-1)

Table II Effective K for oblate spheroids with an aspect ratio 0.667 and 15.7 percent concentration

ka	Monte Carlo Simulation		Equival Volume Assumption		Circumscribing sphere Assumption		Single Scattering Theory
	$K_1/k$	$K_2/k$	$K_1/k$	$K_2/k$	$K_1/k$	$K_2/k$	$K_2/k$

0.1			1.1088	0.6620(-5)	1.1087	0.3493(-5)	0.2146(-4)
0.2	1.1094	0.5203(-5)	1.1094	0.5380(-4)	1.1093	0.2862(-4)	0.1733(-3)
0.3	1.1105	0.5655(-4)	1.1105	0.1865(-3)	1.1103	0.1008(-3)	0.5937(-3)
0.4	1.1121	0.2614(-3)	1.1121	0.4591(-3)	1.1116	0.2541(-3)	0.1436(-2)
0.5	1.1141	0.6498(-3)	1.1141	0.9409(-3)	1.1134	0.5352(-3)	0.2875(-2)
0.6	1.1167	0.1287(-2)	1.1167	0.1723(-2)	1.1157	0.1008(-2)	0.5103(-2)
0.7	1.1199	0.2360(-2)	1.1197	0.2927(-2)	1.1185	0.1770(-2)	0.8328(-2)
0.8	1.1236	0.4144(-2)	1.1231	0.4719(-2)	1.1219	0.2978(-2)	0.1274(-1)
0.9	1.1277	0.6882(-2)	1.1270	0.7318(-2)	1.1258	0.4893(-2)	0.1846(-1)
1.0	1.1320	0.1077(-1)	1.1309	0.1098(-1)	1.1302	0.7909(-2)	0.2545(-1)

# MULTIPLE SCATTERING OF WAVES IN RANDOM MEDIA CONTAINING NON-SPHERICAL SCATTERERS

by

Vasundara V. Varadan, Vijay K. Varadan and Yushieh Ma  
Center for the Engineering of Electronic and Acoustic Materials  
and

Department of Engineering Science and Mechanics  
The Pennsylvania State University  
University Park, PA 16802  
U.S.A.

## SUMMARY

In this paper we wish to consider the effect of multiple scattering, scatterer geometry, statistics of the positional and orientational distribution functions on the propagation of time harmonic electromagnetic waves in a medium containing a random distribution of non-spherical scatterers. Some of the features that complicate the analysis are - (1) the size of the scatterers is comparable to the wavelength of the propagating wave; (2) the volume fraction occupied by the scatterers need not necessarily be small; (3) the impedance mismatch between the scatterers and the host medium need not necessarily be small. These in turn necessitate some of the effects we wish to focus on namely - detailed modeling of scatterer geometry and scatterer response, multiple scattering effects and the effect of correlations. We have already addressed many of these factors [1] and in our proposed talk we wish to present some recent results using non-spherical statistics for the second moment of the field.

In collaboration with Professor William A. Steele of Chemistry Department at Penn State, we have generated by Monte Carlo simulation the pair correlation function for spheroidal particles as a function of the distance between them and the direction of the vector joining their centers. At present we are generating the pair correlation function for randomly oriented spheroids and are also considering the effects of inter-particle forces as well as higher order correlation functions for clusters of particles. All of these have been incorporated into the multiple scattering calculations and compared with available experimental results. In contrast to previous work more attention will be focussed on the second moment of the field.

This paper will fit in very well with the scope of the symposium in the areas of mathematical methods for random media, characterization and modeling of random media and also interface quite well with some of the other papers in this area that we expect will be presented at the ACARD symposium.

## 1. PREFACE

The average or effective properties of a random medium containing inclusions of one material or voids distributed in some fashion in a second material called the host or matrix material can be conveniently studied by analyzing the propagation of plane waves in such materials and solving the resulting dispersion equations. Since waves propagating in such a two phase system will undergo multiple interactions with the scatterer phase, it becomes natural to consider multiple scattering theory and ensemble averaging techniques if the distribution of the inclusion phase is random. In this paper, a multiple scattering theory is presented that utilizes a T-matrix to describe the response of each scatterer to an incident field. The T-matrix is simply a representation of the Green's function for a single scatterer in a basis of spherical functions. In this definition, it simply relates the expansion coefficients of the field that is incident on or excites a scatterer to the expansion coefficients of the field scattered when both fields are expanded in the same spherical wave basis [1]. In theory, the T-matrix is infinite, but in practice the T-matrix is truncated at some size that depends on the ratio of size of scatterer to the wavelength and the complexity of the geometry. Formally, the T-matrix includes a multipole description of the field scattered by the inclusion and this requires a propagator for multipole fields to describe the propagation from one scatterer to the next. Finally, the technique presented here is for a random distribution of scatterers which requires an ensemble average over the position of the scatterers and requires a knowledge of the positional correlation functions.

In previous studies [2,3] we relied on spherical statistics for hard spheres, generated by Monte Carlo simulation

or by the Percus-Yevick approximation even for non-spherical scatterers. Essentially, this increased the exclusion volume surrounding the non-spherical scatterer, and artificially restricted us to smaller concentrations in order to prevent the statistical spheres from overlapping. In the present study, these restrictions are removed by using a new Monte Carlo simulation developed by Steele [4] for non-spherical scatterers, that is based on expanding the two body correlation functions in Legendre polynomials. This permits us to consider the angular correlations that exist for non-spherical oriented scatterers. The final equation for the formalism is the dispersion equation which describes the propagation characteristics of the coherent or average field in the effective medium. The numerical solution of this equation yields the effective complex, frequency dependent propagation number which is also a function of the size, geometry and distribution of the inclusion phase. The effective wavenumber is a function of the direction of propagation in the effective medium if the medium is effectively anisotropic. If, for example, the scatterers are spheres or if the non-spherical scatterers are randomly oriented, the effective medium will be isotropic, but if the medium contains aligned non-spherical scatterers the effective medium will be anisotropic. The effective wavenumber can be related to the effective material properties of the medium which are also complex and frequency dependent. For anisotropic materials, by solving the dispersion equation for different directions of propagation with respect to the aligned non-spherical scatterers, we can construct all components of the material property tensors of the effective medium such as the elastic stiffness tensor or the dielectric tensor, see [5].

In this paper, a systematic study is also made of first order contributions to the second moment or incoherent intensity of the wave field propagating in a discrete random medium. The second moment, which is traditionally defined as the correlation function of the component of the field fluctuations in any direction  $\hat{u}$ , is denoted by  $I_u = \langle (\hat{u} \cdot \Delta E) (\hat{u} \cdot \Delta E)^* \rangle$ , where  $\Delta E = E - \langle E \rangle$  is the fluctuation of the field. Since the field fluctuations can be expanded in a multiple scattering series, each term of which contains sums on all possible scatterers, it is evident that we can divide the resulting terms into two sets; one involves considering only those terms in which the same scatterer contributes to a particular order term in each field fluctuation, and the other involves distinct scatterers. This latter set of terms will contribute to the incoherent intensity only if statistical correlations between scatterers are taken into account. The first category of terms are equivalent in spirit to radiative transfer theory since it is essentially the intensity of the field scattered by each scatterer that propagates from one site to another. Even for this set of terms, positional correlations between scatterers should be taken into account at volume fractions exceeding a few percentage, but these terms contribute to the incoherent intensity even if correlations are neglected.

Numerical results for aligned and randomly oriented oblate and prolate spheroids using the new correlation functions have been obtained and compared with previous calculations for spheroids that used spherical statistics. We foresee important applications of these new results to electromagnetic wave propagation through aerosols, which are non-spherical and often consist of aggregates and also in other cases where non-spherical scatterers are involved.

## 2. EFFECTIVE WAVENUMBER FOR THE AVERAGE FIELD IN A DISCRETE RANDOM MEDIUM

Let the random medium contain  $N$  scatterers in a volume  $V$  such that  $N \rightarrow \infty$ ,  $V \rightarrow \infty$ , but  $n_0 = N/V$  the number density of scatterers is finite. Let  $u$ ,  $u^0$ ,  $u_i^e$ ,  $u_i^s$  be respectively the total field, the incident or primary plane, harmonic wave of frequency  $\omega$ , the field incident or exciting the  $i$ -th scatterer and the field which is in turn scattered by the  $i$ -th scatterer. These fields are defined at a point  $r$  which is not occupied by any one of the scatterers. In general, these fields or potentials which can be used to describe them satisfy the scalar or vector wave equation. Let  $\text{Re } \phi_n$  and  $\text{Ou } \phi_n$  denote the basis of orthogonal functions which are eigenfunctions of the Helmholtz equation, see Morse and Feshbach [6]. As explained in the introduction the subscript 'n' is an abbreviated superindex and vector notation is implied. The qualifiers  $\text{Re}$  and  $\text{Ou}$  denote functions which are regular at the origin (Bessel functions) and outgoing at infinity (Hankel functions) which are respectively appropriate for expanding the field which is incident on a scatterer and that which it scatters. Thus, we can write the following set of self-consistent equations:

$$u = u^0 + \sum_{i=1}^N u_i^s = u_i^e + u_i^s = u^0 + \sum_{j \neq i} u_j^s + u_i^s, \quad (1)$$

$$u^0(r) = p \exp(ik k_0 \cdot r) = \sum_n a_n^i \text{Re } \phi_n(r - r_i), \quad (2)$$

$$u_i^e = \sum_n \alpha_n^i \text{Re } \phi_n(r - r_i); \quad a < |r - r_i| < 2a, \quad (3)$$

$$u_i^s = \sum_n f_n^i \text{Ou } \phi_n(r - r_i); \quad |r - r_i| > a, \quad (4)$$

where  $\alpha_n^i$  and  $f_n^i$  are unknown expansion coefficients. We observe in Eqs. (3) and (4) that "a" is the radius of the

sphere circumscribing the scatterer and that all expansions are with respect to a coordinate origin located in a particular scatterer.

The T-matrix, by definition simply relates the expansion coefficients of  $u_i^e$  and  $u_i^s$  provided  $u_i^e + u_i^s$  is the total field which is consistent with the definitions in Eq. (1). Thus [1],

$$f_n^i = \sum_{n'} T_{nn'}^i \alpha_{n'}^i, \quad (5)$$

and the following addition theorem for the basis functions is invoked:

$$\text{Ou } \phi_n(r - r_j) = \sum_{n'} \sigma_{nn'}(r_i - r_j) \text{Re } \phi_{n'}(r - r_i). \quad (6)$$

Substituting Eqs. (2) - (6) in Eq. (1), and using the orthogonality of the basis functions we obtain

$$\alpha^i = a^i + \sum_{j \neq i} \sigma(r_i - r_j) T^j \alpha^j. \quad (7)$$

This is a set of coupled algebraic equations for the exciting field coefficients which can be iterated and leads to a multiple scattering series.

For randomly distributed scatterers, an ensemble average can be performed on Eq. (7) leading to

$$\langle \alpha^i \rangle_i = a^i + \langle \sigma(r_i - r_j) T^j \alpha^j \rangle_{ij} \quad (8)$$

where  $\langle \rangle_{ijk}$  denotes a conditional average and Eq. (8) is an infinite hierarchy involving higher and higher conditional expectations of the exciting field coefficients. In actual engineering applications, a knowledge of higher order correlation functions is difficult to obtain, usually the hierarchy is truncated so that at most only the two body positional correlation function is required.

To achieve this simplification the Quasi-Crystalline Approximation (QCA), first introduced by Lax [7] is invoked, which is stated as

$$\langle \alpha^j \rangle_{ij} \equiv \langle \alpha^j \rangle_j. \quad (9)$$

Then, Eq. (8) simplifies to

$$\langle \alpha^i \rangle_i = a^i + \langle \sigma(r_i - r_j) T^j \alpha^j \rangle_j; \quad (10)$$

an integral equation for  $\langle \alpha^i \rangle_i$  which, in principle, can be solved. In particular, the homogeneous solution of Eq. (10) leads to a dispersion equation for the effective medium in the quasi-crystalline approximation. Defining the spatial Fourier transform of  $\langle \alpha^i \rangle_i$  as

$$\langle \alpha^i \rangle_i = \int e^{iK \cdot r_i} C^i(K) dK \quad (11)$$

and substituting in Eq. (10), we obtain for the homogeneous solution

$$C^i(K) = \sum_{j \neq i} \int \sigma(r_i - r_j) T^j P(r_j | r_i) e^{iK \cdot (r_i - r_j)} dr_j C^j(K). \quad (12)$$

If the scatterers are identical, then

$$C^i(K) = C^j(K) = C(K), \quad (13)$$

and thus for a non-trivial solution to  $\langle \alpha^i \rangle_i$ , we require that

$$|1 - \sum_{j \neq i} \int \sigma(r_i - r_j) T^j P(r_j | r_i) e^{iK \cdot (r_i - r_j)} dr_j| = 0. \quad (14)$$

In Eqs. (12) and (14),  $P(r_j | r_i)$  is the joint probability distribution function. In order to perform the integration in Eq. (14), we need a model for the pair correlation function. For non-spherical scatterers, the pair correlation function depends not only on the length of the vector connecting the centers of the scatterers, but also on the direction of this vector and the orientation of each scatterer. If the scatterers are spherical, then there is no dependence on direction and



orientation and the statistics are said to be spherical or isotropic. In both cases, the scatterers are not allowed to overlap, i.e. an infinite repulsive potential is assumed between scatterers.

For aligned spheroids which are rotationally symmetric, the dependence is only on the angle  $\theta$  between the separation vector and the symmetry axis which is taken to be the z-axis of the coordinate system, as shown in Fig. 1. There is no dependence on the azimuthal angle  $\phi$ . The joint probability distribution function is then written as

$$P(r_i | r_j) = \begin{cases} 0; & |r_i - r_j| < R(\theta) \\ G(x)/V; & |r_i - r_j| > R(\theta) \end{cases} \quad (15)$$

In the above equation,  $G(x)$  is the pair correlation function for aligned spheroidal scatterers,  $x = r_i - r_j$ , and  $R(\theta)$  is the minimum center to center distance when the spheroids just touch one another at one point, such that the line joining their centers subtends an angle  $\theta$  with the symmetry or z-axis of the spheroids. In this case the statistics are not isotropic but are a function of direction. Equation (14) can hence be simplified to

$$\left| I - n_0 \int \sigma(x) T G(x) e^{iK \cdot x} dx \right| = 0 \quad (16)$$

where  $(1/V) \sum_{j \neq i} = (N-1)/V \approx n_0$ . The integral in Eq. (16) is simply the spatial Fourier transform of  $\sigma T G$ . The zeroes of the determinant as expressed by Eq. (16), yield the allowed values of  $K$  as a function of the microstructure as determined by the T-matrix, the number density  $n_0$  and the statistics of the distribution as determined by the pair correlation function. In general  $K$ , the effective wavenumber is complex and frequency dependent.

The dispersion equation as given in Eq. (16) is very well suited for computation. Using appropriate forms of the basis functions  $\phi_n$  which are solutions of the field equations, the T-matrix of the single scatterer can be computed; for example, see Varadan and Varadan [1]. The translation matrix  $\sigma$ , although complicated in form for spherical functions, can nevertheless be computed in a straightforward manner. The spatial Fourier transform of  $\sigma T G$  is fairly easy to compute because the integrand is well behaved for large values of the interparticle distance. In recent years, considerable progress has been made in Monte Carlo simulation to describe the statistics for non-spherical hard (impenetrable) particles by Steele. The joint probability functions have been expanded in a series of spherical harmonics and radial functions with unknown coefficients. The coefficients are evaluated directly in the Monte Carlo simulation. For aligned prolate and oblate spheroids, these results have just become available. The excluded volume for these geometries is also spheroidal. This has been implemented in calculations of the effective wavenumber in media containing random distributions of aligned spheroidal particles [8]. It can be seen that correct statistics conforming to the shape of the particle is needed to get correct results at volume fractions exceeding 5%.

## 2. INCOHERENT INTENSITY

The total scattered intensity is directly proportional to the second moment of the scattered field. It is known that the total scattered field is a combination of the average scattered field and the fluctuation of the field due to the random distribution of scatterers, i.e.,  $u = \langle u \rangle + u$ , the incoherent component of the scattered intensity can be obtained as

$$\langle u u^* \rangle = \langle u u^* \rangle - \langle u \rangle \langle u^* \rangle, \quad (17)$$

To first order, that is taking only the single scattering contribution to each scattered field, we obtain

$$\begin{aligned} \langle u u^* \rangle &= \langle |u|^2 \rangle = \langle \sum_j u_j^* \sum_k u_k \rangle = \sum_j \langle u_j^* \rangle \sum_k \langle u_k \rangle \\ &= \sum_{j \neq k} \sum_k \langle u_j^* u_k \rangle + \sum_j \langle |u_j|^2 \rangle = \sum_j \sum_k \langle u_j^* \rangle \langle u_k \rangle. \end{aligned} \quad (18)$$

The ensemble averages in Eq. (18) can be written by integrating over the random positions  $r_j, r_k$ , etc. of the scatterers. Thus,

$$\begin{aligned} \langle |u|^2 \rangle &= n_0^2 \iint [(N-1)/N] \langle u_j^* u_k \rangle_{jk} - \langle u_j \rangle_j^* \langle u_k \rangle_k \, dr_j dr_k \\ &\quad + n_0 \int \langle |u_j|^2 \rangle_j \, dr_j. \end{aligned} \quad (19)$$

The second term in the above equation, which is proportional to  $n_0$ , is the ordinary single scattering approximation to the incoherent intensity and the magnitude of the incoherent intensity in any direction is proportional to the bistatic cross section of a single scatterer. The first term proportional to  $n_0^2$  is due to the effect of positional correlations between pairs of scatterers.

For sparse concentrations, the scatterers are uncorrelated, and

$$\langle u_j^* u_k \rangle_{jk} = \langle u_j \rangle_j^* \langle u_k \rangle_k$$

and the first term of Eq. (19) vanishes.

In order to obtain the incoherent intensity for higher concentrations, the pair correlation function  $G(x)$  is taken into consideration. Recently Twersky [1983] has modified Eq. (19) for a dense distribution of scatterers. The incoherent intensity has the form:

$$\begin{aligned} \langle |u|^2 \rangle = & n_0^2 \iint [G(r_j - r_k) - 1] \langle u_j \rangle_j^* \langle u_k \rangle_k dr_j dr_k \\ & + n_0 \int \langle |u_j|^2 \rangle_j dr_j. \end{aligned} \quad (21)$$

Equation (21) is the final form used in our computation for the incoherent intensity up to the first order. However, the higher order contributions to the incoherent intensity become more and more important if the impedance mismatch between the scatterers and the host medium as well as the propagation distance are increasing. A detailed picture using the ladder diagrams in explaining the higher order multiple scattering processes can be found in our previous paper [1984]. In the calculation, a knowledge of the coherent field is still required since the average scattered field  $\langle u_j \rangle_j$  is involved in the formalism. The average scattered field  $\langle u_j \rangle_j$  holding the  $j$ -th scatterer fixed can be expressed as, using Eq. (4)

$$\langle u_j \rangle_j = \sum_n T_{nn} \langle \alpha_n^j \rangle_j \phi_n(r - r_j). \quad (22)$$

The exciting field coefficients  $\alpha_n^j$  are initially unknown in Eq. (22). However, the average field  $\langle \alpha_n^j \rangle_j$  exciting the  $j$ -th scatterer is known after defining an effective propagation constant  $K$  which is complex ( $K = k_0 + iK_2$ ). Following this definition, the average or effective exciting field  $\langle \alpha_n^j \rangle_j$  can be written as

$$\langle \alpha_n^j \rangle_j = A_n e^{iK k_0 \cdot r_j}, \quad (23)$$

where  $k_0$  is the propagation direction of the incident wave. The unknown effective exciting amplitudes  $A_n$  however, can be solved by invoking the extinction theorem.

If we substitute Eq. (22) in (21), we obtain

$$\begin{aligned} \langle |u|^2 \rangle = & n_0^2 \iint [G(r_j - r_k) - 1] \sum_n T_{nn} \langle \alpha_n^j \rangle_j \phi_n \sum_{n''} T_{n''n''}^* \langle \alpha_{n''}^{k*} \rangle_{k''}^* \phi_{n''} dr_j dr_k \\ & + n_0 \int \left| \sum_n T_{nn} \langle \alpha_n^j \rangle_j \phi_n \right|^2 dr_j. \end{aligned} \quad (24)$$

We notice that in Eq. (24), the multiplication of the  $T$ -matrix and the effective exciting field is independent of the integral and the pair correlation function. In fact, the integral of the pair correlation function turns out to be the dimensional spatial Fourier transform of the pair correlation function  $[G(x)-1]$ . In order to investigate the behavior of the incoherent intensity, we calculate the major normalized quantity which is defined as follows

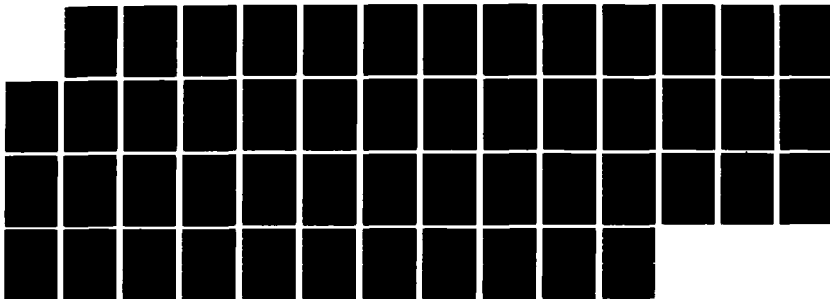
$$\begin{aligned} \langle I_u \rangle = & (I_s/I_0) (kr)^2 (v/V) \\ = & 2c (\sum T_{nn} A_n Y_n) (\sum T_{n''n''}^* A_{n''} Y_{n''})^* F(k_0, K, r) / [(K_2/k_0)(ka)^3 Z] a \end{aligned}$$

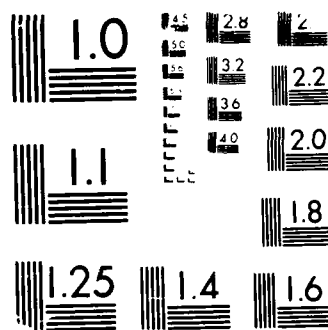
where  $Y_n$  are the normalized spherical harmonics,  $\{Y_{lm}(\theta, \phi)\}$ ,  $Z$  is the distance of penetration,  $n$  ( $n'$  or  $n''$ ) is the index representing  $l$  and  $m$ ;  $r$  is the radial distance from the center of the scatterer to the observation point,  $v$  is the volume of a single scatterer and  $V$  is the whole scattering volume. The function  $F$  in Eq. (25) is given as

$$F = 1 + n_0 \int [G(x) - 1] \exp[i(Kk_0 - k r/r) \cdot x] dx$$

For spheres, the radial distribution function depends only on the separation distance  $x$ . The integration in Eq. (25) is performed numerically using tabulated values of  $G(x)$  from Monte Carlo simulation [1983] or from the integral equation for non-overlapping spheres. For non-spherical scatterers, the integration is performed on integrations on orientation and distance and the integration is more time consuming. The function  $F$  can be again obtained from Monte Carlo simulation.

AD-A191 068 MULTIPLE SCATTERING OF WAVES IN DISCRETE RANDOM MEDIA 2/2  
(U) PENNSYLVANIA STATE UNIV UNIVERSITY PARK LAB FOR  
ELECTROMAGNET V K VARADAN ET AL 31 DEC 87  
UNCLASSIFIED ARO-21825 17-GS DAAG29-84-K-0187 F/G 20/11 NL





MICROCOPY RESOLUTION TEST CHART  
NATIONAL BUREAU OF STANDARDS 1963-A

### 3. RESULTS AND DISCUSSION

In order to study the characteristics of the incoherently scattered wave intensity, we choose electromagnetic waves as probing waves simply because there are a number of applications in remote sensing.

By sending plane electromagnetic waves through scatterers we intend to find, first, the angular dependence of the incoherent intensity and the influence of different polarizations, e.g., vertical and horizontal polarizations. If it is not specifically mentioned, scatterers are assumed to be spherical or spheroidal ice particles with a relative dielectric constant  $\epsilon = 3.168$  embedded in air. Fig. 2 presents the normalized incoherent intensity versus observation (scattering) angles. The forward scattering angle is, in our case  $0^\circ$  and therefore the backscattering direction is  $180^\circ$ . The nondimensional frequency considered is 0.6 which is equivalent to a physical frequency of about 14 GHz if a 2 mm particle is considered.

Taking a further look at Fig. 3, we can conclude that the vertical polarization gives more angular dependence of the incoherent intensity than the horizontal one. There is an extremely low intensity (i.e., a deep minimum in the curve) that occurs at  $90^\circ$  at a  $ka=0.6$ . This phenomenon happens again, however, at a higher observation angle of  $125^\circ$  when the frequency  $ka$  is raised to 2. There is no polarization difference at the forward and backscattering directions for the incoherent intensities.

In Fig. 4, we compare the backscattered intensity calculations with and without the effect of pair correlations. These results tell us that if the intensity is calculated without considering the pair correlation function when the concentration becomes even moderately high, i.e., 5%, one is able to see the difference in the magnitude particularly in the low frequency range.

Finally, we want to say something about the effect of the pair correlation function. In order to tell the importance of its effect on the final first order scattered intensity, we simply calculate the function  $F$  which appears in Eq. (25) and has been defined in Eq. (26). As can be seen from Eq. (26), it involves a Fourier transform of the pair correlation function and it contains an effective propagation constant  $K$ ; hence it depends on the properties of the scatterers, the concentration, frequency and angle of observation. In Figs. 5 and 6, we can see that the Fourier transform of the pair correlation function dominates the scattering response particularly in the low frequency range and in the forward direction. In the high frequency range, it does not affect the scattered intensity much. Also, we observed that the intensity decreases after a volume fraction  $c = 15\%$ , which is also a fact pointed out in Kuga's experiments.

From Fig. 7, it is clear that the difference in obtaining the effective  $K$  is quite large if the spherical statistics is employed in approximating the nonspherical statistics. Therefore, for nonspherical scatterers of considerable concentrations, the incoherent intensity can be mistakenly estimated using Eqs. (22), (23) and (24) which all involve the effective wavenumber  $K$ . In addition, the pair correlation function  $G(x)$  in Eq. (26) may even contribute more to the difference depending on the concentration and the observation angle considered.

### ACKNOWLEDGEMENT

The work reported here was supported in part by the U.S. Army Research Office through contract # DAAG29 - 84 - K - 0187 and DAAG29 - 85 - K - 0234 awarded to the Pennsylvania State University. The authors are grateful to Dr. Walter A. Flood for several helpful discussions and suggestions during the course of this work. They also wish to express their appreciation to Professor W. A. Steele who provided tabulated values of the pair statistics using Monte Carlo simulation.

### REFERENCES

- (1) V.K. Varadan and V.V. Varadan, editors, Acoustic, Electromagnetic and Elastic Wave Scattering - Focus on the T-Matrix Method, Pergamon Press (1980).
- (2) V. N. Bringi, V. V. Varadan and V. K. Varadan, "Effects of the Pair Correlation Function on Coherent Wave Attenuation in Discrete Random Media," *IEEE Trans. AP-30*, pp. 805 - 808 (1982).
- (3) V. N. Bringi, V. K. Varadan and V. V. Varadan, "Average Dielectric Properties of Discrete Random Media Using Multiple Scattering Theory," *IEEE Trans. AP-31*, pp. 371 - 375 (1983).
- (4) Y. D. Chen and W. A. Steele, *J. Chem. Phys.* **50**, p. 1428 (1969).
- (5) V.K. Varadan, Y. Ma and V.V. Varadan, "Multiple Scattering of Compressional and Shear Waves by Fiber Reinforced Composite Materials", *J. Acoust. Soc. Am.* **80**, 333 - 339 (1986).
- (6) P. M. Morse and H. Feshbach, Methods of Theoretical Physics, Vol. II, p. 1865, McGraw-Hill (1953).
- (7) M. Lax, "Multiple Scattering of Waves II. The Effective Field in Dense Systems," *Phys. Rev.* **85**, pp. 621 - 629 (1952).
- (8) V.V. Varadan, V.K. Varadan, Y. Ma and W.A. Steele, "Effects of Non-Spherical Statistics on EM Wave Propagation in Discrete Random Media," *Radio Science*, submitted (1987).
- (9) V. V. Varadan, Y. Ma and V. K. Varadan, "Propagator Model including Multipole Fields for Discrete Random Media," *J. Opt. Soc. Am.* **A2**, pp. 2195 - 2201 (1985).

- (10) V. Twersky, "Multiple Scattering of Sound by Correlated Monolayers," J. Acoust. Soc. Am. **73**, pp. 68 - 84 (1983).
- (11) Y. Kuga and A. Ishimaru, "Retroreflectance from a Dense Distribution of Spherical Particles," J. Opt. Soc. Am. **A1**, pp. 831 - 835 (1984).

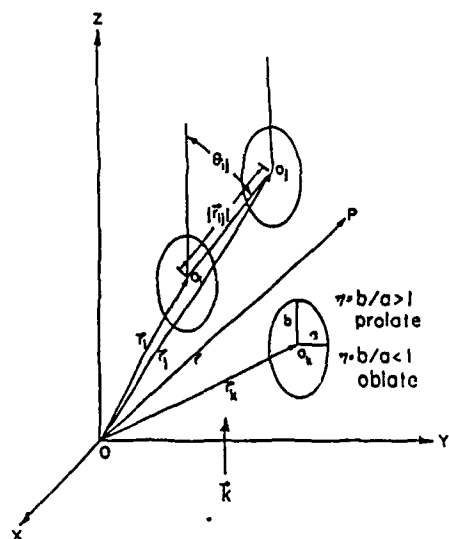


Figure 1 Multiple scattering of waves in discrete random media with positionally and orientationally correlated non-spherical scatterers.

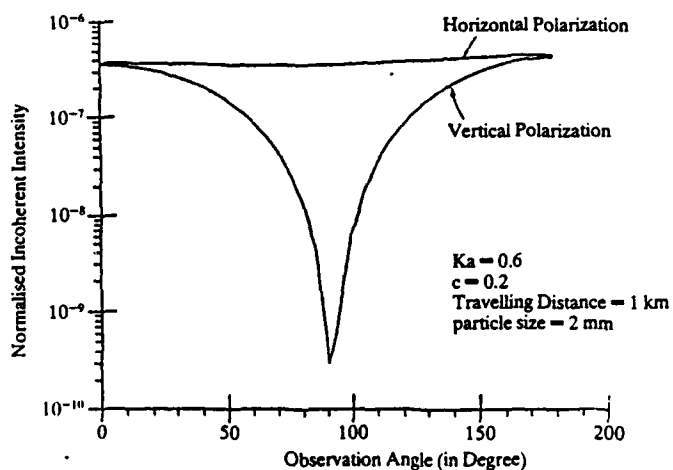


Figure 2 Normalized incoherent intensity vs. observation angle for ice particles ( $ka = 0.6$ ).

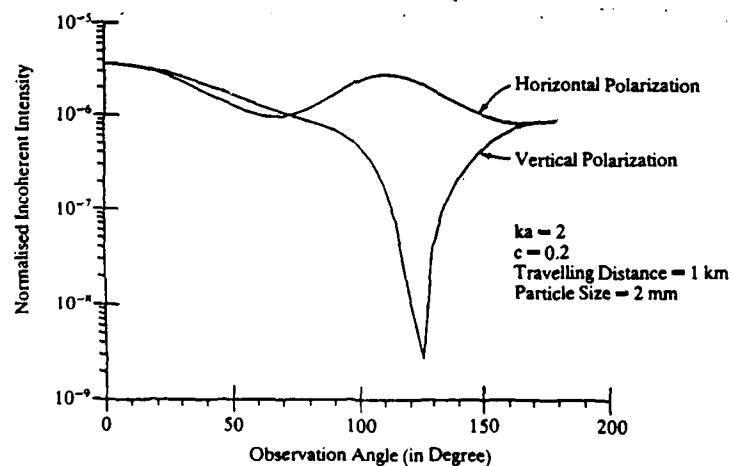


Figure 3 Same as Fig.2 except  $ka = 2$ .

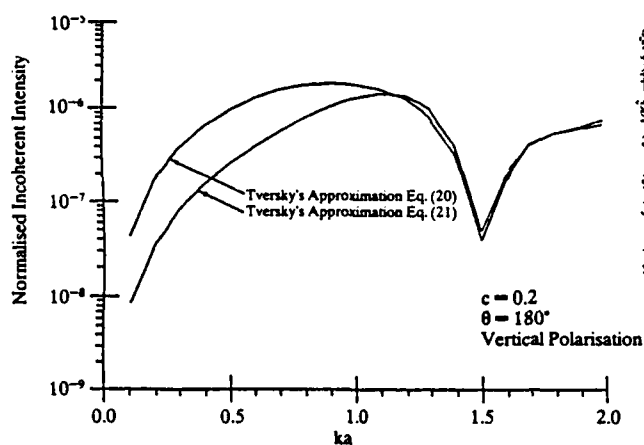


Figure 4 Normalized backscattered intensity vs. nondimensional frequency ( $c = 0.2$ ).

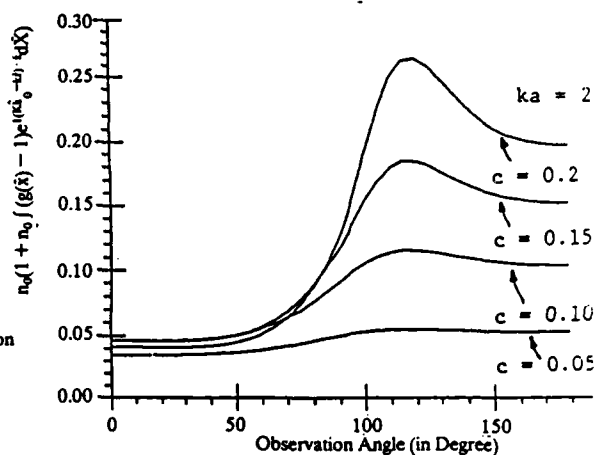


Figure 5 Effect of pair correlation function vs. observation angle.

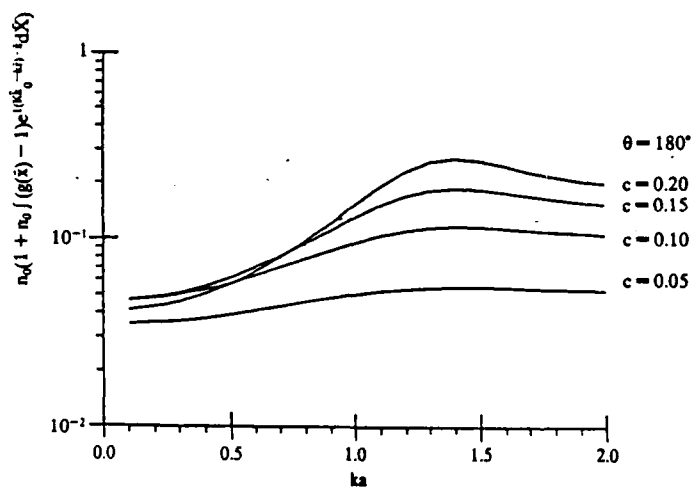


Figure 6 Effect of pair correlation function vs. nondimensional frequency  $ka$ .

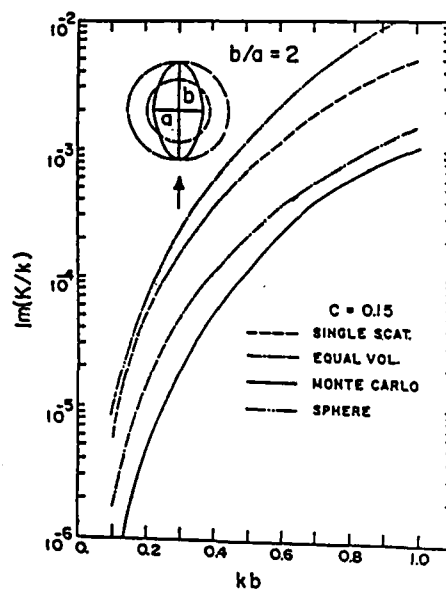


Figure 7 Imaginary part of effective wavenumber  $K$  vs. nondimensional frequency  $kb$  for prolate spheroids

## BACKSCATTERING ENHANCEMENT OF WAVES IN RANDOM MEDIA

V.K. Varadan, V.V. Varadan and Y. Ma  
*Research Center for the Engineering of Electronic and Acoustic Materials*  
*Department of Engineering Science and Mechanics*  
*The Pennsylvania State University*  
*University Park, PA 16802*

### RECENT SUBMITTALS FOR PUBLICATION AND PRESENTATIONS:

- A) V.V. Varadan, V.K. Varadan and Y. Ma, "Multiple scattering of waves in random media containing nonspherical scatterers," presented at the Electromagnetic Wave Propagation Panel Symposium sponsored by AGARD, NATO, Italy, April 1987.
- B) V.V. Varadan, Y. Ma and V.V. Varadan, "Scattered intensity of a wave propagating in a discrete random medium," submitted to *Applied Optics*, August 1987.
- C) V.K. Varadan, Y. Ma and V.V. Varadan, "Enhanced backscattering of optical waves due to densely distributed scatterers," submitted to SPIE's 1988 technical Symposium Southeast on Optics, Electro-Optics, and Sensors.

### ABSTRACT

Recently, an interesting phenomenon has been reported as a result of a series of optical backscattering experiments conducted using collimated light sources (lasers). A locally high intensity maximum has been observed in the range of  $\pi - \epsilon < \theta < \pi + \epsilon$  where  $\epsilon$  is of the order of milliradians and  $\theta = \pi$  is the backscattering direction. Albeit similar phenomena found in backscattering from various random media, e.g., scattering of electrons by impurities in metals and light scattering from random rough surfaces, this is the first observation of enhanced backscattering from suspensions.

In this paper, based on multiple scattering theory, we use the improved two scatterers T matrix program, which takes all back and forth scattering into account between two scatterers and considers the multiple scattering effect, in the intensity calculation. The widths and magnitudes of the backscattered intensity peak of our computations compare favorably with those of optical experiments.

### INTRODUCTION

Backscattering enhancement or similar phenomena have been observed in various backscattering experiments, for example, the Anderson localization from scattering of electrons by impurities in metals [Abrahams et al., 1979 ; Bergmann, 1984], scintillation in turbulent media [Yeh et al., 1975; Rino et al., 1982] and speckling from light scattering by random rough surfaces [Dainty, 1984; Hecht, 1986]. And generally speaking, the enhanced backscattering can happen when (i) waves scattered by turbulent media - continuous random media (e.g., atmosphere); (ii) waves scattered by a collection of randomly distributed scatterers with high concentration; (iii) waves scattered by moving scatterers or by scatterers having Brownian motion; (iv) waves scattered by scatterers (moving or stationary) in a turbulent medium ; (v) waves scattered from random rough surfaces; (vi) waves scattered by scatterers in front of a rough



boundary.

The reason for this is partly that although waves are travelling in random media, the propagation of waves in such media (cases (i) - (vi)) is accompanied by multiple scattering as well as specific coherent effects and the enhancement is caused by positive interference of all the scattered waves. The recently observed enhanced backscattering phenomenon from dense suspensions appears to be the similar result which cannot be explained by radiative-transfer theory. Albeit the cyclic diagram in conjunction with point scatterer approximation introduced in multiple scattering theory to explain the enhanced backscattering [Tsang and Ishimaru, 1985], however, the experimental observations all deal with scatterer's size large compared with the incident wavelength [Kuga and Ishimaru, 1983; Albada and Lagendijk, 1985; Wolf and Maret, 1985], and therefore a detailed computation based on anisotropic scattering for finite size scatterers is essential. In addition, the back and forth scattering between a pair of scatterers, which has been neglected in the ladder approximation, may have major contribution toward backscattering rather than in the forward direction mentioned in one previous paper [Bringing et al., 1980] coauthored with us.

In this paper, based on multiple scattering theory, we use the improved two scatterers T matrix program, which takes all back and forth scattering into account between two scatterers and considers the multiple scattering effect, in the intensity calculation. The widths and magnitudes of the backscattered intensity peak of our computations compare favorably with those of optical experiments.

#### INCOHERENT INTENSITY FORMULATION

The detailed derivations and intermediate steps in obtaining the final expression for intensity can be referred to our paper [Varadan et al., 1987]. The average incoherent intensity  $\langle I \rangle$  can be obtained as follows

$$\begin{aligned} \langle I \rangle = & n_0 \int \langle |u_j|^2 \rangle_j dr_j \\ & + n_0^2 \iint \langle u_k u_j^* \rangle_{jk} g(r_{jk}) dr_k dr_j \\ & - n_0^2 \iint \langle u_k \rangle_k \langle u_j^* \rangle_j dr_k dr_j \end{aligned} \quad (1)$$

where  $n_0$  is the number density ( $n_0 = N/V$ ),  $u_k$  is the scattered field from the  $k$ -th scatterer,  $\langle \rangle_j$  and  $\langle \rangle_{jk}$  are conditional configuration averages holding the positions of the  $j$ -th and both the  $j$ -th and  $k$ -th scatterers fixed, respectively, and  $g(r_{jk})$  the radial distribution function for spherical scatterers. Equation (1) is an exact expression for the incoherent intensity  $\langle I \rangle$ .

In order to perform the computation, we need to make approximations for the expression of  $\langle |u_j|^2 \rangle_j$  and  $\langle u_k u_j^* \rangle_{jk}$ , which are both unknown, in terms of the effective exciting field  $\langle u_k \rangle_k$  which is known [Varadan et al., 1985]. By neglecting higher order statistics and considering only the two particle pair correlation function [Varadan et al., 1987], we can obtain

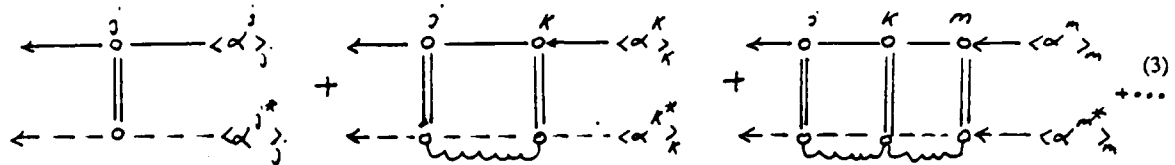
$$\begin{aligned} \langle I \rangle = & n_0 \sum \int [ \psi^j T^j \langle \alpha^j \rangle_j ] [ \psi^j T^j \langle \alpha^j \rangle_j ]^* dr_j \\ & + n_0^2 \sum \iint [ \psi^j T^j \sigma_{jk} T^k \langle \alpha^k \rangle_k ] [ \psi^j T^j \sigma_{jk} T^k \langle \alpha^k \rangle_k ]^* g(r_{jk}) dr_j dr_k \\ & + n_0^3 \sum \iiint [ \psi^j T^j \sigma_{jk} T^k \sigma_{km} T^m \langle \alpha^m \rangle_m ] \times \\ & \times [ \psi^j T^j \sigma_{jk} T^k \sigma_{km} T^m \langle \alpha^m \rangle_m ]^* g(r_{jk}) g(r_{km}) dr_j dr_k dr_m \end{aligned}$$

+ ... ( ladder diagrams )

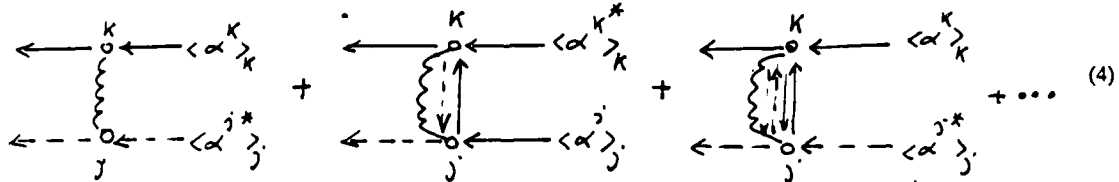
$$\begin{aligned}
 & + n_0^2 \Sigma \iint [ \Psi^k T^k < \alpha^k >_k ] [ \Psi^j T^j < \alpha^j >_j ]^* [ g(r_{jk}) - 1 ] dr_j dr_k \\
 & + n_0^2 \Sigma \iint [ \Psi^k T^k \sigma_{kj} T^j < \alpha^j >_j ] [ \Psi^j T^j \sigma_{jk} T^k < \alpha^k >_k ]^* g(r_{jk}) dr_j dr_k \\
 & + n_0^2 \Sigma \iint [ \Psi^k T^k \sigma_{kj} T^j \sigma_{jk} T^k < \alpha^k >_k ] \times \\
 & \times [ \Psi^j T^j \sigma_{jk} T^k \sigma_{kj} T^j < \alpha^j >_j ]^* g(r_{jk}) dr_j dr_k \\
 & + \dots \text{ ( cyclic diagrams )}
 \end{aligned} \tag{2}$$

In Eq. (2)  $T^j$  is the T - Matrix of the j-th scatterer [Varadan and Varadan, 1980],  $\Psi^k$  is the outgoing function (Hankel function) of the k-th scatterer and  $\sigma_{kj}$  the translation operator. Each term of the two series in (2) represents a certain order of scattering. For the same order of scattering, the cyclic terms are proportional to a higher power in the number density. Thus at low concentrations cyclic terms contribute less than the ladder terms to the the same order of scattering. Eq. (2) can be represented diagrammatically as follows,

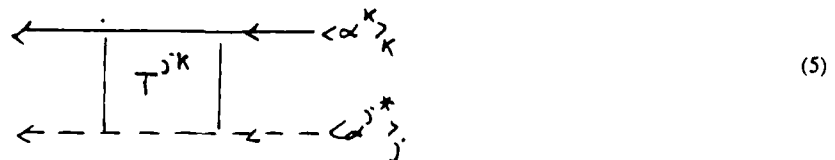
(a) Ladder Diagram



(b) Cyclic Diagram



In fact the so called cyclic terms can all be summed if one replaces the infinite series in (4) with the T-matrix of a pair of scatterers which considers all the back and forth scattering between them. The back and forth scattering between a pair of scatterers, which has been neglected in the ladder approximation, may have major contribution toward backscattering rather than in the forward direction mentioned in one previous paper [Bringi et al., 1980] coauthored with us. Eq. (4) may hence be written diagrammatically as



where  $T^{jk}$ , the two scatterer T - matrix has the following form [Varadan and Varadan, 1981]

$$T^{jk} = R(r_0) T^j [ 1 - \sigma(r_{jk}) T^k \sigma(r_{kj}) T^j ]^{-1} [ 1 + \sigma(r_{jk}) T^k R(r_{kj}) ] R(-r_0)$$

$$+ R(r_0) T^k [1 - \sigma(r_{kj}) T^j \sigma(r_{jk}) T^k]^{-1} [1 + \sigma(r_{kj}) T^j R(r_{jk})] R(-r_0) \quad (6)$$

In the above expression,  $R(r_0)$  is the regular part of the translation matrix  $\sigma(r_0)$ ,  $r_{jk} = r_j - r_k$  and  $r_0 = (r_j + r_k)/2$ .

## RESULTS AND DISCUSSION

In general, at low concentrations, both the magnitude of scattered intensity and multiple scattering contribution are not strong enough to reach the threshold of the enhanced backscattering. When the enhanced backscattering happens, the width of the intensity peak is proportional to the imaginary part of the effective wavenumber. In other words, the width is inversely proportional to the mean free path which is getting smaller when the concentration is getting larger (the average separation distance between two scatterers is getting smaller). The calculated mean free path length, which compares very well with that of the experiment, and the data used in the intensity calculation are shown in Table 1.

To perform the calculation, one needs to adopt the cylindrical coordinates instead of the spherical one to match the experimental set-up which brings the complexities in converting the spherical functions to their cylindrical counterparts. Furthermore, in order to compare with the experimental results, especially the magnitude and the width of the intensity peak, the proper integration limits must be taken care of very carefully. The widths and the magnitudes of the backscattered intensity peak of our computations compare favorably with those of Albada's experiments in which the receiver used has a very small field of view and, hence, gives a much better signal resolution (see Fig. 1). However, due to the truncation of the orders of scattering due to the tremendous amount of CPU time required, we did not obtain a full match.

## REFERENCES

- E. Abrahams, P.W. Anderson, D.C. Licciardello and T.V. Ramakrishnan, *Phys. Rev. Lett.* **42**, 673 (1979).
- E. Akkermans, P.E. Wolf, and R. Maynard, *Phys. Rev. Lett.* **56**, 1471 (1986).
- M.P. Van Albada and A. Lagendijk, *Phys. Rev. Lett.* **55**, 2692 (1985).
- G. Bergmann, *Phys. Rev.* **107**, 1 (1984).
- V.N. Brinl, T.A. Seliga, V.K. Varadan and V.V. Varadan, "Bulk propagation characteristics of discrete random media," in *Multiple Scattering and Waves in Random Media*, edited by P.L. Chow, W.E. Kohler and G.C. Papanicolaou, North-Holland, 1981.
- J.C. Dalnty (ed.), *Laser Speckle and Related Phenomena*, Springer-Verlag, 1984.
- Y. Kuga and A. Ishimaru, *J. Opt. Soc. Am.* **A1**, 831 (1984).
- C.L. Rino, *IEEE Trans. Antennas Propagat.* **AP-24**, 912 (1976).
- L. Tsang and A. Ishimaru, *J. Opt. Soc. Am.* **A2**, 1331 (1985).
- V.K. Varadan and V.V. Varadan, Eds., *Acoustic, Electromagnetic and Elastic Wave Scattering - Focus on the T-Matrix Approach*, Pergamon Press, New York, 1980.
- V.V. Varadan and V.K. Varadan, *J. Acoust. Soc. Am.* **70**, 213 (1981).

V.V. Varadan, Y. Ma and V.K. Varadan, J. Opt. Soc. Am. A2, No. 12, 2195 (1985).

V.V. Varadan, Y. Ma and V.V. Varadan, "Scattered intensity of a wave propagating in a discrete random medium," submitted to *Applied Optics*, August 1987.

P.E. Wolf and G. Maret, *Phys. Rev. Lett.* 55, 2696 (1985).

K.C. Yeh, *Radio Sci.* 18, 159 (1983).

**Table 1. Data used in the calculation [Ref : Albada and Lagendijk, 1985]**

Concentration $n_0$	(i)	$14.1 \times 10^{16} / \text{m}^3$ (corresponding volume fraction $c = 0.09587$ )
	(ii)	$3.48 \times 10^{16} / \text{m}^3$ ( $c = 0.02366$ )
	(iii)	$1.49 \times 10^{16} / \text{m}^3$ ( $c = 0.01013$ )

Particle size  $d = 1.091 \mu\text{m}$  (in diameter)

Refractive index  $n$  (latex 5100) = 1.6

Refractive index  $n$  (distilled water) = 1.33

He-Ne laser wavelength  $\lambda = 633 \text{ nm}$

Nondimensional frequency  $kd$  ( $2\pi d/\lambda$ ) = 10.8294 ( $\gg 1$ )

Calculated effective  $K = K_1 + iK_2$

(i)	$K_1/k_w = 1.01266, K_2/k_w = 0.1514 \times 10^{-1}$ ( $c = 0.09587$ )
(ii)	$K_1/k_w = 1.00231, K_2/k_w = 0.3839 \times 10^{-2}$ ( $c = 0.02366$ )
(iii)	$K_1/k_w = 1.00093, K_2/k_w = 0.1618 \times 10^{-2}$ ( $c = 0.01013$ )

Mean free path (Albada's experiment) =  $2.6 \mu\text{m}$  (for  $n_0 = 14.1 \times 10^{16} / \text{m}^3$ )

Calculated mean free path (from  $K_2$ ) =  $2.5 \mu\text{m}$

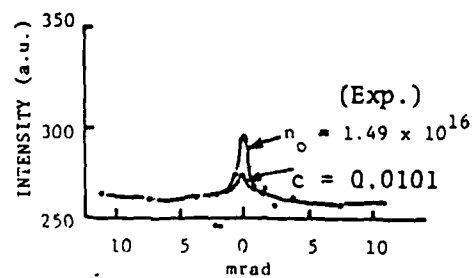
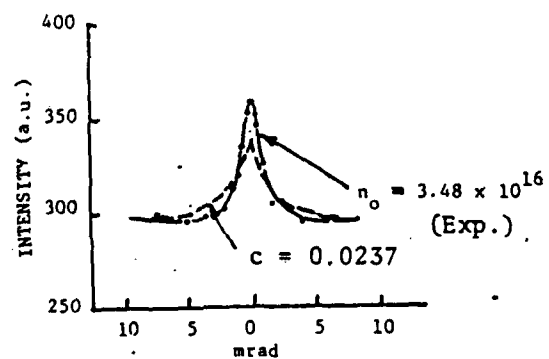
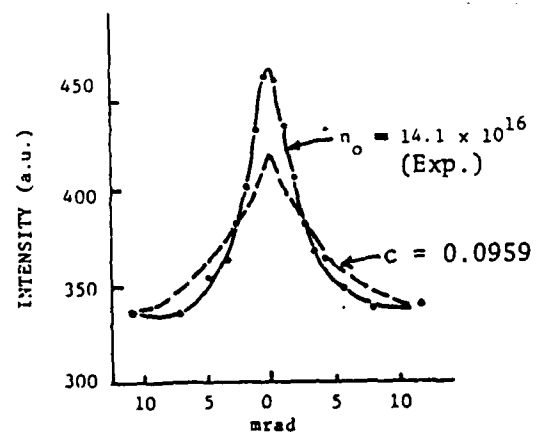


Fig. 1 Backscattered intensity : Comparison with optical experiments [Albada and Legendijk, 1985]

## AVERAGE INTENSITY SCATTERED BY DENSELY DISTRIBUTED NONSPHERICAL PARTICLES

Y. Ma, V.V. Varadan and V.K. Varadan

*Laboratory for Electromagnetic and Acoustic Research  
Department of Engineering Science and Mechanics*

*and*

*Center for the Engineering of Electronic and Acoustic Materials  
The Pennsylvania State University, University Park, PA 16802*

### RECENT PUBLICATIONS, SUBMITTALS FOR PUBLICATION AND PRESENTATIONS:

V.V. Varadan, V.K. Varadan and Y. Ma, "EM wave propagation in discrete random media: nonspherical statistics," in Proceedings of the 1986 CRDC Scientific Conference on Obscuration and Aerosol Research.

V.V. Varadan, V.K. Varadan, Y. Ma, and W.A. Steele, "Effects of nonspherical statistics on EM wave propagation in discrete random media," *Radio Science* 22, No. 4, 491 (1987).

Y. Ma, V.V. Varadan and V.K. Varadan, "Calculations of the incoherent intensity for random media containing nonspherical scatterers," Presented at the URSI Radio Science Meeting, Blacksburg, Virginia, June 1987.

V.V. Varadan, Y. Ma and V.K. Varadan, "Scattered intensity of a wave propagating in a discrete random medium," submitted to *Applied Optics*, August 1987.

### ABSTRACT

This paper investigates the second moment (average intensity) of an EM wave field propagating in a medium containing densely distributed nonspherical scatterers whose positions are random. The effective propagation constant  $K$  obtained from our previous work, using the nonspherical statistics in the investigation of multiple EM wave scattering by aligned prolate and oblate dielectric spheroids, and the appropriate pair correlation function for nonspherical scatterers obtained by the Monte Carlo method are required in implementing the moment equation to get the numerical results for intensity. The comparison between the results using correct nonspherical statistics and approximated spherical statistics indicates that even a small difference for the effective propagation constant  $K$  will produce a remarkable difference in intensity. Numerical results for average intensity scattered by spherical particles using our intensity formalism are also presented and compared with some microwave measurements. The extension of the present work is to study wave propagation in a medium containing a random distribution of randomly oriented nonspherical scatterers and investigate the isotropic properties of the medium.

### INTRODUCTION

The statistical moments of a wave propagating in a random medium are of great interest for use in communication, probing and remote sensing. The present paper following the trace of our previous work, in which the first moment of a random wave field has been carefully investigated using appropriate statistics, starts to examine the effects of nonspherical statistics on the second moment (average intensity) of a wave field propagating in a medium consisting of randomly distributed nonspherical scatterers. In our intensity formalism, shape factor, size distribution, orientation distribution and physical properties of scatterers can all be considered, however, the

intensity equation for densely distributed scatterers requires the pair correlation function which is available at the present time only for simple shaped scatterers with special alignments.

To make the problem tractable, nonspherical scatterers with rotational symmetry properties randomly distributed in free space are first considered. Scatterers of this kind whose scattering responses are able to be represented by the T-matrix [Varadan and Varadan, 1980]. Further, we consider only the aligned case which means the symmetry axes of the scatterers are all parallel to the direction of the incident wave.

In the calculation of intensity, without losing generality, we used the distorted Born approximation in the intensity equation in which the required effective propagation constant  $K$  is obtained from our previous work [Varadan et al., 1986, 1987] using the nonspherical statistics in the investigation of multiple EM wave scattering by aligned prolate and oblate dielectric spheroids. The pair correlation function for nonspherical scatterers is obtained by the Monte Carlo method which has been introduced in our paper [Varadan, et al, 1987]. The comparison between the results using correct nonspherical statistics and approximated spherical statistics indicates that even a small difference for the effective propagation constant  $K$  will produce a remarkable difference in intensity. Numerical results for average intensity scattered by spherical particles using our intensity formalism are also presented and compared with some microwave measurements.

#### MULTIPLE SCATTERING FORMULATION FOR THE INTENSITY

We consider  $N(N \rightarrow \infty)$  rotationally symmetric oriented scatterers randomly distributed in a volume  $V(V \rightarrow \infty)$  so that the number of particles per unit volume  $n_0 = N/V$  is finite. For the scattering of waves by those scatterers located at  $r_1, r_2, \dots, r_N$ , we represent the total field outside the scatterer by

$$U(r) = u_0(r) + \sum u_j(r - r_j). \quad (1)$$

where  $u_0$  is the incident wave field and  $u_j$  the field scattered from the  $j$ -th scatterer. If the scatterers are randomly distributed in space, the total field can be divided into two parts and expressed as

$$U(r) = \langle U(r) \rangle + v. \quad (1-a)$$

We call  $\langle U(r) \rangle$  or  $\langle U \rangle$  the average or coherent field and  $v$  the fluctuation or incoherent field. The angular brackets  $\langle \rangle$  represent the configuration or ensemble average whose definition is quite common in statistics.

Similarly, we average the "intensity" (or the second moment of the field)  $|U|^2$  over the ensemble, and write the "average total intensity" as

$$\begin{aligned} \langle |U|^2 \rangle &= \langle |\langle U \rangle|^2 + |v|^2 \rangle \\ &= |\langle U \rangle|^2 + V \end{aligned} \quad (2)$$

where  $|\langle U \rangle|^2$  is the coherent intensity and can be determined if the average field  $\langle U \rangle$  is known. However, the incoherent intensity  $V$  which is the ensemble average of the absolute square of the field fluctuation is not a directly obtainable quantity. By the use of (1) and some operation rules for the configuration average, the incoherent intensity  $V$  in (2) can be written as

$$V = \sum \langle |u_j|^2 \rangle + \sum \sum \langle u_k u_j^* \rangle - \sum \sum \langle u_k \rangle \langle u_j^* \rangle \quad (3)$$

where the superscript "\*" represents the complex conjugate of the attached quantity. (3) is a finite sum though "N", the number of scatterers, can be fairly large; its computation becomes impractical even for a moderate  $N$  and in most

cases impossible. In terms of an appropriate probability distribution function and the conditional configuration average, (3) can be expressed in the following integral form

$$V = n_0 \int \langle |u_j|^2 \rangle_j dr_j + n_0^2 \iint \langle u_k u_j^* \rangle_{jk} G(r_{jk}) dr_k dr_j - n_0^2 \iint \langle u_k \rangle_k \langle u_j^* \rangle_j dr_k dr_j \quad (4)$$

where  $\langle \rangle_j$  and  $\langle \rangle_{jk}$  are conditional configuration averages holding the positions of the j-th and both the j-th and k-th scatterers fixed, respectively.  $G(r_{jk})$  the pair correlation function, for aligned spheroidal particles, can be expanded in the Legendre polynomials as [Varadan et al., 1987]

$$G(r) = \sum_n g_n(r) P_n(\cos\theta)$$

where the coefficients depend on the distance between particles and azimuthal angle and implicitly on the concentration of scatterers. For spherical scatterers, the pair correlation function becomes the radial distribution function  $g(r_{jk})$  upon which spherical statistics bases. Eq. (4) is an exact expression for the incoherent intensity  $V$ .

If the scatterer locations are random and independent of one another, only the first term on the RHS of (4) remains. This is the single scattering approximation to the intensity. Otherwise, in addition to incoherent single scattering, a relatively coherent intensity appears as the contribution of the second term grows. As the concentration of scatterers increases a local order is introduced in the near field of the scatterers since the particles can only be packed in a limited number of ways. In order to proceed further with the computation of the incoherent intensity as stated in (4), we need expressions for  $\langle u_j \rangle_j$ ;  $\langle |u_j|^2 \rangle_j$ ; and  $\langle u_k u_j^* \rangle_{jk}$ .

#### Distorted Born Approximation

In order to calculate the incoherent intensity  $V$  from (4) an approximation needs to be made for  $\langle |u_j|^2 \rangle_j$  as well as for  $\langle u_k u_j^* \rangle_{jk}$ , which are both unknown. If we consider only first order scattering, we can use the distorted Born approximation (DBA) as follows:

$$\langle u_k u_j^* \rangle_{jk} \approx \langle u_k \rangle_k \langle u_j^* \rangle_j \quad (5)$$

This approximation was used by Twersky [Twersky, 1957] in solving the rough surface scattering problems and has subsequently been used by several other authors. Using (5), in the distorted Born approximation, (4) can thus be written as

$$V = n_0 \int \langle u_j \rangle_j \langle u_j^* \rangle_j dr_j + n_0^2 \iint \langle u_k \rangle_k \langle u_j^* \rangle_j [G(r_{jk}) - 1] dr_k dr_j \quad (6)$$

Equation (6) represents the incoherent intensity in the DBA. Its source is the coherent field,  $\langle u_j \rangle_j$ . Later we show that the average scattered field  $\langle u_j \rangle_j$  is related to the average exciting field when we neglect the field fluctuations in the field exciting a scatterer. Equation (6) tells us that the second term has a contribution to the intensity whenever the i-th and j-th scatterers are close to each other (position dependence), otherwise the contribution can be neglected. Eq. (6) is a deterministic equation since only the average exciting field is involved and the calculation is straight forward as long as the pair correlation function is known.



### Implementation of the T-Matrix

To compute the intensity in the DBA, or to proceed further with the analysis of (4), we need an expression for the coherent field. For a single scatterer, the scattered field from the  $j$ -th scatterer can be expressed as

$$u_j = \sum_n f_n^j \Psi_n^j \quad (7)$$

where  $f_n^j$  are the scattered field coefficients and  $\Psi_n^j$  the outgoing functions (Hankel functions). The scattered field coefficients  $f_n^j$  and the exciting field coefficients  $\alpha_n^j$  are related through the T matrix [Varadan and Varadan, 1980] :

$$f_n^j = \sum_{nn'} T_{nn'}^j \alpha_{n'}^j. \quad (8)$$

Substituting (8) into (7) and taking the conditional configuration average, we have

$$\langle u \rangle_j = \sum_n \sum_{nn'} T_{nn'}^j \alpha_{n'}^j \Psi_n^j \rangle_j. \quad (9)$$

Further, to simplify the computation, we assume the shape, size, and physical properties of all the scatterers are independent of their positions. In such a case, (9) can be written as

$$\langle u \rangle_j = \sum_n \sum_{nn'} T_{nn'}^j \langle \alpha_{n'}^j \rangle_j \Psi_n^j. \quad (10)$$

where the exciting field coefficients of the  $j$ -th scatterer can be shown to be [Varadan et al., 1985]

$$\alpha_n^j = a_n^j + \sum_{nn'} \sum_{kk'} \sigma_{nn'}(r_k - r_j) T_{n'n}^{kk'} \alpha_{n'}^{k'}. \quad (11)$$

In (11),  $a_n^j$  are the incident field coefficients of the  $j$ -th scatterer and  $\sigma_{nn'}$  is the translation matrix for spherical wave functions. Although  $\alpha_n^j$  are, in general, unknown for a random distribution of scatterers, their conditional average  $\langle \alpha_n^j \rangle_j$  (average exciting field coefficients of the  $j$ -th scatterer whose position is fixed) are assumed to have the following form [Varadan et al., 1985]

$$\langle \alpha_n^j \rangle_j = X_n \exp(i K k_0 \cdot r_j) \quad (12)$$

which states that for an incident plane wave field, the average exciting field propagates with a new propagation constant  $K$  along the incident wave direction  $k_0$ . The new propagation constant  $K$  is complex and frequency dependent and can be obtained by solving the dispersion equation [Varadan et al., 1986].

## RESULTS AND DISCUSSION

In order to show the effect of nonspherical statistics on intensity, results based on the approximation for randomly distributed spheroids using single scattering theory and the spherical statistics (Circumscribing Sphere Approximation and Equivalent Volume Approximation [Varadan et al., 1986]) are compared with those using nonspherical statistics. We have picked values of the effective wavenumber, which is obtained using the nonspherical statistics in the investigation of multiple EM wave scattering by aligned prolate and oblate dielectric spheroids [Varadan et al., 1987], and used them to compute the intensity and show the results in Figs 1 and 2. One sees from both figures that, off-forward scattering at the fixed frequency as well as forward scattering at different frequencies, without using the correct pair statistics for nonspherical scatterers, the computed intensities are quite different from case to case. This fact explains why it is necessary to introduce the nonspherical statistics into the intensity calculation.

To check the validity of our formalism, we compared our incoherent intensity calculations with the microwave experiments conducted by Beard et al. [1965]. The transmitted intensity was calculated using the DBA as given in (6) where  $\theta = 0^\circ$  represents the forward direction. This calculation is based on the experimental set-up which

consists of a slab region styrofoam container, for various concentrations of scatterers at the fixed frequency. For the case  $ka = 20.8$  for tenuous scatterers with relative index of refraction 1.016 the computed results match very well with the measurements for off-forward scattering as depicted in Fig. 3.

#### REFERENCES

- C.I. Beard, T.H. Kays and V. Twersky, "Scattered intensities for random distributions - microwave data and optical applications," *App. Opt.* 4, 1299 (1965).
- V. Twersky, "On scattering and reflection of sound by rough surfaces," *J. Acoust. Soc. Am.* 29, 209 (1957).
- V.K. Varadan and V.V. Varadan, eds., *Acoustic, Electromagnetic and Elastic Wave Scattering-Focus on the T-matrix Approach*, Pergamon Press, New York, 1980.
- V.V. Varadan, Y. Ma and V.K. Varadan, "Propagator model including multiple fields for discrete random media," *J. Optical Soc. Am.* 78(5), 1879 (1985).
- V.V. Varadan, V.K. Varadan and Y. Ma, "EM wave propagation in discrete random media: nonspherical statistics," in the Proceedings of the 1986 CRDC Scientific Conference on Obscuration and Aerosol Research.
- V.V. Varadan, V.K. Varadan, Y. Ma, and W.A. Steele, "Effects of nonspherical statistics on EM wave propagation in discrete random media," *Radio Science* 22, No. 4, 491 (1987).
- V.V. Varadan, V.K. Varadan and Y. Ma, "Multiple scattering of waves in random media containing non-spherical scatterers," in the Electromagnetic Wave Propagation Panel Symposium sponsored by AGARD, NATO, 1987.
- V.V. Varadan, Y. Ma and V.K. Varadan, "Scattered intensity of a wave propagating in a discrete random medium," submitted to *Applied Optics*, August 1987.

(6) where  $\theta = 0^\circ$  represents the forward direction. This calculation is based on the experimental set-up which consists of a slab region styrofoam container, for various concentrations of scatterers at the fixed frequency. For the case  $ka = 20.8$  for tenuous scatterers with relative index of refraction 1.016 the computed results match very well with the measurements for off-forward scattering as depicted in Fig. 3.

#### REFERENCES

- C.I. Beard, T.H. Kays and V. Twersky, "Scattered intensities for random distributions - microwave data and optical applications," *App. Opt.* 4, 1299 (1965).
- V. Twersky, "On scattering and reflection of sound by rough surfaces," *J. Acoust. Soc. Am.* 29, 209 (1957).
- V.K. Varadan and V.V. Varadan, eds., *Acoustic, Electromagnetic and Elastic Wave Scattering-Focus on the T-matrix Approach*, Pergamon Press, New York, 1980.
- V.V. Varadan, Y. Ma and V.K. Varadan, "Propagator model including multiple fields for discrete random media," *J. Optical Soc. Am.* 78(5), 1879 (1985).
- V.V. Varadan, V.K. Varadan and Y. Ma, "EM wave propagation in discrete random media: nonspherical statistics," in the Proceedings of the 1986 CRDC Scientific Conference on Obscuration and Aerosol Research.
- V.V. Varadan, V.K. Varadan, Y. Ma, and W.A. Steele, "Effects of nonspherical statistics on EM wave propagation in discrete random media," *Radio Science* 22, No. 4, 491 (1987).
- V.V. Varadan, V.K. Varadan and Y. Ma, "Multiple scattering of waves in random media containing non-spherical scatterers," in the Electromagnetic Wave Propagation Panel Symposium sponsored by AGARD, NATO, 1987.
- V.V. Varadan, Y. Ma and V.K. Varadan, "Scattered intensity of a wave propagating in a discrete random medium," submitted to *Applied Optics*, August 1987.

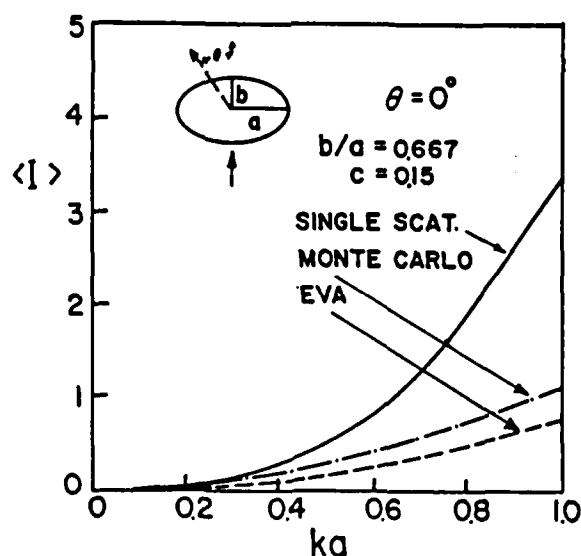


Fig. 1 Forward scattered incoherent intensity versus nondimensional frequency  $ka$ . (oblate spheroid  $b/a = 0.667$ ,  $c = 0.15$ )

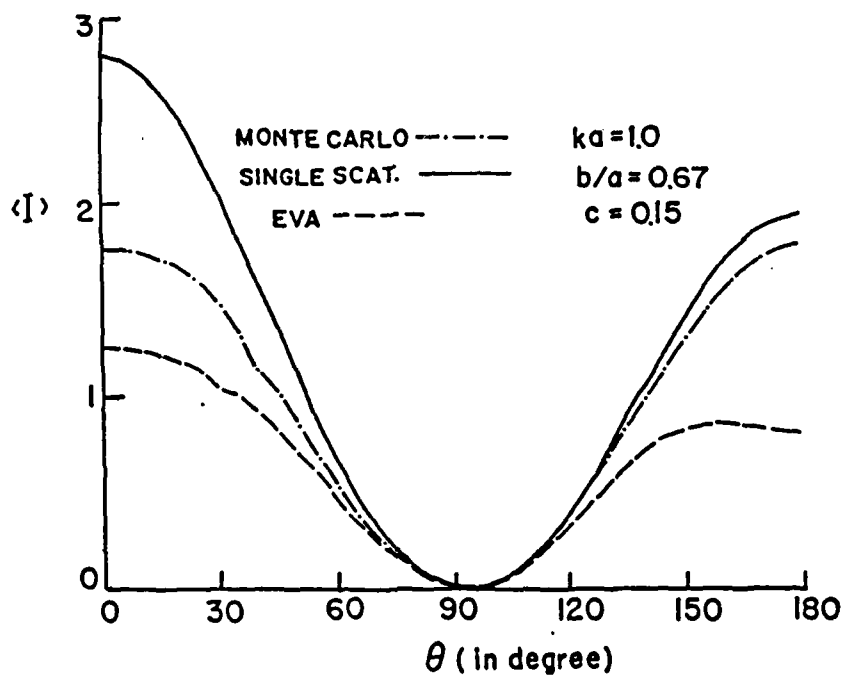


Fig. 2 Incoherent intensity versus scattering angle at  $ka = 1.0$ .  
 (oblate spheroid  $b/a = 0.667$ ,  $c = 0.15$ )

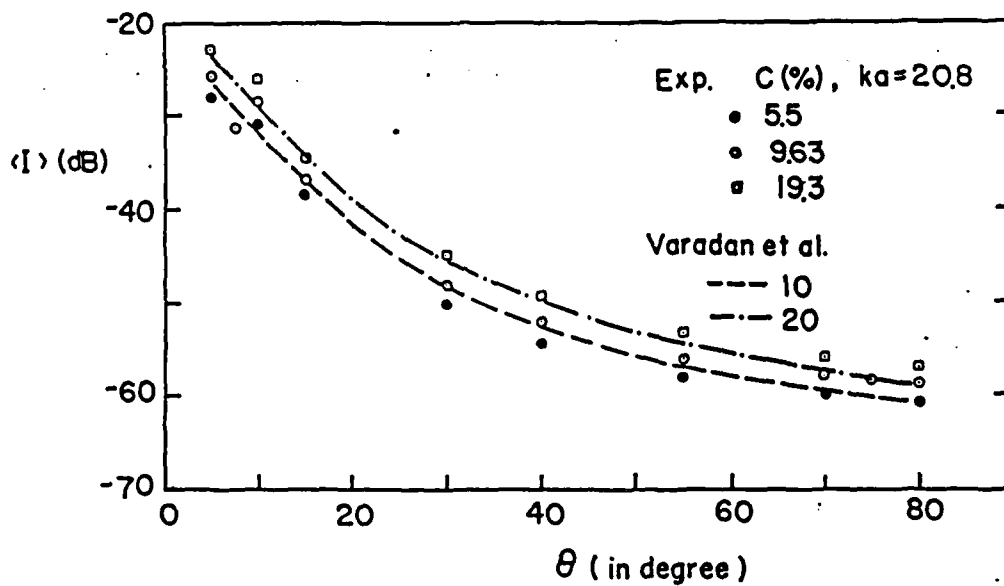


Fig. 3 Incoherent intensity : Comparison with microwave experiments [Beard et al., 1965]

## Effects of nonspherical statistics on EM wave propagation in discrete random media

V. V. Varadan, V. K. Varadan and Y. Ma

Research Center for the Engineering of Electronic and Acoustic Materials, Department of Engineering Science and Mechanics, The Pennsylvania State University, University Park

W. A. Steele

Department of Chemistry, The Pennsylvania State University, University Park

(Received October 30, 1986; revised February 24, 1987; accepted February 24, 1987.)

Earlier results for electromagnetic wave propagation in discrete random media assumed spherical statistics for describing the spatial distribution of even nonspherical scatterers. The appropriate pair correlation function for nonspherical scatterers can, in general, be obtained by the Monte Carlo method which is essential in analyzing nonspherical statistics. This paper presents new results using nonspherical statistics in the investigation of multiple electromagnetic wave scattering by aligned dielectric prolate as well as oblate spheroids randomly distributed in space. Comparison between previous results using spherical statistics and present calculations show that approximating the spatial distribution of nonspherical scatterers using spherical statistics will yield effective medium characteristics that differ quite widely. Of all approximations using spherical statistics for non-spherical scatterers that using an equal volume sphere appears to be the best if the actual statistics are not available."

### 1. INTRODUCTION

In many radar applications, multiple scattering effects cannot be ignored [Ishimaru, 1978; Oguchi, 1981; Olsen, 1982]. In most theoretical investigation, scatterers are assumed to be spherical in shape and bear a uniform size distribution, although this may not be practical [Bringing et al., 1983; Mathur and Yeh, 1964; Twersky, 1978; Varadan et al., 1979, 1983]. When the volume fraction occupied by the spheres becomes large enough to consider their relative positions, detailed knowledge of the positional distribution of the scatterers is needed. This entails a consideration of inter-body forces as in the many body problem of statistical mechanics. At a minimum, the pair correlation function is required in analyzing the problem. In nature, unfortunately, scatterers are not simple in shape and some results have been reported for nonspherical particles [Tsang, 1984; Lang et al., 1986; Varadan et al., 1985]. However, to appropriately model the real situation, deviation from a spherical scatterer still keeping the rotational symmetry of the scatterer appears to be an improvement to the previous model that permit us to study the shape effect. A simple nonspherical scatterer happens to be a prolate or oblate

spheroid. The scattering response of a single spheroid can be simply represented by the T-matrix [Varadan and Varadan, 1980]. If the concentration of the spheroidal scatterers (in this case, lossless dielectric prolate(oblate) spheroids) happens to be small, random lattice gas statistics can apply, otherwise the spatial distribution of these nonspherical scatterers cannot be described by spherical statistics. The reason, which is quite obvious, is that the pair correlation function, instead of being a function of only the separation distance between a pair of scatterers, becomes also a function of the orientation of the vector joining the two nonspherical scatterers. To just see the shape effect and distinguish this from the previous approximations using spherical statistics, we consider only the aligned case. Further the direction of wave propagation is restricted to be along the rotational axis of symmetry of the aligned spheroids. We emphasize that arbitrary orientation (including random orientation) of nonspherical scatterers will not cause major difficulties in the theoretical analysis but we leave this to a future analysis.

The nonspherical statistics involved in the analysis is the pair correlation function for aligned spheroids. It is well known that the Monte Carlo simulation method has yielded superior numerical results for the radial distribution function of densely distributed hard spheres [Barker and Henderson, 1971], with the help of advanced digital computers. Therefore, in this paper, we will briefly discuss the application of the Monte Carlo method in obtaining the pair correlation function for aligned spheroids.

Copyright 1987 by the American Geophysical Union.

Paper number 7S0205.

0048-6604/87/007S-0205\$08.00

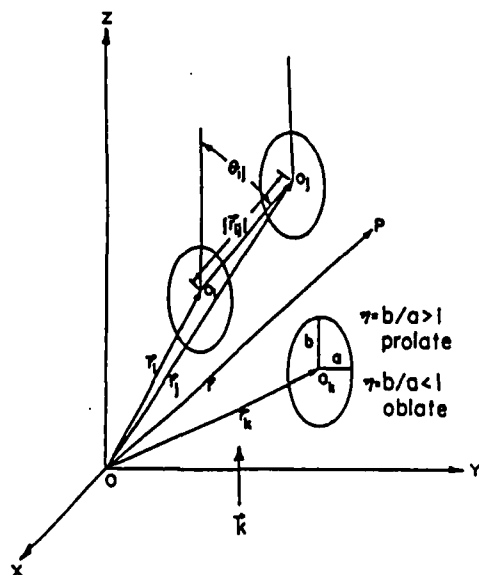


Fig. 1 Multiple scattering of waves in discrete random media with positionally and orientationally correlated nonspherical scatterers.

Finally, computations of the effective attenuation rate using nonspherical statistics in studying electromagnetic wave propagation through randomly distributed aligned spheroids are performed. Comparison between previous results using spherical statistics and present calculations show that approximating the spatial distribution of nonspherical scatterers using spherical statistics will yield effective medium characteristics that differ quite widely. Of all approximations using spherical statistics for non-spherical scatterers that using an equal volume sphere appears to be the best if the actual statistics are not available.

## 2. MULTIPLE SCATTERING FORMULATION

In this section, the average field in the random medium is written as a partial summation of a multiple scattering series. By assuming that the average field is a plane wave with an effective wave number  $K$ , the resulting dispersion equation is solved. The formalism is general and applicable to any types of wave. Only the most important details that lead to the dispersion equation involving the pair correlation are presented and for all intermediate steps, we refer the reader to [Varadan et al., 1979]. Vector notation is dispensed with, but the formalism is equally applicable to acoustic fields satisfying the scalar Helmholtz equation, or the electromagnetic field satisfying the vector Helmholtz equation.

Let the medium contain  $N$  aligned, randomly distributed spheroidal scatterers in a volume  $V$  such that  $N \rightarrow \infty$ ,  $V$

$\rightarrow \infty$  but  $n_0 = N/V$  the number density of scatterers is finite, see Figure 1. Let  $u$ ,  $u^0$ ,  $u_i^e$ ,  $u_i^s$  be respectively the total field; the incident or primary plane, harmonic wave of frequency  $\omega$ ; the field incident or exciting the  $i$ th scatterer; and the field which is in turn scattered by the  $i$ th scatterer. The time dependence  $\exp(-i\omega t)$  of all fields is the same and not written explicitly.

These fields are defined at a point  $r$  which is not occupied by one of the scatterers. In general, these fields or potentials which can be used to describe them satisfy the scalar or vector wave equation. Let  $\text{Re } \phi_n$  and  $\text{Ou } \phi_n$  denote the basis of orthogonal functions which are eigenfunctions of the vector Helmholtz equation. The qualifiers  $\text{Re}$  and  $\text{Ou}$  denote functions which are regular at the origin and outgoing at infinity which are, respectively, appropriate for expanding the field which is incident on a scatterer and that which it scatters which in turn must satisfy outgoing or radiation conditions. Thus, we can write the following set of self-consistent equations:

$$u = u^0 + \sum_{i=1}^N u_i^s = u_i^e + u_i^s$$

$$= u^0 + \sum_{j \neq i} u_j^s + u_i^s \quad (1)$$

$$u^0(r) = \beta \exp(ik k_0 \cdot r) = \sum_n \alpha_n^i \text{Re } \phi_n(r - r_i) \quad (2)$$

$$u_i^e = \sum_n \alpha_n^i \text{Re } \phi_n(r - r_i); \quad a < |r - r_i| < 2a \quad (3)$$

$$u_i^s = \sum_n f_n^i \text{Ou } \phi_n(r - r_i); \quad |r - r_i| > a \quad (4)$$

where  $\alpha_n^i$  and  $f_n^i$  are unknown expansion coefficients. We observe in (3) and (4) that  $a$  is the radius of the sphere or cylinder (for two-dimensional problems) circumscribing the scatterer and that all expansions are with respect to a coordinate origin located in a particular scatterer.

The T-matrix by definition simply relates the expansion coefficients of  $u_i^e$  and  $u_i^s$  provided  $u_i^e + u_i^s$  is the total field which is consistent with the definitions in (1). Thus, see Varadan and Varadan [1980],

$$f_n^i = \sum_{n'} T_{nn'} \alpha_{n'}^i \quad (5)$$

and the following addition theorem for the basis functions is invoked

$$\text{Ou } \phi_n(r - r_j) = \sum_{n'} \sigma_{nn'}(r_i - r_j) \text{Re } \phi_{n'}(r - r_i) \quad (6)$$

Substituting Eqs. (2) - (6) in Eq. (1), and using the orthogonality of the basis functions we obtain

$$\alpha^i = \alpha^i + \sum_{j \neq i} T^j \sigma(r_i - r_j) \alpha^j \quad (7)$$

This is a set of coupled algebraic equations for the exciting field coefficients which can be iterated and leads to a multiple scattering series.

For randomly distributed scatterers, an ensemble average can be performed on Eq. (7) leading to

$$\langle \alpha^i \rangle_i = \alpha^i + \langle \sigma(r_i - r_j) T^j \langle \alpha^j \rangle_{ij} \rangle_i \quad (8)$$

where angle brackets and  $ijk\dots$  denotes a conditional average and (8) when iterated is an infinite hierarchy involving higher and higher conditional expectations of the exciting field coefficients. In actual engineering applications, a knowledge of higher order correlation functions is difficult to obtain, and usually the hierarchy is truncated so that at most only the two body positional correlation function is required.

To achieve this simplification the *quasi-crystalline approximation* (QCA), first introduced by Lax [1952] is invoked, which is stated as

$$\langle \alpha^j \rangle_{ij} \approx \langle \alpha^j \rangle_j \quad (9)$$

Then, (8) simplifies to

$$\langle \alpha^i \rangle_i = \alpha^i + \langle \sigma(r_i - r_j) T^j \langle \alpha^j \rangle_j \rangle_i \quad (10)$$

an integral equation for  $\langle \alpha^i \rangle_i$  which in principle can be solved. We observe that the ensemble average in (10) only requires  $P(r_j|r_i)$ , the joint probability distribution function. In particular, the homogeneous solution of (10) leads to a dispersion equation for the effective medium in the quasi-crystalline approximation. Defining the spatial Fourier transform of  $\langle \alpha^i \rangle_i$  as

$$\langle \alpha^i \rangle_i = \int e^{iK \cdot r_i} X^i(K) dK \quad (11)$$

and substituting in (10), we obtain for the homogeneous solution

$$X^i(K) = \sum_{j \neq i} \int \sigma(r_i - r_j) T^j p(r_j|r_i) \times e^{iK \cdot (r_i - r_j)} dr_j X^j(K) \quad (12)$$

If the scatterers are identical

$$X^i(K) = X^j(K) = X(K) \quad (13)$$

and thus for a nontrivial solution to  $\langle \alpha^i \rangle_i$ , we require

$$\left| 1 - \sum_{j \neq i} \int \sigma(r_i - r_j) T^j p(r_j|r_i) e^{iK \cdot (r_i - r_j)} dr_j \right| = 0 \quad (14)$$

In (12) and (14),  $P(r_j|r_i)$  is the joint probability distribution function. For isotropic or spherical statistics,

$$P(r_j|r_i) = \begin{cases} 0; & |r_i - r_j| < 2a \\ g(|r_i - r_j|) / V; & |r_i - r_j| > 2a \end{cases} \quad (15)$$

where we have assumed that the scatterers are impenetrable with a minimum separation between the centers, and in (15),  $2a$  could be the diameter of the circumscribing sphere in three-dimensional and circle in two-dimensional, or  $2a$  could be the diameter of a sphere of equal volume. Equation (15) is the one that has been used in previous calculations for nonspherical scatterers and hence this equation leads to the use of spherical statistics for nonspherical scatterers. We observe that in (15), the joint probability distribution depends only on the interparticle distance and not on the orientation of the vector joining the centers and the function  $g(|r_i - r_j|)$  is called the radial distribution function.

If the concentration of nonspherical particles is not small, then it is incorrect or at best approximate to assume that isotropic statistics are valid. In this case we assume that the radial distribution function depends not just on the magnitude of the vector joining the centers of two spheroids but also on the orientation of this vector. For aligned spheroids which are rotationally symmetric, the dependence is only on the angle  $\theta$  between the separation vector and the symmetry axis which is taken to be the  $z$  axis of the coordinate system, as shown in Figure 1. There is no dependence on the azimuthal angle  $\phi$ . The joint probability distribution function is then written as

$$P(r_j|r_i) = \begin{cases} 0; & |r_i - r_j| < R(\theta) \\ G(r, \theta) / V; & |r_i - r_j| > R(\theta) \end{cases} \quad (16)$$

In the above equation,  $G(r, \theta)$  is the pair correlation function for aligned spheroidal scatterers (details in the next section), and  $R(\theta)$  is the minimum center to center distance when the spheroids just touch one another at one point, such that the line joining their centers subtends an angle  $\theta$  with the symmetry or  $z$ -axis of the spheroids. In this case the statistics are not isotropic but are a function of direction.

If (16) is substituted in (14), we get the following integral involving the pair distribution function when the explicit form of the translation matrix is substituted and  $\exp(iK \cdot (r_i - r_j))$  is written as an expansion in regular wave functions [Bringer et al., 1981]

$$[JH_\lambda] = 2\pi n_0 (2\lambda + 1) \int_0^\pi \sin \theta d\theta \times \quad (17)$$

$$\int_{R(\theta)}^\infty G(r, \theta) j_\lambda(Kr) h_\lambda(Kr) P_\lambda(\cos \theta) P_\lambda(\cos \theta) r^2 dr$$

where  $P_\lambda(\cos \theta)$  is the Legendre polynomials and  $j_\lambda$  and  $h_\lambda$  are the spherical Bessel and Hankel functions, respectively. We note that the lower limit of the integration on the  $r$ -variable

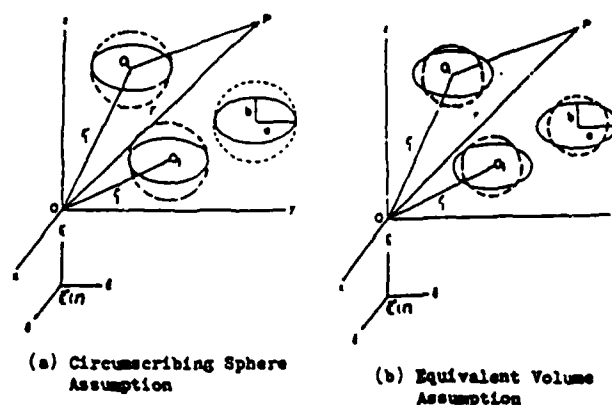


Fig. 2 The equal volume sphere and the circumscribing sphere assumption.

depends on the angle  $\theta$ . This double integral must hence be performed numerically. If isotropic statistics are used on the other hand, i.e., (15) is substituted in (14) and as in (17) the explicit form of the translation theorem is used, then (17) simplifies to

$$\begin{aligned}
 [JH_\lambda] = & 6c [ 2ka j'_\lambda(2Ka) h'_\lambda(2ka) - \\
 & 2Ka j'_\lambda(2Ka) h_\lambda(2ka) ] / \{ (ka)^2 - (Ka)^2 \} \\
 & + 24c \int [g(x) - 1] j_\lambda(2Kax) h_\lambda(2Kax) x^2 dx
 \end{aligned} \quad (18)$$

Equation (18) is actually a special case of (17) and  $c$  is the concentration ( $c = 4\pi a^3 n_0 / 3$ ) or volume fraction occupied by the scatterers and  $a$  is the radius of a sphere of volume equal to the scatterer. The prime denotes derivatives with respect to the argument of the Bessel and Hankel functions. The first term in (18) is usually referred to as the "hole correction" term. This only takes into effect that the scatterers cannot penetrate one another and does not take into account positional correlations. We further notice that the integral in (18) is only in one variable unlike (17) which contains a nested double integral. The "hole correction" appears in analytical form in (18), since

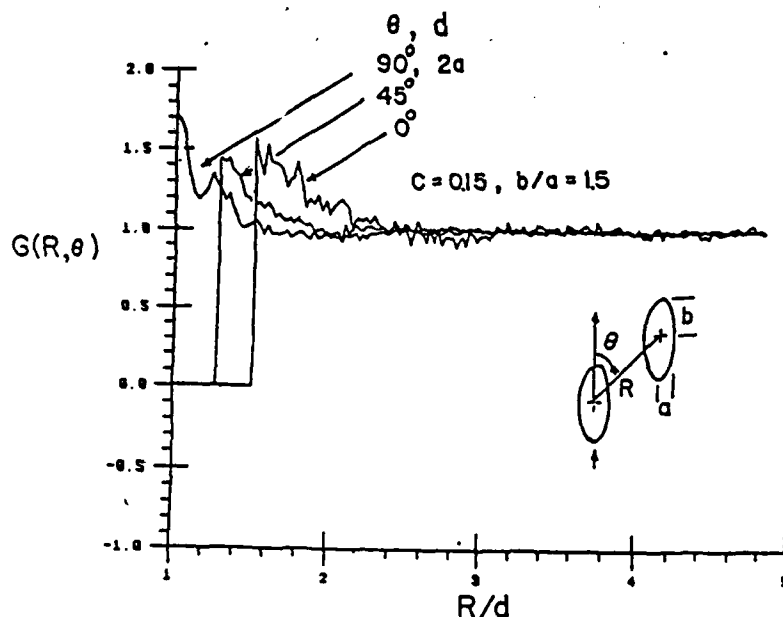


Fig. 3 Pair distribution function for random prolate spheroids using Monte Carlo simulation.



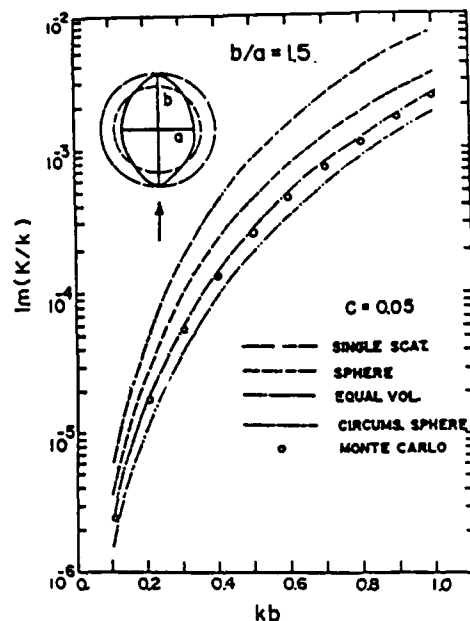


Fig. 4 Attenuation vs. nondimensional wave number using different statistics, and comparison with single scattering approximation for prolate spheroids of aspect ratio  $b/a = 1.5$  and concentration of 5%.

the excluded volume is a sphere of radius  $2a$ , where  $a$  is the radius of the equal volume sphere. In (17), it is difficult to separate the "hole correction" term since that must also be done numerically.

Equation (14) is a determinantal equation, the roots of which can be solved for numerically to yield the values of the effective wave number  $K = K_1 + iK_2$  as a function of the frequency via  $k = \omega/c$ , the shape, size and orientation of the scatterer via the T-matrix, and the statistics of the distribution via the joint probability distribution function. The effective wave number which describes wave propagation characteristics in the composite medium.

The details of numerically simulating the pair correlation function for spheroids is outlined in the next section.

### 3. THE PAIR CORRELATION FUNCTION FOR ALIGNED SPHEROIDS

The pair correlation function for aligned spheroidal particles can be expanded in Legendre polynomials as

$$G(r, \theta) = \sum_l g_l(r) P_l(\cos \theta) \quad (19)$$

where the coefficients  $g_l(r)$  depend only on the distance between particles (see Figure 1). The coefficients  $g_l(r)$  can be evaluated

during the Monte Carlo simulation by using the orthogonality of the Legendre polynomials and (18) can be inverted to give [Street and Tildesley, 1976]

$$g_l(r) = (2l+1) \langle P_l(\cos \theta) \rangle_{\text{shell}} / n_0 V(r, \Delta r) \quad (20)$$

where  $\langle \rangle$  is the average for all particles in the spherical shell with radius  $r$  to  $r + \Delta r$  of volume  $V(r, \Delta r)$ .

The Monte Carlo method in statistical mechanics refers to a computational scheme for estimating averages of the following form

$$\langle f \rangle = \int_{\Omega} f(X) P(X) dX / \int_{\Omega} P(X) dX \quad (21)$$

where  $X = (r_1, r_2, \dots, r_n)$  with  $r_i$  the position vector of the  $i$ th particle and  $f(X)$  is any well-behaved function of  $X$  and  $P(X)$  is a probability density function of  $X$  and for hard bodies has the form

$$P(X) = \exp\{-\beta U(X)\}, \quad \beta = 1/kT \quad (22)$$

where  $U(X)$  is the potential energy of the system and  $k$  is the Boltzmann constant.

Furthermore, the Monte Carlo method in its basic form consists of defining and realizing a Markov process in  $X$  space, which is the configuration space in this case. Chain averages

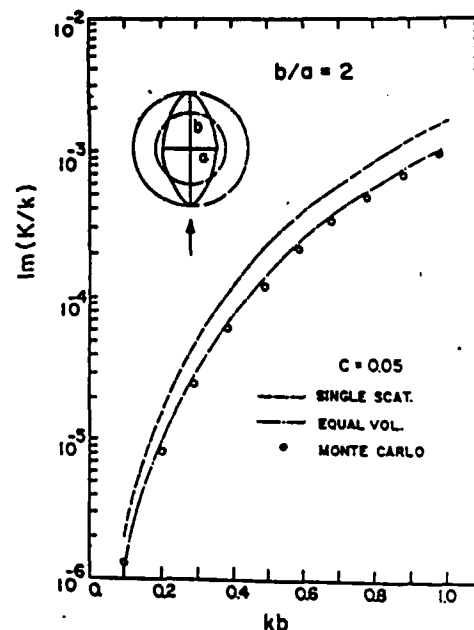


Fig. 5 Same as Figure 4 but for prolate spheroids of aspect ratio  $b/a = 2$ .

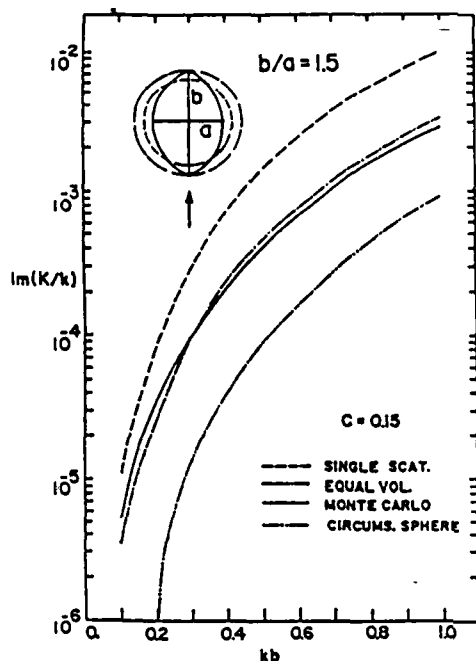


Fig. 6 Same as Figure 4 but for a concentration of 15%.

are evaluated based on whether the required probability appeared in different configurations. Readers are encouraged to go through the work of either Metropolis et al [1953] or Wood [1968] for details. For a system of hard particles, the required probability in accepting the configurations consists of simply checking the overlap criterion. Overlap is decided by checking whether the center to center distance for a pair of spheroids is less than  $d$  which is defined by

$$d = 2b [1 - \cos^2\theta + \cos^2\theta / \eta^2]^{-1/2} / \eta \quad (23)$$

where  $\eta$  is the aspect ratio of the spheroid such that  $\eta > 1$  for prolate and  $\eta < 1$  for oblate spheroids and  $b$  is half the length of the axis of symmetry for the spheroid (see Figure 1).

#### 4. RESULTS AND DISCUSSION

The imaginary part  $K_2$  of the effective wave number  $K$ , which is related to the attenuation in the effective medium, can be obtained by solving the dispersion equation in (17). In order to judge the effects of the pair correlation function, results based on calculations for spheroids using spherical statistics are also presented, i.e., using (18). In one calculation it is assumed that the relative position of a pair of spheroids can be approximated by that for a pair of spheres, each of which has the same volume as the spheroid (we call this the equivalent volume assumption). The other calculation employs the

approximation that the relative position of a pair of spheroids may be replaced by that for a pair of spheres which circumscribe the spheroids (we call this the circumscribing sphere assumption). These two assumptions are explained graphically in Figure 2. Some representative plots of the pair correlation function  $G(R, \theta)$  is plotted as a function of the interspheroid distance for various angles for prolate spheroids of aspect ratio 1.5 at a concentration of 15% in Figure 3. In Figure 4, the equivalent volume spherical statistics and the circumscribing sphere statistics are compared with the spheroidal statistics for an aspect ratio of 1.5 at a concentration of 5%. We note that the circumscribing sphere statistics are limited to very low volume fractions at high or low aspect ratios because the circumscribing spheres begin to overlap even at low spheroid concentrations.

In Figure 4, the attenuation which is normalized with respect to  $k$ , i.e.  $(K_2 / k)$  is plotted against the nondimensional frequency  $kb$  for prolate spheroids with an aspect ratio 1.5 and 5% concentration. If we do not consider the pair correlation at all, i.e., the calculation done using single scattering theory, one sees that the results give much higher attenuation than all other cases and this has been observed for all the computations. Although the circumscribing sphere assumption predicts lower attenuation, for such a moderate concentration, the equivalent volume assumption produces relatively good results when compared with the attenuation using the Monte Carlo method. This is also true for prolate spheroids of aspect ratio 2 which

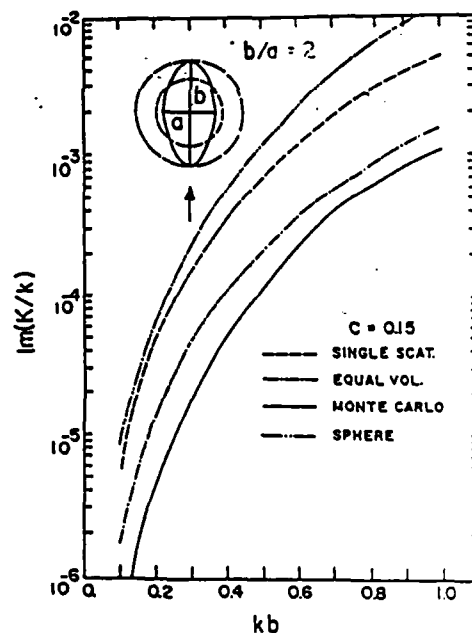


Fig. 7 Same as Figure 4 but for  $b/a = 2$  and concentration of 15%.

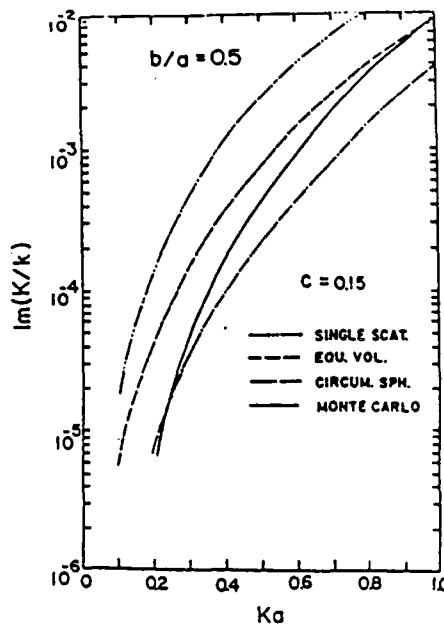


Fig. 8 Same as Figure 4 but for oblate spheroids with  $b/a = 0.5$  and concentration of 15%.

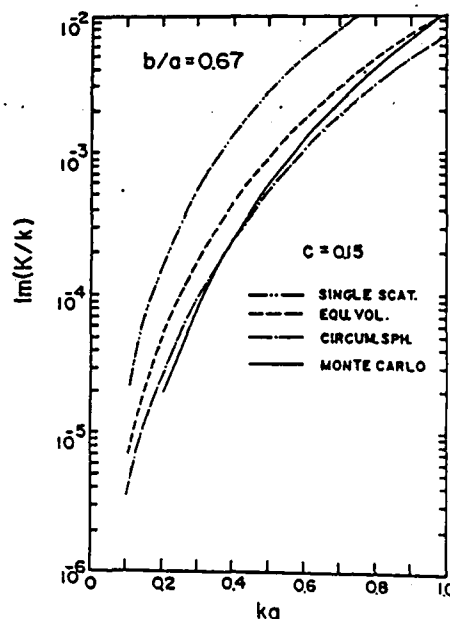


Fig. 9 Same as Figure 4 but for oblate spheroids of aspect ratio  $b/a = 0.67$  and concentration of 15%.

can be seen in Figure 5. However, when the concentration is increased to 15%, even the equivalent volume assumption fails to correctly predict the attenuation and, in general, it overpredicts the attenuation. These can be observed in Figures 6 and 7.

For oblate spheroids, the attenuation is similar to that for the prolate spheroids when the concentration is low. Two sets of calculation for aspect ratios 0.5 and 0.67 are presented as in Figures 8 and 9 for 15% concentration. At such a high concentration, for both aspect ratios, we find that the circumscribing sphere assumption predicts the attenuation quite well in the low frequency range while the equivalent volume assumption yields better results when the frequency is increased. However, both approximations cannot be compared with the Monte Carlo method in a certain band width when the concentration is high.

In conclusion, we would like to emphasize the importance of using nonspherical statistics in analyzing the scattering from densely distributed nonspherical scatterers. The approximations made for the spatial distribution of nonspherical scatterers can produce results which either over or under-estimate the effective properties which, in this case, is the attenuation of the effective medium. The effective phase velocity which is a relatively slowly varying function of frequency and concentration is insensitive to the differences between nonspherical statistics and the equal volume spherical statistics. Hence the phase velocity plots have not been included here.

**Acknowledgment.** This research was supported by contract DAAG-85-K-0234 and DAAG29-84-K-0187 awarded by the U. S. Army Research Office to the Pennsylvania State University.

## REFERENCES

- Barker, J. A. and D. Henderson, Monte Carlo values for the radial distribution function of a system of fluid hard spheres, *Mol. Phys.*, 21, 187-191, 1971.
- Bringi, V. N., T. A. Seliga, V. K. Varadan, and V. V. Varadan, Bulk propagation characteristics of discrete random media, in *Multiple Scattering of Waves in Random Media*, edited by P. L. Chow, W. E. Kohler and G. Papanicolaou, North-Holland, Amsterdam, 1981.
- Bringi, V. N., V. K. Varadan, and V. V. Varadan, Coherent wave attenuation by a random distribution of particles, *Radio Sci.*, 18, 321-327, 1983.
- Ishimaru, A., *Wave Propagation and Scattering in Random Media*, vol. 2, Academic, Orlando, Florida, 1978.
- Lang, R. H., S. S. Seker, and D. M. LeVine, Vector solution for the mean electromagnetic fields in a layer of random particles, *Radio Sci.*, 21, 771-787, 1986.
- Lax, M., Multiple scattering of waves, II, Effective field in dense systems, *Phys. Rev.*, 85, 621-629, 1952.
- Mathur, N. C. and K. C. Yeh, Multiple scattering of

- electromagnetic waves by random scatterers of finite size, *J. Math. Phys.*, 5, 1619-1628, 1964.
- Metropolis, N., A. W. Rosenbluth, N. Rosenbluth, A. H. Teller, and E. Teller, Equation of state calculation by fast computing machines, *J. Chem. Phys.*, 21 (6), 1087-1092, 1953.
- Oguchi, T., Scattering from hydrometeors: A survey, *Radio Sci.*, 16, 691-729, 1981.
- Olsen, R. I., A review of theories of coherent radio wave propagation through precipitation media of randomly oriented scatterers, and the role of multiple scattering, *Radio Sci.*, 17, 913-928, 1982.
- Street, W. B. and D. J. Tildesley, Computer simulation of polyatomic molecules, I. Monte Carlo studies of hard diatomics, *Proc. R. Soc. London*, Ser AA348, 485-510, 1976.
- Tsang, L., Scattering of electromagnetic waves from a half space of nonspherical particles, *Radio Sci.*, 19, 1450-1460, 1984.
- Twersky, V., Coherent electromagnetic waves in pair-correlated random distributions of aligned scatterers, *J. Math. Phys.*, 19, 215-230, 1978.
- Varadan, V. K. and V. V. Varadan, (eds.) *Acoustic, Electromagnetic and Elastic Wave Scattering: Focus on the T-Matrix Approach*, Pergamon, New York, 1980.
- Varadan, V. K., V. N. Bringi, and V. V. Varadan, Coherent electromagnetic wave propagation through randomly distributed dielectric scatterers, *Phys. Rev. D*, 19, 2480-2489, 1979.
- Varadan, V. K., V. N. Bringi, V. V. Varadan and A. Ishimaru, Multiple scattering theory for waves in discrete random media and comparison with experiments, *Radio Sci.*, 18, 321-327, 1983.
- Varadan, V. V., Y. Ma and V. K. Varadan, Anisotropic dielectric properties of media containing aligned nonspherical scatterers, *IEEE Trans. Antennas Propag.*, AP-33, 886-890, 1985.
- Wood, V. V., Monte Carlo studies of simple liquid models, in *Physics of Simple Liquids*, edited by H. N. V. Temperley, J. S. Rowlinson, and G. S. Rushbrooke, pp. 115-230, North Holland, Amsterdam, 1968.

---

Y. Ma, V. K. Varadan, and V. V. Varadan, Research Center for the Engineering of Electronic and Acoustic Materials, Department of Engineering Science and Mechanics, The Pennsylvania State University, 227 Hammond Building, University Park, PA 16802.

W. A. Steele, Department of Chemistry, The Pennsylvania State University, 127 Pond Laboratory, University Park, PA 16802.

## Scattered Intensity of a Wave Propagating in a Discrete Random Medium

by

Yushieh Ma, Vasundara V. Varadan, and Vijay K. Varadan  
Center for the Engineering of Electronic and Acoustic Materials  
and  
Department of Engineering Science and Mechanics  
The Pennsylvania State University  
University Park, PA 16802

The present paper aims at a computational scheme to obtain numerical results for the second moment (average intensity) of a wave field propagating in a medium consisting of randomly distributed scatterers, not necessarily simple in shape. A formalism is presented that parallels the diagram method and shows the approximations made in the intensity computation of anisotropic scattering whenever finite size scatterers with a considerable concentration are considered. The back and forth scattering between a pair of scatterers, which has been neglected in the ladder approximation, automatically appears in our formalism taking into account all the multiple scattering between two particles through the pair statistics. Sample numerical results for average intensity scattered by particles are presented and compared with some microwave and optical measurements.

### I. Introduction

Scattering of waves from random distribution of objects has received attention ever since Rayleigh's pioneering work in explaining the color of the sky.<sup>1</sup> The statistical moments of a wave propagating in a random medium are of great interest for use in communication, probing and remote sensing. Numerous papers have reported a study of moment equations of various kinds (acoustic, electromagnetic and elastic) for waves in both continuous and discrete random media. As a result, it has been shown that the first moment called the coherent field satisfies a Dyson-type equation,<sup>2</sup> whereas the second moment or intensity satisfies a Bethe-Salpeter type equation.<sup>3,4</sup>

In spite of the abundant literature on wave propagation in continuous random media, an uneven progress still exists in scattering from dense distributions of scatterers which has an increasing application in lidar, radar, and sonar remote sensing. The present paper aims at a computational scheme to obtain numerical results for the second moment (average intensity) of a wave field propagating in a medium consisting of randomly distributed scatterers, not necessarily simple in shape. In a previous paper<sup>5</sup> this has been shown with the help of Feynman diagrams.<sup>6</sup> however, formal derivations and a detailed expression of the average intensity in terms of the T-matrix, dressed propagators and pair correlation function were not given. The formalism

presented here parallels the diagram method and shows the approximations made in the intensity computation of anisotropic scattering whenever finite size scatterers with a considerable concentration are considered.

Unlike diffusion theory,<sup>7</sup> which treats mainly isotropic scattering for point scatterers and large scatterers embedded in a medium with a large optical distance, our concern is the range between those extremes where the validity of the diffusion approximation is fairly limited. In addition, the recently observed enhanced backscattering phenomenon<sup>8</sup> appears to be a result of multiple scattering which cannot be explained by radiative-transfer theory in which the average intensity is treated in a way analogous to the ladder approximation of the Bethe-Salpeter equation. In the formal derivation of the second moment equation based on Twersky's previous work,<sup>9</sup> we clearly show different orders of scattering which involve different orders of statistics and the approximation made in order to implement the computation using the ladder diagram. The cyclic diagrams which involve back and forth scattering between a pair of scatterers was introduced in an ad hoc manner to explain the enhanced backscattering,<sup>10</sup> and is neglected in the ladder approximation. In the derivation presented here, it appears automatically and takes into account all multiple scattering between two particles through the pair statistics. This is essential for high concentrations of scatterers, since in this case their positions are not totally random but there is partial order. The observation that back and forth scattering may have a major contribution to backscattering rather than the forward direction has also been made in one of our previous papers<sup>11</sup>.

In our formalism, shape factor, size distribution, orientation distribution and physical properties of scatterers can all be considered, however, till now, the most reliable calculations are performed for scatterers with rotational symmetry.<sup>12,13</sup> The reason is partly that the intensity equation which best predicts the scattering characteristics beyond some threshold concentrations (when deviations from the single scattering approximation become prominent) requires information about the pair correlation function which is available at the present time only for simple shaped

scatterers which are aligned. Sample numerical results for the average intensity scattered by such particles are presented and compared with available microwave and optical measurements.

## II. Multiple Scattering Formulation for the Intensity

For the scattering of waves by  $N$ , not necessarily identical, scatterers located at  $r_1, r_2, \dots, r_N$ , we represent the total field outside the scatterer by

$$U(r) = u_0(r) + \sum_{j=1}^N u_j(r - r_j). \quad (1)$$

where  $u_0$  is the incident wave field and  $u_j$  the field scattered from the  $j$ -th scatterer. If the scatterers are randomly distributed in space, the total field can be divided into two parts and expressed as

$$U(r) = \langle U(r) \rangle + v. \quad (1a)$$

We call  $\langle U(r) \rangle$  or  $\langle U \rangle$  the average or coherent field and  $v$  the fluctuation or incoherent field. The angular brackets  $\langle \rangle$  represent the configuration or ensemble average whose definition is well known.

Similarly, we average the "intensity" (or the second moment of the field)  $|U|^2$  over the ensemble, and write the "average total intensity" as

$$\begin{aligned} \langle |U|^2 \rangle &= \langle | \langle U \rangle |^2 + |v|^2 \rangle \\ &= | \langle U \rangle |^2 + V \end{aligned} \quad (2)$$

where  $| \langle U \rangle |^2$  is the coherent intensity and can be determined if the average field  $\langle U \rangle$  is known. However, the incoherent intensity  $V$  which is the ensemble average of the absolute square of the field fluctuation is not a directly obtainable quantity. By the use of Eq. (1) and some operation rules for the configuration average, the incoherent intensity  $V$  in Eq. (2) can be written as

$$V = \sum_{j=1}^N \langle |u_j|^2 \rangle + \sum_{\substack{k \neq j \\ k, j=1}}^N \langle u_k u_j^* \rangle - \sum_{k=1}^N \sum_{j=1}^N \langle u_k \rangle \langle u_j^* \rangle \quad (3)$$

where the superscript "\*" represents the complex conjugate of the attached quantity. Eq. (3) is a

finite sum, though "N", the number of scatterers, can be fairly large. The computation of V becomes impractical even for a moderate N and in most cases impossible. In terms of an appropriate probability distribution function and the conditional configuration average, Eq. (3) can be expressed in the following integral form

$$\begin{aligned} V = & n_0 \int \langle |u_j|^2 \rangle_j dr_j \\ & + n_0^2 \iint \langle u_k u_j^* \rangle_{jk} g(r_{jk}) dr_k dr_j \\ & - n_0^2 \iint \langle u_k \rangle_k \langle u_j^* \rangle_j dr_k dr_j \end{aligned} \quad (4)$$

where  $n_0$  is the number density ( $n_0 = N/V$ ),  $\langle \rangle_j$  and  $\langle \rangle_{jk}$  are conditional configuration averages holding the positions of the j-th and both the j-th and k-th scatterers fixed, and  $g(r_{jk})$  is the pair correlation function which is called the radial distribution function for the case of spherical scatterers. Equation (4) is an exact expression for the incoherent intensity V. Even if the number density and pair statistics are known, unless the conditional averages appearing in the integrand are known the integral cannot be evaluated. We also note that this expression can be used to calculate the intensity of the field scattered by a random rough surface provided the integration variables  $r_i$ ,  $r_j$ ,  $r_k$  etc are confined to the rough surface.<sup>14</sup>

For regular distributions, i.e., scatterer at fixed positions, there is no incoherent scattering ( $V = 0$ ) due to the fact that the averaging process is not required. If the scatterer locations are random and independent of one another, only the first term on the RHS of Eq. (4) remains. This is the single scattering approximation to the intensity. Otherwise, in addition to incoherent single scattering, a relatively coherent intensity appears as the contribution of the second term grows. As the concentration of scatterers increases a local order is introduced in the near field of the scatterers since the particles can only be packed in a limited number of ways. In order to proceed further with the computation of the incoherent intensity as stated in Eq. (4), we need expressions for  $\langle u_j \rangle_j$ ;  $\langle |u_j|^2 \rangle_j$ ; and  $\langle u_k u_j^* \rangle_{jk}$ . The Distorted Born Approximation which is discussed next avoids further analysis by making straight forward approximations to the first two terms of Eq. (4).



### III. Distorted Born Approximation ( DBA )

In order to calculate the incoherent intensity  $V$  from Eq. (4) an approximation needs to be made for  $\langle |u_j|^2 \rangle_j$  as well as for  $\langle u_k u_j^* \rangle_{jk}$ , which are both unknown. If we consider only first order scattering, we can use the distorted Born approximation as follows:

$$\langle u_k u_j^* \rangle_{jk} \equiv \langle u_k \rangle_k \langle u_j^* \rangle_j. \quad (5)$$

This approximation was used by Twersky<sup>15</sup> in solving the rough surface scattering problems and has subsequently been used by several other authors. Using Eq. (5), in the distorted Born approximation, Eq. (4) can thus be written as

$$V = n_0 \int \langle u_j \rangle_j \langle u_j^* \rangle_j dr_j + n_0^2 \iint \langle u_k \rangle_k \langle u_j^* \rangle_j [g(r_{jk}) - 1] dr_k dr_j. \quad (6)$$

Equation (6) represents the incoherent intensity in the DBA. Its source is the coherent field,  $\langle u_j \rangle_j$ . Later we show that the average scattered field  $\langle u_j \rangle_j$  is related to the average exciting field when we neglect the field fluctuations in the field exciting a scatterer. Equation (6) tells us that the second term has a contribution to the intensity whenever the  $i$ -th and  $j$ -th scatterers are close to each other (position dependence), otherwise the contribution can be neglected (for small concentration,  $g(r_{jk}) \approx 1$ ). Equation (6) is a deterministic equation since only the average exciting field is involved and the calculation is straight forward for spherical scatterers, by using tabulated values of the pair correlation function. However, attention should be paid to the implementation of the equation since the integrals in Eq. (6) depend upon the receiver position through  $\langle u_j \rangle_j$ . For line-of-sight propagation, the receiver can be placed either in the scattering medium or outside the medium and the axis of the receiver may not be parallel to the propagation direction (see Fig. 1). Furthermore, in order to compare with real measurements, the calculated incoherent intensity, must take into account the characteristics of the transmitter and the receiver and the spreading factor. In other words, the beam patterns of the transmitter and the receiver, especially for off-forward scattering, must be built into the equation which makes the calculation a little more complicated.<sup>16</sup>

In general, using the distorted Born approximation, the incoherent intensity in the far field is

directly proportional to:

$$V \propto \{ I_0 |A|^2 n_0 / (kr)^2 \} [ 1 + n_0 \int [g(x) - 1] \exp(i \mathbf{q} \cdot \mathbf{x}) d\mathbf{x} ] \quad (6a)$$

where  $I_0$  is the incident wave intensity,  $|A|$  the modified bistatic scattering amplitude (by this we refer to the scattered amplitude when the excitation is the coherent field),  $g(x)$  is the pair correlation function,  $\mathbf{x} = \mathbf{r}_j - \mathbf{r}_k$ , and  $\mathbf{q} = K\mathbf{k}_0 - k\mathbf{r}$ ; where  $K$  is the effective wavenumber,  $k_0$  the unit vector along the incident wave direction,  $k$  the wavenumber of the host medium,  $\mathbf{r}$  the unit vector in the direction of observation.

In the integral of Eq. (6a), we find that if the concentration of scatterers is small, the pair correlation function  $g(x)$  is independent of  $x$  and equals unity, therefore the second term on the RHS of Eq. (6a) simply vanishes and only single scattering terms remain. If  $g(x) \neq 1$ , the incoherent intensity is comprised of single scattering contributions from each scatterer plus multiple scattering effects. Only if  $n_0 = 0$ , i.e. no scatterers are present in the medium, the incoherent intensity  $V$  is zero and the total intensity is just the incident wave intensity if the medium itself is lossless.

The other extreme is when the whole medium is occupied by scatterers, the incoherent intensity again vanishes. This implies that one composite medium (two phase medium) has been converted to a single phase homogeneous medium, therefore no scattering occurs. This can be most easily explained by considering the low frequency limit, i.e.  $q \cdot x \ll 1$ . In this case,

$$\exp(i\mathbf{q} \cdot \mathbf{x}) \approx 1 \text{ and } 1 + n_0 \int [g(x) - 1] d\mathbf{x} = (1 - c)^4 / (1 + 2c)^2$$

which is the statistical-mechanics packing factor for spherical scatterers distributed in three dimensional space. The volume fraction  $c (= n_0 4\pi a^3 / 3$  for spherical scatterers with radii  $a$ ) is unity and the structure factor vanishes so does the incoherent intensity. When the volume fraction is between 0 and 1, the incoherent intensity is proportional to  $c(1 - c)^4 / (1 + 2c)^2$ , in the long wavelength limit.

#### A. The Coherent or Average Scattered Field $\langle u \rangle$

To compute the intensity in the DBA, or to proceed further with the analysis of Eq. (4), we

need an expression for the coherent field. For a single scatterer, the scattered field from the  $j$ -th scatterer can be expressed as

$$u_j = \sum f_n^j \Psi_n^j \quad (7)$$

where  $f_n^j$  are the scattered field coefficients and  $\Psi_n^j$  the outgoing functions (Hankel functions). The scattered field coefficients  $f_n^j$  and the exciting field coefficients  $\alpha_n^j$  are related through the  $T$  matrix:<sup>17</sup>

$$f_n^j = \sum T_{nn'}^j \alpha_{n'}^j. \quad (8)$$

Substituting Eq. (8) into Eq. (7) and taking the conditional configuration average, we have

$$\langle u \rangle_j = \sum \sum \langle T_{nn'}^j \alpha_{n'}^j \Psi_n^j \rangle_j. \quad (9)$$

Further, to simplify the computation, we assume the shape, size, and physical properties of all the scatterers are independent of their positions. In such a case, Eq. (9) can be written as

$$\langle u \rangle_j = \sum \sum T_{nn'}^j \langle \alpha_{n'}^j \rangle_j \Psi_n^j. \quad (10)$$

where the exciting field coefficients of the  $j$ -th scatterer can be shown to be<sup>5</sup>

$$\alpha_n^j = a_n^j + \sum \sum \sum \sigma_{nn'}(\mathbf{r}_k - \mathbf{r}_j) T_{n'n''}^k \alpha_{n''}^k. \quad (11)$$

In Eq. (11),  $a_n^j$  are the incident field coefficients of the  $j$ -th scatterer and  $\sigma_{nn'}$  is the translation matrix for spherical wave functions. Although  $\alpha_n^j$  are, in general, unknown for a random distribution of scatterers, their conditional average  $\langle \alpha_n^j \rangle_j$  (average exciting field coefficients of the  $j$ -th scatterer whose position is fixed) are assumed to have the following form<sup>5</sup>

$$\langle \alpha_n^j \rangle_j = X_n \exp(i \mathbf{K} \mathbf{k}_0 \cdot \mathbf{r}_j) \quad (12)$$

which states that for an incident plane wave field, the average exciting field propagates with a new propagation constant  $K$  along the incident wave direction  $\mathbf{k}_0$ . The above form results directly as a result of the assumption that the average medium is a statistically homogenous medium described by different properties but that preserves the plane wave nature of the original incident plane wave. The new propagation constant  $K$  is complex and frequency dependent and can be obtained by solving the following dispersion equation<sup>5</sup>

$$\langle \alpha_n^j \rangle_j = a_n^j + \sum \sum \sum n_0 \int \sigma_{nn'}(\mathbf{r}_k - \mathbf{r}_j) T_{n'n''}^k g(\mathbf{r}_{jk}) \langle \alpha_{n''}^k \rangle_k d\mathbf{r}_k \quad (13)$$

in which the Quasi-crystalline approximation (QCA),<sup>18</sup> i.e.,

$$\langle \alpha_n^k \rangle_{jk} \cong \langle \alpha_n^k \rangle_k, \quad (14)$$

has been introduced.

#### IV. Improvements to the Distorted Born Approximation

We can now proceed with further evaluation of the first and second terms of Eq. (4) which involve  $\langle u_j u_j^* \rangle_j$  and  $\langle u_k u_j^* \rangle_{jk}$ . These are, respectively, the ensemble average of the intensity of the field scattered by one scatterer in the presence of other scatterers and the correlation of the fields scattered by two distinct scatterers. These can also be expressed in terms of the T-matrix, exciting field coefficients and outgoing functions, as follows:

$$\langle u_j u_j^* \rangle_j = \sum \sum \sum \sum T_{nn''}^j T_{n'n''}^{j*} \langle \alpha_n^j \alpha_n^{j*} \rangle_j \Psi_n^j \Psi_n^{j*}, \quad (15)$$

$$\langle u_k u_j^* \rangle_{jk} = \sum \sum \sum \sum T_{nn''}^k T_{n'n''}^{j*} \langle \alpha_n^k \alpha_n^{j*} \rangle_{jk} \Psi_n^k \Psi_n^{j*}. \quad (16)$$

If we do not use the distorted Born approximation and instead Eq. (11) is substituted into Eqs. (15) and (16) for  $\alpha_n$  and for simplicity all the obvious subscripts are omitted to obtain

$$\begin{aligned} \langle \alpha^j \alpha^{j*} \rangle &= \langle \left( a^j + \sum_{\substack{k=1 \\ k \neq j}}^N \sigma_{jk} T^k \alpha^k \right) \left( a^j + \sum_{\substack{m=1 \\ m \neq j}}^N \sigma_{jm} T^m \alpha^m \right)^* \rangle \\ &= a^j a^{j*} + a^j [\langle \alpha^j \rangle - a^j] + a^{j*} [\langle \alpha^j \rangle - a^j] \\ &\quad + \sum \sum \sigma_{jk} T^k \sigma_{jm}^* T^{m*} \langle \alpha^k \alpha^m \rangle. \end{aligned} \quad (17)$$

Therefore,

$$\begin{aligned} \langle \alpha^j \alpha^{j*} \rangle_j &= a^j \langle \alpha^j \rangle_j + a^{j*} \langle \alpha^j \rangle_j - a^j a^{j*} \\ &\quad + \sum_{k=m}^N \int \sigma_{jk} T^k \sigma_{jk}^* T^{k*} \langle \alpha^k \alpha^{k*} \rangle_{jk} P(r_j; r_k) dr_k \\ &\quad + \sum_{k \neq m}^N \sum_{m=1}^N \iint \sigma_{jk} T^k \sigma_{jm}^* T^{m*} \langle \alpha^k \alpha^m \rangle_{jkm} P(r_j; r_k, r_m) dr_k dr_m \end{aligned} \quad (18)$$

We are now ready to proceed with a similar evaluation of  $\langle u_k u_j^* \rangle_{jk}$ . Using Eq. (11), we can write

$$\begin{aligned}
\langle \alpha^k \alpha^{j*} \rangle_{jk} &= \langle (a^k + \sum_{\substack{p=1 \\ p \neq k}}^N \sigma_{kp} T^p \alpha^p) (a^j + \sum_{\substack{m=1 \\ m \neq j}}^N \sigma_{jm} T^m \alpha^m)^* \rangle_{jk} \\
&= a^k a^{j*} + a^k [\langle \alpha^{j*} \rangle_{jk} - a^{j*}] + a^{j*} [\langle \alpha^k \rangle_{jk} - a^k] \\
&\quad + \sum' \sum' \sigma_{kp} T^p \sigma_{jm}^* T^{m*} \langle \alpha^p \alpha^{m*} \rangle_{jk}
\end{aligned} \tag{19}$$

where the last term can be further expressed as the sum of the following

$$\begin{aligned}
\sum \sum \sigma_{kp} T^p \sigma_{jm}^* T^{m*} \langle \alpha^p \alpha^{m*} \rangle_{jk} &= \sigma_{kj} \sigma_{jk}^* T^j T^{k*} \langle \alpha^j \alpha^{k*} \rangle_{jk} \\
&+ \sum \int \sigma_{kp} \sigma_{jp}^* T^p T^{p*} \langle \alpha^p \alpha^{p*} \rangle_{jk} p(r_k, r_j; r_p) dr_p \\
&+ \sum \int \sigma_{kj} \sigma_{jp}^* T^j T^{p*} \langle \alpha^j \alpha^{p*} \rangle_{jk} p(r_k, r_j; r_p) dr_p \\
&+ \sum \int \sigma_{kp} \sigma_{jk}^* T^p T^{k*} \langle \alpha^p \alpha^{k*} \rangle_{jk} p(r_k, r_j; r_p) dr_p \\
&+ \sum \int \int \sigma_{kp} \sigma_{jm}^* T^p T^{m*} \langle \alpha^p \alpha^{m*} \rangle_{jk} p(r_k, r_j; r_p, r_m) dr_p dr_m.
\end{aligned} \tag{20}$$

Equations (18) and (20) can be substituted into Eqs. (15) and (16) and finally into Eq. (4) to yield an expression for the incoherent intensity which can be evaluated in principle provided complete statistics are known. It can be seen that Eqs. (18) and (20) involve correlation functions of all orders. In practice, this is not known for any system unless approximations are made for the correlation functions or the statistics are Gaussian. In this case, higher order correlation functions can be written in terms of products of lower order ones or the higher order statistics can be completely neglected. This is pursued in the next section.

## V. Corrections to the DBA Keeping only Two Point Statistics

### A. Ladder Approximation

In order to carry out the intensity computation, we need to make approximations based on the statistics we considered for the coherent field. Up to this point, statistics higher than the pair correlation function has not been employed in the truncation of the hierarchy of equations for the coherent field.<sup>5</sup> Therefore, we neglect terms involving  $p(r_j; r_k, r_m)$  which is the conditional probability of finding the scatterer at  $r_j$  with respect to a pair of scatterers at  $r_k$  and  $r_m$ . Further, in the spirit of the QCA we assume that

$$\langle \alpha^k \alpha^{k*} \rangle_{jk} \approx \langle \alpha^k \alpha^{k*} \rangle_k. \tag{21}$$

Equation (18) can then be written as

$$\begin{aligned} \langle \alpha^j \alpha^{j*} \rangle_j &= \langle \alpha^j \rangle_j \langle \alpha^{j*} \rangle_j \\ &+ n_0 \int \sigma_{jk} T^k \sigma_{jk}^* T^{k*} \langle \alpha^k \alpha^{k*} \rangle_{jk} g(r_{jk}) dr_k. \end{aligned} \quad (22)$$

If we keep iterating  $\langle \alpha^k \alpha^{k*} \rangle_k$  and use Eq. (21) as an approximation in Eq. (22), we obtain

$$\begin{aligned} \langle \alpha^j \alpha^{j*} \rangle_j &= \langle \alpha^j \rangle_j \langle \alpha^{j*} \rangle_j + n_0 \int \sigma_{jk} T^k \sigma_{jk}^* T^{k*} \langle \alpha^k \rangle_k \langle \alpha^{k*} \rangle_k g(r_{jk}) dr_k \\ &+ n_0^2 \iint \sigma_{jk} T^k \sigma_{jk}^* T^{k*} \sigma_{km} T^m \sigma_{km}^* T^{m*} \langle \alpha^m \rangle_m \langle \alpha^{m*} \rangle_m g(r_{jk}) g(r_{km}) dr_k dr_m \\ &+ n_0^3 \iiint \sigma_{jk} T^k \sigma_{jk}^* T^{k*} \sigma_{km} T^m \sigma_{km}^* T^{m*} \times \\ &\times \sigma_{mp} T^p \sigma_{mp}^* T^{p*} \langle \alpha^p \rangle_p \langle \alpha^{p*} \rangle_p g(r_{jk}) g(r_{km}) g(r_{mp}) dr_k dr_m dr_p \\ &+ \dots = \text{Distorted Born + Higher Order Correction.} \end{aligned} \quad (23)$$

Equation (23) when substituted into Eq. (15) and then in Eq. (4) will enable us to compute the first term of the incoherent intensity  $V$  to accuracy higher than the DBA, but involves only the pair correlation function. This is explained further when the results in Table I are discussed. In Eq. (21), an approximation analogous to the QCA for the exciting field has been made for the exciting field intensity.

The above equation is analogous to the equation associated with a continuous random medium with fluctuations of the physical properties whose distributions are Gaussian. In this case, all correlation functions appearing in the averaging process can be written in terms of the two point correlation function.<sup>4</sup> If we use diagrammatic techniques, which were first introduced by Feynman in quantum mechanics,<sup>6</sup> and were later, employed in the study of wave propagation in random media by Bourret,<sup>19</sup> Furutsu,<sup>20</sup> Tatarski<sup>21</sup> and Frisch,<sup>4</sup> it can be shown that Eq. (23) is equivalent to the ladder approximation (neglect the cross terms, i.e. 1-2' and 2-1', in Eq. (24a)) of the Bethe-Salpeter equation:

$$\begin{aligned} \langle U(r, r_0) U^*(r', r'_0) \rangle &= \langle U(r, r_0) \rangle \langle U^*(r', r'_0) \rangle + \iiint dr_1 dr_2 dr'_1 dr'_2 G(r, r_1) \times \\ &\times G^*(r', r'_1) I(r_1, r_2; r'_1, r'_2) \langle U(r_2, r_0) U^*(r'_2, r'_0) \rangle \end{aligned} \quad (24)$$

The above equation can also be represented diagrammatically as

$$(24a)$$

where  $(\mathbf{r}, \mathbf{r}')$  and  $(\mathbf{r}_0, \mathbf{r}'_0)$  are the vectors associated with the incident and observation positions respectively. The vectors  $\mathbf{r}_1, \mathbf{r}_2, \mathbf{r}_1'$  and  $\mathbf{r}_2'$  denote position vectors of the scatterers 1, 2, 1' and 2' respectively and  $G(\cdot)$  is the propagation function. In most cases it is difficult to calculate an explicit expression for the intensity operator  $I(\mathbf{r}_1, \mathbf{r}_2; \mathbf{r}_1', \mathbf{r}_2')$ . In order to evaluate the correlation function of the field, it is necessary to resort to approximate representations. The ladder approximation to the intensity operator based on Eq. (23) is

$$+ \dots (25)$$

We note that only the first term of Eq. (4) which involves only  $\langle |u_j|^2 \rangle$  contributes to the ladder approximation.

The so called "dressed" diagrams shown above have a multiple scattering interpretation and in this approximation, the coherent exciting field is the original source of the final incoherent radiation. The upper (or lower) line corresponds to a wave, scattered by the  $m$ -th scatterer which is excited by the coherent field, propagating in an effective medium, characterized by the effective wavenumber  $K$ , to the  $k$ -th scatterer which is again scattered and propagates to the next scatterer, and so on. The curly and dash lines joining two scatterers represent the dressed propagators which consist of the translation operator  $\sigma$  and the pair correlation function. Each double diagram in Eq. (25) is the product ( scalar or vector or tensor product depending upon the nature of the problem) of the operator corresponding to the upper line with its complex conjugate corresponding to the lower line. Therefore, different order ladder approximations of the incoherent intensity rely on the number of sequential scattering processes considered in the calculation. Without truncation of the series,

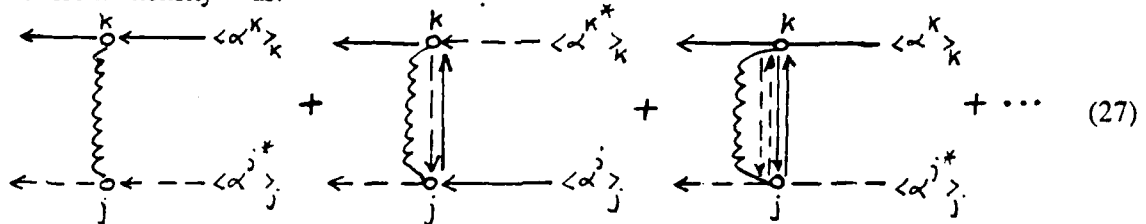
the calculation cannot be done. The truncation depends critically on the concentration of scatterers, the propagation distance or the thickness of the scattering medium, physical properties of the scatterers, the incident wavelength, etc.

### B. Cyclic Diagrams

It will be now shown that the so called cyclic diagrams involving back and forth scattering between a pair of scatterers results from the second term of Eq. (4). In order to carry out the computation, higher order statistics, i.e.  $p(r_k, r_j; r_p)$  and  $p(r_k, r_j; r_p, r_m)$ , are neglected in Eq. (19). Finally, we have, after some manipulations in iterating  $\langle \alpha^j \alpha^{k*} \rangle_{jk}$ ,

$$\begin{aligned} \langle \alpha^k \alpha^{j*} \rangle_{jk} &\approx \langle \alpha^k \rangle_k \langle \alpha^{j*} \rangle_j + \sigma_{kj} \sigma_{jk}^* T^j T^{k*} \langle \alpha^j \rangle_j \langle \alpha^{k*} \rangle_k \\ &\quad + \sigma_{kj} \sigma_{jk}^* T^j T^{k*} \sigma_{kj}^* \sigma_{jk} T^k T^{j*} \langle \alpha^{j*} \rangle_j \langle \alpha^k \rangle_k \\ &\quad + \dots \\ &= \text{Distorted Born + Higher Order Correction.} \end{aligned} \quad (26)$$

After substituting Eq. (26) into Eq. (16) and then in Eq. (4), we can diagrammatically write the incoherent intensity  $V$  as:

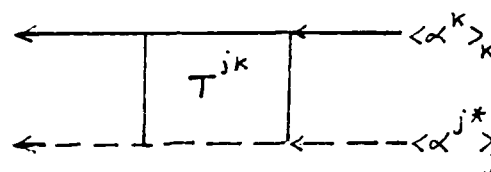


$$+ \dots \quad (27)$$

In the above equation, one sees that beyond the distorted Born approximation the cross terms imply that back and forth multiple scattering processes between a pair of scatterers. This is over and beyond the ladder approximation to the intensity. It may be mentioned that although excellent agreement was obtained between theory and experiment when similar terms were neglected in the computation of the coherent field,<sup>5</sup> this may not be the case for the intensity calculation. Recently, an interesting enhanced backscattering phenomenon has been observed<sup>8,22,23</sup> and some analytical work was tried to explain this using cyclic scattering and point scatterers.<sup>10</sup> However, the experimental observations deal with scatterers large when compared with the incident wavelength,



and therefore a detailed computation based on anisotropic scattering for finite size scatterers is essential. From the published experimental results it is not possible to observe backscattering enhancement when the scatterer size is small compared to the wavelength. It is also advisable to use the T-matrix for a pair of scatterers as mentioned in our earlier work.<sup>11</sup> In fact the so called cyclic terms can all be summed if one replaces the infinite series in Eq. (27) with the T-matrix of a pair of scatterers as given by.<sup>24</sup> Equation (27) may hence be written diagrammatically as


(28)

where  $T^{jk}$ , the two scatterer T-matrix has the following form

$$T^{jk} = R(r_0) T^j [1 - \sigma(r_{jk}) T^k \sigma(r_{kj}) T^j]^{-1} [1 + \sigma(r_{jk}) T^k R(r_{kj})] R(-r_0) \\ + R(r_0) T^k [1 - \sigma(r_{kj}) T^j \sigma(r_{jk}) T^k]^{-1} [1 + \sigma(r_{kj}) T^j R(r_{jk})] R(-r_0) \quad (29)$$

where  $R(r_0)$  is the regular part of the translation matrix  $\sigma(r_0)$ ,  $r_{jk} = r_j - r_k$  and  $r_0 = (r_j + r_k)/2$ .

We are now in a position to write an expression for  $V$  as given in Eq. (4) which is exact if only two point correlations are retained. We emphasize that this is different from making approximations to higher order statistics such as Kirkwood's superposition approximation for the three point correlation function. To this end we substitute Eqs. (23) and (26) in Eqs. (15) and (16) and the last two in Eq. (4) to yield

$$V = n_0 \sum \int [\Psi^j T^j \langle \alpha^j \rangle_j] [\Psi^j T^j \langle \alpha^j \rangle_j]^* dr_j \\ + n_0^2 \sum \iint [\Psi^j T^j \sigma_{jk} T^k \langle \alpha^k \rangle_k] [\Psi^j T^j \sigma_{jk} T^k \langle \alpha^k \rangle_k]^* g(r_{jk}) dr_j dr_k \\ + n_0^3 \sum \iiint [\Psi^j T^j \sigma_{jk} T^k \sigma_{km} T^m \langle \alpha^m \rangle_m] \times \\ \times [\Psi^j T^j \sigma_{jk} T^k \sigma_{km} T^m \langle \alpha^m \rangle_m]^* g(r_{jk}) g(r_{km}) dr_j dr_k dr_m \\ + \dots \text{ (ladder diagrams)} \\ + n_0^2 \sum \iint [\Psi^k T^k \langle \alpha^k \rangle_k] [\Psi^j T^j \langle \alpha^j \rangle_j]^* [g(r_{jk}) - 1] dr_j dr_k \\ + n_0^2 \sum \iint [\Psi^k T^k \sigma_{kj} T^j \langle \alpha^j \rangle_j] [\Psi^j T^j \sigma_{jk} T^k \langle \alpha^k \rangle_k]^* g(r_{jk}) dr_j dr_k$$

$$\begin{aligned}
& + n_0^2 \sum \iint [ \Psi^k T^k \sigma_{kj} T^j \sigma_{jk} T^k < \alpha^k >_k ] \times \\
& \times [ \Psi^j T^j \sigma_{jk} T^k \sigma_{kj} T^j < \alpha^j >_j ]^* g(r_{jk}) dr_j dr_k \\
& + \dots \text{ (cyclic diagrams) }
\end{aligned} \tag{30}$$

Each term of the two series in Eq. (30) represents a certain order of scattering. For the same order of scattering, the cyclic terms are proportional to a higher power in the number density. Thus at low concentrations cyclic terms contribute less than the ladder terms to the the same order of scattering. Equation (30) has been used in the computations presented in the next section.

## VI. Numerical Results and Discussion

To check the validity of our formalism, we compared our incoherent intensity calculations with the microwave experiments conducted by Beard et al.<sup>16</sup> The transmitted intensity was calculated using the DBA as given in Eq. (6) where  $\theta = 0^\circ$  represents the forward direction. This calculation is based on the experimental set-up (see Fig. 1) which consists of a slab region styrofoam container, for various concentrations of scatterers at the fixed frequency. For the case  $ka = 20.8$  for tenuous scatterers with relative index of refraction 1.016 the computed results match very well with measurements (see Fig. 2). Similar computations were also performed for off-forward scattering and a good comparison is again presented in Fig. 3.

The contribution of different orders of scattering is also investigated for the propagation of an electromagnetic wave through randomly distributed spherical ice particles (see Fig. 4). In this calculation, the intensity in the far field of the scattering medium is computed and is normalized with respect to the number density, receiving area and the distance  $D$  traveled by the wave in order to consider the general nature of the problem without reference to specific measurements. Table I gives the magnitudes of the different order scattered incoherent intensities in the forward direction for two different concentrations at two different frequencies. The distorted Born approximation uses only 1st (A) and 1st (B) terms described in the remark of Table I. Although the calculation converges quite rapidly for this scattering medium at small and moderate frequencies ( $ka = 0.1$  and  $1.0$ , respectively), no conclusion can be drawn when high frequencies and different scattering

media are considered. Higher order terms in the intensity calculation not only increase the amount of CPU time but also require knowledge of higher order statistics for densely distributed finite size scatterers.

If the scatterers are not spherical in shape, the calculation of the scattered intensity for a dense distribution of nonspherical scatterers, using spherical statistics, may deviate from measurement s by a considerable amount unless a correct pair correlation function, is employed in the calculation. To show the effect of pair statistics on the intensity calculation, we have picked values of the effective wavenumber from a previous investigation<sup>13</sup> and used them to compute the intensity and show the results in Figs 5 and 6. The geometry of this problem is, again, described by Fig. 4. But the scatterers are either oblate or prolate spheroids and the rotational axis symmetry for all scatterers is parallel to the direction of the incident wave. The details in obtaining the appropriate pair correlation function using Monte Carlo techniques have been discussed by the authors.<sup>13</sup>

As for the backscattered intensity, we have included the T-matrix of a pair of scatterers which takes into account all the so called 'cyclic' terms and considers multiple scattering up to the second order for the calculation of the incoherent intensity . Among three similar optical experiments<sup>8,22,23</sup> of laser light scattered by densely distributed latex particles in distilled water, Albada's measurements are, in our opinion, of the best quality for comparison purposes. The reason is partly that the receiver used has a very small field of view and, hence, gives a much better angular resolution. The widths and the magnitudes of the backscattered intensity peak of our computations compare favorably with those of Albada's experiments (see Fig. 7) for three different number densities which have been converted to the corresponding volume fractions in our intensity calculation. However, due to the truncation of the orders of scattering due to the tremendous amount of CPU time required, we did not obtain a full match.

In a previous paper,<sup>5</sup> the multiple scattered intensity was represented intuitively using diagrams which included possibly all the complicated multiple scattering processes, whereas in the present case, one can see that it also involves approximating higher order statistics in terms of the

pair statistics. Without a priori knowledge of higher order statistics, one may be able to make various approximations and, as a result, different diagrams can be generated but these nonunique subsets of the intensity operator of the Bethe-Salpeter equation. As for the validity of the approximations – can higher order statistics be satisfactorily approximated by lower order statistics or should they be neglected – is still an open question.

**Acknowledgement:** This research was supported by the U.S. Army Research Office through contract # DAAG-29-84-K-0187 awarded to the Pennsylvania State University. The authors wish to thank Dr. Walter Flood for helpful discussions.

### References

1. Lord Rayleigh, "On the transmission of light through an atmosphere containing small particles in suspension, and on the origin of the blue sky," *Philos. Mag.* **47**, 375 (1899).
2. F.J. Dyson, "The radiation theories of Tomonaga, Schwinger, and Feynman," *Phys. Rev.* **75**, 486 (1949).
3. E.E. Salpeter and H.A. Bethe, "A relativistic equation for bound-state problems," *Phys. Rev.* **84**, 1232 (1951).
4. U. Frisch, "Wave propagation in random media," in *Probabilistic Methods in Applied Mathematics*, edited by A.T. Bharucha-Reid, Academic, New York, 1968.
5. V.V. Varadan, Y. Ma and V.K. Varadan, "Propagation model including multiple fields for discrete random media," *J. Opt. Soc. Am.* **A2**, 2195 (1985).
6. R.P. Feynman, "Space-time approach to nonrelativistic quantum mechanics," *Rev. Modern. Phys.* **20**, 367 (1948).
7. A. Ishimaru, *Wave Propagation and Scattering in Random Media*, Academic Press, New York, 1978.
8. Y. Kuga and A. Ishimaru, "Retroreflectance from a dense distribution of spherical particles," *J. Opt. Soc. Am.* **A1**, 831 (1984).
9. V. Twersky, "On propagation in random media of discrete scatterers," in *Proceedings of Symposia in Applied Mathematics*, vol. 16, American Mathematical Society, 1964.
10. L. Tsang and A. Ishimaru, "Theory of backscattering enhancement of random discrete isotropic scatterers based on the summation of all ladder and cyclical terms," *J. Opt. Soc. Am.* **A2**, 1331 (1985).
11. V.N. Brongi, T.A. Seliga, V.K. Varadan and V.V. Varadan, "Bulk propagation characteristics of discrete random media," in *Multiple Scattering and Waves in Random Media*, edited by P.L. Chow, W.E. Kohler, and G.C. Papanicolaou, North-Holland, Amsterdam, 1981.

12. V.K. Varadan, V.N. Bringi, V.V. Varadan, and A. Ishimaru, "Multiple scattering theory for waves in discrete random media and comparison with experiments," *Radio Sci.* **18**, 321 (1983).
13. V.V. Varadan, V.K. Varadan, Y. Ma and W.A. Steele, "Effects of nonspherical statistics on EM wave propagation in discrete random media," *Radio Science* **22**, 491 (1987).
14. V. Twersky, "Multiple scattering of sound by correlated monolayers," *J. Acoust. Soc. Am.* **73**, 68 (1983).
15. V. Twersky, "On scattering and reflection of sound by rough surfaces," *J. Acoust. Soc. Am.* **29**, 209 (1957).
16. C.I. Beard, T.H. Kays and V. Twersky, "Scattered intensities for random distributions - microwave data and optical applications," *App. Opt.* **4**, 1299 (1965).
17. V.K. Varadan and V.V. Varadan (Eds.), *Acoustic, Electromagnetic and Elastic Wave Scattering - Focus on the T-matrix Approach*, Pergamon, New York, 1980.
18. M. Lax, "Multiple scattering of waves. II. The effective field in dense systems," *Phys. Rev.* **88**, 621 (1952).
19. R.C. Bourret, "Propagation of randomly perturbed fields," *Can. J. Phys.* **40**, 782 (1962).
20. K. Furutsu, "On the statistical theory of electromagnetic waves in a fluctuating medium," *J. Res. Natl. Bur. Standards, D* **67**, 303 (1963).
21. V.I. Tatarski, *Wave Propagation in a Turbulent Medium*, McGraw-Hill, New York, 1961.
22. M.P. Van Albada and A. Lagendijk, "Observation of weak localization of light in a random medium," *Phys. Rev. Lett.* **55**, 2692 (1985).
23. P.E. Wolf and G. Maret, "Weak localization and coherent backscattering of photons in disordered media," *Phys. Rev. Lett.* **55**, 2696 (1985).
24. V.V. Varadan and V.K. Varadan, "Configurations with finite numbers of scatterers - A self-consistent T-matrix approach," *J. Acoust. Soc. Am.* **70**, 213 (1981).

Table I Comparison of Orders of Scattering

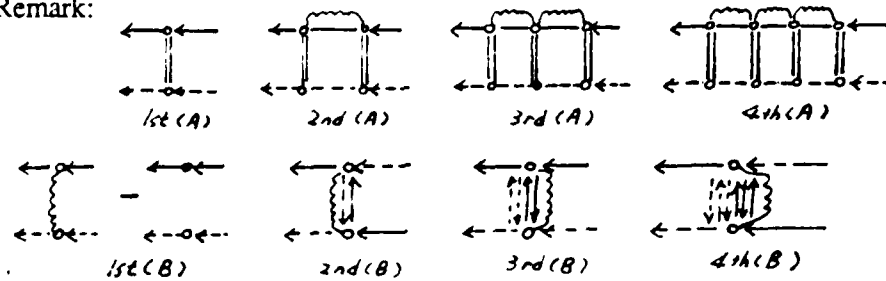
 $(\theta = 0^\circ, ka = 0.1)$ 

$c = 0.05$		$c = 0.20$	
Order	Normalized Intensity	Order	Normalized Intensity
1st (A)	$0.1796 \times 10^{-6}$	1st (A)	$0.1839 \times 10^{-6}$
(B)	$-0.6050 \times 10^{-7}$	(B)	$-0.1469 \times 10^{-6}$
2nd (A)	$0.7689 \times 10^{-15}$	2nd (A)	$0.1076 \times 10^{-13}$
(B)	$0.7544 \times 10^{-15}$	(B)	$0.1062 \times 10^{-13}$

 $(\theta = 0^\circ, ka = 1.0)$ 

$c = 0.05$		$c = 0.20$	
Order	Normalized Intensity	Order	Normalized Intensity
1st (A)	0.3009	1st (A)	0.2999
(B)	-0.1016	(B)	-0.2393
2nd (A)	$0.8369 \times 10^{-3}$	2nd (A)	$0.1123 \times 10^{-1}$
(B)	$0.8665 \times 10^{-3}$	(B)	$0.1160 \times 10^{-1}$
3rd (A)	$0.1419 \times 10^{-7}$	3rd (A)	$0.6044 \times 10^{-3}$
(B)	$0.4653 \times 10^{-5}$	(B)	$0.7246 \times 10^{-3}$
4th (A)	$0.6054 \times 10^{-10}$	4th (A)	$0.3428 \times 10^{-4}$
(B)	$0.2777 \times 10^{-6}$	(B)	$0.4759 \times 10^{-4}$

Remark:



# LIST OF FIGURES

Fig. 1 Geometry of scattering from layered media.

(In Beard's experiment  $\alpha = 6^\circ$ ,  $\beta = 3^\circ$

T = 69.9 cm, R = 264 cm, D = 25.4 cm)

Fig. 2 Transmitted incoherent intensity vs. concentration.

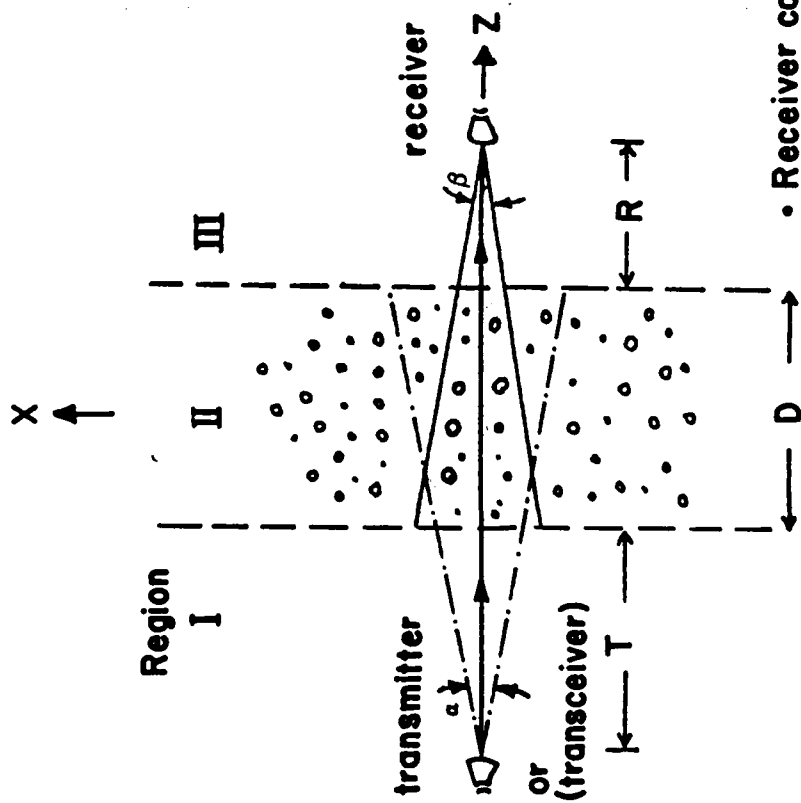
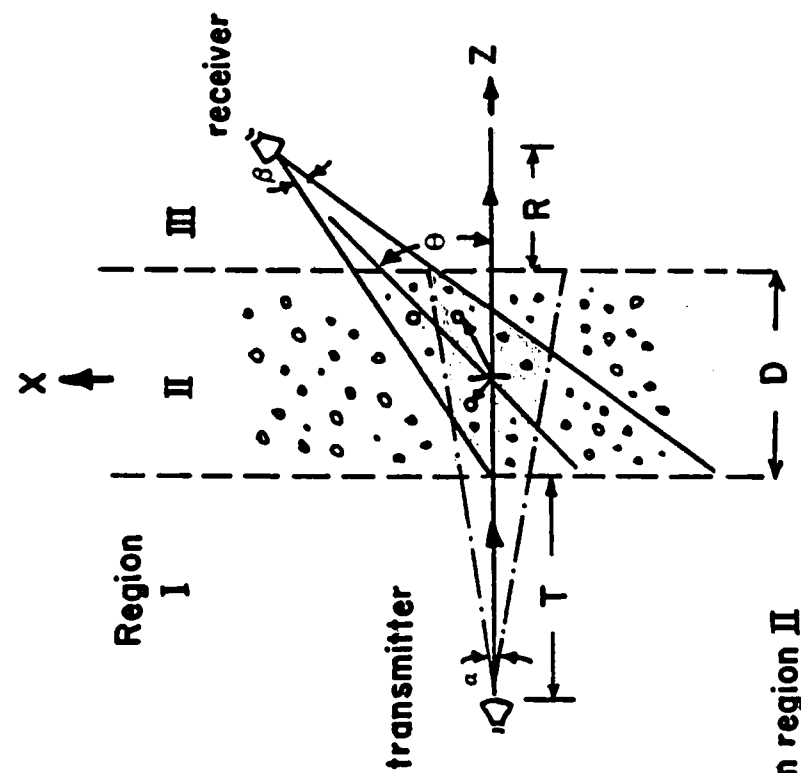
Fig. 3 Off-forward scattering of incoherent intensity for different concentrations.

Fig. 4 Geometry of scattering from a volume of scatterers.

Fig. 5 Normalized incoherent intensity of EM wave scattered by oblate ice spheroids in free space.

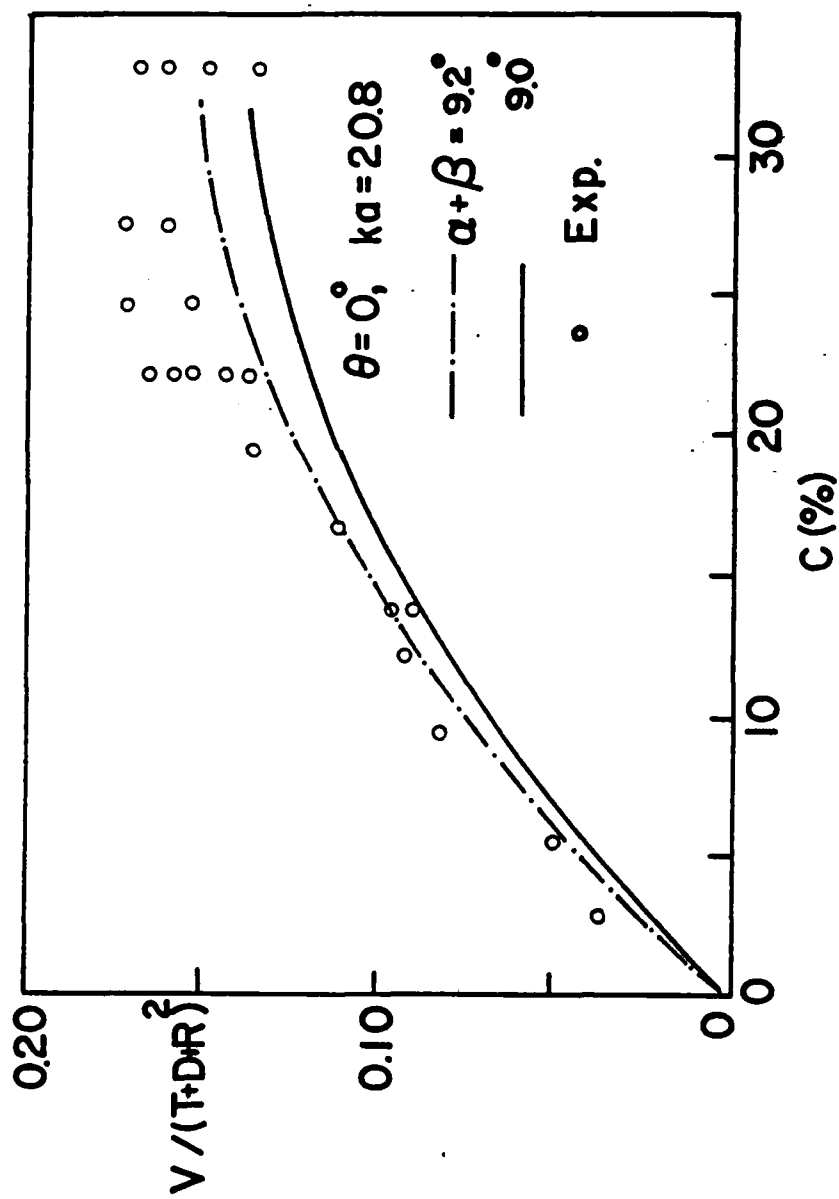
Fig. 6 Normalized incoherent intensity of EM wave scattered by prolate ice spheroids in free space.

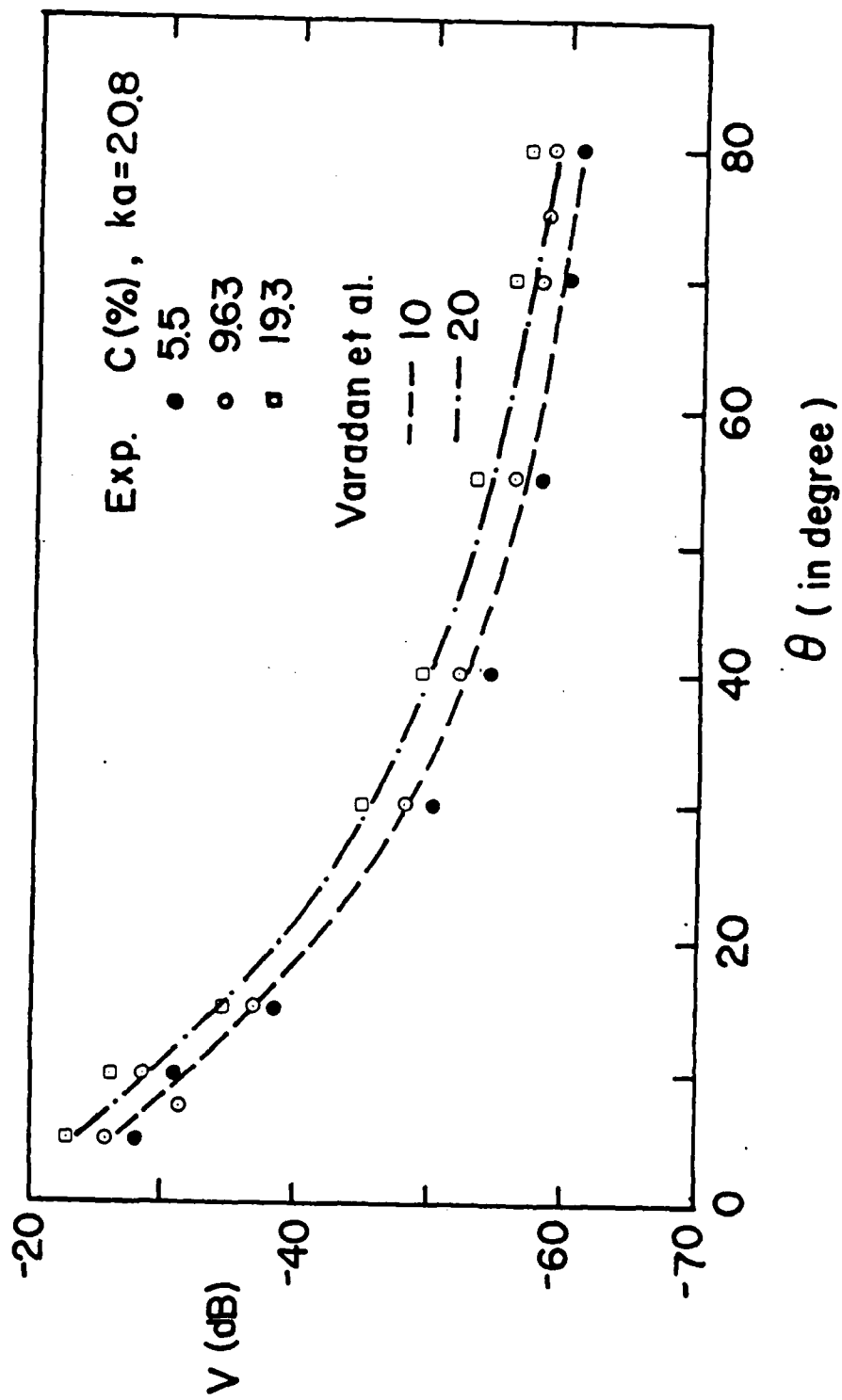
Fig. 7 Backscattered intensity for latex spheres in water (0 mrad is the backscattering direction).

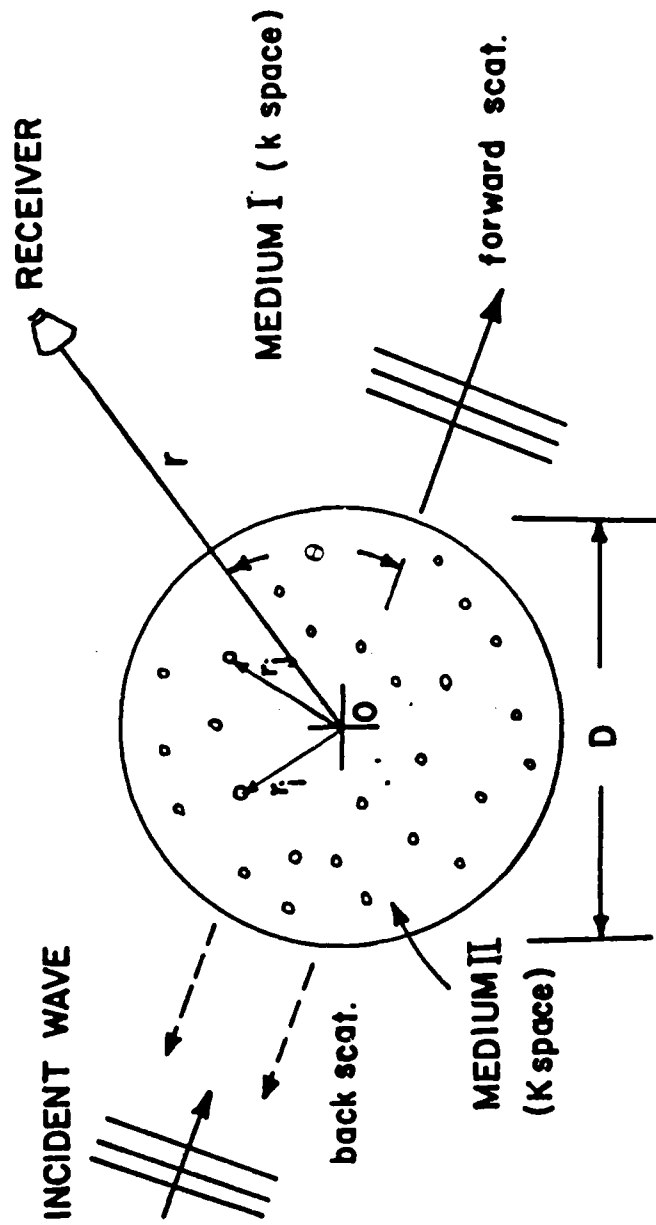


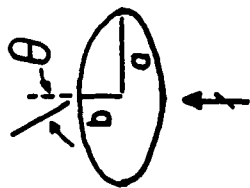
- Receiver can be in region II
- $D$  can be very large







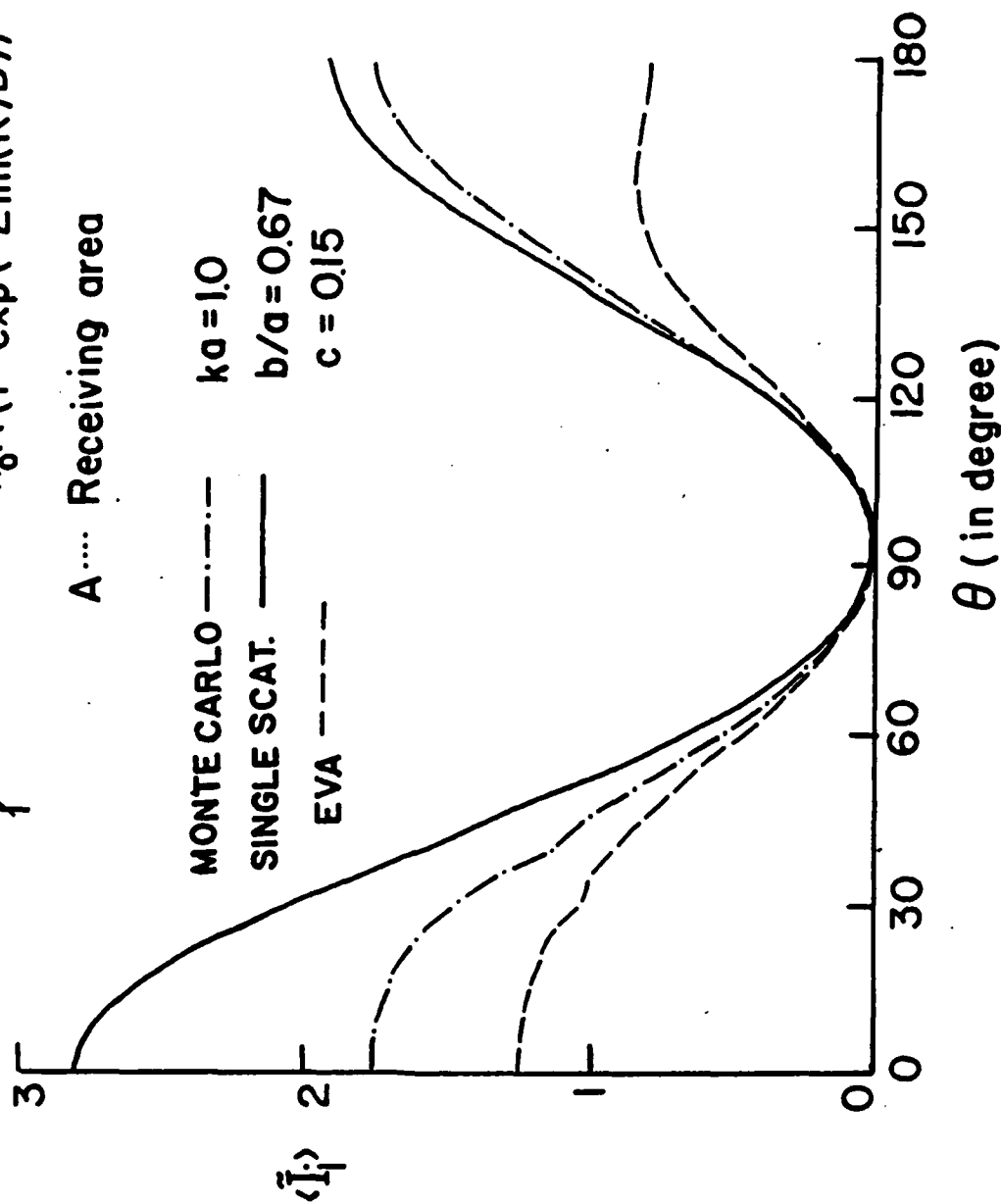


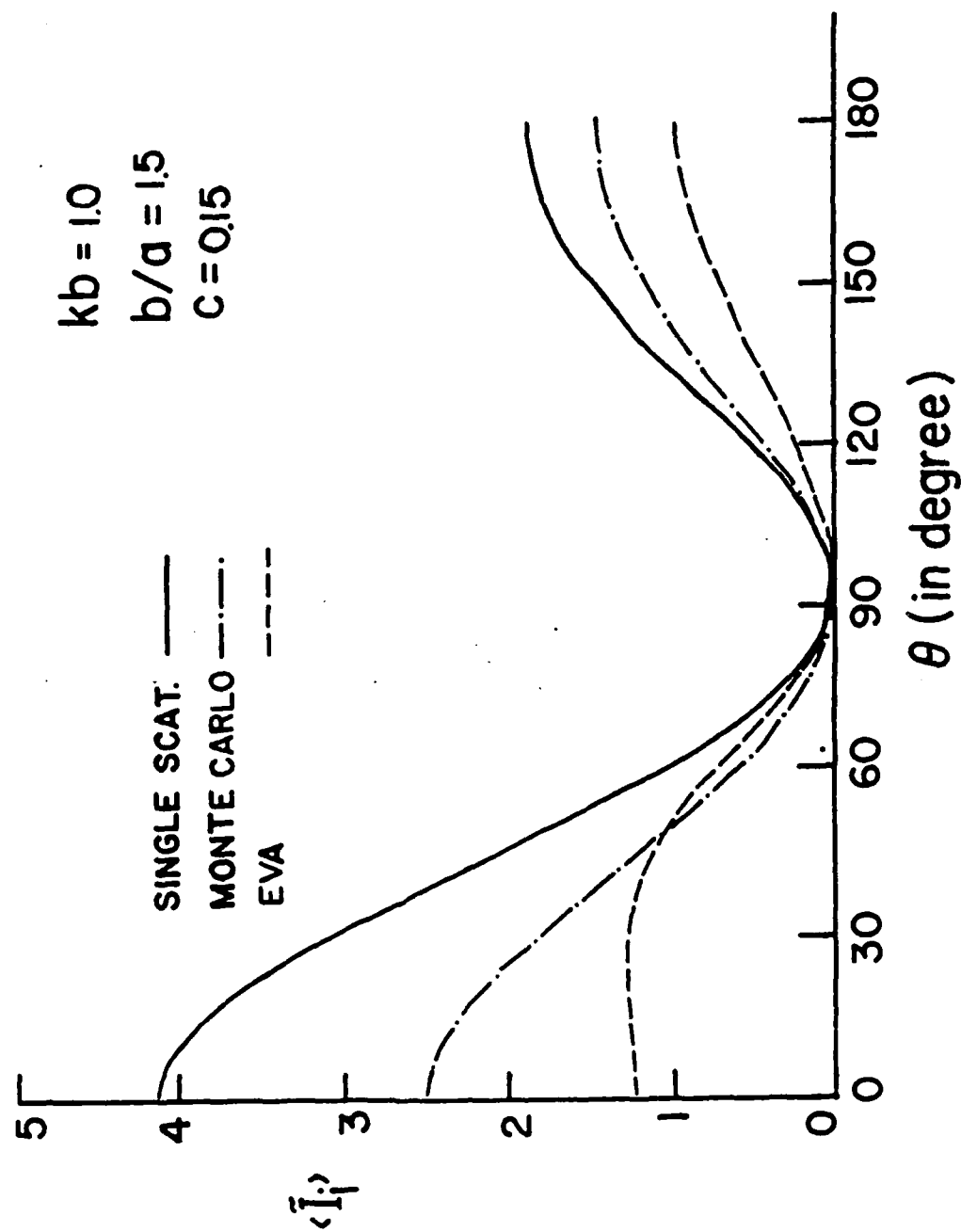


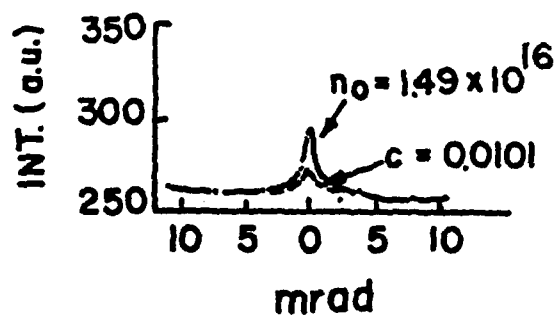
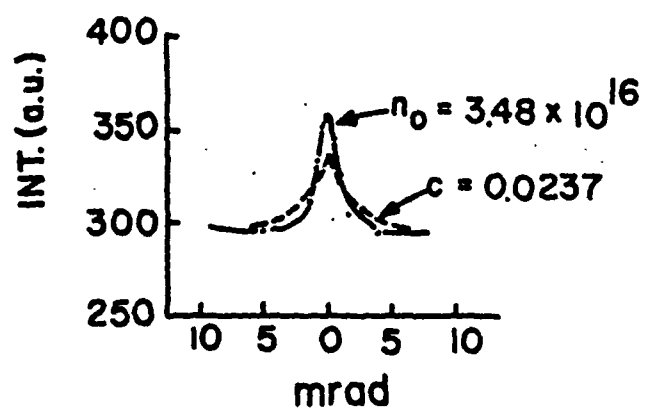
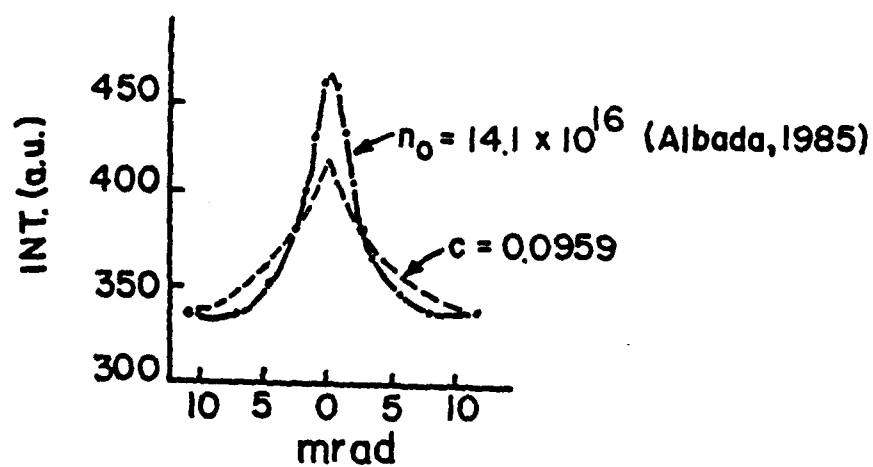
$$\langle \tilde{I}_r \rangle = \frac{V(kr)^2 2 \ln(K)}{n_0 A (1 - \exp(-2 \ln(K) D))}$$

A... Receiving area

MONTE CARLO — · — · —  $ka = 1.0$   
 SINGLE SCAT. —  $b/a = 0.67$   
 EVA — — —  $c = 0.15$







END

DATE

FILMED

5-88

DTIC